

Doctoral Thesis

**Phytoplankton community occurring in the
southern coast of Myanmar especially focusing on
potentially harmful dinoflagellates**

Su Myat

**Graduate School of Biosphere Science
Hiroshima University**

March 2013

Doctoral Thesis

**Phytoplankton community occurring in the
southern coast of Myanmar especially focusing on
potentially harmful dinoflagellates**

Su Myat

**Department of Environmental Dynamics and Management
Graduate School of Biosphere Science
Hiroshima University**

March 2013

ABSTRACT

Myanmar has been one of the world's top ten countries for capture fisheries, and the catches are constantly increasing after 1990's. Such growth in the marine capture fishery relies on high productivity of the coastal environment. However, over-fishing surpassing that ocean productivity and recent rapid coastal developments, which often lead eutrophication and subsequent harmful algal blooms, are concerned. Any of these issues should be primarily regarded in a view of phytoplankton, however, researches and information are totally lacking in the Myanmar coasts. Therefore, detail phytoplankton surveys were firstly carried out in pre- and post-rainy seasons at the foremost marine fishery area, Tanintharyi coastal region. The surveys were conducted thrice: May, 2010 (pre-rainy season), December, 2010 (post-rainy season) and March, 2012 (pre-rainy season).

Total of 64 diatom species and 100 dinoflagellates species were listed from these three surveys. Diverse diatom species were mainly found in the December survey and the dinoflagellate species were rather in the May and March surveys. The massive occurrence of diverse diatom species in the December survey can be explained by the flooding of nutrient-rich terrestrial water into the coastal areas in prolonged rainy weather during the southwest monsoon, and drift of these terrestrial waters to the entire coastal area due to shift to the northeast wind. The diverse dinoflagellate occurrences in the May and March surveys were probably due to the oligotrophic environment in the late dry season. Simultaneous occurrence of the oceanic and the neritic species in the May and March surveys were unique and explained the oceanic water mixing with the

coastal waters in this coastal area. High diversities of heterotrophic dinoflagellate cysts were also characteristic in the Myanmar coast.

In the dinoflagellate list from three surveys, 21 species were identified as potentially harmful species. Among them, 10 species were reexamined with detail morphological observation and DNA (28S rRNA gene) analyses. In here, red-tide forming species such as *Alexandrium affine*, *Gonyaulax polygramma* and *Prorocentrum shikokuense*, and shellfish poisoning causative species such as *Alexandrium tamiyavanichii* and *Gymnodinium catenatum* were recognized. These harmful species were mainly detected in the May and March surveys, and these late dry seasons should be regarded as to potentially cause HAB events. Accidentally, red-tide of *Prorocentrum* spp. was found near the northeast part of Kadan Island on the March survey. This red-tide was noteworthy by comprising three different harmful dinoflagellates, namely *P. rhathymum*, *P. shikokuense* and *A. affine*. Culture strains of these three species were successfully established from this red-tide water, and subjected to growth experiment under different temperatures, to understand their blooming capabilities. The experiments were carried out at four different temperature regimes (15, 20, 25, 30°C). The results of *A. affine* exhibited the low tolerant to the low temperature (15°C), irrespective to its records in northern temperate region, hence this strain adapted to the tropical environment in Myanmar. *P. rhathymum* and *P. shikokuense* exhibited strong tolerance to the all given temperature ranges and rather high division rates, providing physiological basis to form red-tide.

Such plankton and cyst surveys were also conducted in the Selangor district, west coast of Malay Peninsula, facing to the Strait of Malacca and connecting to the Myanmar coast. Selangor coast is an important area for culture industries of a bivalve,

blood cockle, in Malaysia. In the result, paralytic shellfish poisoning (PSP) causative species of *G. catenatum* (motile and cyst forms) and *A. tamiyavanichii* (thecate form) were detected. The detection of toxic dinoflagellates from the cockle culture grounds suggested that PSP risk might present in the Selangor district, and the management plan will be needed in this area. Such awareness is or will be applied also to the Myanmar coast.

In conclusion, this study firstly showed remarkable diversities of diatoms and dinoflagellates off the coast of Myeik. These diversities were largely influenced by two distinctive seasons caused by monsoon, and largely supported by nutrient loads from native rivers or oceanic water extensions, which all characteristics of the Myanmar coasts. These plankters are, of course, primary producers and support high ocean productivity in Myanmar. At the same time, some of harmful dinoflagellates species were recognized, and indeed, a red-tide comprising three potentially harmful species was found on the site. On those grounds, perspectives for those risk-managements should be raised soon.

ACKNOWLEDGEMENTS

First of all, I would like to thank my supervisor Dr. Kazuhiko Koike, for providing me with the opportunities to dinoflagellate research, and his guidance and teaching over the years. I would like to extend my thanks to committee member Dr. Kazumi Matsuoka, for his teaching and comments on the dinoflagellate cysts study. I would like to acknowledge to all committee members, Dr. Shin-ichi Uye, Dr. Kazuo Iseki and Dr. Keizo Nagasaki, for their valuable comments and questions.

I would like to thank Minister of Livestock and Fisheries, Myanmar and Director General U Khin Ko Lay (Department of Fisheries) for all supporting on my research survey in the Tanintharyi coast, and thanks to Dr. Swe Thwin, (U Myint Pe) and all Myeik DOF members for their supporting in my field surveys. I would also like to acknowledge Dr. Tatsuya Yurimoto (JIRCAS), Mohd Nor Azman Bin Ayub and Alias Bin Man (FRI, Penang, Malaysia) for allowing me to participate in their joint research and supporting the samples of Selangor district.

I wish to thank Koike team's members especially to Taro Arimoto for helping on experiment and nutrients analysis, and Kohei Shintaku for sharing knowledge on DNA analysis. I am deeply grateful to Saw Htoo Thaw for investing time and energy assisting in my surveys and discussing ideas. My special thanks and loves to my best friend Lisa Fujise for her assistance, knowledge sharing and generous encouragement. I wish to thank also to graduated senior Dr. Hiroshi Yamashita, Dr. Ryosuke Makabe, Nanami Honge and Yohei Takaya for their teaching. I wish to acknowledge Dr. Vera Pospelova and Manuel Bringue (University of Victoria, Canada), and Dr. Kenneth Neil Mertens (Ghent University, Belgium) for their teaching and supporting literatures. I will forever be thankful to my lab members from Hiroshima University and Matsuoka's lab members from Nagasaki University for their kindly helps.

I would also like to acknowledge the Ministry of Education, Culture, Sports, Science, and Technology, Japan (Monbukagakusho scholarship) for financially supporting throughout my research in Japan.

I am deeply indebted to retired Deputy Minister U Aung Thein (Chairman of GIS Group of Companies, Yangon), for his nurturing that made me into a researcher. I am always keep in mind the gratitude of retired Deputy Director U Minn Thein, retired Director General U Than Tun and retired Deputy Director General U Hla Win for their generous guidance and supports. I will never forget the encouragement and supporting of Dr. Tatsuya Umino, Himiko Koi and my dear friend Dr. Ione Madinabeitia. Finally, a big thank to my father, mother, brothers, husband and all of my relatives for their everlasting encouragement and loving-kindness.

TABLE OF CONTENT

ABSTRACT	i
ACKNOWLEDGEMENTS	iv
TABLE OF CONTENT	v
LIST OF TABLES	viii
LIST OF FIGURES	x
CHAPTER 1: GENERAL INTRODUCTION	1
1.1. General overview of Myanmar fisheries and coastal environments	1
1.2. Phytoplankton	3
1.3. Dinoflagellate cysts	4
1.4. Potential risks in Myanmar fisheries	5
1.5. Needs to avoid possible risks for Myanmar fisheries	6
1.6. General objectives of this study	6
CHAPTER 2: PHYTOPLANKTON OCCURRENCES IN THE SOUTHERN MYANMAR COAST	8
2.1. Introduction	8
2.2. Materials and Methods	10
2.2.1. Study area	10
2.2.2. Survey	10
2.2.3. Microscopy for plankton	11
2.2.4. Sediment sample preparation and microscopy for cysts	13
2.2.5. Nutrient analysis	14
2.3. Results	14
2.3.1. Diatom and dinoflagellate species occurrence	14
2.3.2. Cysts occurrence	18
2.3.3. Nutrients	20
2.4. Discussion	21
2.4.1. Species diversity in pre- and post-rainy seasons: overview	21
2.4.2. Characters of species occurrences	23

2.4.3. Dinoflagellate cyst assemblage	28
CHAPTER 3: OCCURRENCES OF POTENTIALLY HARMFUL DINOFLAGELLATES	75
3.1. Introduction	75
3.2. Materials and Methods	77
3.2.1. Sampling	77
3.2.2. Isolation and culture	78
3.2.3. Morphological observation and identification	78
3.2.4. Analyzes of DNA sequences and their phylogenies	79
3.3. Results	81
3.3.1. Morphological analysis	81
3.3.2. DNA phylogeny	90
3.4. Discussion	95
3.4.1. Species confirmation and their phylogenetic position	95
3.4.2. Potential implications of red-tide forming species	100
3.4.3. Potential implications of shellfish poisoning causative species	101
CHAPTER 4: GROWTH CHARACTERS OF THREE RED-TIDE FORMING SPECIES (<i>Prorocentrum rhathymum</i> , <i>P. shikokuense</i> , <i>Alexandrium</i> <i>affine</i>) AT DIFFERENT TEMPERATURES	122
4.1. Introduction	122
4.2. Materials and Methods	124
4.2.1. Study area	124
4.2.2. <i>Prorocentrum rhathymum</i> cell densities in red-tide water	124
4.2.3. Organism and culture conditions	124
4.2.4. Temperature experiments	125
4.3. Results	126
4.3.1. <i>P. rhathymum</i> densities in the field sample	126
4.3.2. Effects of temperature on growth	126
4.4. Discussion	127

4.4.1. Effects of temperature on growth	127
CHAPTER 5: OCCURRENCE OF DINOFLAGELLATE CYSTS IN THE SURFACE SEDIMENT, AND FINDING OF TOXIC <i>Gymnodinium catenatum</i> AND <i>Alexandrium tamiyavanichii</i> FROM COASTAL WATERS OF SELANGOR, MALAY PENINSULA	133
5.1. Introduction	133
5.2. Materials and Methods	134
5.2.1. Study area and cyst survey	134
5.2.2. Sample preparation and microscopy	135
5.2.3. Plankton sampling and microscopy	135
5.3. Results	136
5.3.1. Cysts	136
5.3.2. Cysts of <i>Gymnodinium catenatum</i>	137
5.3.3. Plankton of <i>Gymnodinium catenatum</i>	138
5.3.4. Plankton of <i>Alexandrium tamiyavanichii</i>	138
5.4. Discussion	139
CHAPTER 6: GENERAL DISCUSSION	170
6.1. General overview of studies	170
6.2. Phytoplankton occurrences in the southern Myanmar coast	170
6.3. Occurrences of potentially harmful dinoflagellates	171
6.4. Growth characters of three red-tide forming species (<i>Prorocentrum rathymum</i> , <i>P. shikokuense</i> and <i>A. affine</i>) at different temperatures	172
6.5. Occurrence of dinoflagellate cysts in the surface sediment, and finding of toxic <i>Gymnodinium catenatum</i> and <i>Alexandrium tamiyavanichii</i> from coastal water of Selangor, Malay Peninsula	173
6.6. Significance of this study	174
6.7. Future studies	176
REFERENCES	178

LIST OF TABLES

Table 2.1.	Sampling locations around Mali and Kadan Islands (May 2010).	55
Table 2.2.	Sampling locations around Kadan Island: depths and environmental parameters (December, 2010).	56
Table 2.3.	Sampling locations around Kadan Island: depths and environmental parameters (March, 2012).	57
Table 2.4.	List of diatom species observed around Kadan Island, southern coast of Myanmar.	58
Table 2.5.	List of dinoflagellate species observed around Mali and Kadan Islands, southern coast of Myanmar.	63
Table 2.6.	List of dinoflagellate cysts recorded around Kadan Island, southern coast of Myanmar.	69
Table 2.7.	Density of dinoflagellate cysts recorded around Kadan Island, southern coast of Myanmar.	72
Table 5.1.	Sampling locations at the west coast of the Malay Peninsula: depths and environmental parameters (September and December, 2011).	151
Table 5.2.	List of dinoflagellate cysts recorded from Selangor area, west coast of the Malay Peninsula.	152
Table 5.3.	Density of autotrophic cysts from Station A (Bagan Nakhoda Omar), Selangor area.	155
Table 5.4.	Density of heterotrophic cysts from Station A (Bagan Nakhoda Omar), Selangor area.	156
Table 5.5.	Density of autotrophic cysts from Station B (Sungai Besar), Selangor area.	158
Table 5.6.	Density of heterotrophic cysts from Station B (Sungai Besar), Selangor area.	159
Table 5.7.	Density of autotrophic cysts from Station C (Sekinchan), Selangor area.	161
Table 5.8.	Density of heterotrophic cysts from Station C (Sekinchan), Selangor area.	162
Table 5.9.	Density of autotrophic cysts from Station D (Kuala Selangor), Selangor area.	164

Table 5.10.	Density of heterotrophic cysts from Station D (Kuala Selangor), Selangor area.	165
Table 5.11.	Density of autotrophic cysts from Station E (Sungai Buloh), Selangor area.	167
Table 5.12.	Density of heterotrophic cysts from Station D (Kuala Selangor), Selangor area.	168

LIST OF FIGURES

Figure 2.1.	Map showing sampling locations around Mali and Kadan Islands, southern Myanmar coast, for the first survey in May, 2010.	30
Figure 2.2.	Map showing sampling locations around Kadan Island, southern Myanmar coast for the second survey in December, 2010 and third survey in March, 2012.	31
Figure 2.3A.	Light and scanning electron microscope (SEM) micrographs of centric looking diatoms.	32
Figure 2.3B.	Light and SEM micrographs of rod-like looking and cylindrical chain forming diatoms.	33
Figure 2.3C.	Light and SEM micrographs of chain forming diatoms with spines and setae.	34
Figure 2.3D.	Light and SEM micrographs of leaf-like looking diatoms.	35
Figure 2.3E.	Light and SEM micrographs of not centric-looking diatoms.	36
Figure 2.3F.	Light and SEM micrographs of pennate diatoms.	37
Figure 2.4A.	Light, fluorescence and SEM micrographs of dinoflagellates, order Prorocentrales.	38
Figure 2.4B.	Light, fluorescence and SEM micrographs of dinoflagellates, order Dinophysiales.	39
Figure 2.4C.	Light, fluorescence and SEM micrographs of dinoflagellates, order Dinophysiales.	40
Figure 2.4D.	Light, fluorescence and SEM micrographs of dinoflagellates, order Gonyaulacales.	41
Figure 2.4E.	Light, fluorescence and SEM micrographs of dinoflagellates, order Gonyaulacales.	42
Figure 2.4F.	Light and fluorescence micrographs of dinoflagellates, order Peridiniales.	43
Figure 2.4G.	Light, fluorescence and SEM micrographs of dinoflagellates, order Peridiniales.	44
Figure 2.4H.	Light, fluorescence and SEM micrographs of dinoflagellates, order Peridiniales.	45

Figure 2.4I.	Light and fluorescence micrographs of dinoflagellates, order Peridiniales.	46
Figure 2.4J.	Light, fluorescence and SEM micrographs of unarmoured dinoflagellates.	47
Figure 2.5.	Dendrogram produced by clustering of 7 stations sampled in May, 2010 based on dinoflagellate species similarity using cluster analysis.	48
Figure 2.6.	Dendrogram produced by clustering of 7 stations sampled in December, 2010 based on dinoflagellate species similarity using cluster analysis.	48
Figure 2.7.	Dendrogram produced by clustering of 7 stations sampled in March, 2012 based on dinoflagellate species similarity using cluster analysis.	48
Figure 2.8.	Graph showing the proportion of dinoflagellates and diatoms cell density, and surface nutrient concentration in each station in December, 2010.	49
Figure 2.9.	Graph showing the proportion of dinoflagellates and diatoms cell density, and surface nutrient concentration in each station in March, 2012.	49
Figure 2.10.	Graph showing species diversity of dinoflagellates and diatoms, and surface nutrient concentration in each station in December, 2010.	50
Figure 2.11.	Graph showing species diversity of dinoflagellates and diatoms, and surface nutrient concentration in each station in March, 2012.	50
Figure 2.12.A	Light micrographs of dinoflagellate cysts.	51
Figure 2.12B	Light micrographs of dinoflagellate cysts.	52
Figure 2.12C	Light micrographs of dinoflagellate cysts.	53
Figure 2.13a	Graph showing the proportion of autotrophic and heterotrophic dinoflagellate cysts in December, 2010.	54
Figure 2.13b	Graph showing the proportion of autotrophic and heterotrophic dinoflagellate cysts in March, 2012.	54

Figure 3.1.	Light, fluorescence and SEM micrographs of potentially harmful dinoflagellates.	105
Figure 3.2.	Light and SEM micrographs of <i>Prorocentrum rhathymum</i> .	106
Figure 3.3.	Light and SEM micrographs of <i>Prorocentrum shikokuense</i> .	107
Figure 3.4.	Light and fluorescence micrographs of <i>Alexandrium tamiyavanichii</i> .	108
Figure 3.5.	Light and fluorescence micrographs of <i>Alexandrium affine</i> .	109
Figure 3.6.	Light and SEM micrographs of <i>Gymnodinium catenatum</i> .	110
Figure 3.7.	Light and fluorescence micrographs of <i>Lingulodinium polyedrum</i> .	111
Figure 3.8.	Fluorescence and SEM micrographs of <i>Gonyaulax spinifera</i> .	112
Figure 3.9.	Fluorescence and SEM micrographs of <i>Gonyaulax polygramma</i> .	113
Figure 3.10.	Light and SEM micrographs of <i>Dinophysis caudata</i> .	114
Figure 3.11.	Light and SEM micrographs of <i>Dinophysis miles</i> .	115
Figure 3.12.	Light and SEM micrographs of <i>Dinophysis rotundata</i> .	116
Figure 3.13.	Light micrographs of <i>Noctiluca scintillans</i> .	117
Figure 3.14.	Maximum-likelihood (ML) tree for <i>Prorocentrum rhathymum</i> .	118
Figure 3.15.	Maximum-likelihood (ML) tree for <i>Prorocentrum shikokuense</i> .	118
Figure 3.16.	Maximum-likelihood (ML) tree for <i>Alexandrium affine</i> .	119
Figure 3.17.	Maximum-likelihood (ML) tree for <i>Alexandrium tamiyavanichii</i> .	119
Figure 3.18.	Maximum-likelihood (ML) tree for <i>Gonyaulax polygramma</i> .	120
Figure 3.19.	Maximum-likelihood (ML) tree for <i>Dinophysis caudata</i> .	120
Figure 3.20.	Maximum-likelihood (ML) tree for <i>Dinophysis rotundata</i> .	121
Figure 3.21.	Maximum-likelihood (ML) tree for <i>Gymnodinium catenatum</i> .	121
Figure 4.1.	Map showing sampling location of red-tide occurring area at the northeast part of Kadan Island, Tanintharyi coast, Myanmar in March 2012 (red circle).	130

Figure 4.2.	Red-tide of <i>Prorocentrum rhathymum</i> at the northeast part of Kadan Island.	131
Figure 4.3.	Graph showing the densities of <i>P. rhathymum</i> , <i>P. shikokuense</i> and <i>A. affine</i> detecting in the red-tide field sample.	131
Figure 4.4.	Growth curves and growth rate of <i>A. affine</i> , <i>P. rhathymum</i> and <i>P. shikokuense</i> .	132
Figure 5.1.	Map of the Selangor area off the west coast of Malay Peninsula, Malacca Strait showing the sampling stations.	142
Figure 5.2.A.	Light micrographs of dinoflagellate cysts.	143
Figure 5.2.B.	Light micrographs of dinoflagellate cysts.	144
Figure 5.3.a.	Graph showing the proportion of autotrophic and heterotrophic cyst densities in each station in September, 2011.	145
Figure 5.3.b.	Graph showing the proportion of autotrophic and heterotrophic cyst densities in each station in December, 2011.	145
Figure 5.4.	Light micrographs of cysts and plankton of <i>Gymnodinium catenatum</i> found in Selangor area.	146
Figure 5.5.	Map of Selangor area showing the occurrence of the cyst of <i>Gymnodinium catenatum</i> in September and December surveys.	147
Figure 5.6.	Graph showing the average density of <i>Gymnodinium catenatum</i> cysts in five sampling lines of Selangor area.	148
Figure 5.7.	Light micrographs of plankton of <i>Alexandrium tamiyavanichii</i> collected from Selangor area.	149
Figure 5.8.	Map showing presences of planktonic cells of <i>Gymnodinium catenatum</i> and <i>Alexandrium tamiyavanichii</i> .	150

CHAPTER 1: GENERAL INTRODUCTION

1.1. General over view of Myanmar fisheries and coastal environments

Myanmar has been one of the world's top ten countries for capture fisheries and the third among Association of Southeast Asian Nations (ASEAN) countries (FAO, 2010). In particular, marine capture fisheries in Myanmar have constantly increased since the late 1990s, and were estimated at over 1.6 million tons in 2008 and over 2 million tons in 2009-2010 (Department of Fisheries, 2010). This constant growth in marine fisheries is a response to the growing efforts of fisheries and market demands, but relies on the high productivity of the coastal environment.

Myanmar coastline stretches about 3,000 km and facing the Bay of Bengal in the west and the Andaman Sea, which is a southwest part of the Bay of Bengal. The Bay of Bengal is a semi-enclosed tropical basin located in the northern Indian Ocean. Since Myanmar has tropical monsoon climate, Myanmar coastal area is influenced by strong monsoon regimes: southwest monsoon (summer monsoon) and northeast monsoon (winter monsoon). In the southwest monsoon season (May-October), the southwesterly wind prevails from the Indian Ocean to the mainland, and which brings moisture-laden air and rain. May is the onset of rainy season, and heavy rain started from June to end of October. During this rainy season, the coastal environment is highly productive with large amount of terrestrial nutrients supplied by river runoffs. In the northeast monsoon season (November-April), the northeasterly trade wind prevails from the continental side to the coastal area. November or December is the onset of dry season, when the northeast trade wind brings cool and dry air. Since November and December are also

just after the rainy season, the coastal water is still rich with terrestrial nutrients. March or April is the end of dry season, when the northeast trade wind brings warm and dry air. At that time, the coastal water has become to be oligotrophic after duration of the long dry period. These monsoon winds strongly influence water movements in the Bay of Bengal and the Andaman Sea. During the southwest wind prevailing, wind-drift currents come from the Indian Ocean to the coastal area, and enhance humid weather. During the northeast wind prevailing, wind-drift currents are in reverse direction, set the nutrient-rich waters off the coast, and lead the coastal environment to be oligotrophic.

Myanmar coastline can be divided into three parts; namely, Rakhine coastal area to the west, Ayeyawaddy Delta in the middle, and Tanintharyi coastal area to the south. The Rakhine coast stretches 740 km, and situates in the western part of Myanmar facing with the Bay of Bengal, and its northern part comprises shallow sea with a chain of islands and some delta areas. The Ayeyawaddy Delta or the Gulf of Mottama (the Gulf of Martaban) stretches about 460 km, and forms mouth of Ayeyawaddy (Irrawaddy) River. The Tanintharyi coastal area stretches about 1,200 km, locating at the southern part, and is composed of 800 offshore islands called Myeik (Mergui) Archipelagos. The coasts facing the Andaman Sea of the Ayeyawaddy Delta region and the Tanintharyi region are especially noteworthy in terms of marine production. Around these regions, rich terrestrial nutrients are supplied from numerous rivers and there are extensive mangrove forests, which cover 425,000 hectares, the third largest mangrove extent in Southeast Asia. Of the total mangrove area in Myanmar, 83 % is located around the Ayeyawaddy and the Tanintharyi regions (Giesen et al., 2006).

The Tanintharyi coast also possesses a considerable extent of coral reefs in the southern part, mostly around the Myeik Archipelagos. The existing of numerous

offshore islands, large mangrove forests and large estuaries support the richness of marine flora and fauna in the Tanintharyi coastal area. Moreover, the offshore islands also protect the mariculture farms along the coastal area from the cyclones. The richest fish diversity and the highest biomass of fish larvae were reported in the East Andaman sea harbor, which is on the Tanintharyi coast, in the Bay of Bengal (Lirdwitayaprasit et al., 2008). As a consequence, the Tanintharyi coastal region is the best fishing ground, with the highest catch rate in Myanmar (SEAFDEC Mission Report, 2006), and the total catch of marine fisheries has shown more than 10 % annual growth since 2005 (Department of Fisheries, 2010).

1.2. Phytoplankton

Photosynthesis is nutritional basis for all higher trophic level consumers. Phytoplankton communities are foundation for marine food chains, and their primary production can be used as a basis for fish catch allowances (Pauly and Christensen, 1995).

Phytoplankton community mainly comprises diatoms and dinoflagellates, and they are the most important primary producers in coastal ecosystem. Meanwhile, some of them, especially some dinoflagellate species, can cause harmful algal blooms (HABs). Modern dinoflagellates comprise over 2,500 species worldwide (Hoppenrath et al., 2009), and approximately 76 species are recognized to form water discoloration and occasional mass-mortalities of fish and producing bio-toxins, which can accumulate in fish and shellfish (Moestrup et al., 2009 onwards, IOC-UNESCO web: <http://www.marinespecies.org/HAB/dinoflag.php>, accessed on 24 December 2012). Harmful algal bloom (HAB) toxins can cause severe illness, with effects ranging from vomiting,

diarrhea, amnesia, paralysis and death (Hallegraeff, 1993). Fishery closures and hygiene countermeasure can also result in considerable economic losses in corresponding fisheries (Hallegraeff, 1993). The impact of HABs on human society has grown with our increased reliance on fisheries and use of coastal oceans for aquaculture (Hallegraeff, 1993). In Southeast Asian region, HAB phenomena have been increased in frequency, widen, and prolonged duration of the occurrences (Fukuyo et al., 2011). A recent increase in HAB incidents is closely linked with increased anthropogenic eutrophication of coastal waters and increased nutrient loading (Hallegraeff, 1993). Such coastal developments have been noteworthy especially in the Southeast Asian countries in last two decades.

1.3. Dinoflagellate cysts

In the marine dinoflagellate community, more than 80 species produce resting cysts. Among them, more than 16 species have been known to cause red-tide and seven species to be toxic (Matsuoka and Fukuyo, 2000). Resting cysts are formed by fusion of gametes (sexual reproduction) in natural plankton population under unfavorable conditions, but also seen during active blooming period. These resting cysts can excyst by the external triggering factors such as temperature increase, light exposure and internal cellular mechanisms (Matsuoka and Fukuyo, 2000). Since dinoflagellate cyst walls are constructed with organic spore-pollenin and calcareous material, the resting cysts in the sediments maintain their morphological features for a long period. Dinoflagellate cysts assemblages in the surface sediment can be a source of recurrence blooms, route for expansion of geographical distribution and toxin source for benthic

shellfish (Matsuoka and Fukuyo, 2000). Dinoflagellate cysts studies are being increased in Southeast Asian countries for HAB monitoring especially paralytic shellfish poisoning (PSP) risks management purpose (Furio et al., 1996; Usup and Azanza, 1998).

1.4. Potential risks in Myanmar fisheries

As mentioned above, currently Myanmar is proud of its high fisheries production due to the high ocean productivities. However, in interview of local fishermen, some of them argued decrease of sizes and amounts of fish catches in the coastal areas. In the statistics, numbers of fishing boats has increase 18 % for last 10 years (from 2000 to 2010), and foreign fishing vessels operating within the Myanmar territorial waters have been estimated 10 times after 2000 (Department of Fisheries, 2010). According to these facts, it might be possible to think that the current fish catch is exceeding over the ocean productivities.

Moreover, coastal development in Myanmar is proceeding at a rapid pace; large numbers of aquaculture facilities are being established for export purposes. Marine finfish culture farms are operating in Tanintharyi coastal areas, shrimp aquaculture farms have increased in coastal areas, and production was over 46,000 tons in 2010 (Department of Fisheries, 2010). Other factories developments and also fisheries industries such as fish processing plants have been increasing in the Myanmar coastal area. These coastal developments, along with the drastic economic progress in Myanmar, might lead to eutrophication of coastal areas and subsequent HAB events.

1.5. Needs to avoid possible risks for Myanmar fisheries

As described above, Myanmar is now or will be soon confronted with difficulties of overfishing or HAB events, which all deteriorate healthy growth of Myanmar fisheries. For estimating fish productivities and risks of HAB, phytoplankton surveys are essential. Despite such concerns, very few phytoplankton studies from the Myanmar coasts have been reported. Early phytoplankton studies in the Andaman Sea, the Bay of Bengal and in the offshore Myanmar waters were conducted by several foreign researchers (Taylor, 1976; Kamba and Yuki, 1980; Boonyapiwat et al., 2007; 2008). Therefore, studies on the recent occurrence of phytoplankton communities, especially from the foremost marine fishery area, Tanintharyi coastal region, are urgently needed.

1.6. General objectives of this study

As mentioned above, primary production is the most important ecological aspect of phytoplankton. In the phytoplankton community, diatoms and dinoflagellates are represented as most important primary producers in coastal ecosystems. At the same time, some phytoplankton species can cause HAB events, which can interrupt coastal fisheries productions. Since phytoplankton community can grant advantages and disadvantages to the coastal fisheries production, phytoplankton studies is required for Myanmar's sustainable fisheries, especially in the Tanintharyi coast, a foremost marine fisheries area in Myanmar. For this requirement, phytoplankton surveys were conducted in the Tanintharyi coastal area for the first time. The basic objective of this study is to understand the phytoplankton species occurrences and to clarify the characters of phytoplankton communities in this region. Another subject of phytoplankton study in

the field is to provide basic information for temporal change of plankton community in future. The next objective is to provide the well understanding of whether the HAB causative dinoflagellates species presence or absence in this region. The further objective is to provide phytoplankton species lists and micrographs for future phytoplankton research in Myanmar.

Not only concerning to plankton communities, dinoflagellate cysts in the bottom sediments were also investigated, since they play an important role in initiation, recurrence and geographical expansion of certain species, especially HAB species. That is, geographical distribution and abundance of cysts in the sediment are very essential information in giving early warning for the presence of toxic species and continuing record of HABs occurrences in a given area, which can interpolate scarce sampling opportunities. In this study, investigations of dinoflagellate cysts in the surface sediments around Kadan Island were conducted for the first time. This is also the first dinoflagellate cyst study from the Andaman Sea area. In addition, an investigation of dinoflagellate cysts from Selangor area, west coast of Malay Peninsula was also conducted. The aim of this investigation was to realize the presence or absence of PSP causative species in the blood cockle cultures ground, and to evaluate PSP risks. Furthermore, since Andaman Sea is directly connected with water body of the Strait of Malacca, the occurrence of HAB species from the Selangor area can be reflected as the recent or future occurrence of in the Myanmar waters, and this information can be useful for future bivalve culture operating system in Myanmar coast. Thus, dinoflagellate study from Selangor area can also provide important basic information not only for this region, and also for Myanmar coast.

CHAPTER 2: PHYTOPLANKTON OCCURRENCES IN THE SOUTHERN MYANMAR COAST

2.1. INTRODUCTION

Phytoplankton community is the primary foundation for marine food chains, and dinoflagellates and diatoms are two of the most important primary producers in coastal ecosystems. As stated in the previous chapter (Chapter 1), fisheries in Myanmar might possibly to face decline of fish resources, due to over-fishing even surpassing the ocean productivities, and environmental deteriorations which can often lead harmful algal blooms. To manage these unwanted events, information of the primary producers or the causative of harmful algal blooms, at least, their occurrence should be known.

However, investigation on phytoplankton community in Myanmar coastal area has been rarely conducted so far. In 1963, the International Indian Ocean Expedition “Anton Bruun” was once conducted, and plankton surveys at the both coastal and open sea areas of the Indian Ocean, including the Bay of Bengal and the Andaman Sea, were performed. Based on these surveys, dinoflagellate species occurring both the Bay of Bengal and the Andaman Sea were reported by Taylor (1976). Another and first phytoplankton survey on the Myanmar coastal territory was conducted by Kamba and Yuki (1980), and they reported a list of microplankton species, including dinoflagellates and diatoms. Phytoplankton species occurring in the Andaman Sea, Bay of Bengal and offshore Myanmar water were also reported by Boonyapiwat et al. (2007; 2008).

The main objective of this chapter is to construct a species list of dinoflagellates and diatoms occurring in the Tanintharyi coastal area, which could be a useful reference

for the future phytoplankton studies in Myanmar, and is to obtain a better understanding on the characteristic of phytoplankton community in this region. Another objective is to construct a species list of dinoflagellate cysts occurring in the surface sediment of the Tanintharyi coast, in order to understand the occurrence of dinoflagellate cysts assemblages for HABs risk management.

Field surveys were carried out thrice in off-coast of Myeik, Tanintharyi Division, which is a foremost marine fishery area in the southern Myanmar. The surveys were also aimed to distinguish phytoplankton communities in the different oceanographic conditions or the season. As described in the Chapter 1, the southwest monsoon season (June-October) is “rainy season” in Myanmar, and long-prolonged heavy rain lead to considerable input of terrestrial nutrients to the ocean. Therefore, at the onset of the season, during the season, and after the season, drastic physical or chemical perturbations can occur and, which can allow drastic changes in the phytoplankton community structure. Seasonal variations in temperature, salinity and nutrients levels are all believed to play a major part in phytoplankton species succession (Hallegraeff and Jeffrey, 1993). Taking these factors into consideration, this study elucidates the modulations in the diatom and dinoflagellate communities in the coastal area and attempts to determine mostly the response of dinoflagellate community to monsoon-influenced seasonal changes.

The first survey was conducted at the onset of rainy season (May, 2010) around the Mali and Kadan Islands. The second survey was at the onset of dry season, namely just after the rainy season (December, 2010) and third survey was at the end of dry season (March, 2012). The latter two surveys were conducted around the Kadan Island.

2.2. MATERIALS AND METHODS

2.2.1. Study area

Mali and Kadan Islands (12°2'-13°3'N latitude, 98°-98°6'E longitude) are among the 800 offshore islands in the Myeik (Mergui) Archipelago, locating along the Tanintharyi coastal region, Tanintharyi Division, in the southern part of Myanmar (Fig. 2.1). These islands are largely influenced by river runoff from the mainland, and open-ocean waters from the Indian Ocean. The east coast of Kadan Island is lined by mangrove forests. We set seven stations around both islands (Fig. 2.1) in the first survey during May 2010, and six stations around Kadan Island (Fig. 2.2) for both December, 2010 and March, 2012 surveys.

2.2.2. Survey

An aim of the first survey in May, 2010 at the seven stations was to visit and cover as wide an area as possible around the two islands (Table 2.1). Therefore, without measuring water depth at the stations by rope, we just concentrated on oblique hauls of a 20- μ m- mesh plankton net from ca. 1-2 m depth. Collected plankton was transferred into 50-ml plastic tubes and immediately fixed with glutaraldehyde at final concentration of 1%.

The second December, 2010 and the third March, 2012 surveys were carried out at six stations around Kadan Island. In these two surveys, phytoplankton samples were collected using vertical hauls of a 20- μ m-mesh plankton net from 1 m above the bottom (Tables 2.2 and 2.3). The samples were immediately transferred to 50-ml bottles,

further concentrated using a 10- μ m mesh to 15-ml total volume, and fixed with glutaraldehyde at final concentration of 1%.

Sediment samples were also collected at 4 stations (Sts. 1, 2, 3 and 6) in the December, 2010 survey and at 3 stations (Sts. 2, 3 and 6) in the March, 2012 survey, using a handy core sampler (TFO gravity corer) (Matsuoka and Fukuyo, 2000), equipped with an inner tube of 1.1 cm diameter to collect dinoflagellate cysts. The upper 2 cm of core samples were preserved with neutralized formalin at final concentration of 10 %.

In the second survey, water temperature and salinity were measured for vertically collected water samples, by using a handy water sampler (No. 15010, The Science Source Co., USA), by using a calibrated mercury thermometer and a refractometer (IS/Mill-E, AS ONE, Japan) respectively. On the third survey, handy-type CTD (Compact-CTD Lite, JFE Advantec, Japan) was used to measure vertical profiles of temperature and salinity (practical salinity unit; PSU) (Tables 2.2 and 2.3). To measure the nutrient concentration, 500 ml of water from appropriate depth were taken by a water sampler at the each station. Nutrient samples were sub-sampled from 500 ml plastic bottles then filtered through cellulose 0.45 μ m syringe filter and were collected into 15 ml bottles, and were stored at -20°C until analysis.

2.2.3. Microscopy for plankton

To identify the diatom species, morphology of cells on valve view and girdle view were observed. Morphological details of the valves like raphe, areolae, labiate process, spines, setae, and chloroplast were carefully observed under inverted light microscope (CKX41,

Olympus, Japan) equipped with phase contrast unit, or inverted DIC (differential interference contrast) microscope (IX71, Olympus). Species identification was made according to literature (Hasle and Syversten, 1997; Hoppenrath et al., 2009).

To identify an armored (thecate) dinoflagellate species, morphological observation was conducted based on overall cell shape, size, characteristics feature of epitheca, hypotheca, sulcus, cingulum, apical and antapical horns and number and arrangement of thecal plates. Among the armored dinoflagellates, species identification in more detail was carried out based on their specific morphological characters in different orders as follow. For order Procoentrales: apical projection, surface of valve and presence and/or arrangement of trichocyst pores; for order Dinophysiales: shape and size of epitheca and hypotheca, cingular and sulcal lists, and ribs of left sulcal list; for order Gonyaulacales: arrangement of thecal plates, torsion of cingulum and shape of apical and antapical spine; for order Peridinales: arrangement of thecal plates and shape of apical and antapical horns. To identify the unarmored (athecate) dinoflagellate species, morphological observation was conducted based on the cell shape, size and the position of nucleus. However, original shape was somewhat deformed. Some species were not preserved. For observing plate tabulations in armored dinoflagellates species, the Calcofluor White M2R was used to stain cellulose theca (Fritz and Triemer, 1985). They were then observed under an inverted microscope (IX71, Olympus) equipped with a fluorescence unit [ultraviolet (UV) excitation light] for M2R visualization and with a DIC unit. Images were captured with a charge-coupled device (CCD) camera (600CL-CU, Pixera, USA).

For detailed observations, small amounts of the plankton samples were subjected to scanning electron microscopy (SEM). The fixed plankton samples were dehydrated

with a graded ethanol series (50, 70, 80, 90, 95, and 100 % each for 5 min), dried in a *t*-butanol dryer (JFD-320, JEOL, Japan), and coated with Pt in a coater (JFC-1600, JEOL). Observations were made under a SEM (JSM-6390LV, JEOL). Species identification was made according to literature (Taylor, 1975; 1976; Abé, 1981; Dodge, 1988; Balech, 1988; 1995; Larsen and Moestrup, 1992; Steidinger and Tangen, 1997; Hoppenrath et al., 2009).

Grouping of stations based on similarity of dinoflagellate species was performed using occurrence data according to Clarke and Warwick (2001). Agglomerative hierarchical cluster analysis was done on the species occurrence (presence/absence). The Bray-Curtis similarity index of species occurrence was used as a clustering metric, and a cluster tree was drawn by group average linkage. Hierarchical cluster analysis was conducted using the PRIMER v6[®] software package (PRIMER-E Ltd., UK).

2.2.4. Sediment sample preparation and microscopy for cysts

Preparation of the sediment samples was based on Matsuoka and Fukuyo (2000); 3-10 g of sediment from each sample was chemically treated with 50 ml of 10% hydrochloric acid and 30 % hydrofluoric acid each for 24 h to remove carbonate and silicate particles, and neutralized with distilled water for one night after each chemical treatment. The samples were then sieved through stainless-steel screens of 100- μ m mesh to remove debris. The refined sediment was sieved by 20- μ m mesh to concentrate the size fraction of dinoflagellate cysts. The sediment remaining on the 20- μ m mesh was transferred into a 50-ml glass container and sonicated for 1 min in a sonic bath (Type USK, AS ONE), and further washed on 20- μ m mesh and finally bottled with 10 ml distilled water. Cysts

were observed under the inverted light microscope with DIC illumination. Dinoflagellate cysts were identified based on the shape of cysts, wall structure, color, ornamentation, and archeopyle type according to relevant literature (Reid, 1977; Harland, 1982; Matsuoka, 1984; 1985; 1987; 1988; McMinn, 1991; Rochon et al., 1999; Matsuoka and Fukuyo, 2000). Dinoflagellate cysts were counted with an inverted light microscope at 200x to 600x magnification. To calculate the water content, about 1 g sediment from each station was weighed, and dried at 70°C for 15 h. Dinoflagellate cyst abundance is expressed as number of cysts g⁻¹ of sediment dry weight.

2.2.5. Nutrient analysis

Nitrate plus nitrite (NO₃+NO₂-N), nitrite (NO₂-N), ammonia (NH₄-N), phosphate (PO₄-P) and silicate (SiO₄-Si) were analyzed using an auto-analyzer (SWAAT, BLTEC, Japan). Nutrient concentrations were determined from the peak heights and calculated using auto analytical software under the analyzer achieved from a five point standard curve prepared in low nutrient artificial seawater matrix.

2.3. RESULTS

2.3.1. Diatom and dinoflagellate species occurrence

Sixty-four species were identified in 40 genera in 26 families of diatoms (Table 2.4) including centric (Fig. 2.3.A-E) and pennate diatoms (Fig. 2.3.F). Centric diatom species were classified into 5 groups (Fig. 2.3.A-E) based on their general morphology according to Hoppenrath et al. (2009): 1) Centric looking diatoms (Fig. 2.3.A), 2) Rod-

like looking and cylindrical chain forming diatoms (Fig. 2.3.B), 3) Chain forming diatom with spines and setae (Fig. 2.3.C), 4) Leaf-like looking diatoms (Fig. 2.3.D) and 5) Not centric-looking diatoms (Fig. 2.3.E). Centric diatoms comprise 45 species under 17 families and pennate diatoms comprise 19 species under 9 families. Among overall diatom species, 57 species in the December survey and 52 species in the March survey were detected. Among them, *Coscinodiscus radiatus* Ehrenberg (Fig. 2.3A. 3), *Cyclotella striata* (Kützing) Grunow (Fig. 2.3A. 9), *Detonula pumila* (Castracane) Gran (Fig. 2.3A. 15), *Lauderia annulata* Cleve (Fig. 2.3A. 17), *Rhizosolenia* spp. (Figs. 2.3B. 1-4), *Guinardia striata* (Stolterfoth) Hasle (Fig. 2.3B. 5-7), *Chaetoceros* spp. (Figs. 2.3C. 3-14), *Bacteriastrum* spp. (Figs. 2.3C. 15-20), *Bellerophon horologicalis* Stosch (Fig. 2.3E. 4-6), *Odontella* spp. (Figs. 2.3D. 2-6), *Eucampia zodiacus* Ehrenberg (Figs. 2.3D. 11,12), *Thalassionema* spp. (Figs. 2.3F. 2-4), *Navicula directa* (Smith) Ralfs (Fig. 2.3F. 5), *Meuniera membranacea* (Cleve) Silva (Fig. 2.3F. 7), *Pleurosigma normanii* Ralfs (Fig. 2.3F. 9), *Surirella fastuosa* Ehrenberg (Fig. 2.3F. 11,12) *Entomoneis paludosa* (Smith) Reimer (Fig. 2.3F. 16), *Pseudo-nitzschia caciantha* Lundholm, Moestrup & Hasle (Fig. 2.3F. 18) and *Nitzschia* spp. (Figs. 2.3F. 19-21) were commonly detected in both December and March surveys. In the December survey, massive diatoms blooms were detected with high density of *Bacteriastrum* spp. (50,500 cells L⁻¹) and *Chaetoceros* spp. (40,500 cells L⁻¹) as dominant species.

In the dinoflagellate species occurrence, 100 species were identified in 22 genera of 14 families of dinoflagellate (Table 2.5; Figs. 2.4 A-J). In overall dinoflagellate species observed, six unarmored species (Fig. 2.4.J) and 94 armored species (Figs. 2.4A-I) were comprised. Among armored dinoflagellates, four *Prorocentrum* species in order Prorocentrales (Fig. 2.4.A), seven *Dinophysis* species, six *Ornithocercus* species

and one *Metadinophysis* species in order Dinophysiales (Figs.2.4.B,C), 13 *Gonyaulax* species, one *Lingulodinium* species, two *Alexandrium* species, two *Pyrophacus* species and eight *Ceratium* species in order Gonyaulacales (Figs. 2.4.D,E), two species of *Peridinium*, 22 species of *Protoperidinium* species, one species of *Preperidinium*, one species of *Oblea*, two species of *Diplopelta*, one species of *Podolampas*, one species of *Goniodoma*, two species of *Scrippsiella*, and two species of *Heterocapsa* in order Peridinales (Figs. 2.4.F-I) were listed. Among unarmored dinoflagellates (Fig. 2.4.J), one *Balechina* species and two *Gymnodinium* species in order Gymnodinales, two *Pyrocystis* species in order Pyrocystales and one *Noctiluca* species in order Noctilucales. Since all samples were fixed with formalin or glutaraldehyde, very few unarmored dinoflagellate species was detected. Due to the chemical fixation, some unarmored dinoflagellates might be loss or deform. In the overall dinoflagellate species listed from this study, 22 species have been reported to be cyst-forming. In addition, several potentially harmful species were found: Toxin-producing species that can cause shellfish poisonings including paralytic shellfish poisoning (PSP) such as *Alexandrium tamiyavanichii* Balech (Fig. 2.4D. 26,27), *Gymnodinium catenatum* Graham (Fig. 2.4J. 8,9), diarrhetic shellfish poisoning (DSP)-causative species such as *Dinophysis caudata* Saville-Kent (Fig. 2.4B. 1-3), *D. miles* Cleve (Fig. 2.4B. 4-7), and *D. rotundata* Claparède & Lachmann (Fig. 2.4B. 18,19), and yessotoxin (YTX)-producing species *Gonyaulax spinifera* (Claparède & Lachmann) Diesing (Figs. 2.4D. 14,15) and *Lingulodinium polyedrum* (Stein) Dodge (Fig. 2.4D. 21-23) [these toxic species are listed on the Intergovernmental Oceanographic Commission (IOC)-United Nations Educational, Scientific, and Cultural Organization (UNESCO) website: <http://www.marinespecies.org/HAB/dinoflag.php>, accessed on 24 December 2012]. We also

found several red-tide forming species such as *Alexandrium affine* (Inoue & Fukuyo) Balech (Fig. 2.4D. 24,25), *Gonyaulax polygramma* Stein (Fig. 2.4D. 7-9), *Scrippsiella trochoidea* (Stein) Balech ex Loeblich III (Fig. 2.4I. 23), *Prorocentrum* spp. including *P. sigmoides* Bohm (Fig. 2.4A. 4-7), *P. micans* Ehrenberg (Fig. 2.4A. 1-3), *P. rathymum* Loeblich, Sherley & Schmidt (Fig. 2.4A. 8-10), *P. shikokuense* Hada ex Balech (Fig. 2.4A. 11-13), and *Ceratium* spp. including *C. furca* (Ehrenberg) Claparède & Lachmann (Fig. 2.4E. 10-13) and *C. fusus* (Ehrenberg) Dujardin (Fig. 2.4E. 7,8) (Fraga et al., 1988; Okaichi, 1997). Rare dinoflagellate species belonging to the genus *Metadinophysis* (Nie and Wang, 1941) was found in all surveys (Fig. 2.4B. 20-26). This is dissimilar to the sole species of *Metadinophysis*, *M. sinensis* Nie & Wang, from its slender lateral view of the hypotheca. This species was previously recorded from Ben Tre Province (South Vietnam coast) in May and February by Nguyen (2009) as *Metadinophysis* sp. 1. As it is still possible to think that the differences in hypothecal shape may be within-species variation, we tentatively treat it here as *Metadinophysis* cf. *sinensis*.

Aside from these neritic species, oceanic species such as *Ornithocercus* spp. (Fig. 2.4C) and *Podolampas bipes* Stein (Fig. 2.4I. 15-17) were found simultaneously at some stations in the May survey and *O. magnificus* was found in the March survey. This diverse species composition indicated a mixture of oceanic and neritic waters in this area.

From the first survey (May, 2010), cluster analysis of seven stations based on the occurring dinoflagellate species (non-quantitatively) showed one distinct group composed of four stations (Sts. 1, 4, 5 and 7) at 35.95% similarity level, apart from Sts. 2, 3, and 6 (Fig. 2.5). In the second (December, 2010) and third (March, 2012) surveys, cluster analysis was conducted on six stations based on the occurring dinoflagellate

species. While no distinct group of similarity was showed in the second survey (Fig. 2.6), the third survey showed one distinct group composed of four stations (Sts. 1, 4, 5 and 6) at 53.27% similarity level, apart from Sts. 2 and 3 (Fig. 2.7).

In December, maximum cell density was recorded at St. 2, as more than 220,000 cells L⁻¹ in diatom species (Fig. 2.8). Even in the March survey (Fig. 2.9), maximum abundance was recorded by diatoms, but the density was slightly lowered to as 18,100 cells L⁻¹. On the contrary, dinoflagellate abundances were higher in March (Fig. 2.11), and average of the six stations was estimated as 1,075 cells L⁻¹, while that in the December was lower (516 cells L⁻¹) (Fig. 2.10). The effloresce of dinoflagellate and fade of diatoms in March are also seen in the numbers of species occurrence: In the December samplings, while 26 dinoflagellate species were counted, much diverse species as high as 67 species were in March (Figs. 2.10 and 11). Among the stations, there was less diatom abundance at St. 4 in both December and March (Figs. 2.8 and 9). That of dinoflagellate in the March sampling was also lowest among the station. Species diversity of this station was lesser in diatom on December. These were probably due to flushing of ocean current in the channel near the St. 4. However, dinoflagellate species were rather diverse at this station on the March sampling (Fig. 2.11), probably may derived from outer ocean, which can carry oceanic species. Indeed, at St. 4, the oceanic species of *O. magnificus* was detected.

2.3.2. Cysts occurrence

At least 44 cyst types were recorded (Table 2.6; Figs. 2.12A,B) based on current paleontological taxonomy (Reid, 1977; Harland, 1982; Matsuoka, 1984; 1985; 1987;

1988; McMinn, 1991; Rochon et al., 1999; Matsuoka and Fukuyo, 2000). Among these 44 types, 22 species could be identified to species level in 11 genera. Total 12 autotrophic cyst types and 32 heterotrophic cyst types were listed from two surveys. The samples were generally dominated by the cysts of heterotrophic species as 80.88 % in December and 60.73 % in March (Table 2.7, Fig. 2.13a,b), mainly *Protoperidinium* spp. including different paleontological genera such as *Brigantedinium* spp. (Figs. 2.12B. 2-4), *Selenopemphix* spp. (Figs. 2.12B. 12-14), *Stelladinium* spp. (Figs. 2.12B. 15,16; 2.12C. 1,2) and cyst forms of *Protoperidinium* spp. (Figs. 2.12C. 5-12). Among these *Protoperidinium* species, the round brown cysts of *Protoperidinium avellanum* (*Brigantedinium cariacense*) (Fig. 2.12B. 4), the spiny round brown cysts of *Protoperidinium* sp. 14 and the brown peridinioid cysts of *Protoperidinium* sp. 15 (new form 1) (Fig. 2.12C. 5,6) were detected as common cyst types throughout the stations. Cysts of *P. avellanum* were found as a dominant species in St. 1 (3.99 cysts g⁻¹), St. 2 (7.62 cysts g⁻¹), and at St. 3, *Protoperidinium* sp. 15 (new form 1) was found to be the dominant species with density of 4.97 cysts g⁻¹ in the December survey. Other heterotrophic species also included a diplopsalid group identified as *Dubridinium caperatum* Reid (Fig. 2.12C. 13,14) and *Oblea acanthocysta* Kawami, Iwataki & Matsuoka (Fig. 2.12C. 15) and one undescribed form (Fig. 2.12C. 16).

Relatively low proportions of 12 autotrophic species including *Gymnodinium catenatum* (Fig. 2.12A. 7), *Alexandrium* cf. *tamiyavanichii*, *Alexandrium affine* (Fig. 2.12A. 1), *Gonyaulax scrippsae* Kofoid (*Spiniferites delicatus*) (Fig. 2.12A. 2) and *Gonyaulax spinifera* (*Spiniferites ramosus*) (Fig. 2.12A. 3), *Lingulodinium polyedrum* (Stein) Dodge (*Lingulodinium machaerophorum*) (Fig. 2.12A. 4) were detected. The highest densities of autotrophic cysts (9.99 cysts g⁻¹) were found at St. 1 in the

December survey and (11.45 cysts g⁻¹) were found at St. 2 in the March survey. Low density of autotrophic cyst comprising only one species of *A. affine* (2.85 cysts g⁻¹) was found at St. 2 in the December survey, however highest density of autotrophic cyst (11.45 cysts g⁻¹) comprising *A. affine*, *Gonyaulax spinifera*, *Gymnodinium catenatum*, *G. impudicum* and *Scrippsiella* sp. were found at same station in the March survey. We should note that identification of *A. affine* from cyst morphology is provisional because some other *Alexandrium* species can also produce spherical cysts, as shown in (Fig. 2.12A. 1). Meanwhile, presence of *A. affine* cyst in the sediments was highly possible because the vegetative cells were found from the same sampling station. Cysts of *Pyrodinium bahamense* Plate (*Polysphaeridium zoharyi* (Wall)), PSP producer, were not observed.

2.3.3. Nutrients

The vertical distribution of nutrients concentrations were listed in Table 2.2 for December, 2010 and Table 2.3 for March, 2010. Also, the differences of those in the surface waters were depicted in Figs. 2.8-2.11. The nitrite plus nitrate concentration ranged between less than the detectable limit (DL; ca. 0.05 µM) to 3.23 µM in the December survey and < DL to 4.33 µM in the March. Ammonia concentrations ranged between undetectable < DL to 20.43 µM in December and < DL to 0.41 µM in March. The ammonia distribution in the December survey was relatively higher than that in the March survey. Low concentration of phosphate showed a similar pattern in both surveys; ranged between 0.14 µM to 0.71 µM in December and ranged between 0.21 µM to 0.64 µM in March. In overall stations, the mean N:P ratio is 15.9:1 in the

December survey and 4.7:1 in the March survey. Silicate concentration ranged between 6.98 μM to 15.4 μM in December and 8.61 μM to 17.69 μM in March.

2.4. DISCUSSION

2.4.1. Species diversity in pre- and post-rainy season: overview

In this study, total thrice surveys were conducted: twice in the pre-rainy season (May 2010 and March 2012) and once in the post-rainy season (December 2010). In the post-rainy season survey, diatoms were much abundant than other two surveys in the pre-rainy season, and total 57 species were observed on this survey. On the other hand, lesser diatoms' abundance and diversity were found in the March survey: total 52 species were recorded.

For dinoflagellates, 57 and 67 species were recorded respectively in the pre-rainy season in the May 2010 and March 2012 surveys, while just 26 species were in the post-rainy season in December 2010. It should be noted here that plankton-net hauling was performed in different manners: oblique in the May survey in 2010 and vertically in the December and March surveys in 2010 and 2012. Nonetheless, the corresponding area is shallow and the water depths are approximately less than 5 or 6 m (St. 3) or even less than 3 m (Sts. 1, 2 and 6) except at Sts. 4 and 5. Therefore, it is assumed that the differences of species diversity between the pre- and post-rainy seasons were not derived from the sampling manners but rather from the significant differences of climate or oceanographic systems.

Diverse occurrences of dinoflagellates in the pre-rainy season are probably explained with oligotrophic condition in the late dry season. Another reason would be transportations of oceanic species by the currents: In the two surveys conducted in pre-rainy season, maximum species number of 44 was detected in St. 2 in the May (2010) survey. In the March survey in 2012, while samplings were not conducted as wide area as the previous survey, maximum species number of 43 was detected in St. 3 (Fig. 2.11). These two stations face to the open ocean, rather than the continental coast. Since the Myanmar coasts are affected by southwest monsoon from May to October, wind stress and surface current from southwest bring oceanic water of southern part of the Bay of Bengal to the Myanmar coast. These two surveys were conducted just before an onset of the rainy season from June, and therefore beginning of southwest wind brought oceanic waters toward the coast. At St. 2 in the first survey, oceanic and neritic waters probably mixed, explaining the coexistence of diverse oceanic species (e.g. *Ornithocercus* spp., *Podolampas bipes*) and neritic species (e.g. *Prorocentrum* spp., *Gonyaulax* spp. and *Alexandrium tamiyavanichii*). In the March survey in 2012, *Ornithocercus magnificus* was found also at St. 4 and Sts. 1 and 6; the latter two stations located inner side of the Island. It indicates the mixing of oceanic water probably reached to the entire coastal area until March. Interestingly, a red-tide of neritic *Prorocentrum* spp. was detected near the St. 6 (see Chapter 4), indicating typical neritic and oceanic characters can coexist in this season.

By contrast, in the survey conducted in the post-rainy season (December, 2010), nutrient-rich terrestrial water had flooded into the coastal areas from prolonged rainy weather during the rainy season, and a shift from southwest winds to northeast winds in December may have carried these terrestrial waters to the entire coastal area. This

explains why diverse diatom species, rather than dinoflagellates, were detected in this survey. The largest number of 19 dinoflagellate species (Fig. 2.10) was found at St. 3 (Fig. 2.2), located opposite the mainland coast, and the smallest number of species at Sts. 1 and 2, facing the rivers from the mainland, at where red-tide of diatoms were detected. Usually diatoms and dinoflagellates compete each other; the former prefer nutrient-rich, terrestrial influenced waters, and after senescence of diatom blooms, dinoflagellates can occur.

This diatom-dinoflagellate competition was also clearly demonstrated in the data obtained in the December and March surveys. Seasonally, while the number of diatoms species was similar in these two surveys, dinoflagellate abundance (Fig. 2.9) and diversity (Fig. 2.11) were higher in the March survey. Spatially, lowest diversity of dinoflagellate composing only neritic species were found at St. 2, at where intensive river runoffs influence and characterized by the massive diatom blooms and lowest salinity in the December survey. Nonetheless, while the climate and oceanographic structure can be understood by seeing dinoflagellate diversity as well, it can be said that diatoms are dominator in any season and their densities were always over 90%.

2.4.2. Characters of species occurrences

(Notes on each species)

Neritic cosmopolitan species of *Prorocentrum micans*, *Dinophysis caudata*, *Ceratium furca*, *C. fusus* and *Scrippsiella trochoidea* were found in the both seasons. Another cosmopolitan species found in the both seasons was *Gonyaulax spinifera*, which is reported to be thermo-tolerant and prefer warmer waters (Taylor, 1987). Other than *G.*

spinifera, diverse *Gonyaulax* species were found in the May and March survey. In the cruise of “Anton Bruun” conducted at Bay of Bengal in 1963 (Taylor, 1976), 20 species of *Gonyaulax* were found in March through June. In other studies conducted at post-rainy season in the Bay of Bengal, Kamba and Yuki (1980) did not recorded *Gonyaulax* species, and three species were recorded in Boonyapiwat’s study (2008), and one species were recorded from west coast of India (D’Costa et al., 2008). Among the total occurrence of 10 species in our study, six species (i.e. *G. digenesis*, *G. kofoidii*, *G. polygramma*, *G. scrippsae*, *G. spinifera* and *G. turbynei*) are coincided to Taylor’s study (1976), and *G. spinifera* matched to Boonyapiwat’s study (2008).

Interestingly, *Prorocentrum rhathymum* was detected at St. 6 in the May survey. This species widely distributes in tropical to temperate waters and potentially be epibenthic. Although specimens were not quantitatively collected in the May survey, many cell-clumps of *P. rhathymum* were observed as dominant species in the St. 6 sample (Fig. 2.4A. 8-10). Morphology of *P. rhathymum* and *P. mexicanum* was taxonomically confused due to overlapping morphological characters. The unique characters of *P. rhathymum* different from *P. mexicanum* is absent of pyrenoid, lack of poroids and ornamentation of a row of six to seven trichocyst pores in the right valve of periflagellar area. It should be noted here that in the previous published report (Su-Myat et al., 2012), this species was identified as *P. mexicanum*, but in further DNA analysis conducted in this work (Chapter 3), the species was finally identified as *P. rhathymum*. In the March survey in 2012, red-tide of *P. rhathymum* was detected near the St. 6 (Fig. 2.2) and this species was also detected in St. 2, which is the same station of St. 6 in the May survey (at where cells-clumps of *P. rhathymum* were detected). Therefore, this area should be regarded to be suitable for the red-tide for coastal dinoflagellate species.

The oceanic species such as *Ornithocercus* spp. and *Podolampas bipes*, which were found at Sts. 2 and 4 in the May survey in 2010 and *O. magnificus*, which was found in the March survey in 2012, at Sts. 1, 4 and 6, were probably transported from the offshore seas due to the prevailing southwest wind. These species were also recorded, including nine species of *Ornithocercus*, in the cruise of Anton Bruun (Taylor, 1976). In his report, six species were found from northeast and east part of the Bay of Bengal and the Andaman Sea. The occurrences of *O. magnificus* Stein, *O. quadratus* Schütt, *O. steinii* Schütt and *O. thumii* (Schmidt) Kofoid & Skogsberg in the current study coincided with Taylor's record.

Through the whole surveys, 41 species of *Protoberidinium* were dominating in this area. They were especially abundant and diverse at St. 2 in May 2010, St. 3 in December 2010 and St. 4, in March 2012, all of which sites exposed to the open ocean. Since *Protoberidinium* species are nonphotosynthetic, their occurrence is often associated with blooms of prey organisms such as diatoms and dinoflagellates (Bralewska and Witek, 1995). Other than these two prey organisms, they may feed on bacteria or nanoflagellates (Naustvoll, 2000; Sherr and Sherr, 2002). The occurrence of diverse *Protoberidinium* species at these three stations might be associated with bacterial concentrations or organic matters supplied by upwelling (Taylor, 1987). Among the *Protoberidinium* species listed in this study, 19 species were previously reported from the Bay of Bengal and the Andaman Sea (Taylor, 1976), four species from the Bay of Bengal (Boonyapiwat et al., 2008), six species from Phuket, Thailand (Taylor, 1975) and four species from west coast of India (D'Costa et al., 2008).

For other species, especially for harmful species, detail discussions will be opened in the separate chapter (Chapter 3), with referencing Myanmar fisheries. For

unarmored dinoflagellates, the possibility for species losing was high by using only fixative samples for microscopic observation. It was noticeable point to detect all species of unarmored dinoflagellates, hence, which comprised many harmful species such as *Karenia* spp., *Cochlodinium polykrikoides* etc.

(Species similarities)

The dendrogram of species similarity in the May survey showed one distinct group including Sts. 1, 4, 5, 7 at 35.95 % similarity level (Fig. 2.5). The group comprised a total of 31 species including nine heterotrophic species. These stations are located in the middle part of the surveyed area (Fig. 2.1) and may largely receive terrestrial nutrients from the mainland coast. The outgroup of the dendrogram consisted of Sts. 2, 3 and 6. St. 2 faces to the open sea and is not protected by offshore islands. Therefore, this station is probably affected by the southwest oceanic current at the onset of rainy season, and thus showed diverse oceanic species. St. 6 showed small number of species occurrences (11 species); however, this is distinct in the dendrogram because of the lack of oceanic species and the presence of two unique coastal species, *Prorocentrum rhathymum* and *Metadinophysis* cf. *sinensis*. St. 6 is surrounded by numerous islands or islets and is influenced by estuarine water from mangrove forests on the east coast of Kadan Island. Only five species were recorded at St. 3, and the data may be insufficient to position the station adequately in the dendrogram. The dendrogram of species similarity in the December survey in 2010 showed no distinct group, due to less dinoflagellate species detected (Fig. 2.6). The dendrogram of species similarity in March 2012 showed one distinct group including Sts. 1, 4, 5 and 6 at 53.27% similarity

level (Fig. 2.7). The group comprised a total of 59 species including 37 heterotrophic species. These stations locate at the inner and upper part of study area (Fig. 2.2) and may largely receive terrestrial nutrients from the mainland coast and mangrove forests, which locate along the inner coast of Kadan Island. Moreover, the occurrence of the oceanic species, *O. magnificus* in Sts. 1, 4 and 6 indicated the mixing of oceanic water seems to be extended to the inner coastal area in March 2012. The outgroup of the dendrogram consisted Sts. 2 and 3, the latter station faces to the open sea and former station locates at the lower part of study area, which are protected by offshore islands. However at the St. 3 is facing to the open sea, any oceanic species was not detected in the March survey in 2012.

(Environmental characters and related phytoplankton occurrences)

In the December survey in 2010, the diatoms blooms were detected near St. 2. The low salinities in the surface waters of Sts. 1 and 2 and lowest silicate concentration (6.98 μM) were detected in St.2 (Fig. 2.10). It is possible that the nutrients transported by the river runoffs were biologically consumed by diatoms. As mentioned in previously, in the March survey in 2012, the dinoflagellates bloom, more specifically *Prorocentrum* bloom, was detected near St. 6. The high salinity (32.42) and lowest nutrients were detected at the surface water of St. 6. This suggests that, in addition to the prolonged dry season until March, nutrient concentrations were extensively consumed by dinoflagellates. The silicate concentration in St. 6 showed as high level as other stations (Fig. 2.11), since the dinoflagellate species do not use silicate for their growth.

2.4.3. Dinoflagellate cyst assemblage

Dinoflagellate cyst concentrations from Sts. 2 and 3 in the December survey in 2010 and from St. 2 in the March survey in 2012 were relatively high, and the bottom environment of these stations was characterized by finer and oxygen-rich (dark-brown-color clay) conditions. This was due to high clay content, which suggests higher cyst concentration (Azanza et al., 2004). Sedimentation rates of tropical regions could be correlated with low cyst concentrations in the surface sediment of Sts. 1 and 6 in the December survey and Sts. 6 in the March survey, at where sediment discharge is high from river runoff from the mainland coast.

In this study, 44 different cyst types including 12 autotrophic and 32 heterotrophic types were recorded. High diversities of heterotrophic cysts were characteristic of the Myanmar coast. In this study, the heterotrophic taxa were mainly composed by one *Polykrikos* species and large diversities of the Protoperidiniaceae. Radi and Vernal (2004) reported that the Peridinales included *Brigantedinium* spp., *Quinquecuspis concreta*, *Islandinium minutum*, *Votadinium* spp., *Selenopemphix* spp., and *Polykrikos kofoidii*, which can be positively linked with high productivity in the northeastern Pacific margin. Based on other studies of dinoflagellate cyst occurrences, especially associated with eutrophication (Matsuoka, 1999; Harland et al., 2006), the existence of high abundance of heterotrophic cysts (80.88 % in the December survey; 60.73 % in the March survey) in this survey area indicates high-nutrient conditions and an abundance of prey organisms.

Among the autotrophic species, spherical *Alexandrium* cysts were not restricted only to the inner coastal stations but also distributed at offshore stations in both surveys.

Based on the morphology of cysts and the finding of vegetative cells of *A. affine*, we assumed that these spherical *Alexandrium* cysts may probably be *A. affine*. In other studies conducted on the west coast of India (D'Costa et al., 2008), *Alexandrium* cf. *affine* was reported in May. Finding of higher density of autotrophic cysts in the March survey, suggests as the newly encysted assemblages which may reflect the plankton population during dry season. Cysts of *Gymnodinium catenatum* were found in low number (0.62 cysts g⁻¹ in the December survey at St. 3; 0.60 cysts g⁻¹ in the March survey at St. 2) (Table 2.7). Although vegetative cells of *G. catenatum* were not found in the December survey, 4-8 cells long chain of *G. catenatum* were detected in Sts. 1 and 3 in the March survey. Boonyapiwat et al. (2007) recorded moderate cell densities of *G. catenatum* (566 cells L⁻¹) in Myanmar water. Cysts of *G. catenatum* and *Gymnodinium* cf. *catenatum* were also recorded from the southwest coast and the west coast of India (Godhe et al., 2000; D'Costa et al., 2008).

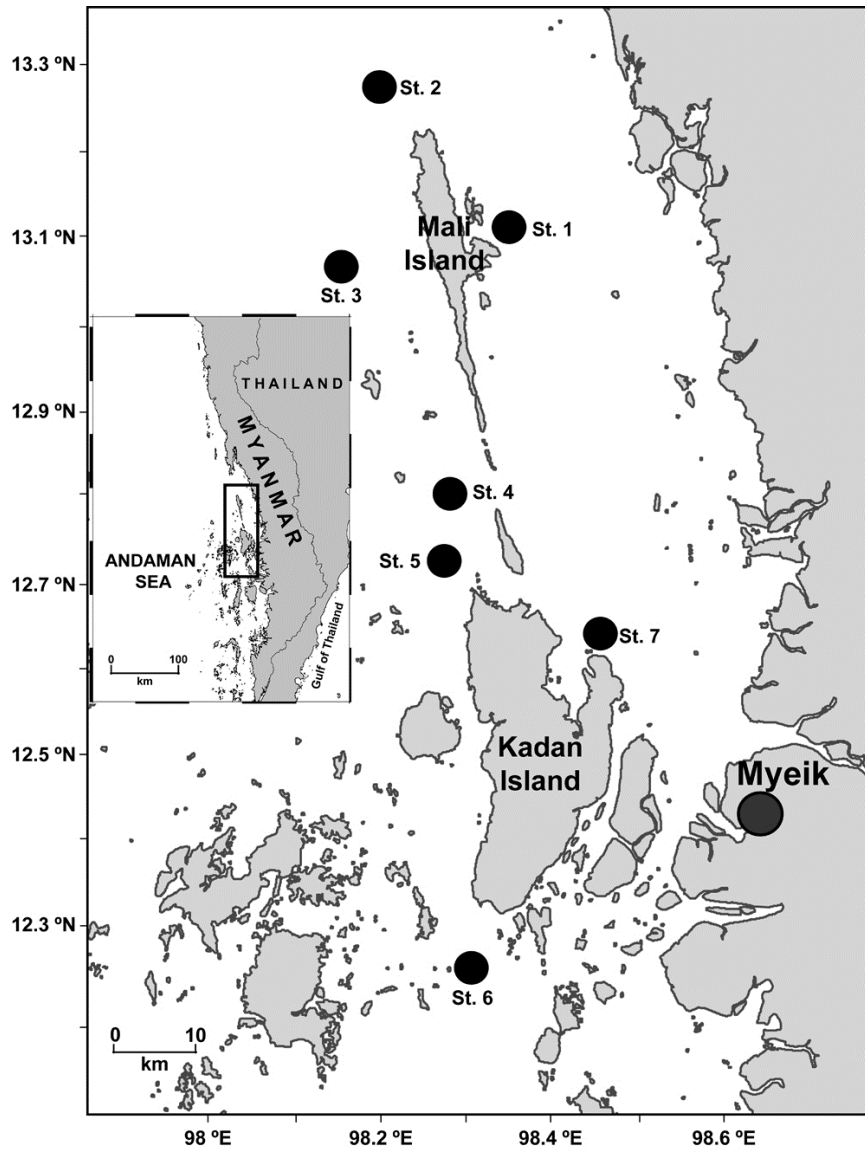


Fig.2.1. Map showing sampling locations around Mali and Kadan Islands, southern Myanmar coast, for the first survey in May, 2010.

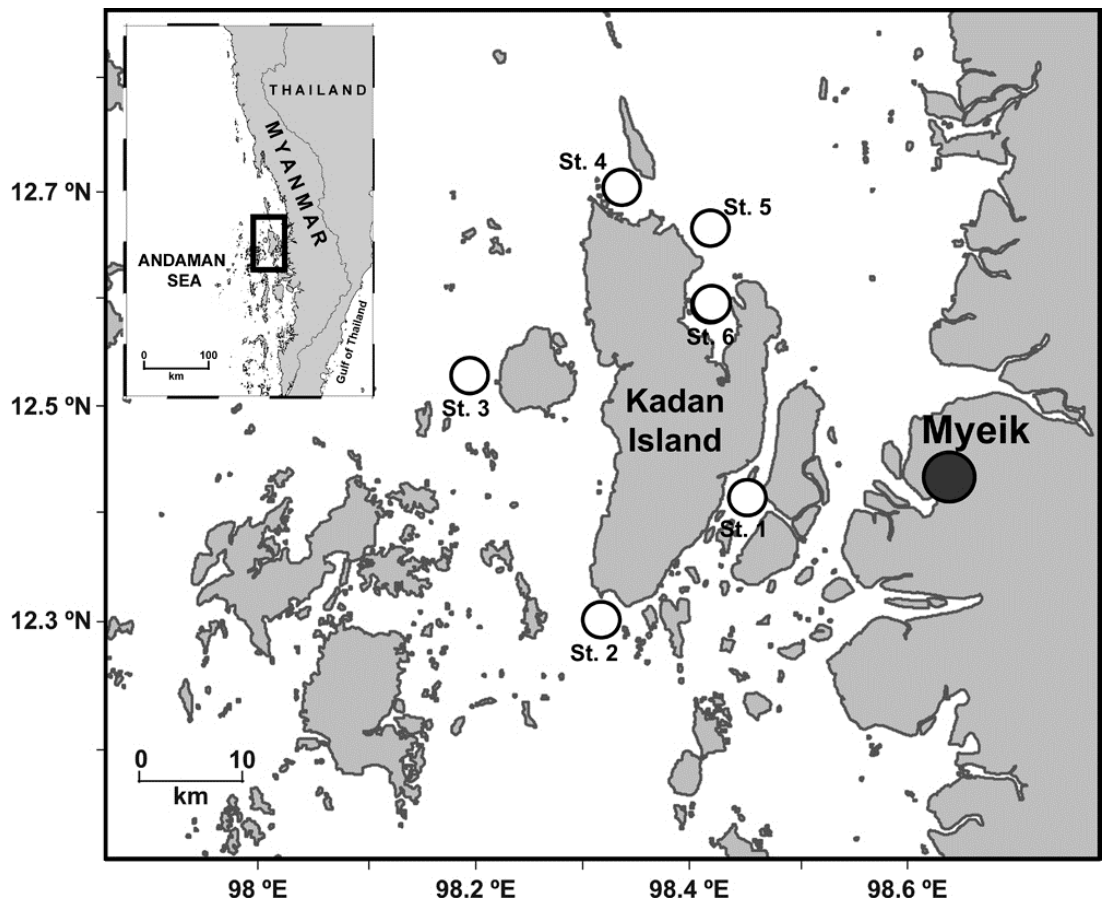


Fig.2.2. Map showing sampling locations around Kadan Island, southern Myanmar coast for the second survey in December, 2010 and third survey in March, 2012.

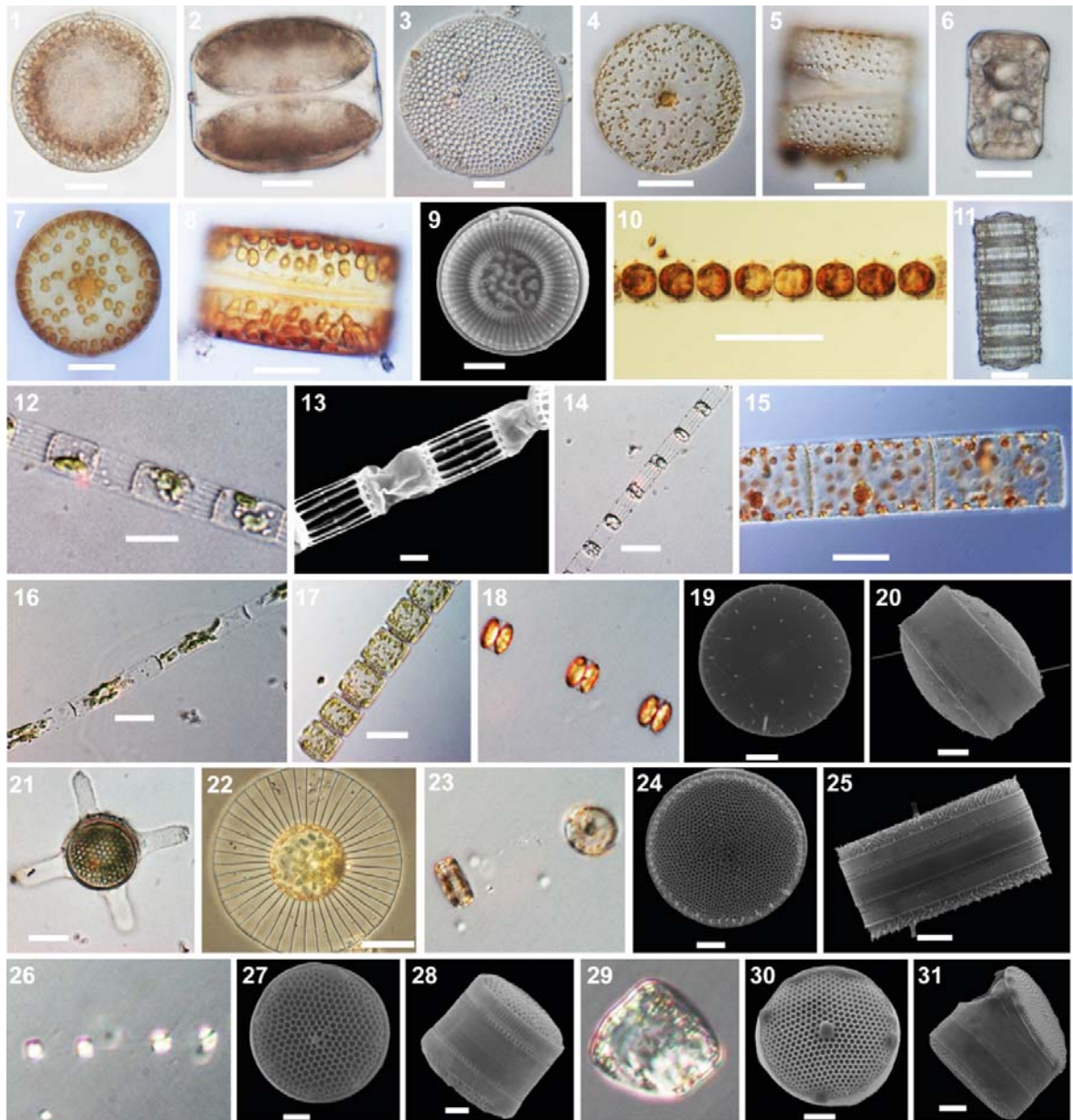


Fig.2.3A. Light and scanning electron microscope (SEM) micrographs of centric looking diatoms. **1,2** *Coscinodiscus concinnus*, **3** *Coscinodiscus radiatus*, **4,5** *Coscinodiscus wailesii*, **6** *Actinocyclus octonarius*, **7,8** *Roperia tessellata*, **9** *Cyclotella striata*, **10** *Melosira moniliformis*, **11** *Paralia sulcata*, **12,13** *Skeletonema costatum*, **14** *Skeletonema menzelii*, **15** *Detonula pumila*, **16** *Detonula confervacea*, **17** *Lauderia annulata*, **18-20** *Porosira glacialis*, **21** *Planktoniella blanda*, **22** *Planktoniella sol*, **23-25** *Thalassiosira eccentrica*, **26-28** *Thalassiosira partheneia*, **29-31** *Thalassiosira oestrupii*. Scale bars = 20 μ m.



Fig.2.3B. Light and SEM micrographs of rod-like looking and cylindrical chain forming diatoms. **1** *Rhizosolenia styliformis*, **2** *Rhizosolenia setigera*, **3,4** *Rhizosolenia imbricata*, **5-7** *Guinardia striata*, **8** *Leptocylindrus danicus*. Scale bars = 20 μ m.

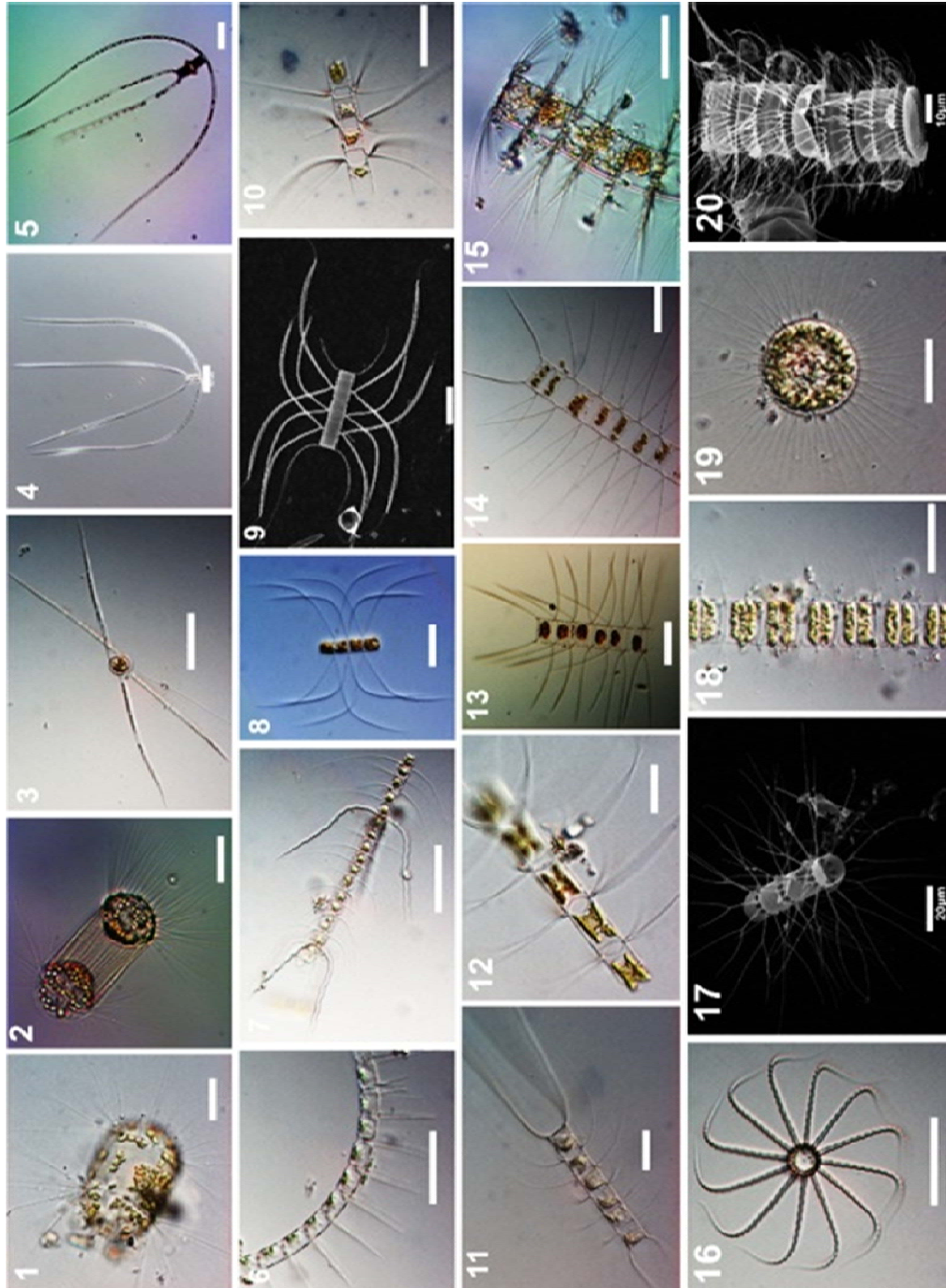


Fig.2.3C. Light and SEM micrographs of chain forming diatoms with spines and setae. **1,2** *Corethron criophilum*, **3** *Chaetoceros danicus*, **4,5** *Chaetoceros peruvianus*, **6** *Chaetoceros curvisetus*, **7** *Chaetoceros compressus*, **8,9** *Chaetoceros diversus*, **10** *Chaetoceros furcellatus*, **11** *Chaetoceros decipiens*, **12** *Chaetoceros mitra*, **13,14** *Chaetoceros lorenzianus*, **15-17** *Bacteriastrium furcatum*, **18-20** *Bacteriastrium hyalinum*. Scale bars = 20 µm.

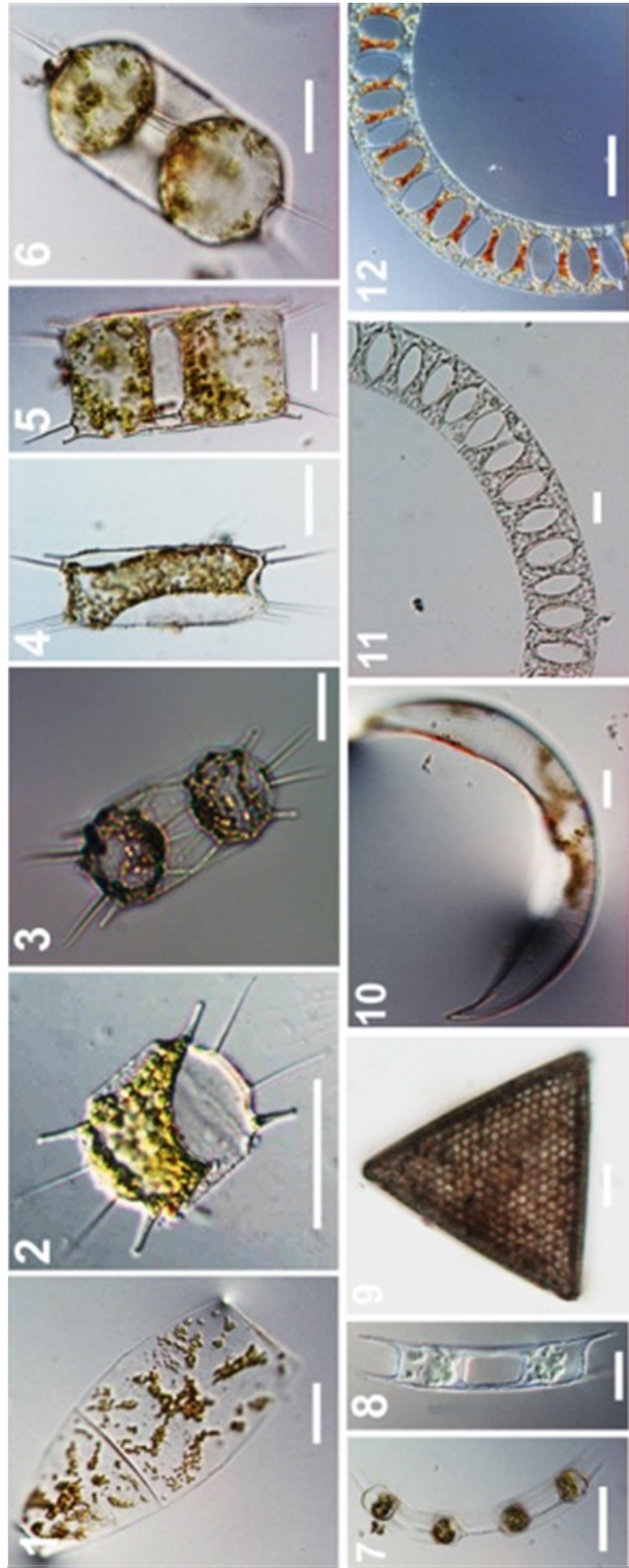


Fig.2.3D. Light and SEM micrographs of leaf-like looking diatoms. **1** *Helicotheca tamesis*, **2,3** *Odontella mobiliensis*, **4-6** *Odontella sinensis*, **7,8** *Hemiaulus hauckii*, **9** *Triceratium favus*, **10** *Neocalyptrella robusta*, **11,12** *Eucampia zodiacus*. Scale bars = 20 μ m.

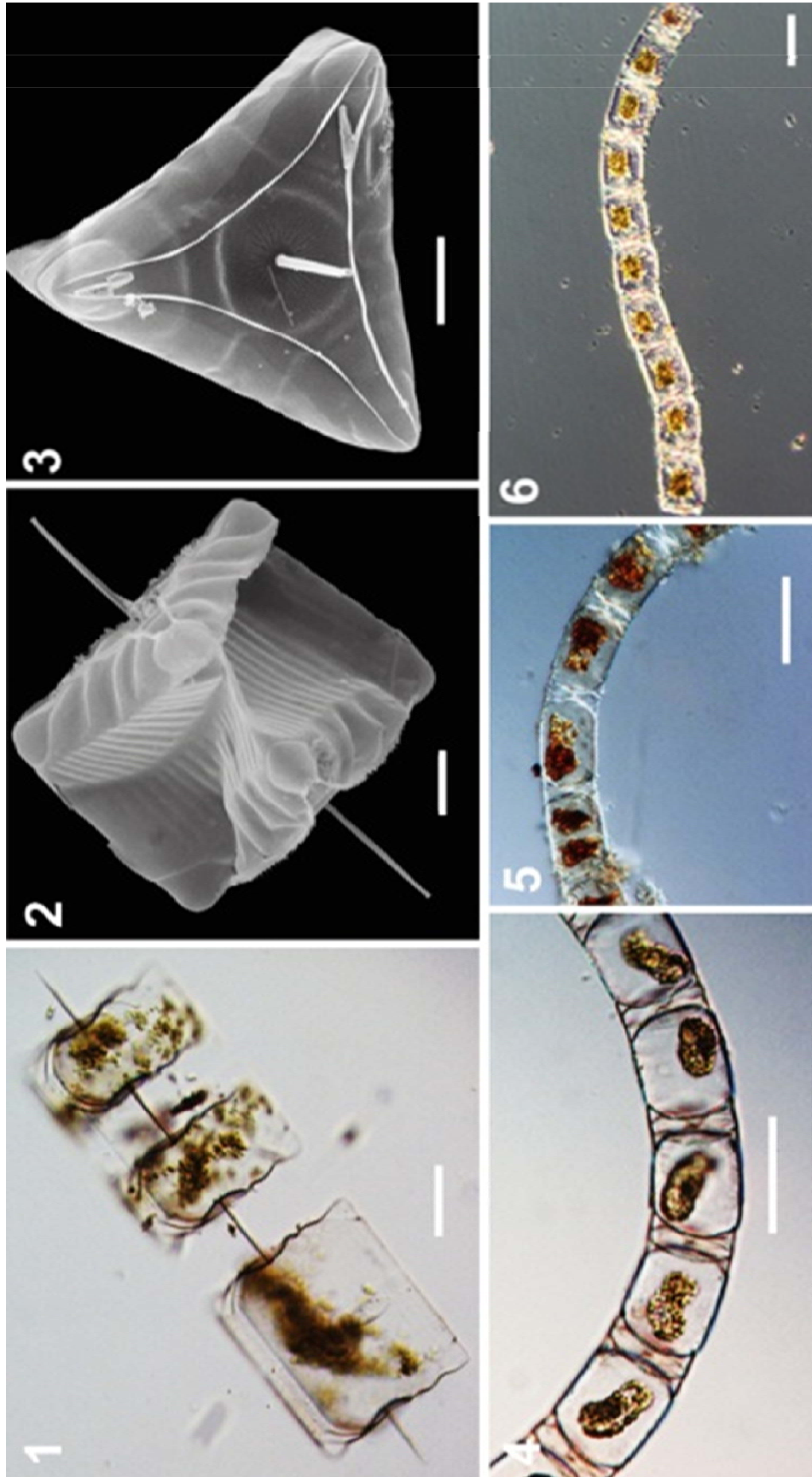


Fig.2.3E. Light and SEM micrographs of not centric-looking diatoms. **1-3** *Ditylum sol*, **4-6** *Bellerochea horologicalis*. Scale bars = 20 μm .

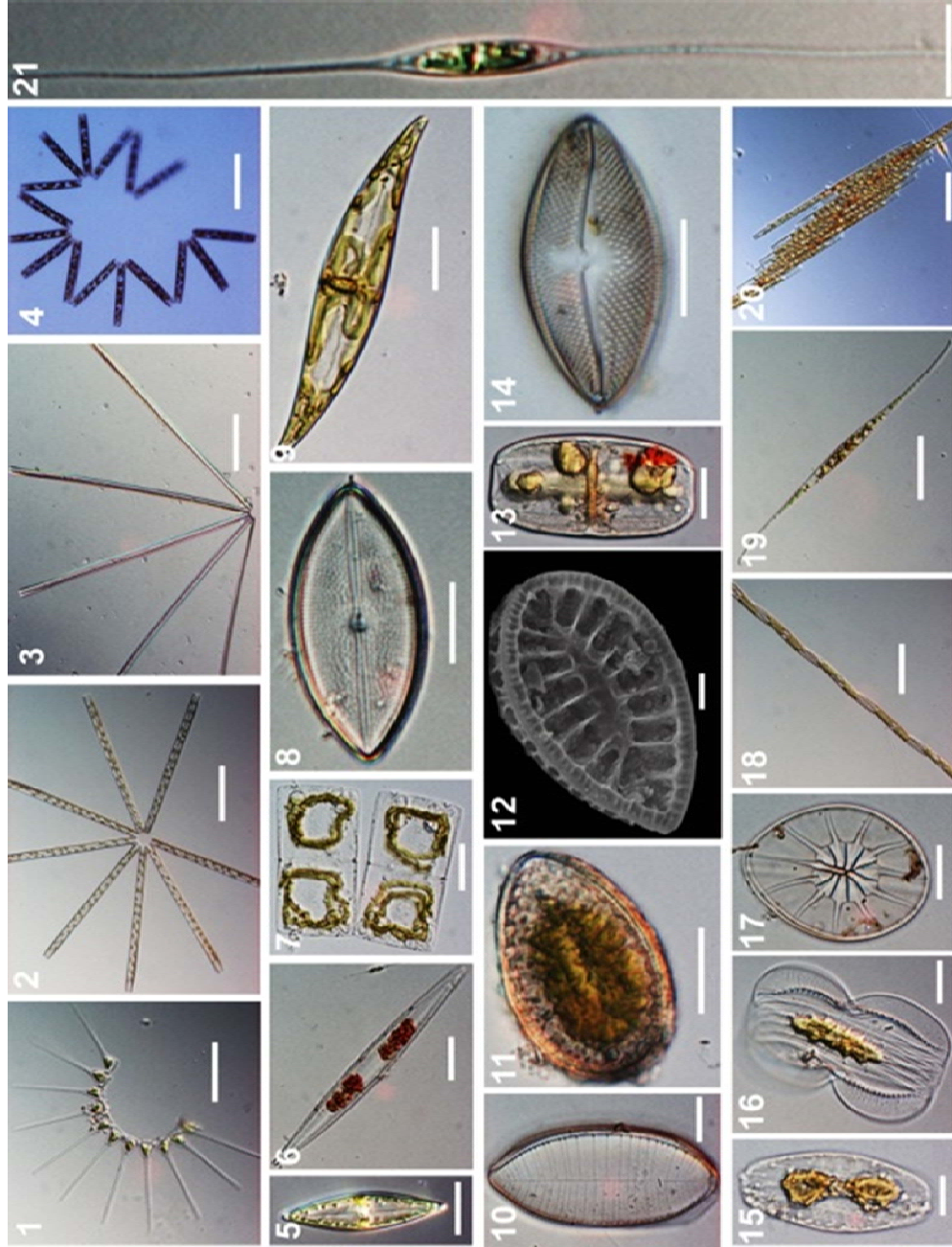


Fig.2.3F. Light and SEM micrographs of pennate diatoms. **1** *Asterionellopsis glacialis*, **2** *Thalassionema frauenfeldii*, **3** *Thalassionema bacillare*, **4** *Thalassionema nitzschioides*, **5** *Navicula directa*, **6** *Haslea trompii*, **7** *Meuniera membranacea*, **8** *Cocconeis placentula*, **9** *Pleurosigma normanii*, **10** *Surirella gemma*, **11,12** *Surirella fastuosa*, **13,14,15** *Amphora commutata*, **15** *Amphora lineolata*, **16** *Entomoneis paludosa*, **17** *Asteromphalus cleveanus*, **18** *Pseudo-nitzschia cacciantha*, **19** *Nitzschia closterium*, **20** *Bacillaria paxillifer*, **21** *Nitzschia longissimas*. Scale bars = 20 μm .

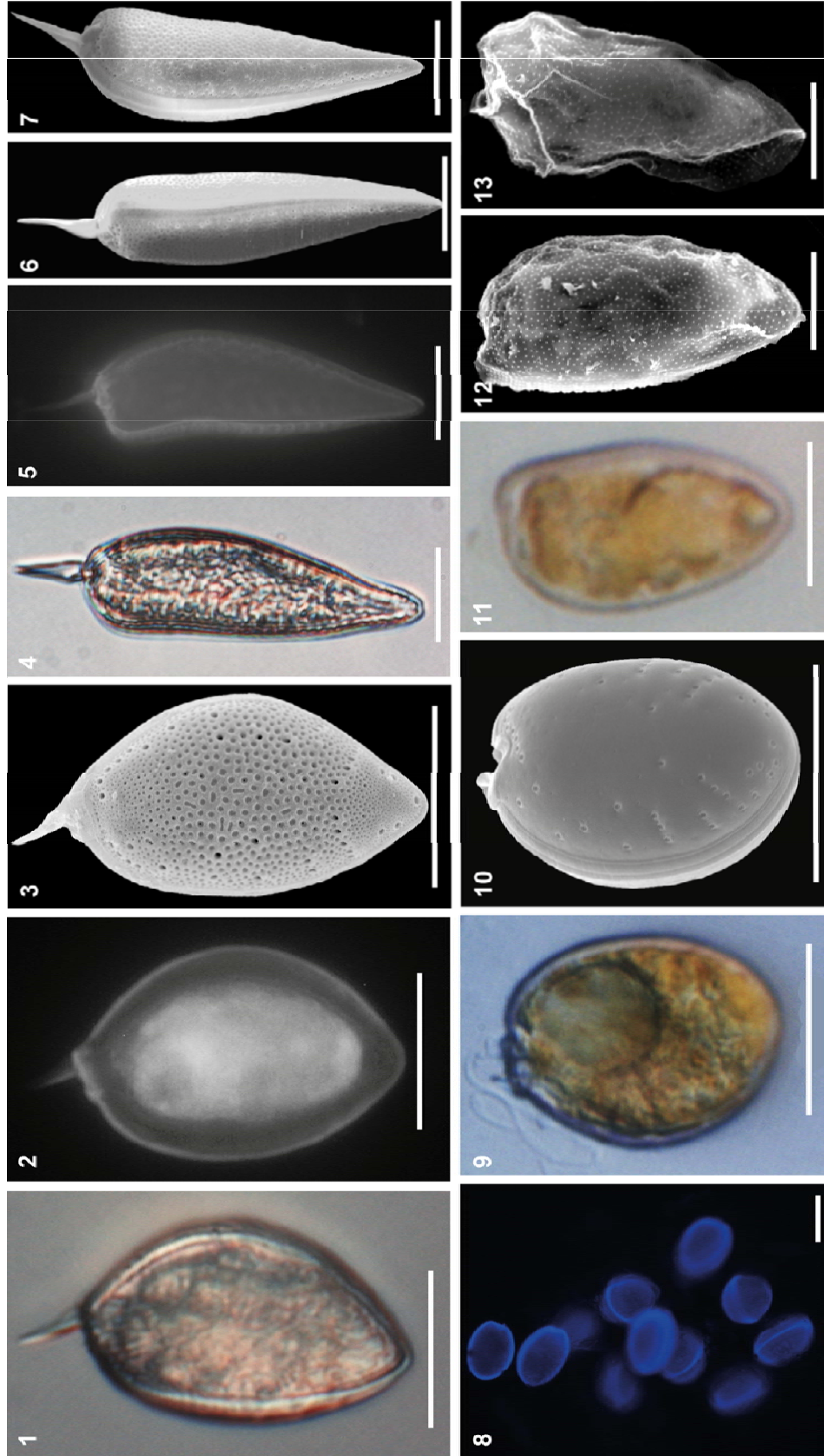


Fig.2.4A. Light (1, 4, 9, 11), fluorescence (2, 5, 8) and SEM (3, 6, 7, 10, 12, 13) micrographs of dinoflagellates, order Prorocentrales. 1-3 *Prorocentrum micans*, 4-7 *Prorocentrum sigmoides*, 8-10 *Prorocentrum rhathymum*, 11-13 *Prorocentrum shikokuense*. (Fluorescence micrographs are taken using Calcofluor, which can stain the cellulose thecal plate). Scale bars = 20 μm , 12, 13= 10 μm .

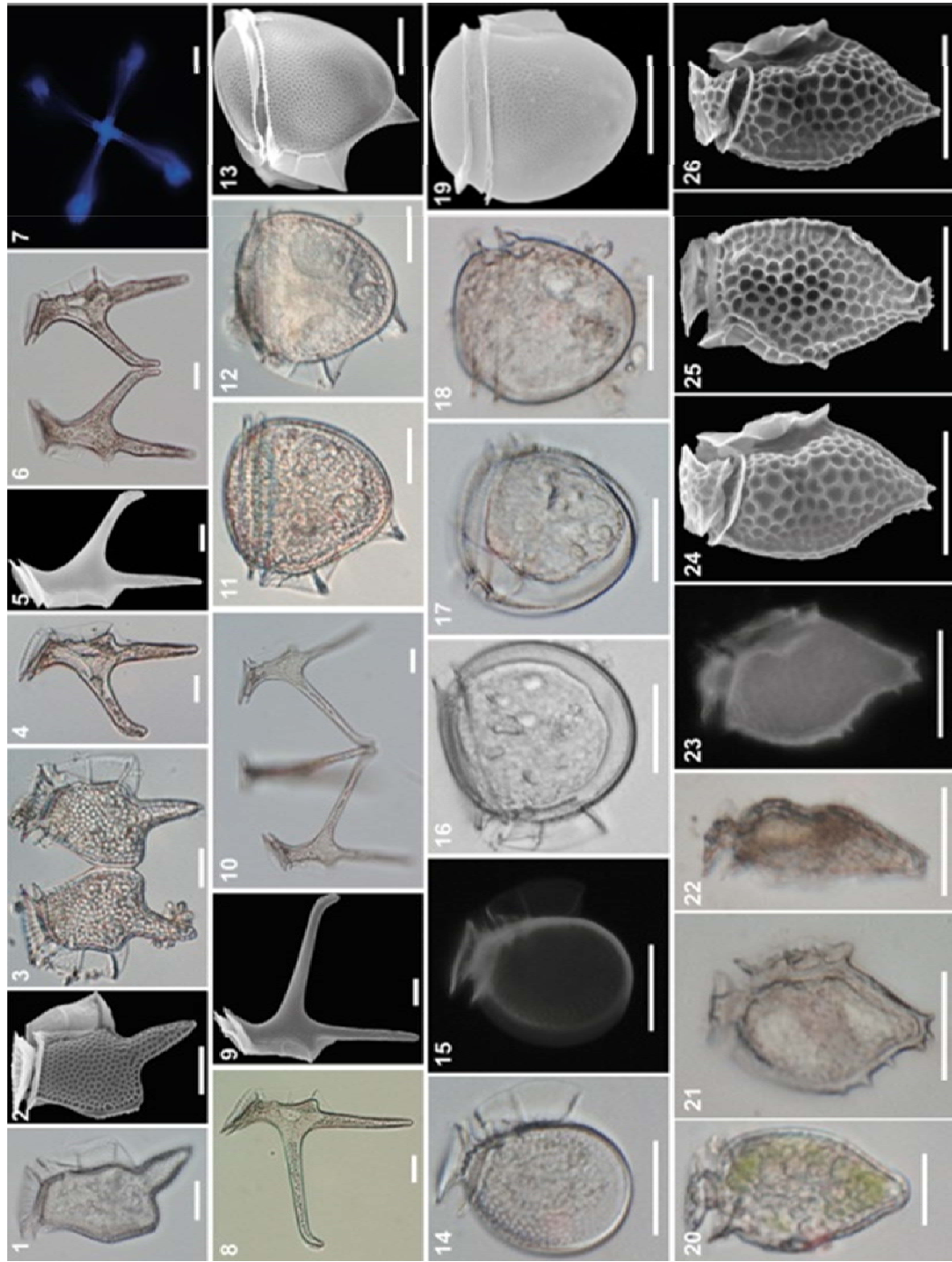


Fig.2.4B. Light (1, 3, 4, 6, 8, 10-12, 14, 16-18, 20-22), fluorescence (7, 15, 23) and SEM (2, 5, 9, 13, 19, 24-26) micrographs of dinoflagellates, order Dinophysiales. 1-3 *Dinophysis caudata*, 4-7 *Dinophysis miles*, 8-10 *Dinophysis miles* var. *schroeteri*, 11-13 *Dinophysis doryphorum*, 14-15 *Dinophysis infundibulus*, 16-17 *Dinophysis parvula*, 18-19 *Dinophysis rotundata*, 20-26 *Metadinophysis* cf. *sinensis*. (Fluorescence micrographs are taken using Calcofluor, which can stain the cellulose thecal plate). Scale bars = 20 μ m.

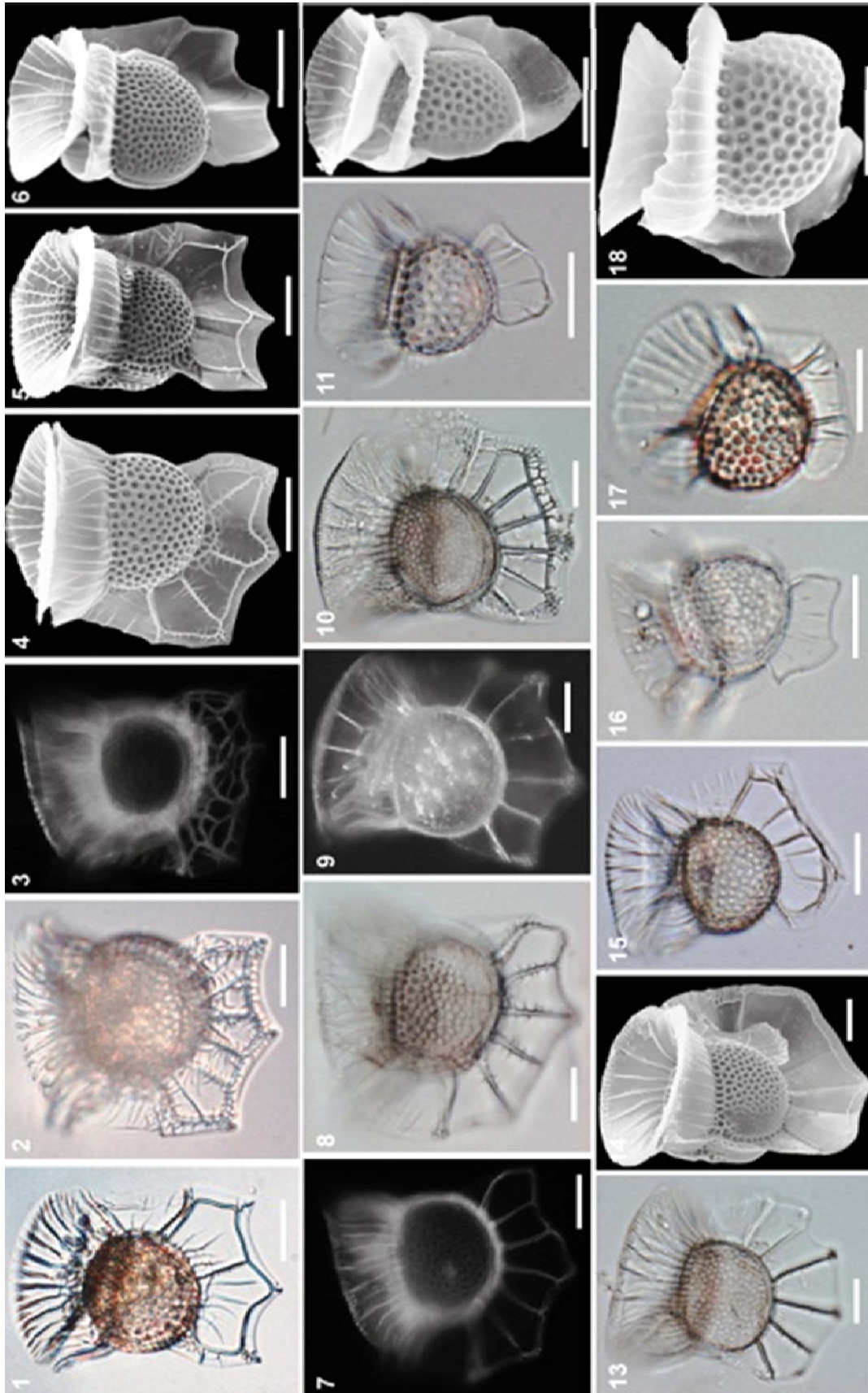


Fig.2.4C. Light (1, 2, 8, 10, 11, 13, 15-17), fluorescence (3, 7, 9) and SEM (4-6, 12, 14, 18) micrographs of dinoflagellates, order Dinophysiales. 1-6 *Ornithocercus magnificus*, 7-9 *Ornithocercus thumii*, 10 *Ornithocercus quadratus*, 11,12 *Ornithocercus cristatus*, 13,14 *Ornithocercus steinii*, 15-18 *Ornithocercus* (immature forms). (Fluorescence micrographs are taken using Calcofluor, which can stain the cellulose thecal plate). Scale bars = 20 μ m.

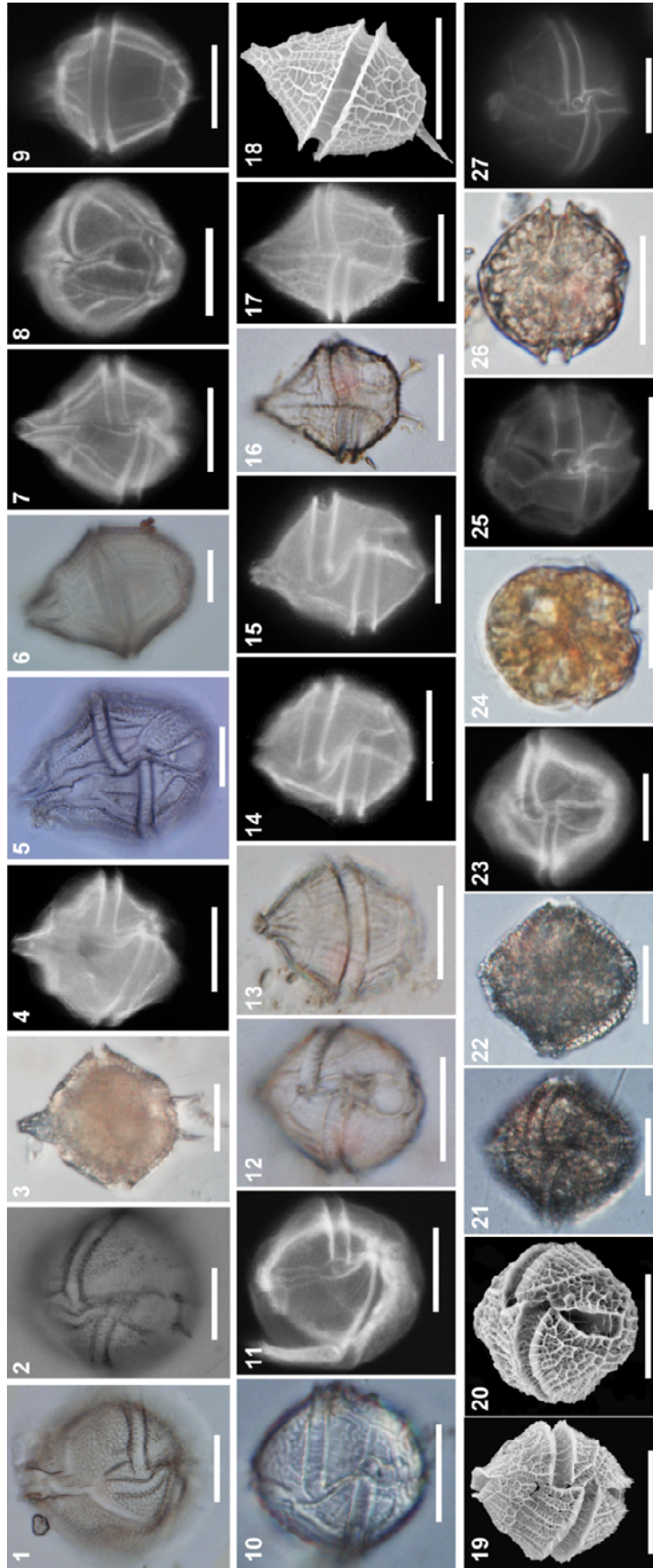


Fig.2.4D. Light (1-3, 5, 6, 10, 12, 13, 16, 21, 22, 24, 26), fluorescence (4, 7-9, 11, 14, 15, 17, 23, 25, 27) and SEM (18-20) micrographs of dinoflagellates, order Gonyaulacales. 1,2 *Gonyaulax digensis*, 3,4 *Gonyaulax digitalis*, 5,6 *Gonyaulax kofoidii*, 7-9 *Gonyaulax polygramma*, 10,11 *Gonyaulax scrippsae*, 12,13 *Gonyaulax turbynei*, 14,15 *Gonyaulax spinifera*, 16-18 *Gonyaulax verior*, 19,20 *Gonyaulax striata*, 21-23 *Lingulodinium polyedrum*, 24,25 *Alexandrium affine*, 26,27 *Alexandrium tamiyavanichii*. (Fluorescence micrographs are taken using Calcofluor, which can stain the cellulose thecal plate). Scale bars = 20 μ m.



Fig.2.4E. Light (1, 4, 7, 8-21, 23-25), fluorescence (2, 3, 5, 6) and SEM (22) micrographs of dinoflagellates, order Gonyaulacales. **1-3** *Pyrophacus horologium*, **4-6** *Pyrophacus steinii*, **7,8** *Ceratium furca*, **9** *Ceratium fusus*, **10-13** *Ceratium furca*, **14,15** *Ceratium macroceros*, **16-18** *Ceratium horridum*, **19-22** *Ceratium breve*, **23-25** *Ceratium tripos*, **26** *Ceratium massiliense*. (Fluorescence micrographs are taken using Calcofluor, which can stain the cellulose thecal plate). Scale bars = 20 μ m.

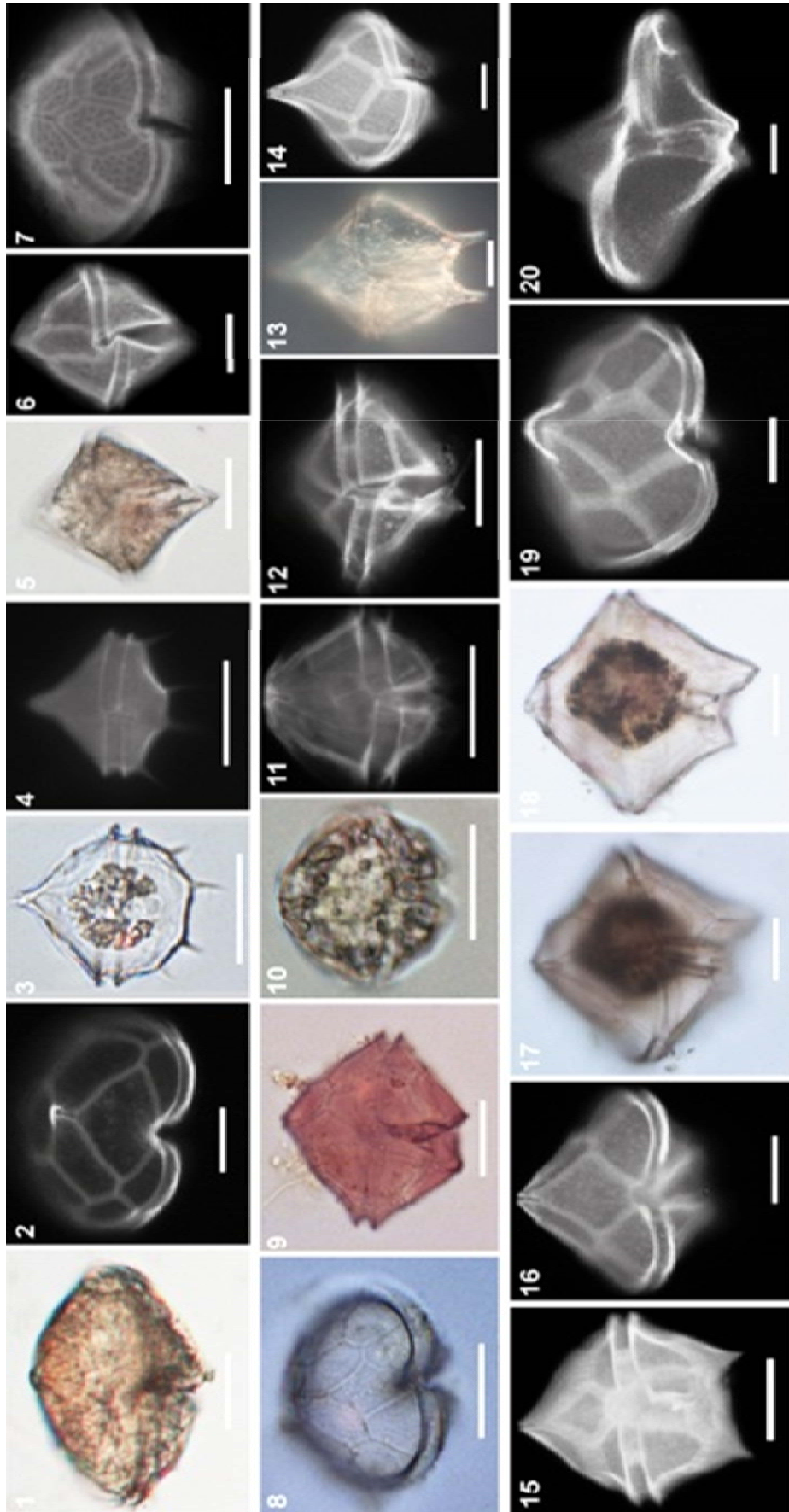


Fig.2.4F. Light (1, 3, 5, 8-10, 13, 17, 18) and fluorescence (2, 4, 6, 7, 11, 12, 14-16, 19, 20) micrographs of dinoflagellates, order Peridinales. 1,2 *Peridinium pervre*, 3,4 *Peridinium quinquecorne*, 5,6 *Protoperidinium abei*, 7 *Protoperidinium avellanum*, 8,9 *Protoperidinium balechii*, 10,11 *Protoperidinium brevipes*, 12 *Protoperidinium capurroi*, 13,14 *Protoperidinium claudicans*, 15 *Protoperidinium compressum*, 16 *Protoperidinium conicoideis*, 17,18 *Protoperidinium conicum*, 19 *Protoperidinium crassipes*, 20 *Protoperidinium curtipes*. (Fluorescence micrographs are taken using Calcoflour, which can stain the cellulose thecal plate).Scale bars = 20 μ m.

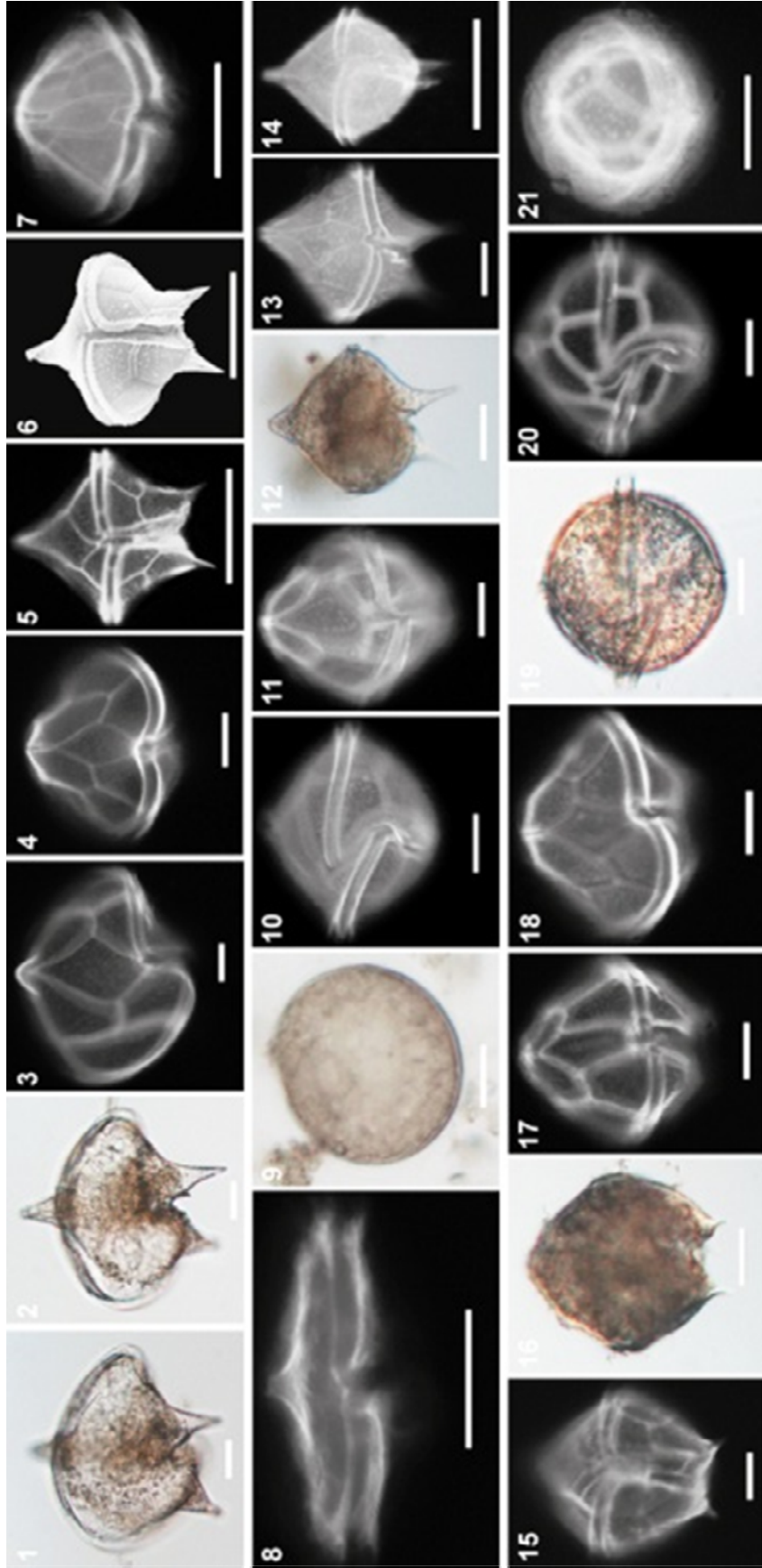


Fig.2.4G. Light (1, 2, 9, 12, 16, 19), fluorescence (3-5, 7, 8, 10, 11, 13-15, 17, 18, 20, 21) and SEM (6) micrographs of dinoflagellates, order Peridinales. 1-3 *Protoperidinium depressum*, 4 *Protoperidinium divaricatum*, 5,6 *Protoperidinium divergens*, 7 *Protoperidinium elongatum*, 8 *Protoperidinium excentricum*, 9,10 *Protoperidinium globiferum*, 11 *Protoperidinium isthmus*, 12,13 *Protoperidinium latidorsale*, 14 *Protoperidinium latissimum*, 15 *Protoperidinium latissimum*, 16,17 *Protoperidinium leonis*, 18 *Protoperidinium mariaelebourae*, 19-20 *Protoperidinium majus*, 21 *Protoperidinium monospinum*. (Fluorescence micrographs are taken using Calcofluor, which can stain the cellulose thecal plate). Scale bars = 20 μ m.

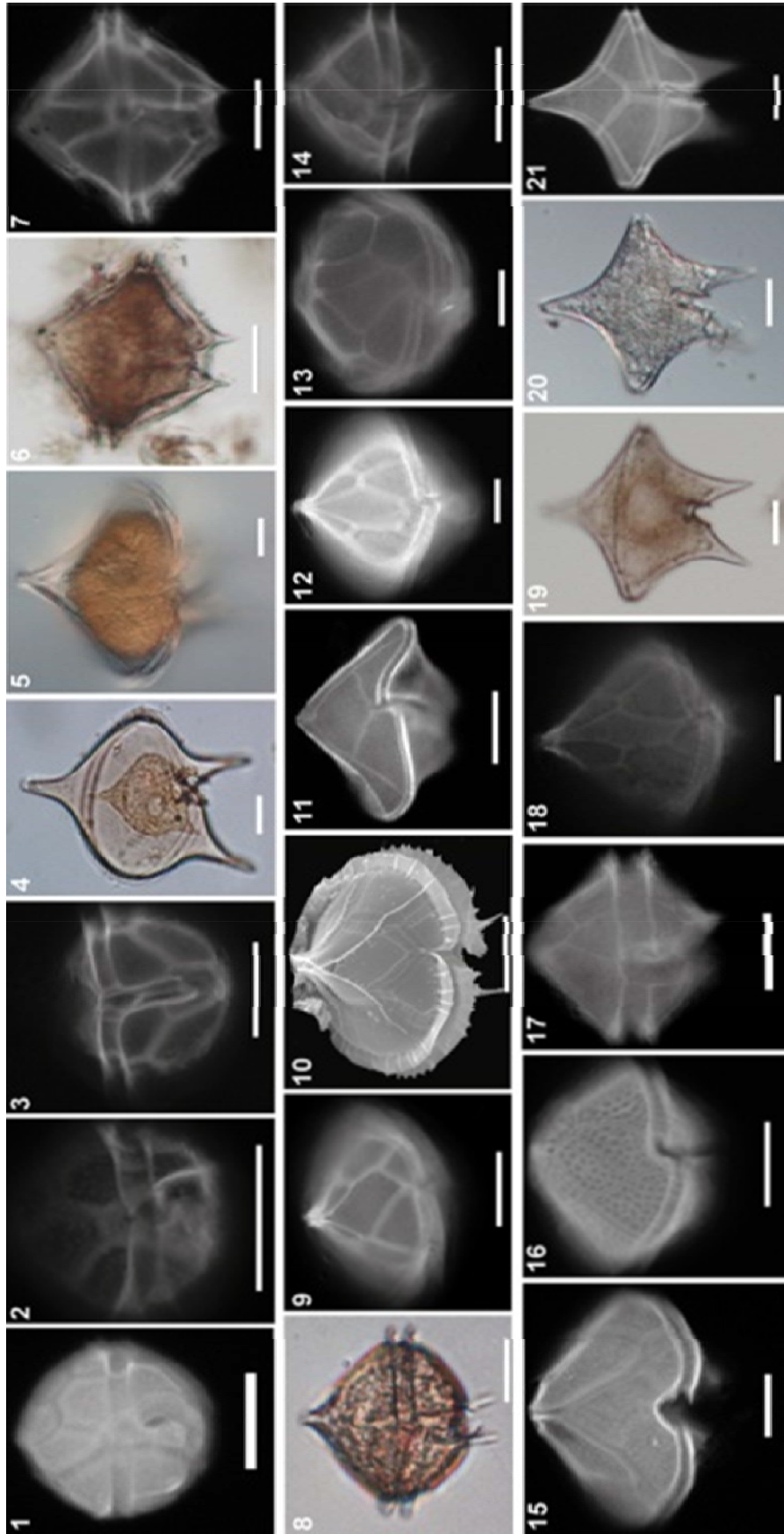


Fig.2.4H. Light (4-6, 8, 19, 20), fluorescence (1-3, 7, 9, 11-18, 21) and SEM (10) micrographs of dinoflagellates, order Peridiniales. **1** *Protoperidinium monovelum*, **2** *Protoperidinium musuensis*, **3** *Protoperidinium nudum*, **4,5** *Protoperidinium oblongum*, **6,7** *Protoperidinium obtusum*, **8-10** *Protoperidinium pallidum*, **11** *Protoperidinium pentagonum*, **12** *Protoperidinium pyriforme*, **13** *Protoperidinium simulum*, **14** *Protoperidinium sphaeroideum*, **15** *Protoperidinium subinerme*, **16** *Protoperidinium thorianum*, **17** *Protoperidinium thulesense*, **18** *Protoperidinium unipes*, **19-21** *Protoperidinium venustum*. (Fluorescence micrographs are taken using Calcofluor, which can stain the cellulose thecal plate). Scale bars = 20 μ m.

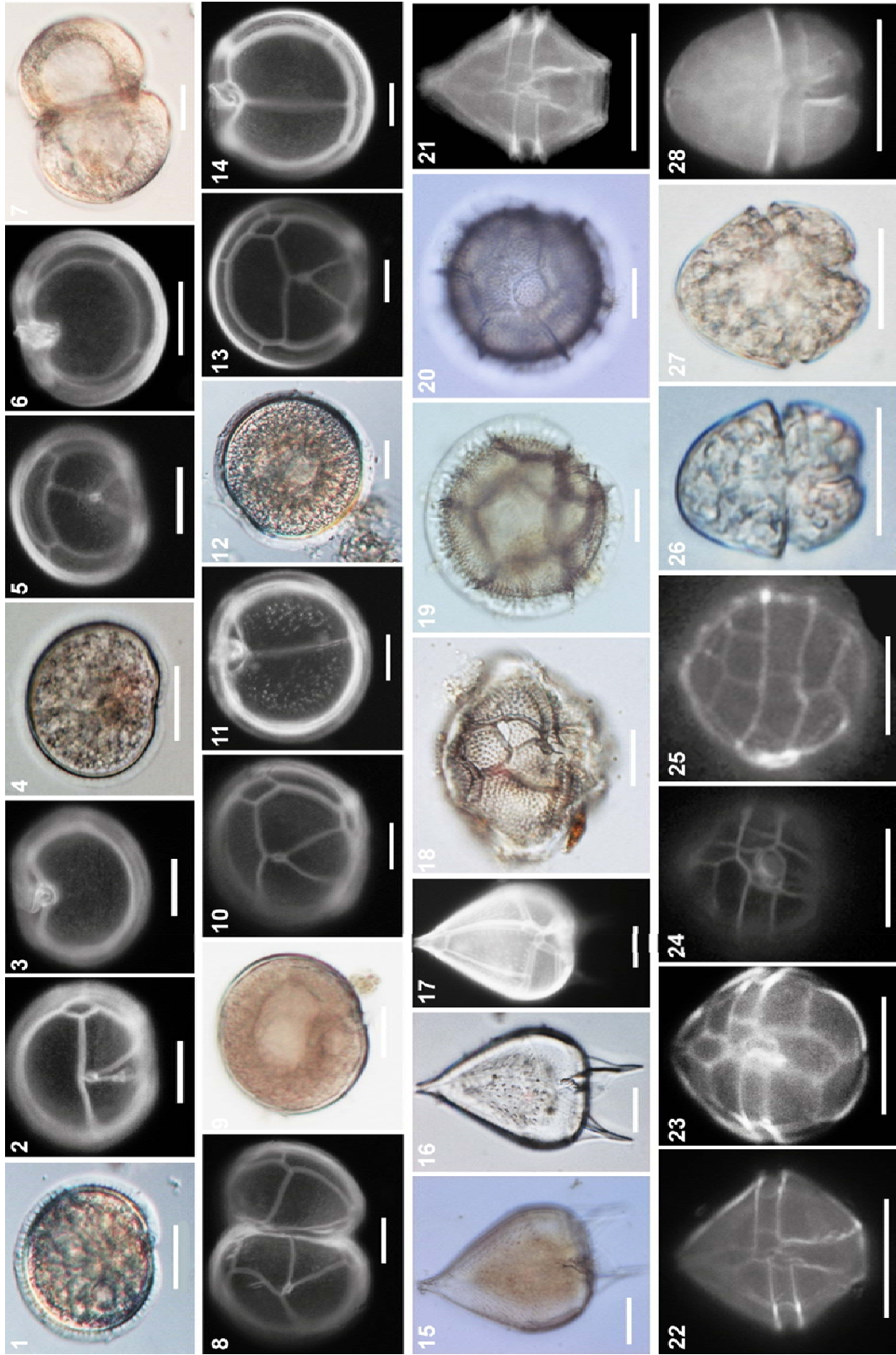


Fig.2.4I. Light (1, 4, 7, 9, 12, 15, 16, 18-20, 26, 27) and fluorescence (2, 3, 5, 6, 8, 10, 11, 13, 14, 17, 21-25, 28) micrographs of dinoflagellates, order Peridinales. 1-3 *Preperidinium meunieri*, 4-8 *Oblea baculifera*, 9-11 *Diplopetla asymmetrica*, 12-14 *Diplopetla bomba*, 15-17 *Podolampas bipes*, 18-20 *Goniodoma polyedricum*, 21,22 *Scrippsiella spinifera*, 23 *Scrippsiella trochoidea*, 24,25 *Heterocapsa niei*, 26-28 *Heterocapsa* sp. (Fluorescence micrographs are taken using Calcofluor, which can stain the cellulose thecal plate). Scale bars = 20 μ m.

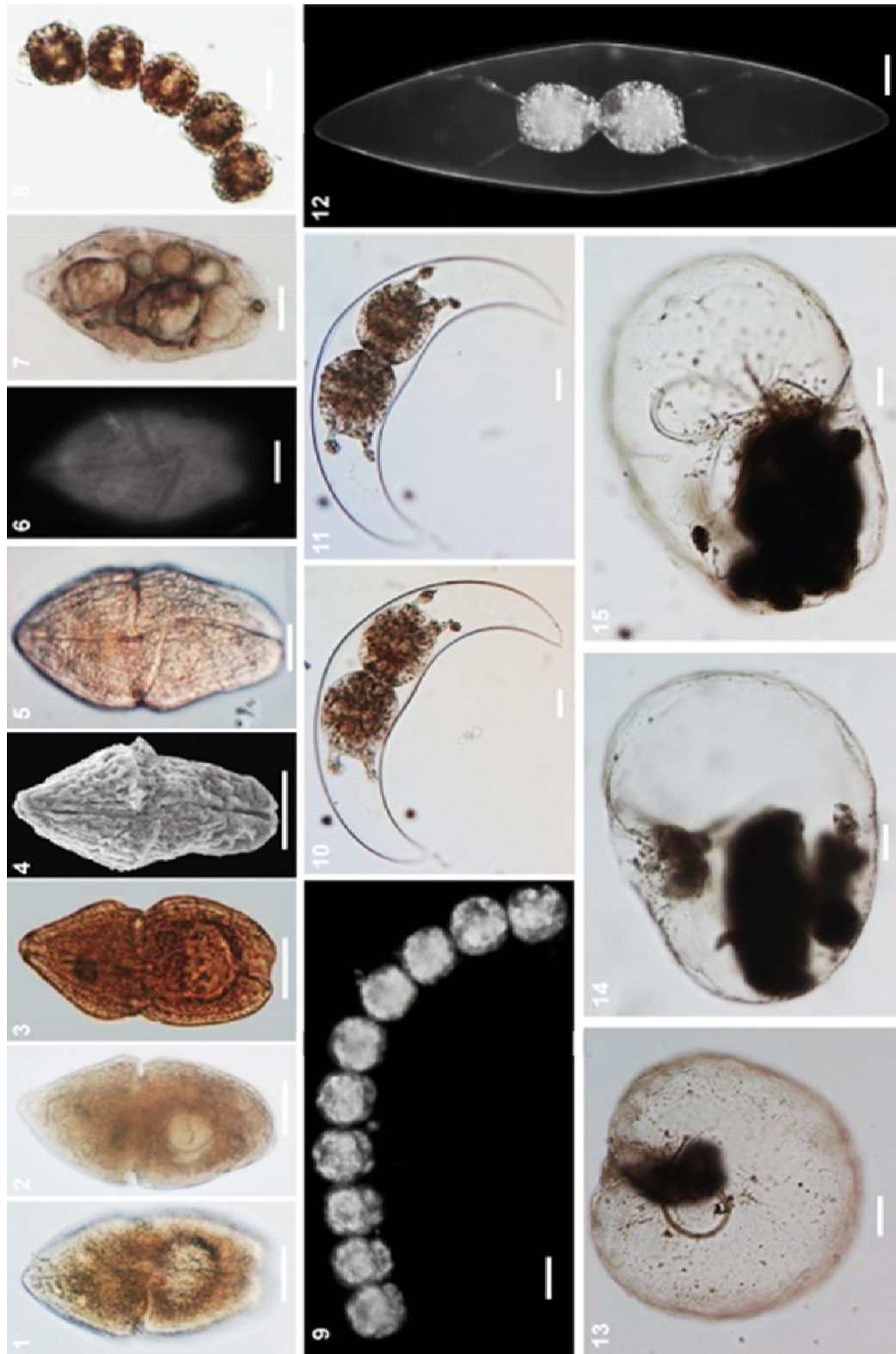


Fig.2.4J. Light (1-3, 5, 7, 8, 10, 11, 13-15), fluorescence (6, 9, 12) and SEM (4) micrographs of unarmoured dinoflagellates. 1-4 *Balechina coerulea*, 5-7 *Gymnodinium lira*, 8,9 *Gymnodinium catenatum*, 10,11 *Pyrocystis lunula*, 12 *Pyrocystis fusiformis*, 13-15 *Noctiluca scintillans*. Scale bars = 20 μm , 8,9= 50 μm .

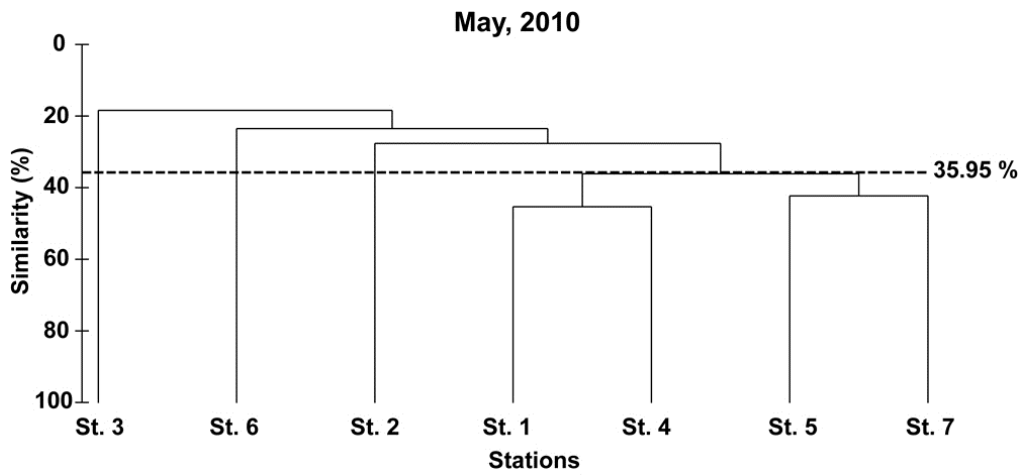


Fig.2.5. Dendrogram produced by clustering of 7 stations sampled in May, 2010 based on dinoflagellate species similarity using cluster analysis.

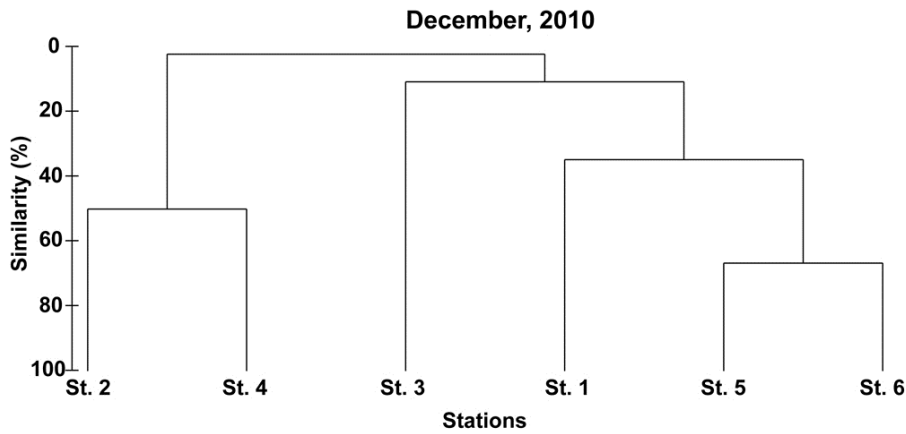


Fig.2.6. Dendrogram produced by clustering of 6 stations sampled in December, 2010 based on dinoflagellate species similarity using cluster analysis.

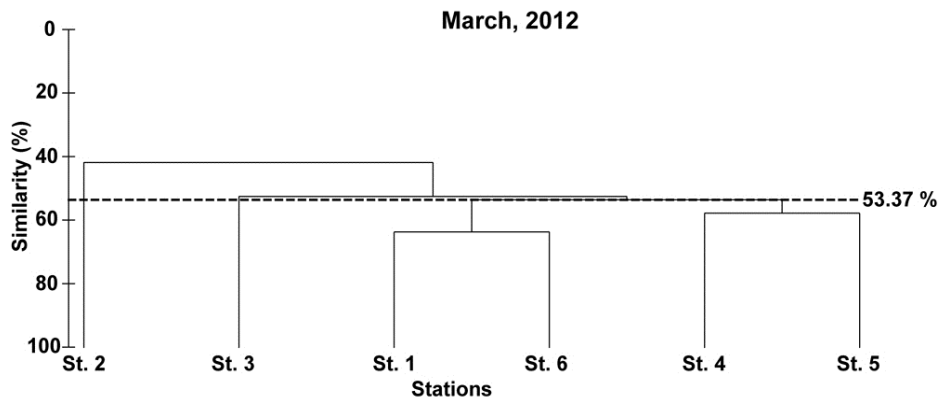


Fig.2.7. Dendrogram produced by clustering of 6 stations sampled in March, 2012 based on dinoflagellate species similarity using cluster analysis.

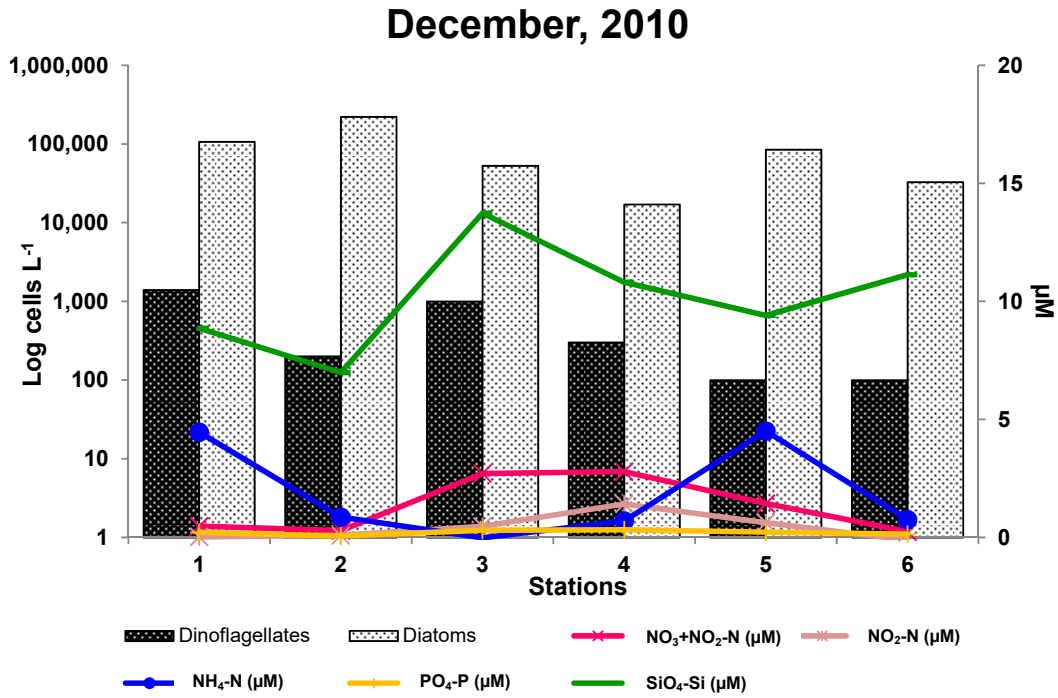


Fig.2.8. Graph showing the proportion of dinoflagellates and diatoms cell density, and surface nutrient concentration in each station in December, 2010.

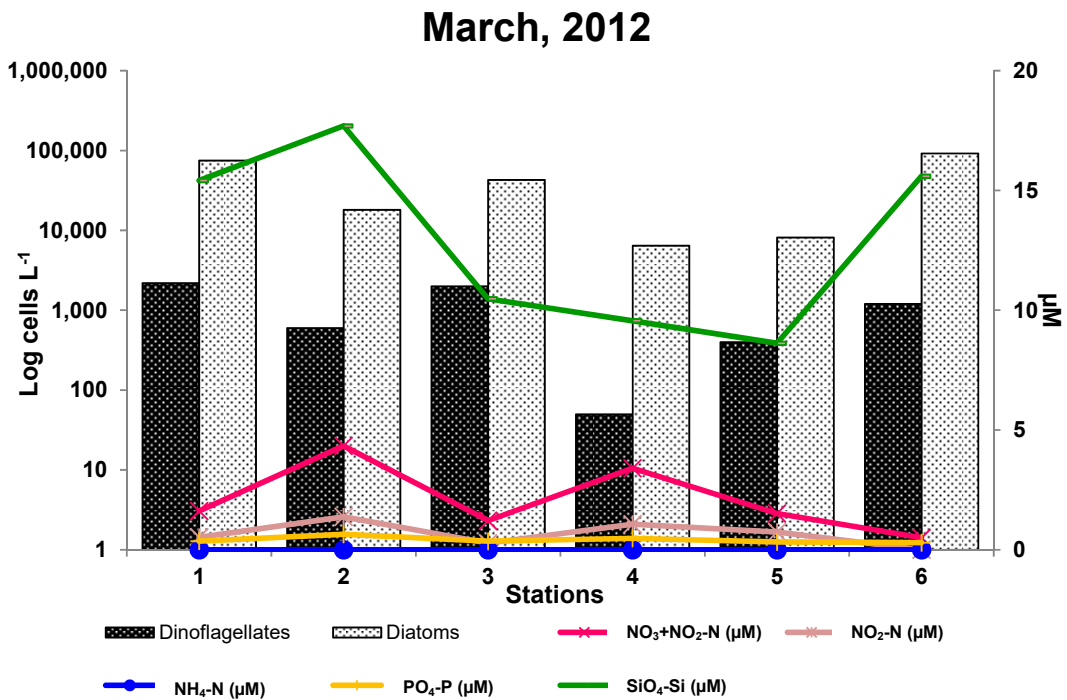


Fig.2.9. Graph showing the proportion of dinoflagellates and diatoms cell density, and surface nutrient concentration in each station in March, 2012.

December, 2010

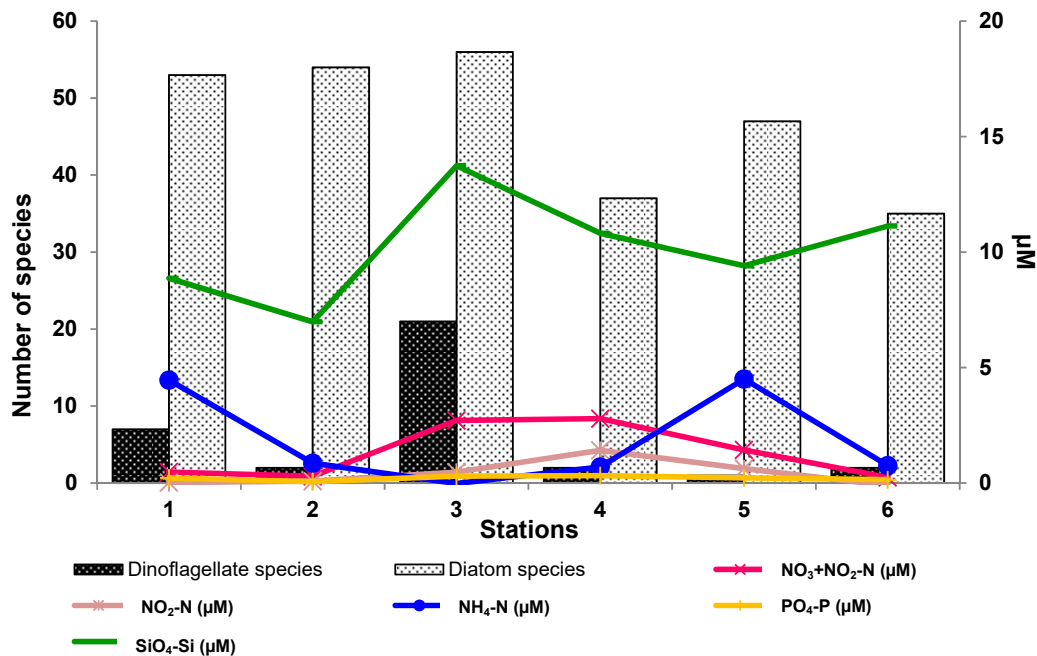


Fig.2.10. Graph showing species diversity of dinoflagellates and diatoms, and surface nutrient concentration in each station in December, 2010.

March, 2012

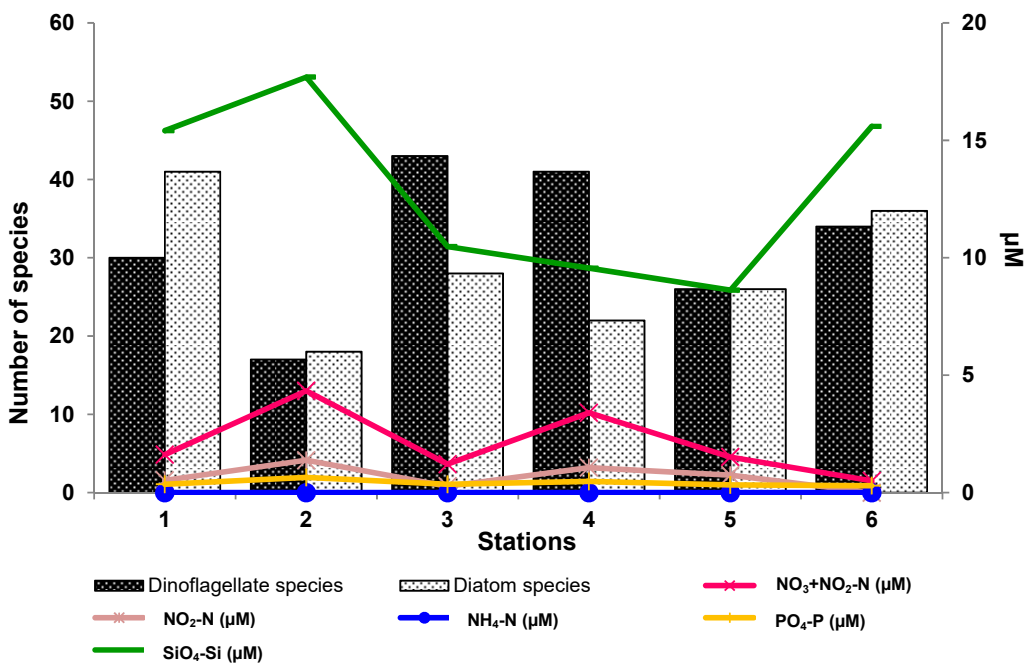


Fig.2.11. Graph showing species diversity of dinoflagellates and diatoms, and surface nutrient concentration in each station in March, 2012.

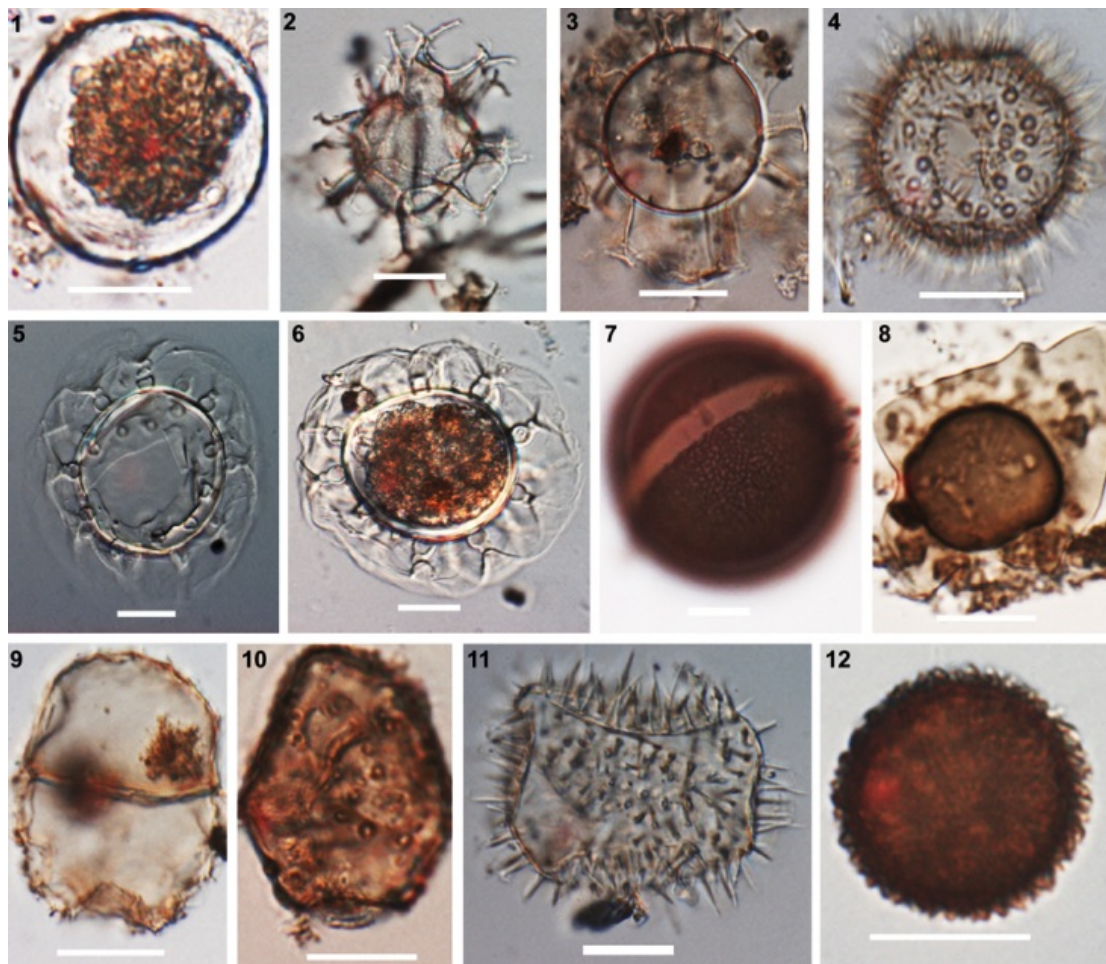


Fig.2.12A. Light micrographs of dinoflagellate cysts. **1** *Alexandrium affine*, **2** *Gonyaulax scrippsae* (*Spiniferites delicatus*), **3** *Gonyaulax spinifera* (*Spiniferites ramosus*), **4** *Lingulodinium polyedrum* (*Lingulodinium machaerophorum*), **5,6** *Pyrophacus steinii* (*Tuberculodinium vancampoae*), **7** *Gymnodinium catenatum*, **8** *Gymnodinium impudicum*, **9** *Gymnodinium* cf. *instriatum*, **10** *Gymnodinium* sp., **11** *Polykrikos hartmannii*, **12** *Scrippsiella* sp. Scale bar = 20 μ m.

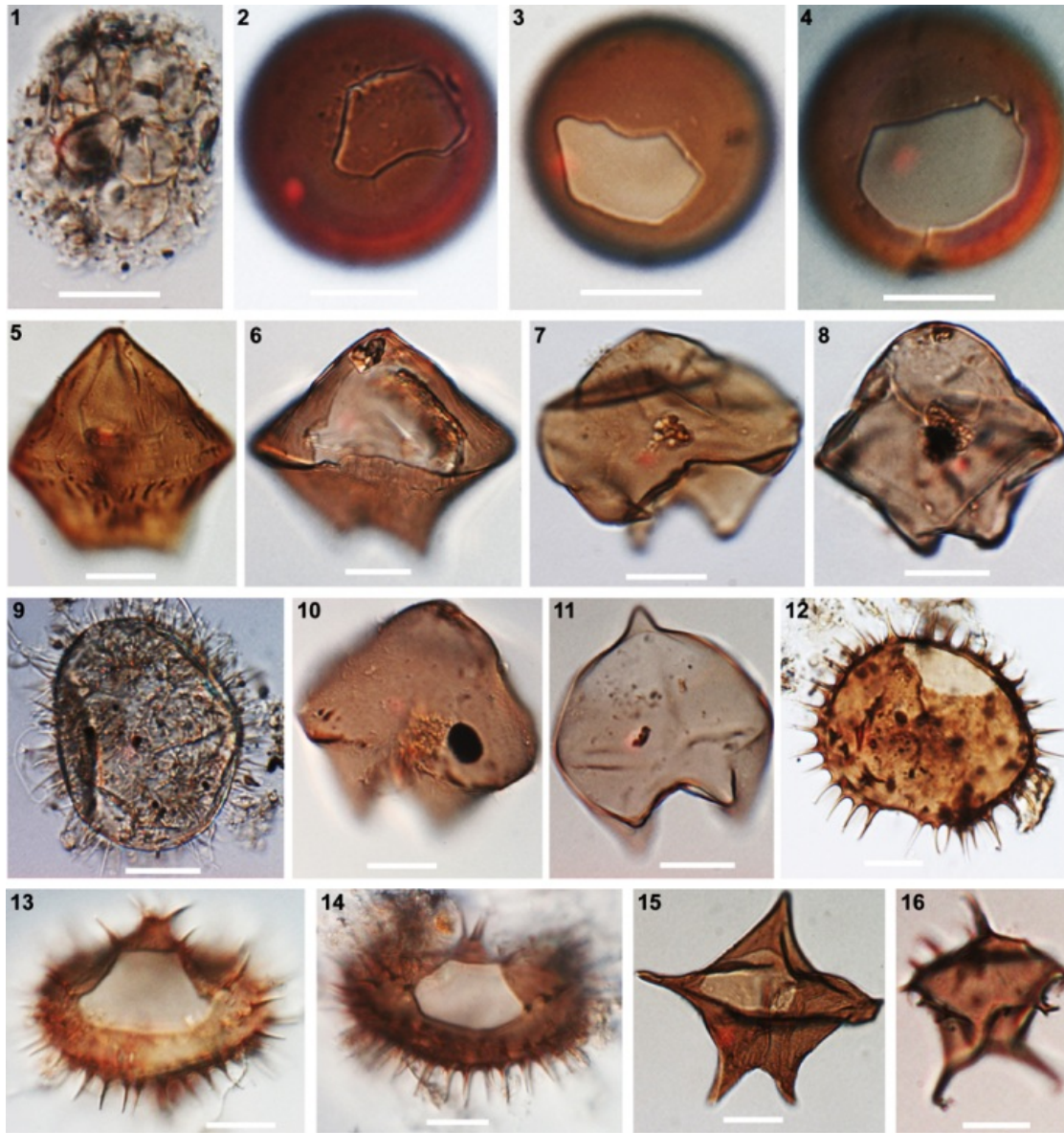


Fig.2.12B. Light micrographs of dinoflagellate cysts. **1** *Polykrikos* cf. *kofoidii*, **2,3** *Protopteridinium denticulatum* (*Brigantedinium irregulare*), **4** *Protopteridinium avellanum* (*Brigantedinium cariacense*), **5** *Protopteridinium* sp. 2 (*Lejeunecysta* sp. 1), **6** *Protopteridinium* sp. 3 (*Lejeunecysta* sp. 2), **7** *Protopteridinium* sp. 4 (*Lejeunecysta* sp. 3), **8** *Protopteridinium* sp. 5 (*Leipokatium* sp.), **9** *Protopteridinium* sp. 6, **10** *Protopteridinium leonis* (*Quinquecuspis concreta*), **11** *Protopteridinium* sp. 7 (*Quinquecuspis* sp.), **12** *Protopteridinium conicum* (*Selenopemphix quanta*), **13** *Protopteridinium nudum* (*Selenopemphix* sp. 1), **14** *Protopteridinium* sp. 8 (*Selenopemphix* sp. 2), **15** *Protopteridinium* cf. *compressum* (*Stelladinium robustum*), **16** *Protopteridinium* sp. 10 (*Stelladinium* sp. 1). Scale bar = 20 μ m.

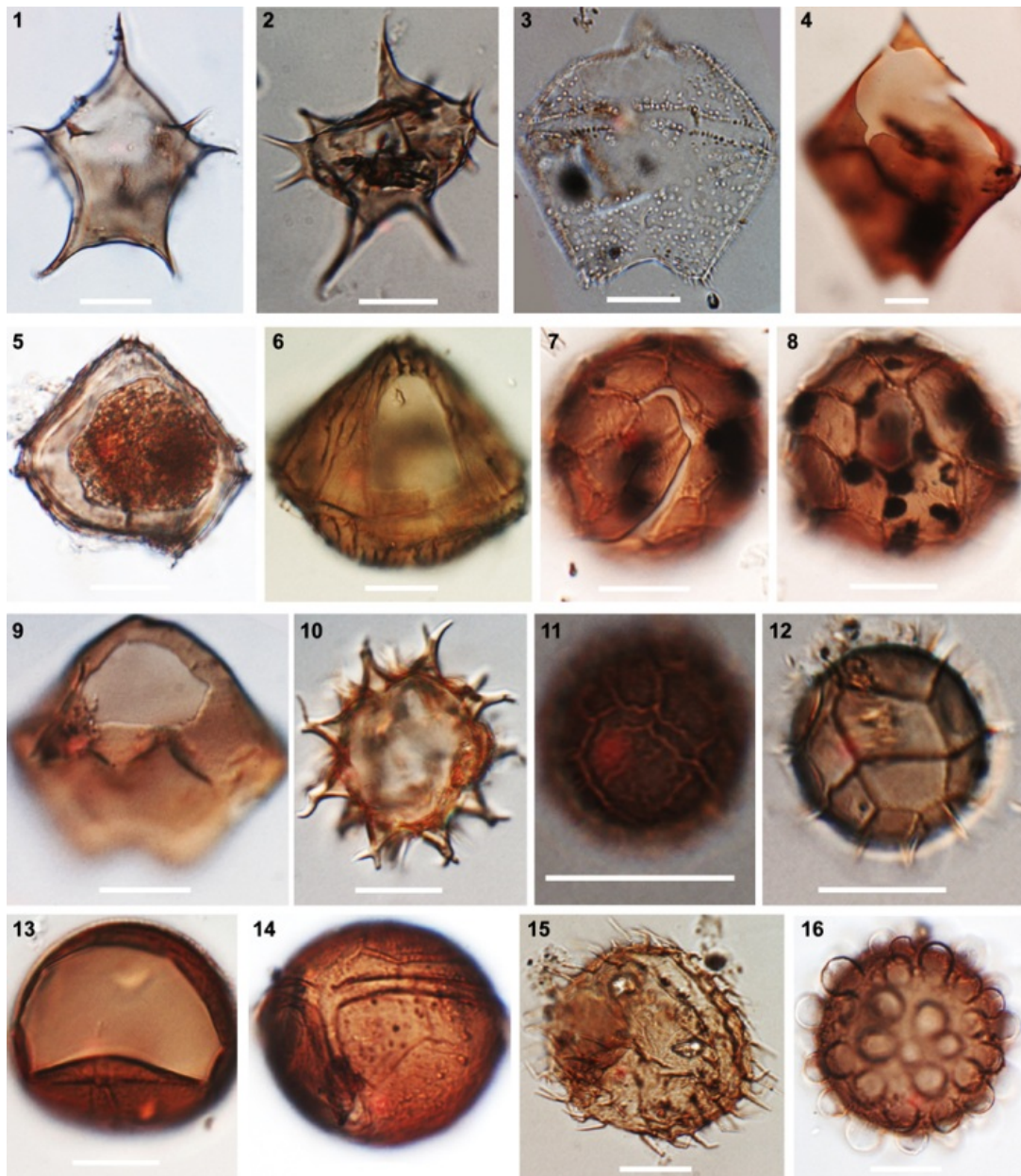


Fig.2.12C. Light micrographs of dinoflagellate cysts. **1** *Protopteridinium* sp. 11 (*Stelladinium* sp. 2), **2** *Protopteridinium* sp. 12 (*Stelladinium* sp. 3), **3** *Protopteridinium pentagonum* (*Trinovantedinium capitatum*), **4** *Protopteridinium latissimum*, **5,6** *Protopteridinium* sp. 15 (new form 1), **7,8** *Protopteridinium* sp. 16 (new form 2), **9** *Protopteridinium* sp. 17 (new form 3), **10** *Protopteridinium* sp. 18 (new form 4), **11,12** *Protopteridinium* sp. 19 (new form 5), **13,14** *Preperidinium maumieri* (*Dubridinium caperatum*), **15** *Oblea acanthocysta*, **16** Diplopsalid new cyst form. Scale bar = 20 μ m.

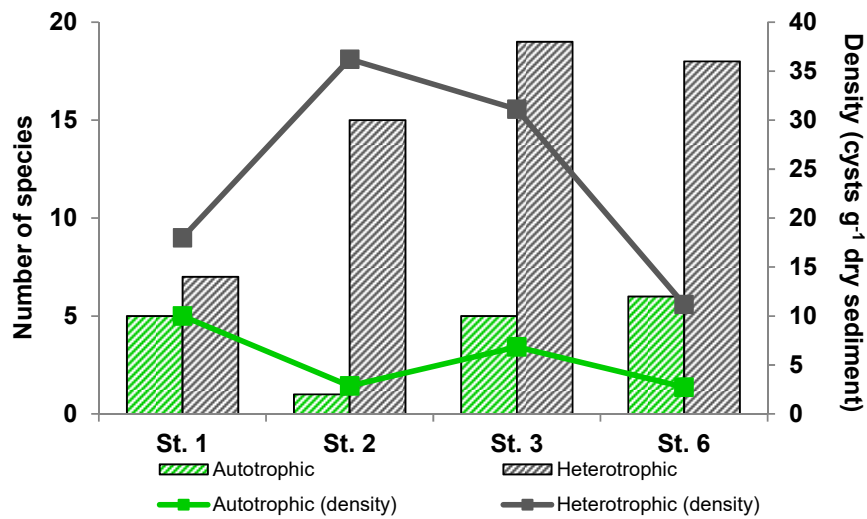


Fig.2.13a. Graph showing the proportion of autotrophic and heterotrophic dinoflagellate cysts in December, 2010

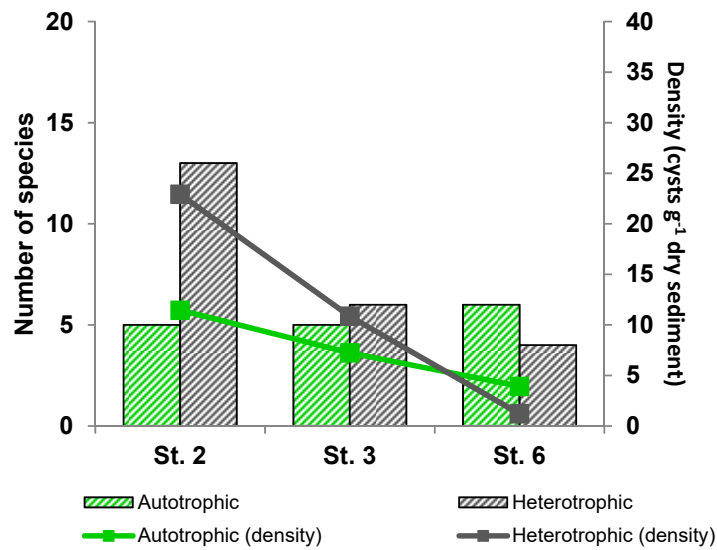


Fig.2.13b. Graph showing the proportion of autotrophic and heterotrophic dinoflagellate cysts in March, 2012.

Table 2.1. Sampling locations around Mali and Kadan Island (May, 2010).

Stations		Latitude (°N)	Longitude (°E)
Mali Island	1	13.107	98.335
	2	13.253	98.193
	3	13.039	98.154
	4	12.777	98.286
Kadan Island	5	12.721	98.283
	6	12.259	98.277
	7	12.542	98.492

Table 2.2. Sampling locations around Kadan Island: depths and environmental parameters (December, 2010).

St.	Latitude (°N)	Longitude (°E)	Depth (m)		Temperature (°C)	Salinity	NO ₃ +NO ₂ -N (µM)	NO ₂ -N (µM)	NH ₄ -N (µM)	PO ₄ -P (µM)	SiO ₄ -Si (µM)
			Total depth	Sampling depths							
1	12.424	98.429	2	0	28.7	25.5	0.477	<DL	4.46	0.215	8.87
				1.5	29.2	26.5	2.11	<DL	20.4	0.710	7.46
2	12.319	98.322	2	0	29.2	21.5	0.291	0.084	0.862	<DL	6.98
				1.5	29.0	29.5	1.12	0.229	<DL	0.243	7.69
3	12.519	98.214	6	0	29.4	32.5	2.71	0.472	<DL	0.302	13.7
				2	28.8	33.0	3.23	0.514	1.27	0.223	15.4
				5	28.6	31.0	2.90	0.636	1.75	0.374	12.2
4	12.700	98.320	-	0	28.7	31.5	2.79	1.42	0.698	0.322	10.8
				5	28.7	32.0	2.80	1.50	10.1	0.243	11.3
				10	28.6	33.5	2.69	1.48	0.615	0.387	11.2
				15	28.6	32.5	2.69	1.38	1.57	0.349	10.5
5	12.650	98.417	22	0	28.4	30.0	1.44	0.623	4.51	0.224	9.40
				5	28.8	30.5	1.19	0.547	0.845	0.257	7.79
				10	28.7	32.0	1.48	0.749	0.330	0.276	8.53
				15	27.5	33.0	1.16	0.558	2.35	0.265	7.96
6	12.588	98.413	3.5	0	29.4	33.5	0.243	<DL	0.758	0.140	11.1
				2	29.2	33.5	0.271	<DL	3.55	0.163	10.4

Table 2.3. Sampling locations around Kadan Island: depths and environmental parameters (March, 2012).

St.	Latitude (°N)	Longitude (°E)	Depths (m)		Temperature (°C)	Salinity	NO ₃ +NO ₂ -N (µM)	NO ₂ -N (µM)	NH ₄ -N (µM)	PO ₄ -P (µM)	SiO ₄ -Si (µM)
			Total depth	Sampling depths							
1	12.381	98.418	13	0	29.59	31.89	1.62	0.522	<DL	0.356	15.4
				5	29.59	31.92	1.00	0.325	<DL	0.215	9.66
2	12.317	98.320	5	0	30.32	31.86	4.34	1.38	<DL	0.645	17.7
				2	30.32	31.87	2.62	0.745	0.412	0.361	10.2
3	12.519	98.214	7	0	29.59	32.52	1.21	0.271	<DL	0.355	10.5
				2	29.59	32.71	1.37	0.306	<DL	0.326	10.3
				5	28.37	32.78	2.47	0.582	<DL	0.429	11.4
4	12.697	98.318	35	0	28.68	30.91	3.40	1.07	<DL	0.476	9.56
				5	28.65	32.76	3.41	1.04	<DL	0.493	9.50
				10	28.62	32.77	4.01	1.26	<DL	0.570	11.5
				15	28.63	32.76	3.44	0.988	<DL	0.487	9.78
5	12.654	98.417	22	0	29.48	32.39	1.51	0.742	<DL	0.326	8.62
				5	29.31	32.48	2.76	1.31	<DL	0.453	9.64
				10	29.11	32.56	3.96	1.79	<DL	0.599	11.9
				15	29.09	32.57	3.12	1.39	<DL	0.468	9.31
6	12.587	98.414	3	0	30.15	32.43	0.498	<DL	<DL	0.298	15.6
				2	30.08	32.41	0.420	<DL	<DL	0.224	14.5

Table 2.4. List of diatom species observed around Kadan Island, southern coast of Myanmar.

No.	Species name	Stations (December, 2010)						Stations (March, 2012)						
		1	2	3	4	5	6	1	2	3	4	5	6	
Family Coscinodiscaceae														
1	<i>Coscinodiscus concinnus</i>							+	+	+	+	+	+	+
2	<i>Coscinodiscus radiatus</i>	+	+	+	+	+		+	+	+		+	+	+
3	<i>Coscinodiscus waitlesii</i>												+	+
Family Hemidiscaceae														
4	<i>Actinocyclus octonarius</i>													
5	<i>Roperia tessellata</i>							+	+	+	+			
Family Stephanodiscaceae														
6	<i>Cyclotella striata</i>	+	+	+	+	+		+	+	+	+	+	+	+
Family Melosiraceae														
7	<i>Melosira moniliformis</i>	+	+	+	+	+						+		
Family Paraliaceae														
8	<i>Paralia sulcata</i>													
Family Skeletonemaceae														
9	<i>Skeletonema costatum</i>	+	+	+	+	+						+	+	+
10	<i>Skeletonema menzeli</i>	+	+	+	+	+						+	+	+
11	<i>Detonula pumila</i>	+	+	+	+	+						+	+	+
12	<i>Detonula confervacea</i>											+	+	+

Table 2.4 continued

No.	Species name	Stations (December, 2010)						Stations (March, 2012)						
		1	2	3	4	5	6	1	2	3	4	5	6	
Family Lauderiaceae														
13	<i>Lauderia annulata</i>	+	+	+	+	+	+	+	+	+	+	+	+	+
Family Thalassiosiraceae														
14	<i>Porosira glacialis</i>	+	+	+	+	+					+			
15	<i>Planktoniella blanda</i>						+			+				+
16	<i>Planktoniella sol</i>						+		+					
17	<i>Thalassiosira eccentrica</i>	+	+	+	+	+	+							+
18	<i>Thalassiosira partheneia</i>		+	+	+	+	+						+	+
19	<i>Thalassiosira oestrupii</i>			+	+									
Family Rhizosoleniaceae														
20	<i>Rhizosolenia styliformis</i>	+	+		+	+	+	+	+	+	+	+	+	+
21	<i>Rhizosolenia setigera</i>	+	+	+	+	+	+	+	+	+	+	+	+	+
22	<i>Rhizosolenia imbricata</i>												+	+
23	<i>Guinardia striata</i>	+	+	+	+	+	+	+	+	+	+	+	+	+
24	<i>Neocalyptrella robusta</i>	+		+	+	+								+
Family Leptocylindraceae														
25	<i>Leptocylindrus danicus</i>	+	+	+	+	+	+	+	+	+	+	+	+	+

Table 2.4 continued

No.	Species name	Stations (December, 2010)						Stations (March, 2012)					
		1	2	3	4	5	6	1	2	3	4	5	6
Family Corethraceae													
26	<i>Corethron criophilum</i>	+	+	+	+	+				+			+
Family Chaetocerotaceae													
27	<i>Chaetoceros danicus</i>	+	+	+		+	+						
28	<i>Chaetoceros peruvianus</i>	+	+	+		+	+					+	+
29	<i>Chaetoceros curvisetus</i>	+	+	+	+	+	+			+	+		+
30	<i>Chaetoceros compressus</i>	+	+	+	+	+	+			+			+
31	<i>Chaetoceros diversus</i>	+	+	+	+	+	+			+			+
32	<i>Chaetoceros furcellatus</i>	+	+	+	+	+	+						
33	<i>Chaetoceros decipiens</i>	+	+	+	+	+	+			+			+
34	<i>Chaetoceros mitra</i>	+	+	+	+	+	+				+		
35	<i>Chaetoceros lorenzianus</i>	+	+	+	+	+	+					+	+
36	<i>Bacteriastrium furcatum</i>	+	+	+	+	+	+			+		+	+
37	<i>Bacteriastrium hyalinum</i>	+	+	+	+	+	+				+		+
Family Lithodesmiaceae													
38	<i>Ditylum sol</i>	+	+	+	+	+	+			+		+	+
39	<i>Helicotheca tamesis</i>	+	+	+	+	+	+			+			
Family Bellerucheaceae													
40	<i>Belleruche horologicalis</i>	+	+	+	+	+	+			+		+	+

Table 2.4 continued

No.	Species name	Stations (December, 2010)						Stations (March, 2012)					
		1	2	3	4	5	6	1	2	3	4	5	6
Family Triceratiaceae													
41	<i>Odontella mobiliensis</i>	+	+	+	+	+	+	+	+	+	+	+	+
42	<i>Odontella sinensis</i>	+	+	+	+	+	+	+	+	+	+	+	+
43	<i>Triceratium favus</i>	+	+	+				+	+	+			
Family Hemiaulaceae													
44	<i>Hemiaulus hauckii</i>	+	+	+	+	+	+						+
45	<i>Eucampia zodiacus</i>	+	+	+	+	+	+	+	+	+	+	+	+
Family Fragilariaceae													
46	<i>Asterionellopsis glacialis</i>	+	+	+									+
Family Thalassionemataceae													
47	<i>Thalassionema frauenfeldii</i>	+	+	+	+	+	+	+	+	+	+	+	+
48	<i>Thalassionema bacillare</i>	+	+	+	+	+	+	+	+	+	+	+	+
49	<i>Thalassionema nitzschioides</i>	+	+	+	+	+	+	+	+	+	+	+	+
Family Naviculaceae													
50	<i>Navicula directa</i>	+	+	+	+	+	+	+	+	+	+	+	+
51	<i>Haslea trompii</i>	+	+	+									
52	<i>Meuniera membranacea</i>	+	+	+	+	+	+	+	+	+	+	+	+
Family Cocconeidaceae													
53	<i>Cocconeis placentula</i>	+										+	+

Table 2.4 continued

No.	Species name	Stations (December, 2010)						Stations (March, 2012)						
		1	2	3	4	5	6	1	2	3	4	5	6	
Family Pleurosigmataceae														
54	<i>Pleurosigma normanii</i>	+	+	+	+	+	+	+	+	+	+	+	+	+
Family Surirellaceae														
55	<i>Surirella gemma</i>	+	+	+										
56	<i>Surirella fastuosa</i>	+	+	+	+	+	+	+	+	+	+	+	+	+
Family Catenulaceae														
57	<i>Amphora commutata</i>	+	+	+	+									
58	<i>Amphora lineolata</i>	+	+	+	+	+	+							
Family Entomoneidaceae														
59	<i>Entomoneis paludosa</i>	+	+	+	+	+	+	+	+	+	+	+	+	+
Family Bacillariaceae														
60	<i>Pseudo-nitzschia caciantha</i>	+	+	+	+	+	+	+	+	+	+	+	+	+
61	<i>Nitzschia longissima</i>	+	+	+	+	+	+	+	+					
62	<i>Nitzschia closterium</i>	+	+	+	+	+	+	+	+	+	+	+	+	+
63	<i>Bacillaria paxillifer</i>	+	+	+	+	+	+	+	+	+	+	+	+	+
Family Asterolampraceae														
64	<i>Asteromphalus cleveanus</i>	+	+	+										

Table 2.5. List of dinoflagellate species observed around Mali and Kadan Island, southern coast of Myanmar.

No.	Species name	Stations (May, 2010)						Stations (December, 2010)						Stations (March, 2012)									
		1	2	3	4	5	6	7	1	2	3	4	5	6	1	2	3	4	5	6			
Family Prorocentraceae																							
1	<i>Prorocentrum micans</i>	+	+	+				+				+				+				+			
2	<i>Prorocentrum rhathymum</i>					+														+			
3	<i>Prorocentrum sigmoides</i>	+	+	+												+				+			
4	<i>Prorocentrum shikokuense</i>																			+			
Family Dinophysiaceae																							
5	<i>Dinophysis caudata</i>	+	+								+					+							
6	<i>Dinophysis doryphorum</i>	+	+								+												
7	<i>Dinophysis infundibulus</i>							+															
8	<i>Dinophysis miles</i>							+															
9	<i>Dinophysis miles</i> var. <i>schroeteri</i>							+															
10	<i>Dinophysis parvula</i>							+	+	+													
11	<i>Dinophysis rotundata</i>									+													
12	<i>Metadinophysis</i> cf. <i>sinensis</i>										+										+		
13	<i>Ornithocercus cristatus</i>							+															
14	<i>Ornithocercus magnificus</i>							+	+														
15	<i>Ornithocercus quadratus</i>							+															
16	<i>Ornithocercus steinii</i>							+															
17	<i>Ornithocercus thumii</i>							+															

Table 2.5 continued

No.	Species name	Stations (May, 2010)						Stations (December, 2010)						Stations (March, 2012)							
		1	2	3	4	5	6	7	1	2	3	4	5	6	1	2	3	4	5	6	
18	<i>Ornithocercus</i> (immature form)		+				+														
Family Gymnodiniaceae																					
19	<i>Balechina coerulea</i>		+				+														
20	<i>Gymnodinium catenatum</i>							+													
21	<i>Gymnodinium lira</i>		+																		
Family Gonyaulacaceae																					
22	<i>Gonyaulax diegensis</i>		+						+												
23	<i>Gonyaulax digitalis</i>		+						+	+									+		
24	<i>Gonyaulax kofoidii</i>																			+	
25	<i>Gonyaulax macroporus</i>		+																		
26	<i>Gonyaulax polygramma</i>		+											+							
27	<i>Gonyaulax scrippsae</i>			+																	
28	<i>Gonyaulax spinifera</i>		+																		
29	<i>Gonyaulax striata</i>		+																		
30	<i>Gonyaulax turbynei</i>		+																		
31	<i>Gonyaulax verior</i>																				
32	<i>Lingulodinium polyedrum</i>																				
33	<i>Alexandrium affine</i>																				
34	<i>Alexandrium tamiyavanichii</i>		+																		

Table 2.5 continued

No.	Species name	Stations (May, 2010)						Stations (December, 2010)						Stations (March, 2012)						
		1	2	3	4	5	6	7	1	2	3	4	5	6	1	2	3	4	5	6
Family Pyrophacaceae																				
35	<i>Pyrophacus horologium</i>	+				+	+							+						
36	<i>Pyrophacus steinii</i>		+			+		+						+						
Family Ceratiaceae																				
37	<i>Ceratum breve</i>	+	+					+						+						
38	<i>Ceratum falcatum</i>																	+		
39	<i>Ceratum furca</i>	+	+	+	+	+	+	+	+					+	+	+	+	+	+	+
40	<i>Ceratum fusus</i>	+										+							+	
41	<i>Ceratum horridum</i>													+						
42	<i>Ceratum tripos</i>	+	+			+	+			+	+									+
43	<i>Ceratum macroeros</i>	+					+													
44	<i>Ceratum massiliense</i>	+	+																	
Family Peridiniaceae																				
45	<i>Peridinium perbreve</i>																	+		+
46	<i>Peridinium quinquecorne</i>									+					+					+
Family Proto-peridiniaceae																				
47	<i>Proto-peridinium abei</i>																	+		+
48	<i>Proto-peridinium avellanum</i>																	+		+
49	<i>Proto-peridinium balechii</i>																+		+	+

Table 2.5 continued

No.	Species name	Stations (May, 2010)						Stations (December, 2010)						Stations (March, 2012)						
		1	2	3	4	5	6	7	1	2	3	4	5	6	1	2	3	4	5	6
50	<i>Protoperidinium brevipes</i>													+						
51	<i>Protoperidinium capurroi</i>										+									
52	<i>Protoperidinium claudicans</i>																			
53	<i>Protoperidinium compressum</i>																			
54	<i>Protoperidinium conicoides</i>																			
55	<i>Protoperidinium conicum</i>																			
56	<i>Protoperidinium crassipes</i>																			
57	<i>Protoperidinium curtipes</i>																			
58	<i>Protoperidinium depressum</i>																			
59	<i>Protoperidinium divaricatum</i>																			
60	<i>Protoperidinium divergens</i>																			
61	<i>Protoperidinium elongatum</i>																			
62	<i>Protoperidinium excentricum</i>																			
63	<i>Protoperidinium globiferum</i>																			
64	<i>Protoperidinium isthmus</i>																			
65	<i>Protoperidinium latidorsale</i>																			
66	<i>Protoperidinium latispinum</i>																			
67	<i>Protoperidinium latissimum</i>																			
68	<i>Protoperidinium leonis</i>																			

Table 2.5 continued

No.	Species name	Stations (May, 2010)						Stations (December, 2010)						Stations (March, 2012)						
		1	2	3	4	5	6	7	1	2	3	4	5	6	1	2	3	4	5	6
69	<i>Protoperidinium mariaelebourae</i>															+				
70	<i>Protoperidinium majus</i>															+	+	+	+	+
71	<i>Protoperidinium monospinum</i>															+				
72	<i>Protoperidinium monovelum</i>															+				
73	<i>Protoperidinium mutsuensis</i>												+							
74	<i>Protoperidinium nudum</i>											+								
75	<i>Protoperidinium oblongum</i>						+													+
76	<i>Protoperidinium obtusum</i>															+				+
77	<i>Protoperidinium pallidum</i>																			+
78	<i>Protoperidinium pentagonum</i>												+							+
79	<i>Protoperidinium pyriforme</i>						+						+							
80	<i>Protoperidinium simulum</i>						+													
81	<i>Protoperidinium sphaeroideum</i>																			
82	<i>Protoperidinium subinerve</i>																			+
83	<i>Protoperidinium subpyriforme</i>																			+
84	<i>Protoperidinium thorianum</i>																			+
85	<i>Protoperidinium thulesense</i>																			+
86	<i>Protoperidinium unipes</i>																			+
87	<i>Protoperidinium venustum</i>												+							+

Table 2.5 continued

No.	Species name	Stations (May, 2010)						Stations (December, 2010)						Stations (March, 2012)							
		1	2	3	4	5	6	7	1	2	3	4	5	6	1	2	3	4	5	6	
88	<i>Preperidinium meunieri</i>		+													+	+	+	+	+	+
89	<i>Obilea baculifera</i>															+		+			+
90	<i>Diplopelta asymmetrica</i>															+	+	+	+	+	+
91	<i>Diplopelta bomba</i>	+	+																		
	Family Podolampadaceae																				
92	<i>Podolampas bipes</i>		+																		
	Family Goniodomataceae																				
93	<i>Goniodoma polyedricum</i>		+							+											
	Family Calciodinellaceae																				
94	<i>Scrippsiella spinifera</i>											+									+
95	<i>Scrippsiella trochoidea</i>										+				+						
	Family Heterocapsaceae																				
96	<i>Heterocapsa niei</i>												+								+
97	<i>Heterocapsa</i> sp.													+							+
	Family Pyrocystaceae																				
98	<i>Pyrocystis fusiformis</i>																				
99	<i>Pyrocystis lunula</i>																			+	
	Family Noctilucaeae																				
100	<i>Noctiluca scintillans</i>															+			+	+	+

Table 2.6. List of dinoflagellate cysts recorded around Kadan Island, southern coast of Myanmar.

No.	Biological name	Paleontological name	Stations						
			(December, 2010)			(March, 2012)			
			1	2	3	6	2	3	6
Autotrophic species									
Gonyaulacales									
1	<i>Alexandrium affine</i>		+	+	+	+	+	+	+
2	<i>Alexandrium</i> cf. <i>tamiyavanichii</i>								
3	<i>Gonyaulax scrippsae</i>	<i>Spiniferites delicatus</i>			+	+		+	
4	<i>Gonyaulax spinifera</i>	<i>Spiniferites ramosus</i>			+	+		+	
5	<i>Lingulodinium polyedrum</i>	<i>Lingulodinium machaerophorum</i>	+			+			
6	<i>Pyrophacus steinii</i>	<i>Tuberculodinium vancampoae</i>	+					+	
Gymnodiniales									
7	<i>Gymnodinium catenatum</i>				+		+		+
8	<i>Gymnodinium</i> sp.				+				
9	<i>Gymnodinium impudicum</i>					+	+		
10	<i>Gymnodinium</i> cf. <i>instriatum</i>		+						
11	<i>Polykrikos hartmannii</i>		+			+			
Peridinales									
12	<i>Scripsiella</i> sp.						+		+
Heterotrophic species									
Gymnodiniales									
13	<i>Polykrikos</i> cf. <i>kofoidii</i>							+	

Table 2.6 continued

No.	Biological name	Paleontological name	Stations						
			(December, 2010)			(March, 2012)			
			1	2	3	6	2	3	6
Peridinales									
14	<i>Protoperidinium avellanum</i>	<i>Brigantedinium cartiacoense</i>	+	+	+	+	+	+	+
15	<i>Protoperidinium denticulatum</i>	<i>Brigantedinium irregulare</i>		+		+	+	+	
16	<i>Protoperidinium</i> sp. 1	<i>Echinidinium</i> sp.			+	+	+		
17	<i>Protoperidinium</i> sp. 2	<i>Lejeunecysta</i> sp. 1		+		+	+		
18	<i>Protoperidinium</i> sp. 3	<i>Lejeunecysta</i> sp. 2				+			
19	<i>Protoperidinium</i> sp. 4	<i>Lejeunecysta</i> sp. 3			+	+	+		+
20	<i>Protoperidinium</i> sp. 5	<i>Leipokatium</i> sp.			+		+		+
21	<i>Protoperidinium</i> sp. 6		+						
22	<i>Protoperidinium leonis</i>	<i>Quinquecuspis concreta</i>		+					
23	<i>Protoperidinium</i> sp. 7	<i>Quinquecuspis</i> sp.	+	+		+			
24	<i>Protoperidinium conicum</i>	<i>Selenopemphix quanta</i>	+	+		+		+	
25	<i>Protoperidinium subinerme</i>	<i>Selenopemphix alticinctum</i>					+		+
26	<i>Protoperidinium nudum</i>	<i>Selenopemphix</i> sp. 1		+	+	+			
27	<i>Protoperidinium</i> sp. 8	<i>Selenopemphix</i> sp. 2		+		+			
28	<i>Protoperidinium</i> sp. 9	<i>Selenopemphix</i> sp. 3			+				
29	<i>Protoperidinium</i> cf. <i>compressum</i>	<i>Stelladinium robustum</i>					+		
30	<i>Protoperidinium</i> sp. 10	<i>Stelladinium</i> sp. 1	+						
31	<i>Protoperidinium</i> sp. 11	<i>Stelladinium</i> sp. 2			+				

Table 2.6 continued

No.	Biological name	Paleontological name	Stations (December, 2010)						Stations (March, 2012)					
			1	2	3	6	6	2	2	3	3	6		
32	<i>Protoperidinium</i> sp. 12	<i>Stelladinium</i> sp. 3			+									
33	<i>Protoperidinium pentagonum</i>	<i>Trinovantedinium capitatum</i>			+									
34	<i>Protoperidinium</i> sp. 13	<i>Trinovantedinium</i> sp.		+										
35	<i>Protoperidinium latissimum</i>				+									
36	<i>Protoperidinium</i> sp. 14	(Spiny round brown cyst)		+										
37	<i>Protoperidinium</i> sp. 15	(new form 1)		+										
38	<i>Protoperidinium</i> sp. 16	(new form 2)												
39	<i>Protoperidinium</i> sp. 17	(new form 3)												
40	<i>Protoperidinium</i> sp. 18	(new form 4)												
41	<i>Protoperidinium</i> sp. 19	(new form 5)												
42	<i>Preperidinium maumieri</i>	<i>Dubridinium caperatum</i>		+										
43	<i>Oblea acanthocysta</i>													
44	Diplopsalid group	Diplopsalid new cyst form		+										

Table 2.7. Density of dinoflagellate cysts recorded around Kadan Island, southern coast of Myanmar.

No.	Biological name	Paleontological name	Density (Cysts g ⁻¹ dry sediment weight)						
			Stations (December, 2010)			Stations (March, 2012)			
			1	2	3	6	2	3	6
Autotrophic species									
1	<i>Alexandrium affine</i>		1.99	2.85	1.86	0.68	7.83	3.61	1.81
2	<i>Alexandrium cf. tamiyavanichii</i>		0	0	0	0	0	1.80	0.90
3	<i>Gonyaulax scrippsae</i>	<i>Spiniferites delicatus</i>	0	0	2.48	0.91	0	0.45	0
4	<i>Gonyaulax spinifera</i>	<i>Spiniferites ramosus</i>	0	0	1.24	0.45	1.20	0.45	0.30
5	<i>Lingulodinium polyedrum</i>	<i>Lingulodinium machaerophorum</i>	1.99	0	0	0.22	0	0	0
6	<i>Pyrophacus steinii</i>	<i>Tuberculodinium vancampoeae</i>	1.99	0	0	0	0	0.90	0.30
7	<i>Gymnodinium catenatum</i>		0	0	0.62	0	0.60	0	0.30
8	<i>Gymnodinium sp.</i>		0	0	0.62	0	0	0	0
9	<i>Gymnodinium impudicum</i>		0	0	0	0.26	0.60	0	0.30
10	<i>Gymnodinium cf. instriatum</i>		1.99	0	0	0	0	0	0
11	<i>Polykrikos hartmannii</i>		1.99	0	0	0.22	0	0	0
12	<i>Scrippsiella sp.</i>		0	0	0	0	1.20	0	0.30
			9.99	2.85	6.84	2.73	11.45	7.23	3.92

Table 2.7 continued

No.	Biological name	Paleontological name	Density (Cysts g ⁻¹ dry sediment weight)						
			Stations (December, 2010)			Stations (March, 2012)			
			1	2	3	6	2	3	6
Heterotrophic species									
1	<i>Polykrikos</i> cf. <i>kofoidii</i>		0	0	0.62	0	0	0	0
2	<i>Protoperidinium avellanum</i>	<i>Brigantedinium cariacense</i>	3.99	7.62	2.48	1.59	6.63	3.61	0.30
3	<i>Protoperidinium denticulatum</i>	<i>Brigantedinium irregulare</i>	0	0.95	0	0.22	2.41	0.45	0
4	<i>Protoperidinium</i> sp. 1	<i>Echinidium</i> sp.	0	0	3.73	2.28	0.60	0	0
5	<i>Protoperidinium</i> sp. 2	<i>Lejeunecysta</i> sp. 1	0	0.95	0	0.22	0.60	0	0
6	<i>Protoperidinium</i> sp. 3	<i>Lejeunecysta</i> sp. 2	0	0	0	0.22	0	0	0
7	<i>Protoperidinium</i> sp. 4	<i>Lejeunecysta</i> sp. 3	0	0	0.62	0.22	2.41	0	0.30
8	<i>Protoperidinium</i> sp. 5	<i>Leipokatium</i> sp.	0	0	0.62	0	0.60	0	0.30
9	<i>Protoperidinium</i> sp. 6		1.99	0	0	0	0	0	0
10	<i>Protoperidinium leonis</i>	<i>Quinquecuspis concreta</i>	0	0.95	0	0	0	0	0
11	<i>Protoperidinium</i> sp. 7	<i>Quinquecuspis</i> sp.	1.99	0.95	0	0.22	0	0	0
12	<i>Protoperidinium conicum</i>	<i>Selenopemphix quanta</i>	1.99	2.85	0	1.59	0	0	0
13	<i>Protoperidinium subinermis</i>	<i>Selenopemphix altinctum</i>	0	0	0	0	1.20	0	0.30
14	<i>Protoperidinium nudum</i>	<i>Selenopemphix</i> sp. 1	0	1.90	4.35	0.22	0	0	0
15	<i>Protoperidinium</i> sp. 8	<i>Selenopemphix</i> sp. 2	0	2.85	0	1.59	0	0	0
16	<i>Protoperidinium</i> sp. 9	<i>Selenopemphix</i> sp. 3	0	0	1.24	0	0	0	0
17	<i>Protoperidinium</i> cf. <i>compressum</i>	<i>Stelladinium robustum</i>	0	0	0	0.45	0	0	0

Table 2.7 continued

No.	Biological name	Paleontological name	Density (Cysts g ⁻¹ dry sediment weight)						
			Stations (December, 2010)			Stations (March, 2012)			
			1	2	3	6	2	3	6
18	<i>Protooperidium</i> sp. 10	<i>Stelladinium</i> sp. 1	3.99	0	0	0	0	0	0
19	<i>Protooperidium</i> sp. 11	<i>Stelladinium</i> sp. 2	0	0	0.62	0	0	0	0
20	<i>Protooperidium</i> sp. 12	<i>Stelladinium</i> sp. 3	0	0	0.62	0.22	0	0	0
21	<i>Protooperidium pentagonum</i>	<i>Trinovantedinium capitatum</i>	0	0	0.62	0.68	1.20	0	0
22	<i>Protooperidium</i> sp. 13	<i>Trinovantedinium</i> sp.	0	1.90	0	0	0.60	0	0
23	<i>Protooperidium latissimum</i>		0	0	0.62	0.68	1.20	0	0
24	<i>Protooperidium</i> sp. 14	(Spiny round brown cyst)	1.99	0.95	3.11	1.14	1.20	3.16	0
25	<i>Protooperidium</i> sp. 15	(new form 1)	1.99	4.76	4.97	0.22	3.01	0.45	0
26	<i>Protooperidium</i> sp. 16	(new form 2)	0	4.76	0.62	0	0	0	0
27	<i>Protooperidium</i> sp. 17	(new form 3)	0	0	0.62	0	0	0	0
28	<i>Protooperidium</i> sp. 18	(new form 4)	0	0	2.48	0.45	0.60	0	0
29	<i>Protooperidium</i> sp. 19	(new form 5)	0	0	0.62	0	0	1.35	0
30	<i>Preperidium maumieri</i>	<i>Dubridinium caperatum</i>	0	2.85	1.86	0	1.80	0	0
31	<i>Oblea acanthocysta</i>		0	0	0	0.45	0	0	0
32	Diplopsalid group	Diplopsalid new cyst form	0	0.95	0	0.22	0	0	0
			17.99	35.27	30.49	11.18	22.91	10.85	1.20

CHAPTER 3: OCCURRENCES OF POTENTIALLY HARMFUL DINOFLAGELLATES

3.1. INTRODUCTION

Modern dinoflagellates comprise over 2,500 species worldwide (Hoppenrath et al., 2009), and approximately 76 species are recognized as harmful, causing water discoloration and mass mortalities of caged fishes, and producing biotoxins, which can accumulate in fish and shellfish (IOC-UNESCO web: <http://www.marinespecies.org/HAB/dinoflag.php>, accessed on 24 December 2012).

An increase in marine fish culture and shellfish farming is leading to an increase in reports of harmful events world-wide. Especially in Southeast Asia, concurrent with the recent economic progress of countries in this region, increasing number of reports concerning harmful algal blooms (HAB) have been coming out. For example, it has been reported; diarrhetic shellfish poisoning due to *Dinophysis* spp. in Singapore (Holmes et al., 1999) and the Philippines (Marasigan et al., 2001), paralytic shellfish poisoning due to *Alexandrium* spp. in Malaysia (Usup et al., 2002) and the Philippines (Relox and Bajarias, 2003), and *Pyrodinium bahamense* var. *compressum* in Malaysia, Brunei Darussalam, the Philippines and Indonesia (Azanza and Taylor, 2001). Blooms of *Gymnodinium catenatum* co-existed with the *Pyrodinium bahamense* var. *compressum* were reported from the Philippine (Fukuyo et al., 1993) and from Malaysia (Mohammad-Noor et al., 2002). Also fish-kills due to *Cochlodinium polykrikoides* were found in Malaysia (Anton et al., 2008) and the Philippines (Relox and Bajarias, 2003; Azanza et al., 2008), etc. These increases in HAB incidents are closely linked with increased scientific awareness of harmful species, increased utilization of coastal waters

for aquaculture, stimulation of plankton blooms by cultural eutrophication and/or unusual climatological conditions, and transport of dinoflagellate resting cysts either the ships' ballast water or associated with movement of shellfish stocks from one area to another (Hallegraeff, 1993).

In Myanmar, although such harmful events have not been reported so far, coastal development in Myanmar is proceeding at a rapid pace; currently large numbers of fish and shrimp aquaculture facilities are being established for export purposes. Marine finfish culture farms are mainly operating in the southern coastal areas, and shrimp aquaculture farms have increased in whole coastal areas, and the latter production was once over 46,000 tons in 2010 (Department of Fisheries, 2010). As consequence, many fisheries industries, such as fishmeal plants and processing plants, and other factories have also been constructed in the coastal areas. These coastal developments, along with the drastic economic progress in Myanmar, might lead to eutrophication of coastal areas and subsequent HAB events.

To seek the possibility of HAB in Myanmar, and if there are, to find ways for the risk-managements, phytoplankton studies focusing on potentially harmful species was conducted in this study. In there, accurate species identification is a ground-work for further HABs investigation. In the identification of harmful dinoflagellate species, basically morphological observation is a sole and indispensable criterion. However, sometimes only morphological observation is not sufficient and moreover difficult for some genus to understand exact species. This is because cellular morphology could sometime change due to the environment, life-cycle transformations and other influences, and culture cells can have more variable morphology than field materials (Hallegraeff, 2004). Indeed, many researchers now use molecular methods to gain clear

understanding on taxonomy over broad geographical ranges (Scholin et al., 1994; Hansen et al., 2000; Kim and Kim, 2007; Lilly et al., 2007; Collins et al., 2009; Anderson et al., 2012).

In the previous chapter, some of potentially harmful dinoflagellate species were listed. The aim of this chapter is to extract these species from the list and surmise their existence and occurrence off the Myeik coast, and discuss their potential implications in the region. For this purpose, as much as possible, ribosomal RNA gene (rDNA) analyzes were employed for confirmation of their species and phylogenetic positions. Moreover, as previously mentioned in the previous chapter, we had encountered notable red-tide event in March 2012. Since this would probably be a first report of red-tide in the region, here detail species identification and their regional phylogeny are given by accomplishing rDNA analyzes.

3.2. MATERIALS AND METHODS

3.2.1. Sampling

The details of the samplings were described in the previous chapter. Briefly, plankton net (20- μ m-mesh size) samples were collected around the Mali and Kadan Islands, southern Myanmar coastal area during three surveys (May 2010, December 2010 and March 2012). 50 ml of plankton samples were concentrated using a 10 μ m mesh to 15 ml total volume, and fixed with glutaraldehyde at final concentration of 1 %. During the March survey, some of plankton net samples were diluted in 500 ml bottle for live samples. For DNA analysis, concentrated plankton samples were fixed in 9 volumes of the standard saline ethanol fixative (a mixture of 25 ml of 90% ethanol, 2 ml H₂O, and

3ml 25× SET buffer [3.75 M NaCl, 25 mM EDTA, 0.5 M Tris-HCl, pH 7.8]) solution (Takahashi et al., 2005) and stored at -20°C.

3.2.2. Isolation and culture

At near the St. 6 in the March survey (2012), we found notable red-tide (see Chapter 2). Therefore clonal cultures of the composed species were established at on the site by capillary pipette isolation from the diluted live samples collected near the station. They were tentatively maintained in 1/10 IMK medium (Wako Jyunyaku Co, Japan). The culture tubes were carefully brought back to Hiroshima University, Japan, and kept in the incubator at a temperature of 25°C and an irradiance of 60 $\mu\text{mol m}^{-2}\text{s}^{-1}$ in a 12:12 h light : dark regime. Cell-growth was checked every day under an inverted light microscope. When the cell densities reached about 100 cells in each culture tube, cultures were transferred to plant-culture tubes, which containing 30 ml of sterilized f/2 medium (Guillard, 1975). The culture strains are named as PRRM01 for *P. rhathymum*, PRSM01 for *P. shikokuense* and ALAM01 for *A. affine*.

3.2.3. Morphological observation and identification

Morphological observations were carried out same method mentioned at previous chapter (Chapter 2). Since culture cells of *Prorocentrum shikokuense* possess thin cell wall than wild cells, fixation and dehydration methods were not used as others species. Culture *P. shikokuense* was washed with distilled water and dried with freeze drier (Aqua FD-6500, Kyowa, Japan), and coated with Pt in a coater (JFC-1600, JEOL).

Observation was made under a SEM (JSM-6390LV, JEOL). For armored dinoflagellates, designation of thecal plates tabulation was basically followed the Kofoidian system and particularly for the sulcal plates by Balech (1995). For the fixed unarmored dinoflagellates, such as *Gymnodinium catenatum*, species identification was also confirmed by DNA analysis as well as the light microscopy. All species identifications were made according to literatures (Taylor, 1976; 1975; Dodge, 1988; Balech, 1988; 1995; Larsen and Moestrup, 1992; Taylor et al., 1995; Steidinger and Tangen, 1997; Hoppenrath et al., 2009).

3.2.4. Analyzes of DNA sequences and their phylogenies

(DNA extraction from clonal culture)

The cultures (15 ml) of *Alexandrium* sp. and two *Prorocentrum* species, which were isolated near St. 6 in the March survey (2012), were harvested at mid-exponential growth phase by centrifugation (1,500 rpm, 5 min, 4°C). Supernatant was removed and the cell-pellet was stored frozen (-20°C) until further analysis. The frozen cell-pellets were thawed in ice box, and total DNA was extracted using a Takara Plant DNA Isolation Reagent Kit (code=9194, Takara Bio, Japan).

(Cell isolation from ethanol fixed sample)

Single cell or a chain of dinoflagellate was isolated individually under the light microscope, using a capillary pipette from the ethanol fixed samples collected as a manner mentioned above. The isolated cells were washed 3 times in Milli-Q water and

transferred into 0.2 ml PCR tube, which was primarily filled with 5 µl autoclaved Milli-Q water, and then stored frozen (-20°C) until further analysis.

(PCR amplification)

A set of primers, D1R and D2C (Scholin et al., 1994), was used for the amplification of D1-D2 regions in 28S rRNA gene (rDNA). Using TaKaRa Ex Taq (TaKaRa-Bio), approximately 700 bp of the 28S rDNA were PCR-amplified with the following thermal cycle conditions: an initial denaturing at 94°C for 5 min; 35 cycles of denaturing at 94°C for 1 min, annealing at 48°C for 1.5 min, 72°C for 0.5 min; and concluded with a final elongation step of 72°C for 7 min followed by a hold at 4°C. Denaturing and annealing cycles were increased to 40 cycles for single cell isolated samples. The amplified products were examined by 1.5% agarose gel containing ethidium bromide for DNA band visualization.

(DNA sequencing and phylogenetic analysis)

Amplified PCR products were subsequently cleaned by the Exo-SAP method (Dugan et al., 2002). DNA sequencing was performed using ABI PRISM 3130xl Genetic Analyzer (Applied Biosystem, USA) in Natural Science Center for Basic Research and Development, Genetic Experiment Division, Hiroshima University. Alignment and phylogenetic analyses for obtained sequences were carried out using MEGA Ver. 5.05 (Tamura et al., 2011). Together with the reference sequences of same or similar species obtained from GenBank data by BLAST search via MEGA 5, the nucleotide sequences

were aligned using Clustal W parameters. The alignments were also visually inspected and manually edited, and some gaps and all ambiguous sites in the alignments were removed. Phylogenetic tree of each species was inferred by using Maximum-Likelihood (ML) (Guindon and Gascuel, 2003). Distance matrices for ML analysis were calculated with appropriate model, estimated by MEGA, for each species. Bootstrap analyses were performed using 1000 replicates.

3.3. RESULTS

3.3.1. Morphological analysis

Twenty-one species of potentially harmful dinoflagellates were found around the Mali and Kadan Islands, southern Myanmar coastal area. These can be subdivided into two groups: one of them including shellfish toxin producing species such as *Alexandrium tamiyavanichii* Balech (Fig. 3.4), *Gymnodinium catenatum* Graham (Fig. 3.6), *Lingulodinium polyedrum* (Stein) Dodge (Fig. 3.7), *Gonyaulax spinifera* (Claparède & Lachmann) Diesing (Fig. 3.8), *Dinophysis caudata* Saville-Kent (Fig. 3.10), *D. miles* Cleve (Fig. 3.11), *D. rotundata* Claparède & Lachmann (Fig. 3.12), *Dinophysis infundibulus* Schiller (Fig. 3.1. m), *Prorocentrum rhathymum* Loeblich (Fig. 3.2), *Protoperidinium crassipes* (Kofoid) Balech (Fig. 3.1. l); the another group comprising of massive bloom (red-tide) forming species such as *Prorocentrum micans* Ehrenberg (Fig. 3.1. a-b), *P. sigmoides* Böhm (Fig. 3.1. c-e), *P. shikokuense* Hada ex Balech (Fig. 3.3), *Alexandrium affine* (Inoue & Fukuyo) Balech (Fig. 3.5), *Gonyaulax polygramma* Stein (Fig. 3.9), *Ceratium furca* (Ehrenberg) Claparède & Lachmann (Fig. 3.1. f-g), *C. fusus* (Ehrenberg) Dujardin (Fig. 3.1. h), *C. tripos* (Müller) Ehrenberg (Fig. 3.1. i),

Peridinium quinquecorne Abé (Fig. 3.1. j), *Scrippsiella trochoidea* (Stein) Balech ex Loeblich III (Fig. 3.1. k) and *Noctiluca scintillans* (Macartney) Kofoid & Swezy (Fig. 3.13). The morphological features of some potentially harmful dinoflagellates species are explained in the following.

Prorocentrum rhathymum Loeblich (Fig. 3.2. a-h)

The cells of *Prorocentrum rhathymum* from Myanmar water are somewhat oval in outline (Fig. 3.2. a-d). Cells are 27-39 μm long and 18-27 μm wide. Cell contains dark yellowish chloroplasts. Nucleus locates toward the posterior end (Fig. 3.2. a-c) and large pusule locates near the anterior end of the cell (Fig. 3.2. b), and pyrenoid absent. The cells were embedded in mucilage in culture condition and not actively motile. Periflagellar area is located in the apical excavation of the right valve with an apical spine. This can be seen as a small pointed spine in light microscopy (Fig. 3.2. c, arrow heads) and prominently as ear-shape in SEM micrographs (Fig. 3.2. d, e, arrows). Two flagella are shown to emerge from the apical depression (Fig. 3.2. b, arrow heads). Apical plates are not able to be clearly observed in the SEM micrographs. The valve surface is smooth, ornamented with rounded trichocyst pores of two different sizes (Fig. 3.2. f). Small pores (Fig. 3.2. f, arrow heads) are scattered randomly over the valves in lesser numbers. The larger pores are lying in shallow circular depressions (Fig. 3.2. f, arrows), and these are radially located near the valve margin rather than central (Fig. 3.2. d, g). Right valve is moderately convex and left valve is somewhat straight or slightly concave in central part (Fig. 3.2. g). There are about 70 trichocyst pores on the right valve including a row of 6-7 pores which locate near the apical excavation of the right

valve (Fig. 3.2. e, arrow heads) and about 80 pores on the left valve. The inner surface is smooth with rounded sac like base of large pores (Fig. 3.2. h, arrows) and openings of the small pores (Fig. 3.2. h, arrow heads). The intercalary band is obviously wide with horizontally striated smooth surface and without poroids (Fig. 3.2. g, arrow). *P. rhathymum* was identified based on the characteristic features: lack of pyrenoid, a row of six or seven trichocyst pores on the right valve near the periplagellar area, smooth valve surface, and small apical spine. *P. rhathymum* was detected at St. 6 in May (2010) and at Sts. 2 and 6 in March (2012) surveys.

Prorocentrum shikokuense Hada ex Balech (Fig. 3.3. a-k)

Cells of *Prorocentrum shikokuense* from Myanmar water are elongate and asymmetric with variable in shape such as sunflower seed shape, elongated rectangular shape and caudate shape. Cells size range between 17-22 μm in length and 5-12 μm in width. Cells were photosynthetic with yellowish chloroplast. Rounded nucleus is located posteriorly (Fig. 3.3. d, e). One side of the anterior end is somewhat extended than the other (Fig. 3.3. a, b, e, arrows). Periplagellar area is slightly concave (Fig. 3.3. f) and bears apical spine, which is difficult to be seen under light microscope. In the SEM micrographs, periplagellar area of the right valve is slightly concaved with ear-shaped collar protrusion which varied in shape and size (Fig. 3.3. i, k, arrow). The surface of the valves is densely covered with knob-like spines (Fig. 3.3. k, small arrows) and randomly ornamented with trichocyst pores (Fig. 3.3. g, arrows). The intercalary band is wide and striated with small channels and ornamented with dense rows of tiny knobs (Fig. 3.3. h, arrow). *P. shikokuense* was identified based on the characteristic features:

slightly extended the one side of anterior end, ear-shaped collar protrusion in the right valve of periflagellar area, densely cover the knob-like spines and randomly ornamented trichocyst pores on the valve surface, and well developed intercalary band. *P. shikokuense* was detected at Sts. 1, 4, 5 and 6 in March survey (2012).

Alexandrium tamiyavanichii Balech (Fig. 3.4. a-h)

Cells of *Alexandrium tamiyavanichii* from Myanmar water are round to slightly wider than long (Fig. 3.4. f). Cells range in size between 30-42 μm in length and 32-38 μm in width. The epitheca is conical shaped and wider than long (Fig. 3.4. c). The hypotheca is slightly longer than the epitheca (Fig. 3.4. f). The first apical plate (1') is large and wide rhomboidal shape, and is direct contact with the apical pore plate (Po) (Fig. 3.4. h). Posterior margin of the plat 1' is slightly concave. A small ventral pore is present in the posterior portion on the anterior right margin of 1' (Fig. 3.4. h, black arrow). The apical pore plate (Po) is wide and oval shaped with centrally located a large comma-shaped foramen, and large connecting pore (pc) is located near the right margin of the comma head (Fig. 3.4. h). The cingulum is deeply excavated (Fig. 3.4. c, f). The sulcus is deep and wide posteriorly (Fig. 3.4. f). The S.a. plate is long (Fig. 3.4. f) and has a trapezoidal-shaped precingular part (Fig. 3.4. c, arrow). Two wing-like sulcal lists project toward the antapex (Fig. 3.4. f, arrow). The round posterior attachment pore (Fig. 3.4. g, arrow) is present in the center of the posterior sulcal plate (S.p). *A. tamiyavanichii* was identified based on these characteristic features: the shape of precingular part, the shape of plate 1' and the shape of Po. These characters are distinctive features to distinguish between the morphologically similar species *A.*

cohorticula. *A. tamiyavanichii* was detected at Sts. 2 and 6 in May (2010) and at Sts. 1, 3, 5 and 6 in March (2012) surveys.

Alexandrium affine (Inoue & Fukuyo) Balech (Fig. 3.5. a-h)

Cells of *Alexandrium affine* from Myanmar water are approximately pentagonal in shape, generally a little longer than wide (Fig. 3.5. b). Cell size ranges 28-44 μm in length and 23-43 μm width. Cell contains yellowish chloroplast, and nucleus (n) was located centrally (Fig. 3.5. b). Commonly single cell form and chains of two cells are rarely found in the culture condition. The epitheca is longer than the hypotheca. Apical pore plate (Po) is narrow and long with a ventrally located small oval-shaped foramen (Fig. 3.5. e), and direct connects with 1' plate (Fig. 3.5. e, black arrow). The connection pore (pc) is located above the apical pore (Fig. 3.5. f). Plate 1' is long rhomboidal shaped with long and slightly convex left margin (Fig. 3.5. e), and has a small ventral pore at the half of the right margin of plate (Fig. 3.5. e, white arrow). Plate 3' is asymmetrically hexagonal shape (Fig. 3.5. e). Plate 6'' is longer than wide, posterior left margin is long and concave and anterior left margin is short and straight (Fig. 3.5. c). The cingulum is descending and deeply excavated. Anterior sulcal plate (S.a.) is somewhat longer than wide (Fig. 3.5. c), anterior margin is nearly straight and right margin is somewhat convex. Posterior sulcal plate (S.p.) is longer than wide, with well projected anterior ends. S.p. has obvious rounded pore, which located near the half of the right margin linked with a small channel (Fig. 3.5. g, arrow). *A. affine* was identified on these characteristic features, and distinguished from other *Alexandrium* species by a

distinctive character of the shape of Po pate. *A. affine* was detected at St. 3 in December (2011) survey, and at Sts. 4 and 6 in March (2012) survey.

Gymnodinium catenatum Graham (Fig. 3.6. a-e)

Cells of *Gymnodinium catenatum* from Myanmar water are observed in long chain as 4, 8 or 16 cells and occasionally more cells. Cell size ranges between 30-45 µm long and 25-40 µm wide (might be decreased in size by fixation). The cells contain numerous chloroplasts. The nucleus is located in the central part of the cell (Fig. 3.6. d, arrow). *G. catenatum* was identified based on the distinct characters of long chain formation and nucleus position. The characters of long chain formation and large cell size are distinct character to distinguish among other *Gymnodinium* species. *G. catenatum* was detected at Sts. 1 and 3 in March (2012) survey.

Lingulodinium polyedrum (Stein) Dodge (Fig. 3.7. a-f)

Cells of *Lingulodinium polyedrum* from Myanmar water are angular, pentagonal and polyhedral in shaped (Fig. 3.7. a,b). Cell size ranges from 39-55 m in length and 35-53 m in width. Apical horn or antapical spines are absent. Thecal plates are coarsely areolated. Distinct ridges are present along the plate sutures (Fig. 3.7. c, e, f). The epitheca has shoulders, and an off-center apex which is flattened or slightly pointed (Fig. 3.7. c). The apical pore plate (Po) contains a raised inner elliptical ridge (Fig. 3.7. e). The first apical plate (1') is long and narrow, directly contacts with the Po and bears a ventral pore on its right side (Fig. 3.7. c). The cingulum is deeply excavated. The sulcus

is deep and slightly invades to the epitheca and widens posteriorly (Fig. 3.7. d). The hypotheca has straight sides and a truncated antapex (Fig. 3.7. b, d). *L. polyedrum* was detected at Sts. 1 and 6 in March (2012) survey.

Gonyaulax spinifera (Claparède & Lachmann) Diesing (Fig. 3.8 a-c)

Cells of *Gonyaulax spinifera* from Myanmar water are small, longer than width. Cells size ranges from 24-42 μm long and 32-35 μm wide. Cell is asymmetry due to torsion. The epitheca bears a small apical horn. The cingulum is deeply excavated. The cingulum starts median ventrally, and turning spirally to the left. The sulcus starts at the beginning of the cingulum and twists posteriorly. The sulcus is deep and wider posteriorly (Fig. 3.8. a, b). The hypotheca bears a few antapical spines (Fig. 3.8. c). *G. spinifera* was identified based on these morphological characters. *G. spinifera* was distinguished from other similar species of *G. digitale* and *G. digenesis* by the distinct features of apical horn, cingulum width and amount of overlapping. *G. spinifera* was detected at Sts. 1, 4, 5 and 7 in May (2010), at St. 3 in December (2011) and at St. 6 in March (2012) surveys.

Gonyaulax polygramma Stein (Fig. 3.9. a-f)

Cells of *Gonyaulax polygramma* from Myanmar water are pentagonal in shape (Fig. 3.9. a-f) and ranges from 27-58 μm long and 25-40 μm wide in size. The epitheca is convex to angular with prominent apical horn. The cingulum is deeply excavated and slightly twisted, somewhat overlapping (Fig. 3.9. a,b,d). The sulcus is slightly excavated and

widened posteriorly (Fig. 3.9. d). The hypotheca truncates with straight sides and bears antapical spines (Fig. 3.9. d, f). Thecal plates are ornamented with longitudinal ridges (Fig. 3.9. a-f). *G. polygramma* was identified based on these morphological characters. *G. polygramma* was detected at St. 2 at May (2010), at St. 3 in December (2011) and at Sts. 1, 3 and 6 in March (2012) surveys.

Dinophysis caudata Saville-Kent (Fig. 3.10. a-g)

Cells of *Dinophysis caudata* from Myanmar water are large, long and laterally compressed. Cells size ranges from 72-100 μm in length and 35-50 μm in dorso-ventral width (excluding the left sulcal list). Epitheca is extremely small. The hypotheca is large irregularly sub-ovate, which comprises four large plates, and ventral margin is generally straight or undulate along the body. The dorsal margin is slightly concave along the anterior half of the hypotheca and straight in the posterior half, which lined with small knob-like spine (Fig. 3.10. f). The hypotheca has a long ventral projection, which extended posteriorly. The extended process varies in length and shape (Fig. 3.10. b, d, e), and is often toothed on its posterior end (Fig. 3.10. c, e, arrow). Left sulcal list (LSL) is long and extends to half of the total length of the cell and widest at the base. Thecal plates are thick and strongly areolated, each areolae with a pore (Fig. 3.10. f). The small epitheca is hidden in lateral views. The cingulum is narrow with two well-developed lists, anterior cingular list (ACL) and posterior cingular list (PCL), supported by ribs (Fig. 3.10. f). Both cingular lists are projected anteriorly. The ACL is wide and deep funnel obscuring the epitheca (Fig. 3.10. c-f). LSL is supported by three ribs. A right sulcal list (RSL) is shorter than left sulcal list (LSL) and narrow posteriorly. *D. caudata*

was detected at Sts. 1, 2, 4 and 5 in May (2010), at St. 1 in December (2011) and at Sts. 1, 3, 4, 5 and 6 in March (2012) surveys.

Dinophysis miles Cleve (Fig. 3.11. a-d)

Cells of *Dinophysis miles* from Myanmar water are large and antero-posteriorly elongated with two long projections: dorsal and posterior projections. Cells size range between 120-150 μm long. Epitheca is small. Ventral side of hypotheca is undulated and dorsal side is concaved anteriorly and extended to the dorsal projections. The distal end of projection bends posteriorly, which lines with small wing (Fig. 3.11. d, arrow). Posterior projection is longer than dorsal projection. Anterior cingular list (ACL) is wide, small funnel shape, supported by many ribs (Fig. 3.11. a). Left sulcal list (RSL) sometime extends until one third of the length of posterior projection and supports with three ribs. Thecal plates are thick with round areolae. *D. miles* was detected at Sts. 1 and 2 in May (2010) survey.

Dinophysis rotundata Claparède & Lachmann (Fig. 3.12. a-c)

Cells of *Dinophysis rotundata* from Myanmar water are broadly rounded with convex ventral and dorsal margins. Cells have numerous vacuoles and a posteriorly located nucleus (n) (Fig. 3.12. a). Cells size ranges from 34-50 μm in length and 30-41 μm in width. The slightly rounded epitheca is convex above the cingulum. The cingulum bears two narrow well developed lists: an anterior cingular list (ACL), and a posterior cingular list (PCL) (Fig. 3.12. b, arrows). The left sulcal list (LSL) is narrow and wider

posteriorly (Fig. 3.12. b) supported by three ribs. The right sulcal list (RSL) is narrower than LSL and extend until the third rib of LSL. The hypotheca comprises four large plates, the ventral margin is slightly concave at the half of the LSL. The dorsal margin is convex. Posterior part is rounded. Thecal plates are areolated, and some areolae with a pore (Fig. 3.12. b,c). *D. rotundata* was detected at St. 3 in May (2010) and at Sts. 3 and 4 in March (2012) surveys.

Noctiluca scintillans (Macartney) Kofoid & Swezy (Fig. 3.13. a-f)

Cells of *Noctiluca scintillans* from Myanmar water are red-colored, large, balloon-like and sub-spherical (Fig. 3.13. a-c). Cells size range from 155-1400 μm in diameter. A large eukaryotic nucleus (n) is located near the ventral groove (Fig. 3.13. A). The ventral groove is deep and wide (Fig. 3.13. b, arrow). The prominent tentacle is extended posteriorly and slightly twisted in fixed specimens (Fig. 3.13. c, arrow). *N. scintillans* was detected at Sts. 1, 2, 3 and 6 in March (2012) survey.

3.3.2. DNA phylogeny

ML phylogenetic tree for *Prorocentrum rhathymum* strain (PRRM01) was constructed using the Kimura-2-parameter model with gamma distribution (G) (Fig. 3.14). The D1-D2 region of 28S rDNA sequences (698 bp) of this species was aligned with eight species of *Prorocentrum* in database. Two strains of *P. triestinum* (Korea and China) were used as the outgroup species. ML tree showed two major clades. First clade further branched into four major groups: the first group comprises four strains of *P. rhathymum*

(Florida Bay, Malaysia, Iran, Australia); the second group comprises three strains of *P. mexicanum* (USA, Denmark) and one strain of *P. rhathymum*; the third group comprises *P. sigmoides* and *P. gracile*; and the fourth group comprises four strains of *P. micans* (UK, USA, Korea). The second lower clade comprises two strains of *P. dentatum* (China and South Pacific) and two strains of *P. minimum* (China and East China Sea). The Myanmar strain of *P. rhathymum* belongs to the first *P. rhathymum* group in the first *P. rhathymum* – *mexicanum* clade, and nests within the four strains of *P. rhathymum* from Florida Bay (FIU9), Sabah, Malaysia (NMN016), Iran and Australia (PRHI01) at the bootstrap value of 93%. Based on this phylogenetic result, the current species could be confirmed as *P. rhathymum*. However, six bases substitution among 698 bp was found in the Myanmar strain comparing to other *P. rhathymum* strains, and this seems to be intraspecies variation.

ML phylogenetic tree for *Prorocentrum shikokuense* strain (PRSM01) was constructed using the Jukes-Cantor model (Fig. 3.15). The D1-D2 region of 28S rDNA sequences (694 bp) of *P. shikokuense* was determined with five *Prorocentrum* species. *Prorocentrum* sp. of strain FIU22 was used as the outgroup species. ML tree showed two major groups. First group comprises four strains of *P. donghaiense* (East China Sea and China) and two strains of *P. dentatum* from China. The second group comprises six strains of *P. minimum* (Spain, USA, Korea and China) and *P. balticum* strain from Korea. The Myanmar strain of *P. shikokuense* belongs to the first group of *P. donghaiense* (East China Sea and China). Based on this phylogenetic result, the current Myanmar strain might be identified under the name of *P. donghaiense*. However, rDNA sequence of *P. donghaiense* (East China Sea strain) was identical to that of *P. shikokuense* from Japan and these two species are now treated as same species (Takano

and Matsuoka, 2011). Since *P. donghaiense* Lu and Goebel (2001) is a junior synonym of *P. shikokuense*, which was formerly identified as *P. shikokuensis* by Hada (1975), we identified the Myanmar strain as *P. shikokuense*, which is still valid and prior in nomenclatural position.

ML phylogenetic tree for *Alexandrium affine* strain (ALAM01) was constructed using the Tamura-Nei model with gamma distribution (G) (Fig. 3.16). The D1-D2 region of 28S rDNA sequences (703 bp) was aligned with 22 *Alexandrium* data. *A. andersoni* of USA strain was used as the outgroup species. The current strain belongs to the clade, which comprising *A. affine* from various geographic areas (Mexico, China, Japan, South China Sea, Malaysia, Gulf of Thailand, France, Spain and Australia). Among this clade, the current strain has genetic identity with a *A. affine* strain (CU1) from the Gulf of Thailand. Based on phylogenetic result, the current Myanmar strain is confirmed as *A. affine*, and it was closely related with *A. affine* from The Gulf of Thailand strain.

ML phylogenetic tree for *Alexandrium tamiyavanichii* was constructed using the Tamura-Nei model with gamma distribution (G) (Fig. 3.17). The D1-D2 region of 28S rDNA sequences (690 bp) of the current species was aligned with 13 *Alexandrium* data. *A. taylori* from Italy strain (AY4T) was used as the outgroup species. *A. tamiyavanichii* shows two distinct clades. First clade comprises *A. tamiyavanichii* from Japan strains (TAMI 2207, TAMI2201, TAMI22012), Brazil strains (PSAA1, PSII, PSAB2) and *A. cohorticula* from the Straits of Malacca. The first clade sub-branched into two groups, one group comprises Japan strains of *A. tamiyavanichii* and *A. cohorticula* from the Strait of Malacca, and the other group comprises Brazil strains of *A. tamiyavanichii*. The Myanmar sequence belongs to the first group, and shows genetic identity with *A.*

tamiyavanichii from Japanese strains. Based on this phylogenetic result, the current cells occurring in Myanmar water is confirmed as *A. tamiyavanichii*.

ML phylogenetic tree for *Gonyaulax polygramma* was constructed using the Tamura-Nei model with gamma distribution (G) (Fig. 3.18). The D1-D2 region of 28S rDNA sequences (703 bp) of the current species was aligned with 12 *Gonyaulax* data, two strains of *Alexandrium pseudogonyaulax* and one strain of *Protoceratium reticulatum*. *Lingulodinium polyedrum* of Mexico strain was used as the outgroup species. ML tree showed three clades. First clade comprises seven strains of *Gonyaulax* species. The second clade comprises two strains of *Alexandrium pseudogonyaulax*, *Protoceratium reticulatum*, *Gonyaulax cochlea* and *G. verior*. The third clade comprises two strains of *Gonyaulax spinifera* from the Andratic Sea and one strain of *G. spinifera* from New Zealand. The Myanmar sequence is belonging to the first clade, which composes of two strains of *G. baltica*, *G. elongata*, *G. digitale*, *G. membranacea*, *G. spinifera* from USA and *G. polygramma* from South Korea. Among this clade, the current Myanmar sequence is genetically closely related with the strain of *G. polygramma*. Based on this phylogenetic result, the Myanmar species is confirmed as *Gonyaulax polygramma*.

ML phylogenetic tree for *Dinophysis caudata* was constructed using the Hasegawa-Kishino-Yano model (Fig. 3.19). The D1-D2 region of 28S rDNA sequences (731 bp) is aligned with 16 *Dinophysis* data. *D. hastata* from the Pacific Ocean is used as the outgroup species. ML tree showed one major clades. This clade has two major groups: first group comprises nine data of *D. caudata* from various geographic regions (Pacific Ocean, Japan, Vietnam, France, and USA); second group comprises two data of *D. tripos* (Japan and France) and three data of *D. miles* (Indian Ocean, China, Vietnam).

D. acuta from Scottish Coastline and *D. acuminata* from Korea are separately branched in this clade. The current Myanmar sequence belongs to the first group and shows identity with three data of *D. caudata* from Japan, two data of *D. caudata* from Vietnam, one data from France and one data from USA. Based on this phylogenetic result, the current *Dinophysis* cells in Myanmar are identified as *Dinophysis caudata*.

ML phylogenetic tree for *Dinophysis rotundata* was constructed using the Tamura-Nei model with gamma distribution (G) (Fig. 3.20). The D1-D2 region of 28S rDNA sequences (701 bp) was aligned with 11 *Dinophysis* data. Two data of *D. parvula* in Japan was used as the outgroup species. ML tree showed two major clades. The first clade comprises *D. odiosa*, *D. schroederi*, *D. norvegica* and *D. acuminata*. The second clade comprises *D. parvula* from the Pacific Ocean and three *D. rotundata* from Japan, France and Norway. The Myanmar sequence belongs to the second clade and closely related with the group of three *D. rotundata* data. Based on this phylogenetic result, the current cells in Myanmar are confirmed as *D. rotundata*.

ML phylogenetic tree for *Gymnodinium catenatum* was constructed using the Tamura-Nei model with gamma distribution (G) (Fig. 3.21). The D1-D2 region of 28S rDNA sequences (716 bp) was aligned with 14 *Gymnodinium* data. *Akashiwo sanguinea* of strain JL36 was used as the outgroup species. ML tree showed two major clades. First clade comprises *G. microreticulatum*, *G. nolleri* and eight strains of *G. catenatum* (Korea, Algeria, China, Spain, Japan, South Australia, Singapore, Hong Kong and Denmark). The second clade comprises *G. impudicum*, *G. fuscum* and two strains of *G. aureolum* (Denmark and USA). The Myanmar sequence belongs to the first clade and shows identity with the all strains of *G. catenatum*. Based on this phylogenetic result, the current cells occurring in Myanmar are confirmed as *G. catenatum*.

3.4. DISCUSSION

Harmful algal blooms (HAB), such as red tides and shellfish poisonings, have yet to be reported on the Myanmar coast. Nevertheless, various potentially harmful species were identified in this study. A total of 21 species of potentially harmful dinoflagellate species were found in the surveys and identified by general morphological features. Among them, 10 species were identified with detail morphological, and some of them were also conducted species confirmation by DNA analysis.

3.4.1. Species confirmation and their phylogenetic position

P. rhathymum was originally described by Loeblich (1979) from Cinnamon Bay, Virgin Island. Morphology of *P. rhathymum* and *P. mexicanum* was taxonomically confused so far due to overlapping morphological characters. Cortés-Altamirano and Sierra-Beltrán (2003) described these two species with detail morphological differences of unique characters such as apical spine, presence or absence of pyrenoid, trichocyst pores around the periflagellar area. In my study, the morphological characters such as cells shape and size, rather smooth valve with a small number of trichopores in *P. rhathymum* coincides with an original description of *P. rhathymum* (Loeblich et al., 1979) and other descriptions from Japan (Fukuyo, 1981), Malaysia (Mohammad-Noor et al., 2005), Tasmania (as oyster spat mortalities: Pearce et al., 2005) and Mexican Pacific (as *P. mexicanum*: Hernández-Becerril et al., 2000). Cells of *P. rhathymum* from Malaysia (strain NMN016) (Mohammad-Noor et al., 2005) showed different characters of two wing-like structures from periflagellar area and possessing a pyrenoid from the original description. Pyrenoid was not observed in the cells of *P. rhathymum* in this study, while

two wing-like structures were observed as Malaysian strain NMN016. Strain of *P. rhathymum* from Malaysia was reported as okadaic acid producer by Caillaud et al. (2010). However this toxic strain was smaller than the Myanmar strains. Massive fish kill of wild and cultured fish event by *P. rhathymum* was reported as *P. mexicanum* from the Kuwait Bay (Al-Yamani et al., 2004). Cell lengths of *P. rhathymum* (44-46 µm) from sediments of Kuwait Bay (Al-Yamani and Saburova, 2010) were longer than Myanmar specimens, however other characters were overlapped. The sequence of *P. rhathymum* Myanmar strain (PRRM01) showed 93% genetic identity with *P. rhathymum* strain FIU9 from Florida Bay, strain NMN016 from Malaysia, strain PRHI01 from Australia and from Iran (Oman Sea) (GenBank JN020161). Based on these morphology and genetic results, Myanmar strain *P. rhathymum* (PRRM01) is closely related with *P. rhathymum* from Malaysia waters and Iran, Oman Sea area. It should be noted here that the strain from Florida Bay (FIU9) was reported to be toxic (An et al., 2010) or *P. rhathymum* from Kuwait Bay cause massive fish kills (Al-Yamani et al., 2004). However Myanmar strain was not exactly situated within these harmful strains, and its exact identity is still unclear.

The morphology of *P. shikokuense* from this study was identical with original description of Hada (1975) and the detail description of Takano and Matsuoka (2011), and also coincided with the description of *P. donghaiense* from East China Sea by Lu et al. (2005). SEM micrographs of *P. shikokuense* from this study showed slightly shrink by using of culture cells, however the important characters of concave periflagellar area, large ear-shaped collar structure, valve surface ornamentation with trichocyst pores and knob-like spines, and intercalary band with row of tiny knobs were clearly observed. Phylogenetic result also showed the genetic identity of *P. shikokuense* Myanmar strain

(PRSM01) with four strains of *P. donghaiense* and two strains of *P. dentatum* from Chinese waters. Although Myanmar strain (PRSM01) closely related with *P. donghaiense* and *P. dentatum* in genetically, I named the Myanmar strain as *P. shikokuense* under the nomenclatural priority. The identity of morphology and molecular data of *P. shikokuense* from Uwajima Bay and Iwamatsu Bay from Japan and *P. donghaiense* from East China Sea have been reported by Takano and Matsuoka (2011). Close genetic relation was also found between Myanmar strain of *P. shikokuense* and *P. donghaiense* from East China Sea strain. This molecular results showed the extend distribution of *P. shikokuense* from the East Asia waters to the Southeast Asia waters of the Indian Ocean area.

Alexandrium affine was originally described as *Protogonyaulax affinis* by Fukuyo et al. (1985), and Balech (1995) reported as *A. affine* latter. This species widely distributes in Europe, North America, Asian and Australian waters. The morphology of the specimens from Myanmar water was identical with original descriptions of Fukuyo et al. (1985) and Balech (1995), and also with the description of *A. affine* from Strait of Malacca, Malaysian water (Usup et al., 2002) and Vietnamese waters (Nguyen-Ngoc, 2004; Hong et al., 2008). Phylogenetic result showed the genetic relation of the strain of Myanmar (ALAM01) with other *A. affine* strains from various geographical areas such as Mexico, China, Japan, Malaysia, Gulf of Thailand, France, Spain and Australia. Among these strains, Myanmar strain was closely related with strain CU1 from the Gulf of Thailand, which locates closest geographical region with Myanmar waters. This phylogenetic result also showed the low genetic diversity *A. affine* and it agree the suggestion of Scholin et al. (1994) as *A. affine* has a unique ribotype within the genus *Alexandrium*.

A. tamiyavanichii was originally described by Balech (1994) from the Gulf of Thailand. This species distributes in South America, East Asia and Southeast Asian waters. Morphology of *A. tamiyavanichii* isolated from Myanmar water was identical with the description of Balech (1995). The phylogenetic results also showed the genetic relation of *A. tamiyavanichii* from this study with the other localities (Japan, Brazil) and *A. cohorticula* from the Strait of Malacca. Molecular results from this study clearly showed that the *A. tamiyavanichii* isolated from Myanmar water was closely related with the toxic strains of *A. tamiyavanichii* isolated from Harima Nada of the Seto Inland Sea, Japan (TAMI2201, TAMI22012, TAMI2207) reported by Kim et al. (2004). Note that *A. cohorticula* is taxonomically accepted as separate species.

The morphology of *Gonyaulax polygramma* isolated from Myanmar was identical to the detail description of Dodge (1988). Phylogenetic result also confirmed the cells isolated from Myanmar water as *G. polygramma*. This species is not toxic, but it causes massive blooms. *G. polygramma* red-tides have been reported from many geographical areas such as Japan (Koizumi et al., 1996), South Africa (Grindley and Taylor, 1962) and Hong Kong (Lam and Yip, 1990). During the *G. polygramma* bloom in Uwajima Bay, Japan, mass mortalities of culture and wild fishes and shellfish stocks due to oxygen depletion were reported by Koizumi et al. (1996), and the same incident of fish and invertebrates death also occurred in False Bay, near Cape Town (Grindley and Taylor, 1962).

The morphology of *G. catenatum* was identified only based on the shape and size of cells body and nucleus position under the fixed specimens in this study. The identification was then confirmed by the phylogenetic result. This result showed the close genetic identity of *G. catenatum* from Myanmar water with *G. catenatum* from

various geographic regions. It has been reported that *G. catenatum* strains from different geographic areas have significant physiological variations (Hallegraeff et al., 2012).

The morphology of *Dinophysis caudata* was identical to the later detail descriptions of Taylor et al. (1995) and Larsen and Moestrup (1992). The cells of *D. caudata* isolated from Myanmar waters showed wide morphological variation even from the same area (Fig.3.10. b, d, e). Nguyen (2009) also reported the morphological variation of *D. caudata* in Vietnamese water. Phylogenetic result showed the genetic identity *D. caudata* from Myanmar water with *D. caudata* from various geographic regions. It suggests that *D. caudata* has low genetic diversity in the analyzed locus, however high morphological diverse within intraspecies level.

The morphology of *Dinophysis rotundata* was identical to the later detail descriptions of Taylor et al. (1995) and Larsen and Moestrup (1992). Phylogenetic result showed genetic relation of *D. rotundata* from Myanmar water with *D. rotundata* from Japan, France and Norway. DSP toxin production of *D. rotundata* has been reported from Mutsu Bay, Japan (Lee et al., 1989), however *D. rotundata* from Atlantic coast did not show reaction against the DSP-antibody (Cembella, 1989).

Morphology of *G. spinifera* isolated from Myanmar water was identical to the detail description of Hoppenrath et al. (2009). *Gonyaulax spinifera* (Fig. 3.8) was detected in all the surveys (May, December and March). YTXs production of *G. spinifera* was reported from New Zealand (Rhodes et al., 2006) and the detection of YTXs in mussels associated of *G. spinifera* was reported from the north-western coasts of the Adriatic Sea (Riccardi et al., 2009).

Morphology of *L. polyedrum* isolated from Myanmar water was identical to the original description of Dodge (1989). *L. polyedrum* (Fig. 3.7) was detected in the March survey. Blooms of *L. polyedrum* have been reported from several locations such as California (Sweeney, 1975), Arabian Sea (Currie et al., 1973) and Spain (Margalef, 1956). YTXs production of cultured *L. polyedrum* was reported from Spain (Paz et al., 2004), and *L. polyedrum* strains from California (Armstrong and Kudela, 2006).

The morphology of *Noctiluca scintillans* was identified based on its distinct characters of ventral groove, tentacle and nucleus. Blooms forming species of *Noctiluca scintillans* (red type) was detected at Sts. 1, 2, 3 and 6 in March (2012) survey. *N. scintillans* widely distributes in temperate, subtropical and tropical regions.

3.4.2. Potential implications of red-tide forming species

In regard to red-tide, *Prorocentrum micans* and *P. sigmoides*, which may cause red coloration of oysters or oxygen depletion due to massive blooms (Pastoureaud and Chrétiennot-Dinet, 2003; Lee et al., 2005), were detected, mainly in the May (2010) and March (2012) surveys. The common red-tide forming species *P. shikokuense* was found in the March (2012) survey. *P. shikokuense* had been once reported as *P. donghaiense* and it was the major organism causing red tide in Chinese coastal water (Lu and Goebel, 2001). *Ceratium fusus* and *C. furca* may potentially cause oxygen depletion or damage to finfish gills and should be listed as harmful also in Myanmar area. Further red-tide forming species of *N. scintillans* was detected in the March survey. The bloom of *N. scintillans* may cause large scale mortality of caged fish (Smayda, 1997) and other finfishes through oxygen depletion, gill clogging and production of NH₄ (Okaichi and

Nishio, 1976; Naqvi et al., 1998). A linkage of red *Noctiluca* (red type: lack endosymbionts) blooming events and progressive eutrophication of coastal waters was reported from the Romanian Black Sea (Porumb, 1992) and from the southwest coast of India (Padmakumar et al., 2010).

Although it is possible that our fixation methods were not suitable for long storage, species lethal to fish or bivalves such as species of the genera *Karenia* and *Cochlodinium*, and *Heterocapsa circularisquama* Horiguchi, were not observed on these occasions.

3.4.3. Potential implications of shellfish poisoning causative species

Latent events of shellfish poisonings should be of more concern in this area. In this study, *Alexandrium tamiyavanichii*, a producer of potent toxin causing PSP was detected in the May (2010) and March (2012) surveys, but not in the December (2010) survey. In 2007, high cell density of *A. tamiyavanichii* and *G. catenatum* from Myanmar waters (the offshore area of Kadan Island and near the Gulf of Martaban) were reported in February (Boonyapiwat et al., 2007). Karunasagar et al. (1990) also reported an outbreak of PSP following consumption of clams harvested from an estuary near the City of Mangalore, southwest India, which caused the death of an infant. The toxin profiles of the clams corresponded to those of a strain of *A. tamiyavanichii* isolated from Thailand (Karunasagar et al., 1990). Based on these previous reports, together with our current findings, occurrences of *A. tamiyavanichii* seem to be extending to the entire Bay of Bengal. Another PSP-causative species, *Gymnodinium catenatum*, was also previously reported from the Myanmar waters by Boonyapiwat et al. (2007); in our

surveys, vegetative cells of *G. catenatum* were detected in Sts. 1 and 3 of the March (2012) survey and its cysts were detected in both surveys (December and March). The reports on the occurrence of *G. catenatum* in Southeast Asian water have increased: Manila Bay of Philippines (Fukuyo et al., 1993), Kota Kinabalu, Malaysia (Mohammad-Noor et al., 2002), Singapore (Holmes et al., 2002), Lombok, Indonesia (Sidharta and Adyadi, 2007) and Thailand (Lirdwitayaprasit et al., 2008). In Myanmar, bivalve cultures have not yet been introduced at a successful level (FAO and NACA, 2003), however domestic consumption of oysters is potentially high, and varieties of bivalves are sold in local markets. Under such circumstances, monitoring of PSP-causative species should be conducted for safer shellfish consumption, especially in post- and pre-rainy seasons.

Not only awareness of PSP, but also the occurrence of *Dinophysis*, which contains causative species of DSP, should be concerning. In my study, potentially toxic species of *Dinophysis caudata*, *D. miles*, *D. rotundata* and *D. infundibulus* were detected sporadically, and *D. caudata* was detected in all surveys (May, December and March). *D. caudata* widely distributes in tropical and warm temperate coastal waters and may occur abundantly (Holmes et al., 1999; Marasigan et al., 2001). Although little is known about actual DSP incidences in tropical waters (Hallegraeff, 1993), DSP toxins in green mussels *Perna viridis* and an occurrence of *D. caudata* in the Johor Strait, Singapore, were reported by Holmes et al. (1999). During blooms of *D. caudata* and *D. miles* in Spain Bay, Philippines, high-level accumulations of DSP toxins in green mussels were also reported (Marasigan et al., 2001). Successful culture experimental data show growth rates of *D. caudata* as high as 1.03 division day⁻¹, and this species is able to grow for a few days without prey (Nishitani et al., 2008). Attention must be paid

of DSP events off the Myanmar coast due to *D. caudata* blooms, in order to predict possible outbreaks of DSP. Furthermore, potentially okadaic acid (OA) producing species of *Prorocentrum rhathymum* was detected in the May (2010) and March (2012) surveys. In the May survey, cells clumps of *P. rhathymum* were detected in St. 6, which located at the southern part of Kadan Island. In the March survey, the red-tide of *P. rhathymum* was encountered near the St. 6, which located between the mainland coast and northeastern coast of Kadan Island. In the toxicological researches, *P. rhathymum* was previously reported to produce haemolytic (Nakajima et al., 1981) and/or fast acting methanol soluble toxins (Pearce et al., 2005), and have lethal effect for *Artemia nauplii* (Aligizaki et al., 2009). In these, OA was not detected in *P. rhathymum*, but recently shown in the Florida Bay (An et al., 2010) and Sabah, Malaysia (Caillaud et al., 2010).

Potentially yessotoxins (YTXs) producing species of *G. spinifera* was detected in all surveys (May, 2010; December, 2010; March, 2012) and that of *L. polyedrum* was detected in March survey. YTXs production of *G. spinifera* from New Zealand was reported by Rhodes et al. (2006). YTXs production of cultured *L. polyedrum* was reported from Spain (Paz et al., 2004), and *L. polyedrum* strains from California (Armstrong and Kudela, 2006). The linkage of yessotoxins detection in Adriatic mussels and the presence of *Protoceratium reticulatum* and *Lingulodinium polyedrum* species was firstly reported from the north-western coasts of the Adriatic Sea in 1995 (Ciminiello et al., 1997), and then Riccardi et al. (2009) reported the detection of YTXs in mussels associated with the presence of *G. spinifera* in the same area in late 2006.

In this study, the existence of potentially harmful dinoflagellate species around the Mali and Kadan Island, southern Myanmar coastal area, was proved by the detail

observation of both morphologically and genetically. The results showed the high diversity of potentially harmful dinoflagellate species in the May and March surveys, both of these two surveys represented the later part of dry season. This study supports an idea for the dinoflagellate monitoring and to pay more attention on the HAB awareness especially in this late dry season.

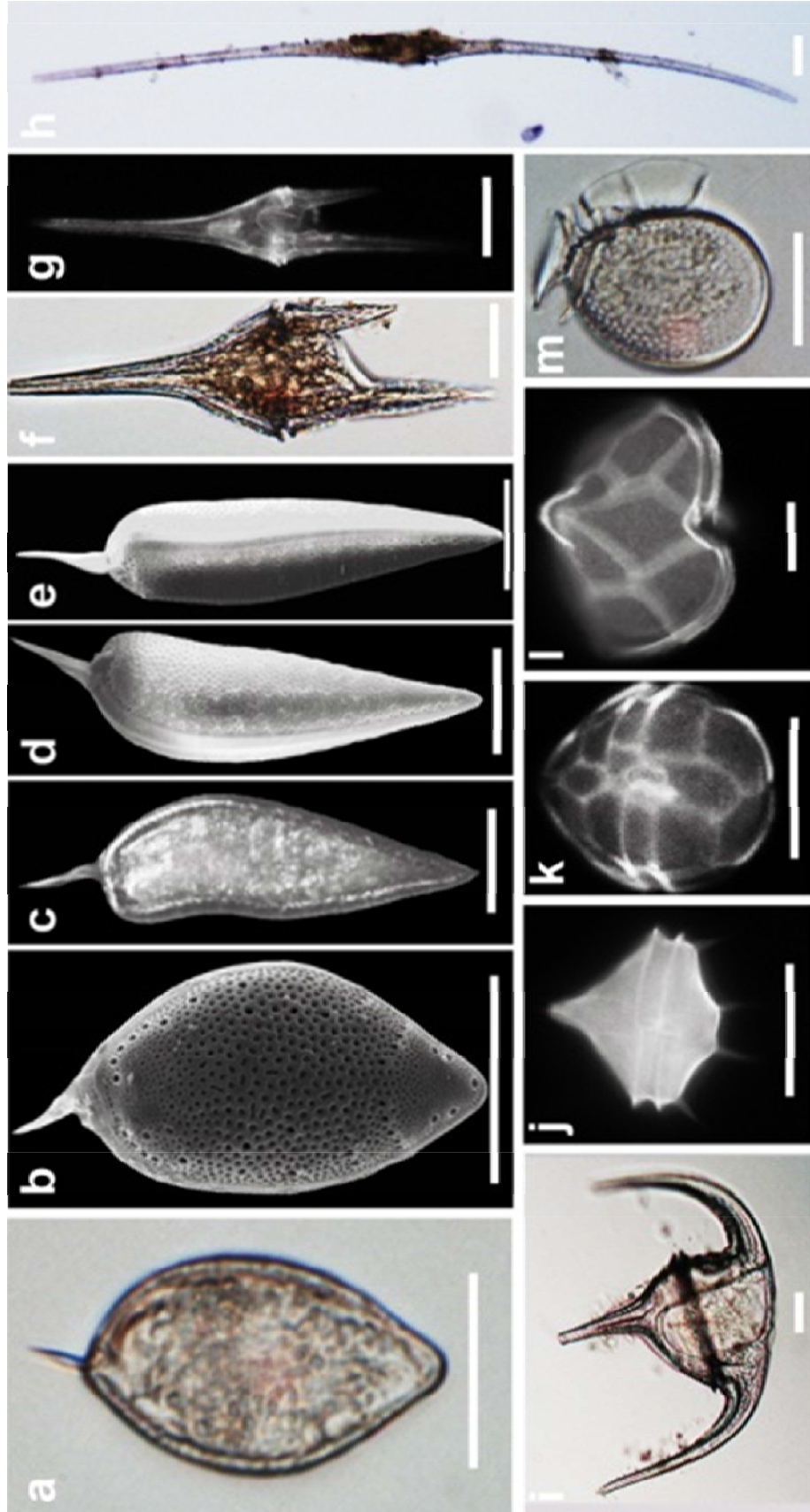


Fig.3.1. Light (**a, f, h, l, m**), fluorescence (**c, g, j-l**) and scanning electron micrographs (**b, d, e**) of potentially harmful dinoflagellates. **a,b** *Prorocentrum micans*, **c-e** *Prorocentrum trochoidea*, **f** *Prorocentrum trochoidea*, **g** *Ceratium furca*, **h** *Ceratium furca*, **i** *Ceratium fusus*, **j** *Peridinium quinquecorne*, **k** *Scrippsiella trochoidea*, **l** *Protoperidinium crassipes*, **m** *Dinophysis infundibulus*. (Fluorescence micrographs are taken using Calcofluor, which can stain the cellulose thecal plate). Scale bar = 20 μm .

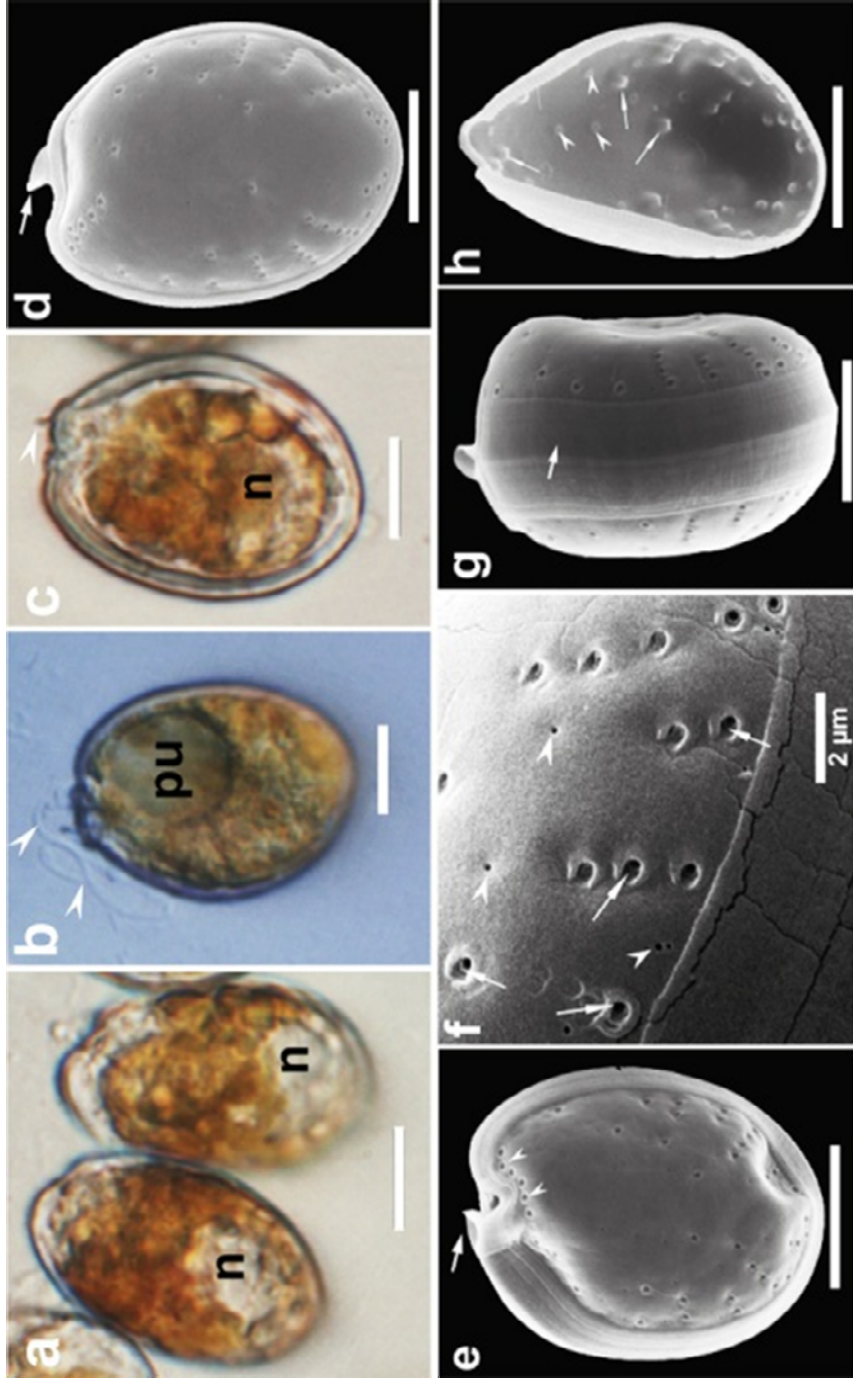


Fig.3.2. a-h Light (a-c) and scanning electron micrographs (d-h) of *Prorocentrum rathymum*. **a** Cells clump in the mucilage showing posteriorly located nucleus (n). **b** Single cell showing anteriorly located large pusulae (pu) and flagella (arrow heads). **c,d** Single cell showing the apical spine (arrow and arrowhead). **e** Right valve view showing the apical spine (arrow) and seven pores along the periflagellar area (arrow heads). **f** Smooth valve surface with randomly scattered small pores (arrow heads) and large pores located in shallow circular depression (arrows). **g** Wide intercalary band with striated smooth surface (arrows). **h** Inner surface showing small pore openings (arrow heads) and rounded sac like base of large pores (arrows). Scale bars: a-e, g-h = 10 μ m.

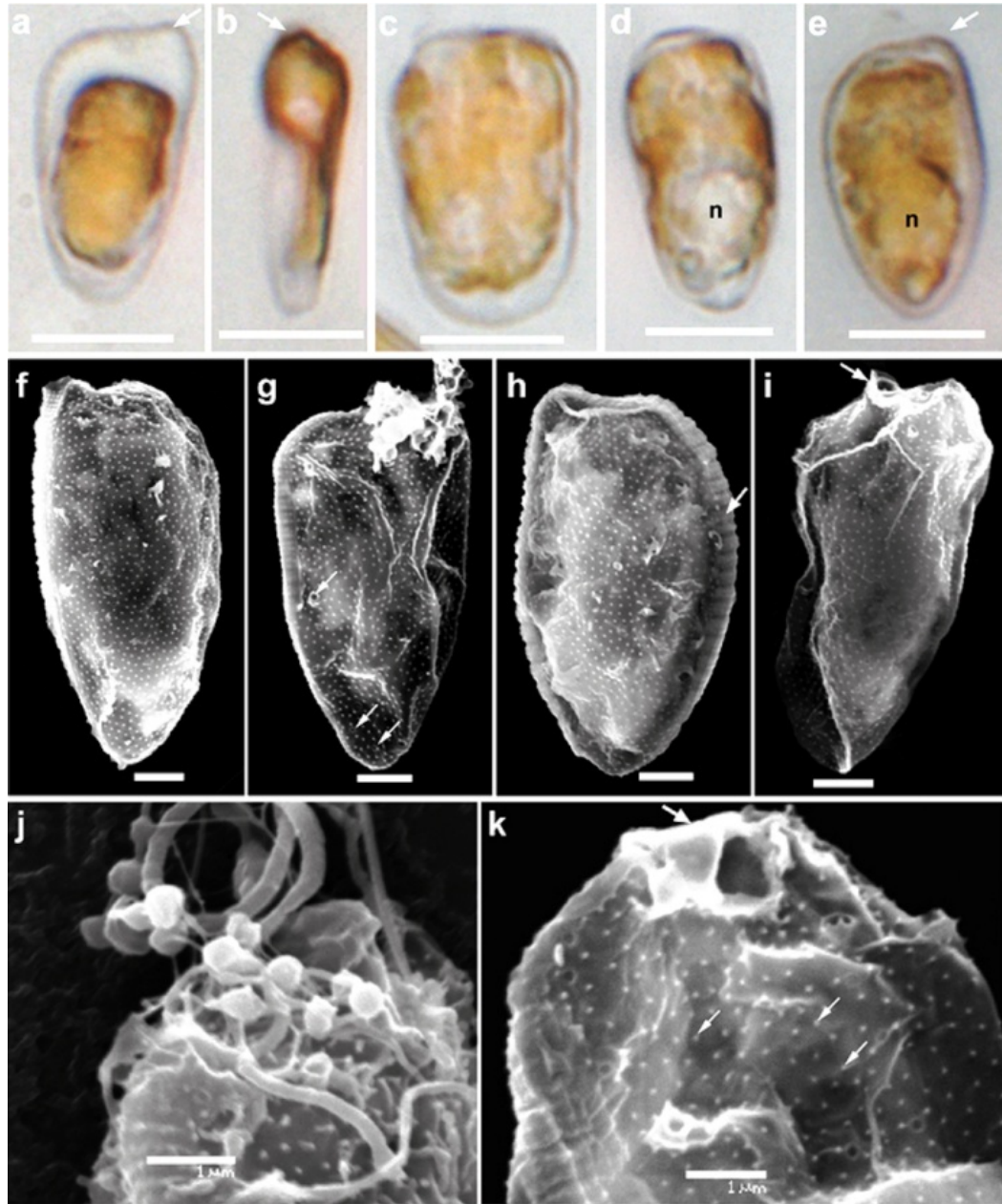


Fig.3.3. **a-k** Light (**a-e**) and scanning electron micrographs (**f-k**) of *Prorocentrum shikokuense*. **a-e** Individual variation in cell shape in size showing rounded nucleus (n) and slightly extended anterior one end (arrow in **a**, **b**, **e**). **f** Right valve showing concave periplagellar area. **g** Left valve showing trichocyst pores (arrows). **h** Right valve view showing wide intercalary band with rows of tiny knobs. **i** Periplagellar area with ear-shaped collar protrusion (arrow). **j** Enlarged view of periplagellar area showing large amount of mucilage. **k** Enlarged view showing the collar protrusion (large arrow) and tiny knob-like spines (small arrows). Scale bars: a-e = 10 μ m, f-i=2 μ m, j-k=1 μ m.

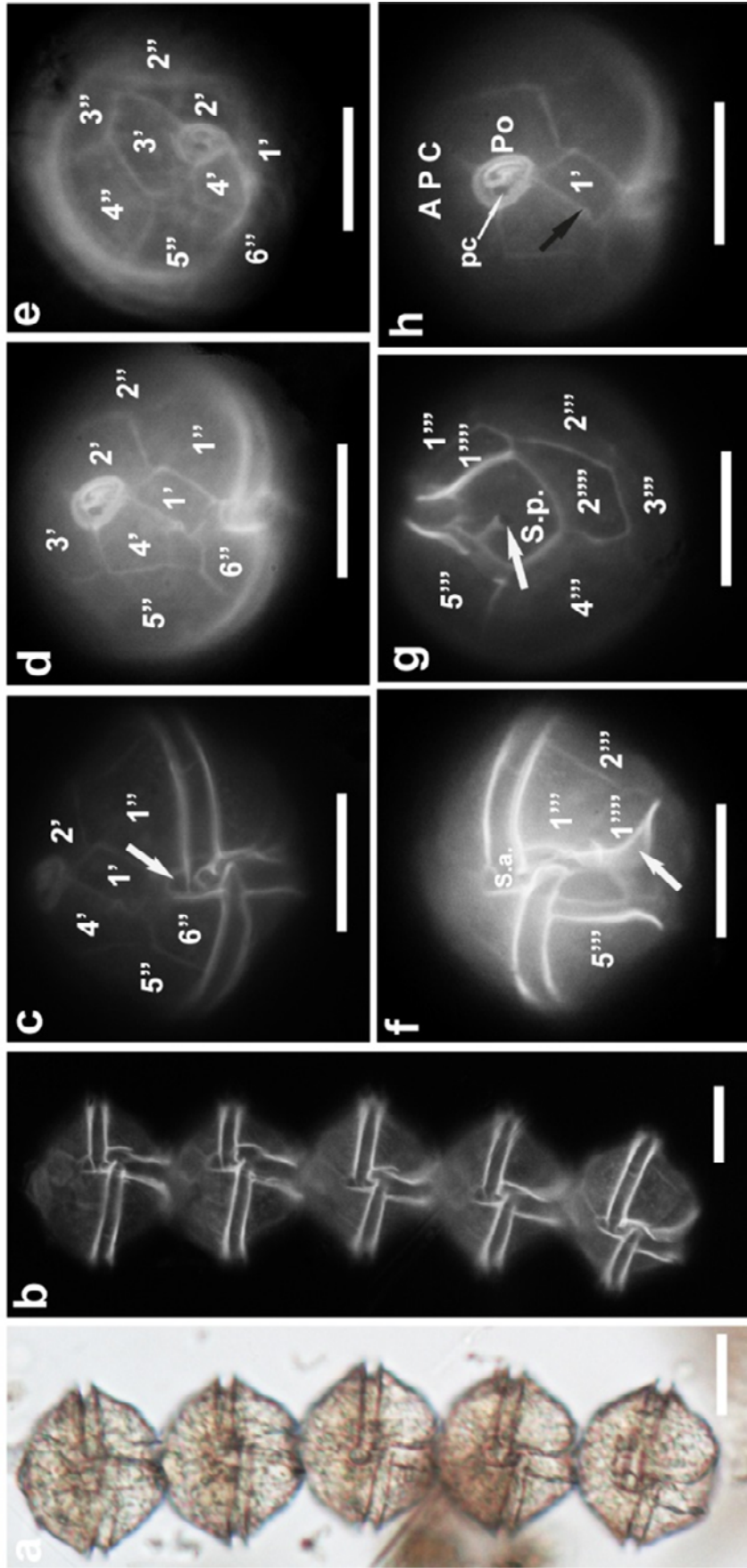


Fig.3.4. Light (a) and fluorescence (b-h) micrographs of *Alexandrium tamiyavanichii* (a-h). a Normal light micrograph of cell chains. b-h Fluorescence light micrographs of cells chain (b) and single cell (c-h). c-d Single cell showing thecal arrangement of epitheca in ventral view. c Ventral view showing the precingular part (arrow). e Apical view showing the third apical plate (3') without an attachment pore. f Ventral view showing the anterior sulcal plate (S.a.) and wing like projecting sulcal list (arrow). g Antapical view showing a posterior sulcal plate (S.p.) with large rounded posterior attachment pore (arrow). h Apical plate complex (APC) showing the oval-shaped apical pore plate (Po) with connecting pore (1') (white arrow), and first apical plate (1') with small ventral pore (black arrow). (Fluorescence micrographs are taken using Calcofluor, which can stain the cellulose thecal plate). Scale bars = 20 μ m.

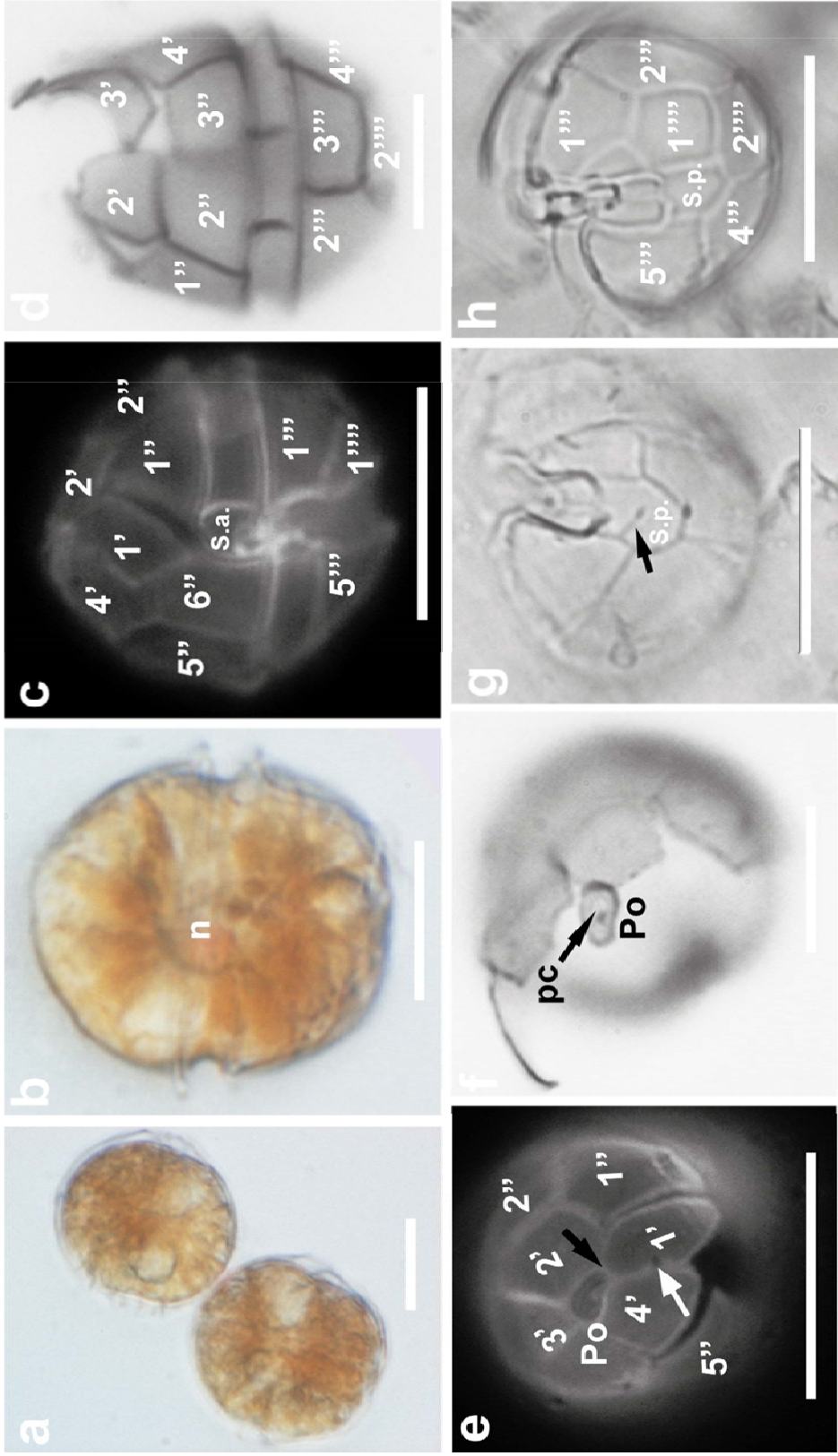


Fig.3.5. Light (a, b, d, f-h) and fluorescence (c, e) micrographs of *Alexandrium affine* (a-h). **a** A pair of vegetative cells. **b** Single cell showing the nucleus (n). **c** Ventral view showing the long plate 6". **d** Dorsal view showing thecal plate arrangement. **e** Apical view showing the first apical plate (1') with ventral pore (white arrow), and direct connection of Po (black arrow). **f** Apical pore plate (Po) showing the connecting pore (pc). **g** Anapical view showing the elongated posterior sucral plate (S.p.) with posterior attachment pore (arrow). **h** Posterior-ventral view thecal plates arrangement. (Fluorescence micrographs are taken using Calcofluor, which can stain the cellulose thecal plate). Scale bars = 20 μm .

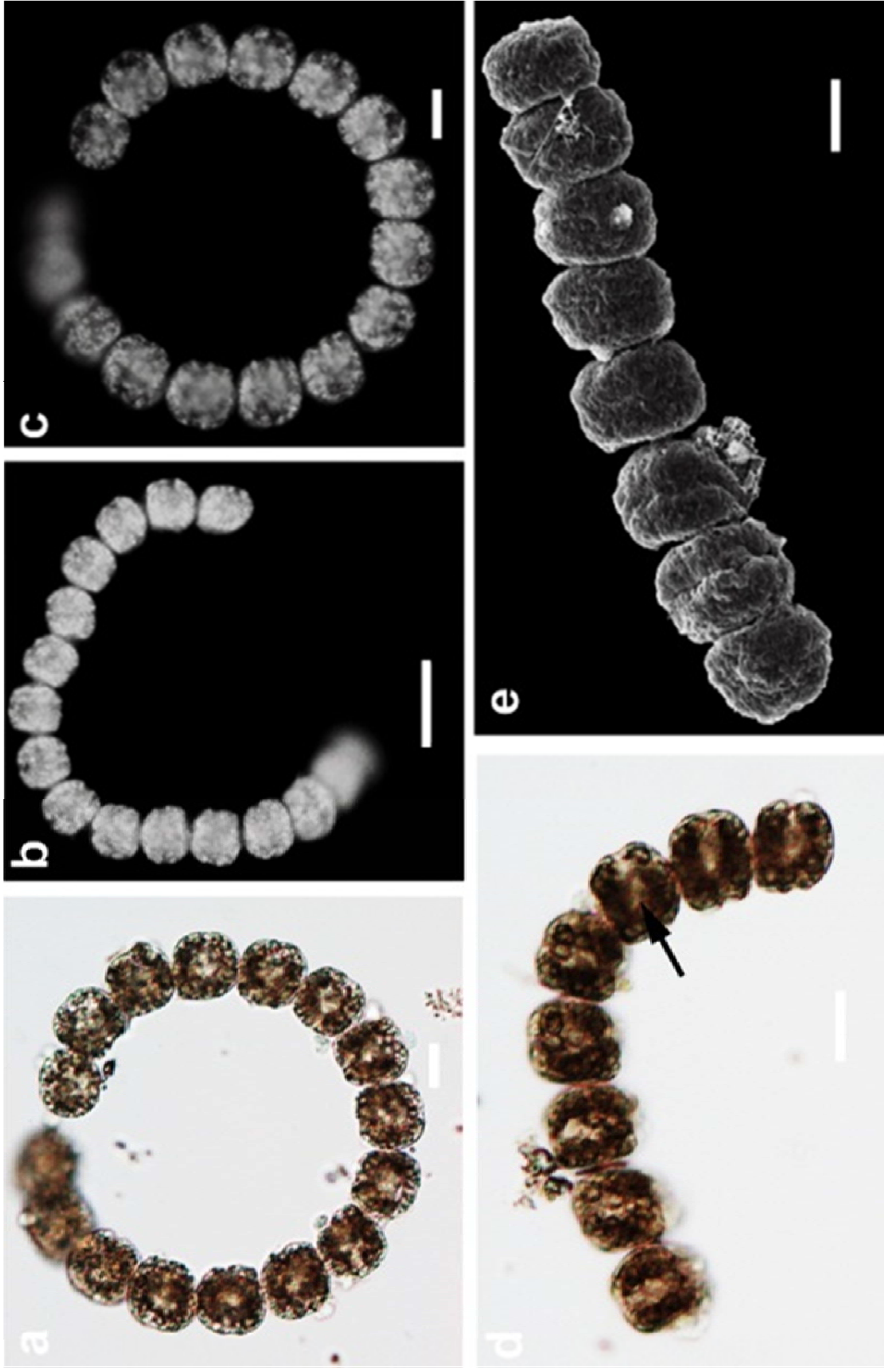


Fig.3.6. Light and scanning electron micrographs (e) of *Gymnodinium catenatum*. **a,d** Normal light micrographs, **b,c** Fluorescence light micrographs, **e** Scanning electron micrograph. **d** Black arrow showing the centrally located nucleus. Scale bars: a,c-e = 20 μ m; b= 50 μ m.

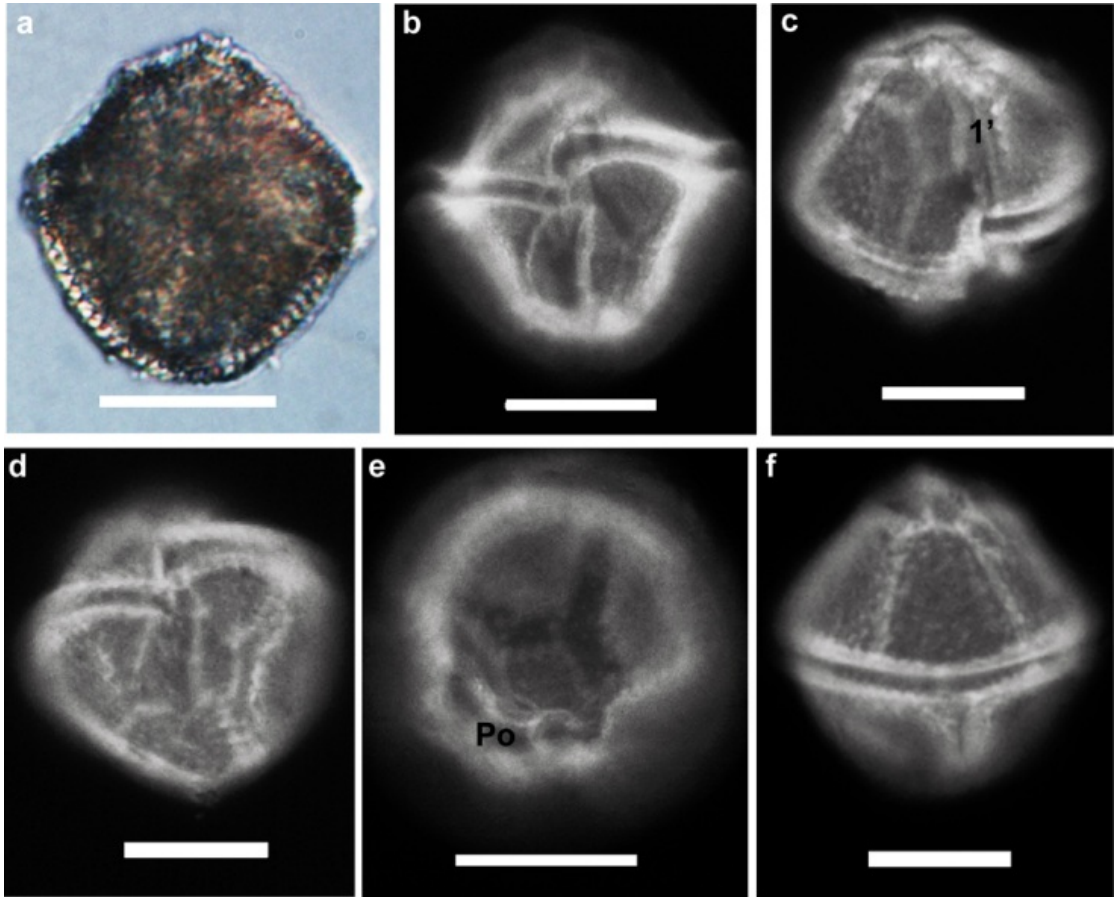


Fig.3.7. Light (a) and fluorescence (b-f) micrographs of *Lingulodinium polyedrum*. **a** Normal light micrograph, **b-f** Fluorescence light micrographs. **a,b** Micrograph showing pentagonal cell outline. **c** Ventral view showing the first apical plate (1'). **d** Ventral view of hypotheca showing the deep sulcus. **e** Apical view showing the apical pore plate (Po) with a raised inner elliptical ridge. **f** Dorsal view showing the distinct ridges along the plate sutures. (Fluorescence micrographs are taken using Calcofluor, which can stain the cellulose thecal plate). Scale bar = 20 μ m.

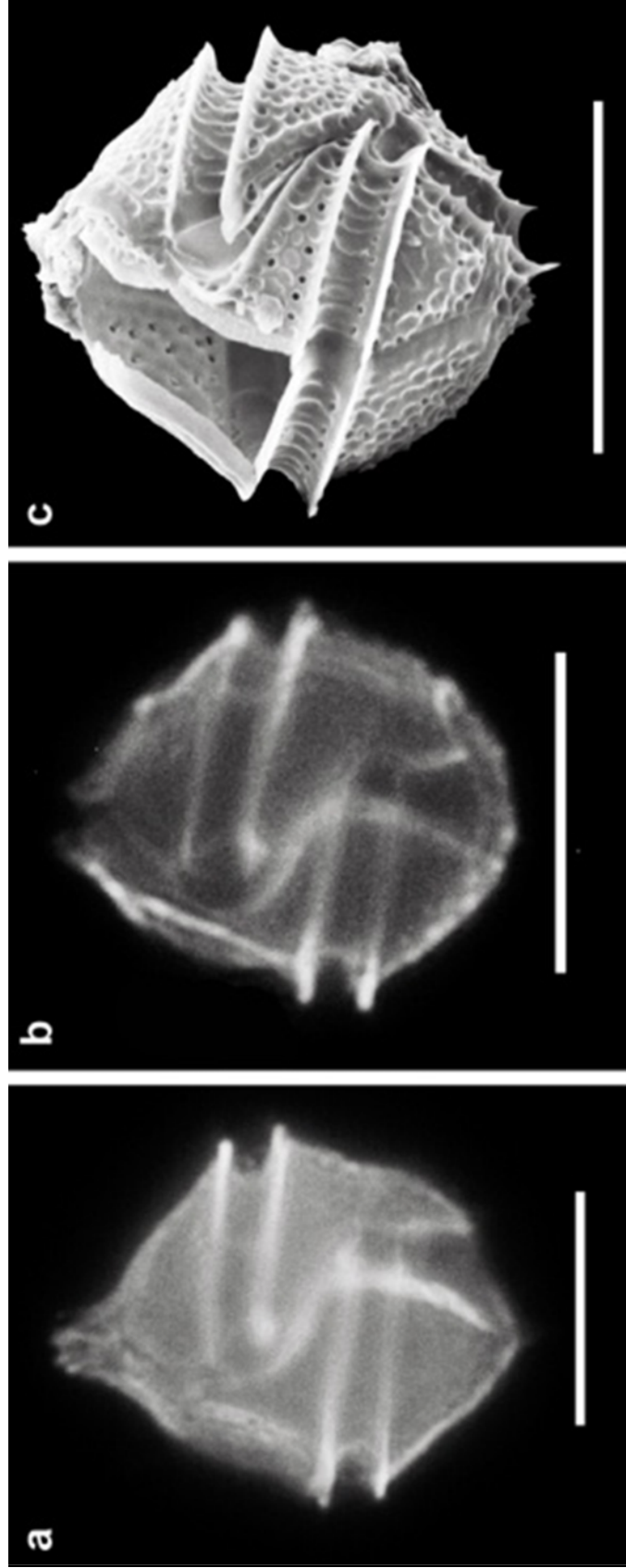


Fig.3.8. Fluorescence (a, b) and scanning electron micrographs (c) of *Gonyaulax spinifera*. a Ventral view showing the asymmetry cell outline and small apical horn. b Ventral view showing the deeply excavated and spirally twisted cingulum, c Showing the posteriorly located small spines. (Fluorescence micrographs are taken using Calcofluor, which can stain the cellulose thecal plate). Scale bar = 20 μ m.

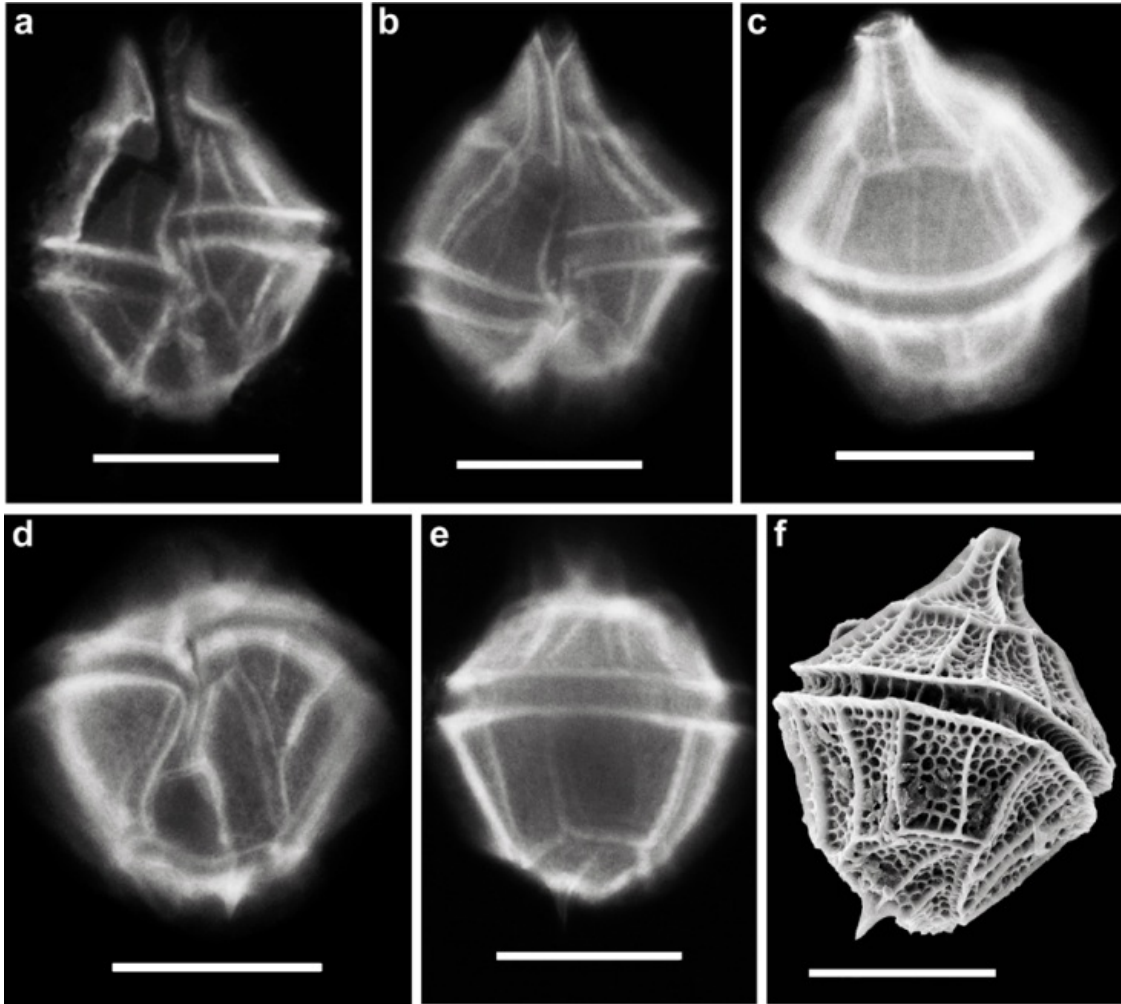


Fig.3.9. Fluorescence (**a-e**) and scanning electron micrographs (**f**) of *Gonyaulax polygramma*. **a** Ventral view of cell outline. **b** Ventral view of epitheca showing the slightly invaded cingulum. **c** Dorsal view of angular epitheca showing the prominent apical horn and deeply excavated cingulum . **d** Ventral view hypotheca showing the posteriorly widened sulcus. **e-f** Dorsal view of truncate hypotheca showing the straight sides and an antapical spine. (Fluorescence micrographs are taken using Calcofluor, which can stain the cellulose thecal plate). Scale bar = 20 μm.

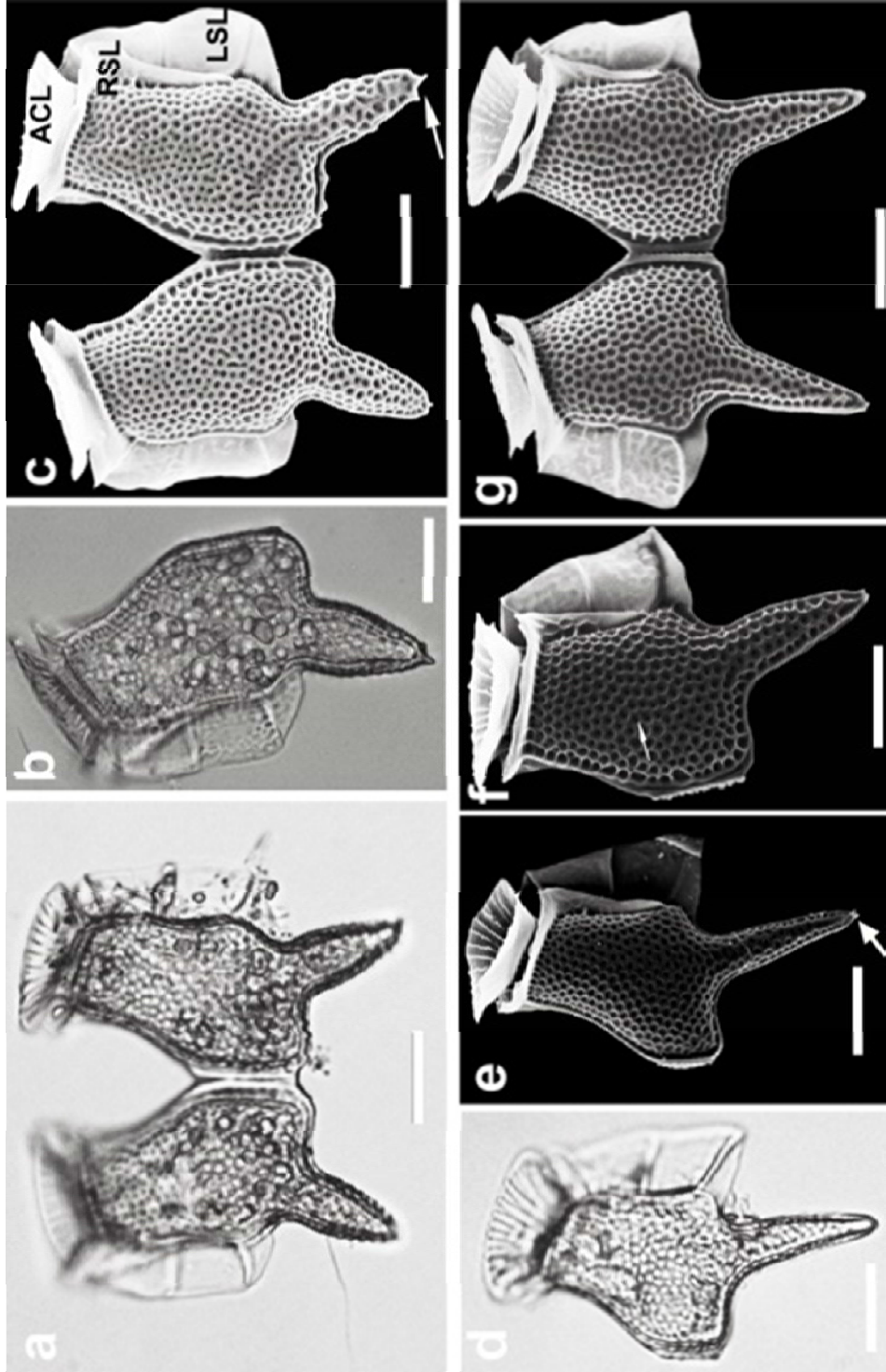


Fig.3.10. Light micrographs (a,b,d) and scanning electron micrographs (c,e-g) of *Dinophysis caudata*. a-g Lateral views showing various morphology of *D. caudata*. a,c,g Paired of cells. b,d-f Single cell. c Showing the large funnel shaped anterior cingular list (ACL), long left sulcal list (LSL), short and narrow right sulcal list (RSL). c,e Single and couple cells showing the toothed posterior end of posterior projection (arrow). f Right lateral view showing the areolae with a pore (arrow). Scale bars = 20 μ m.

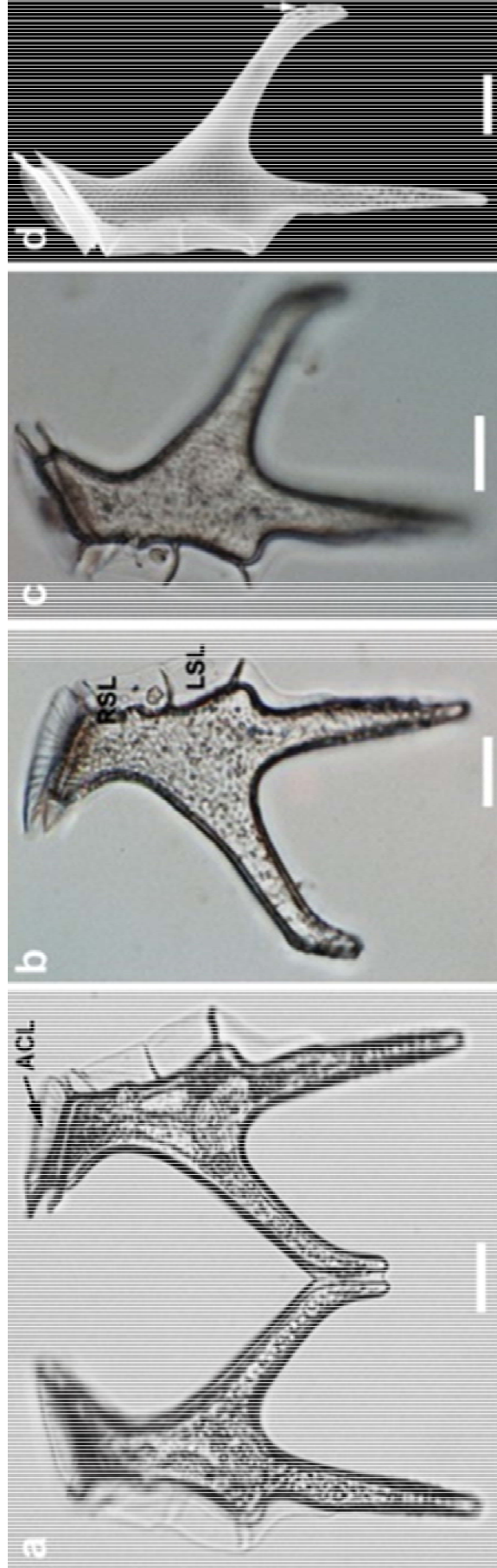


Fig.3.11. Light micrographs (a-c) and scanning electron micrograph (d) of *Dinophysis miles*. a Pair of cells showing the small funnel shaped anterior cingular list (ACL). b Right lateral view showing the left sulcal list (LSL) and right sulcal list (RSL). c Left lateral view showing the ribs of LSL. d Left lateral view showing the small wing at the distal end of dorsal projection (arrow). Scale bar = 20 μ m.

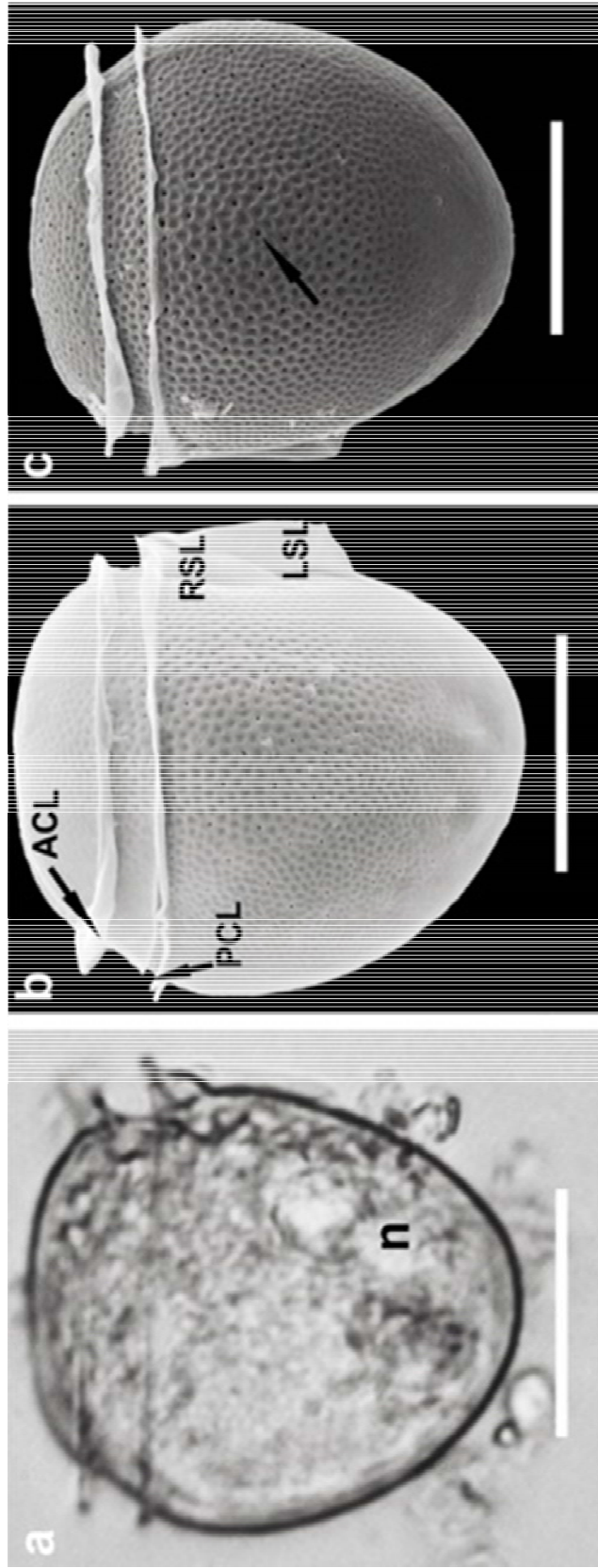


Fig.3.12. Light and scanning electron micrographs of *Dinophysis rotundata*. **a** Light micrograph showing the posteriorly located nucleus (n). **b,c** Scanning electron micrographs: **b** Right lateral view showing the anterior cingular list (ACL), posterior cingular list (PCL), left sulcal list (LSL) and right sulcal list (RSL). **c** Left lateral view showing the areolated surface bearing pores in some areolae. Scale bar = 20 μ m.

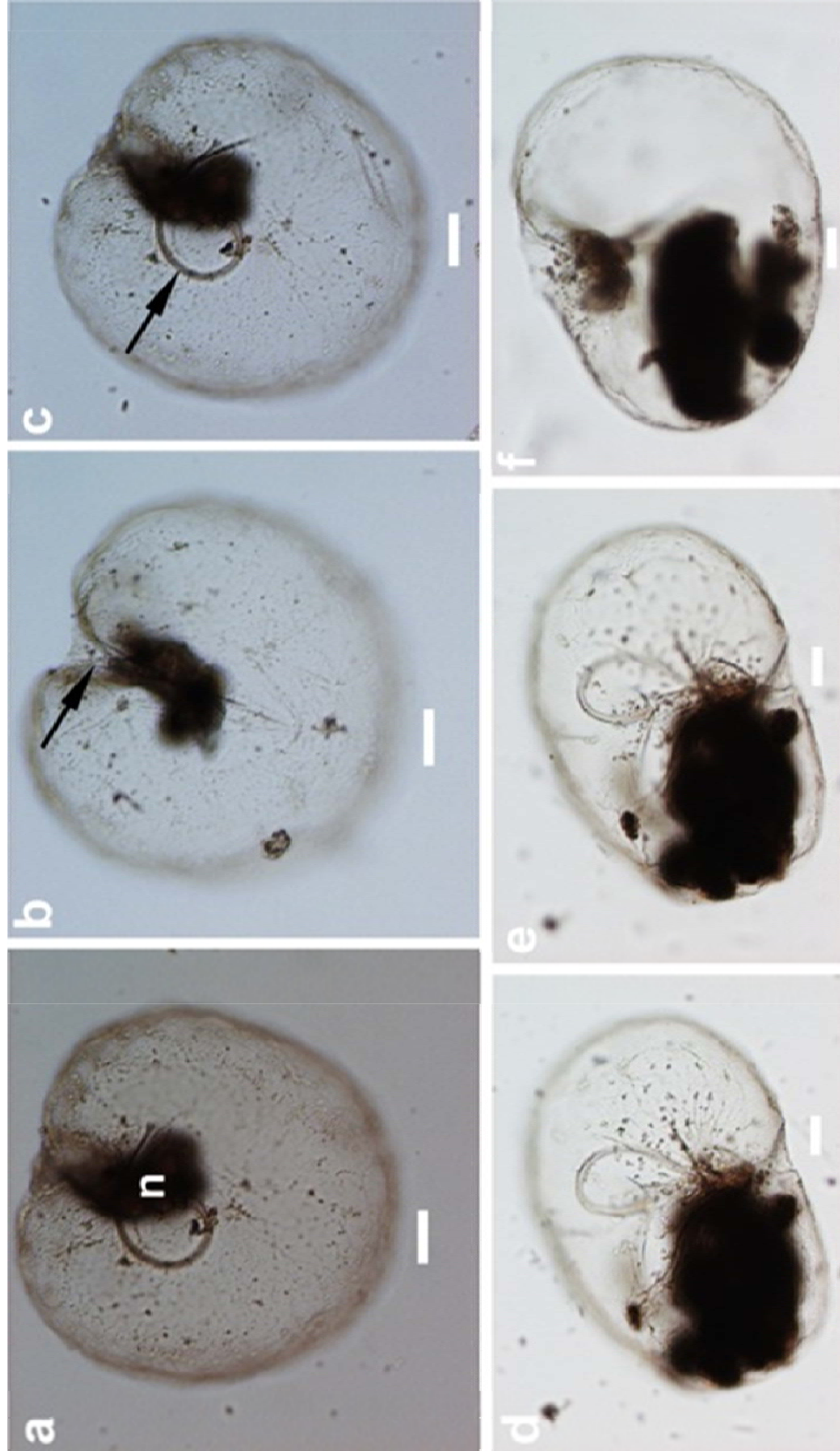


Fig.3.13. Light micrographs of *Noctiluca scintillans* (red *Noctiluca*) (a-f). **a** Cell with arrow pointing the nucleus. **b** Cell with arrow showing the ventral groove. **c** Cell with arrow showing the tentacle. **d-f** Ventral view of cells. Scale bar = 50 μ m.

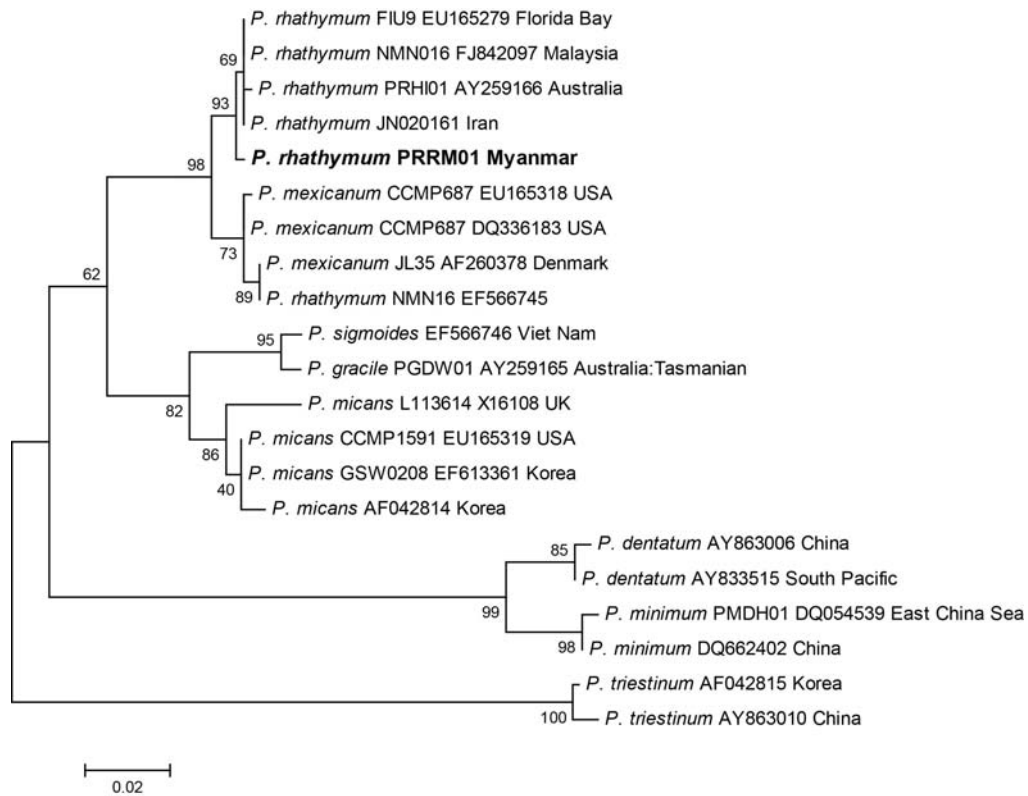


Fig.3.14. Maximum-likelihood (ML) tree for *Prorocentrum rhathymum* based on the nuclear 28S rRNA gene. An evolution model of Kimura-2-parameter (with G distributions) was used to construct a tree. Numbers at nodes are boot-strap values calculated with 1,000 replicates. Strain sequenced in this work is in bold.

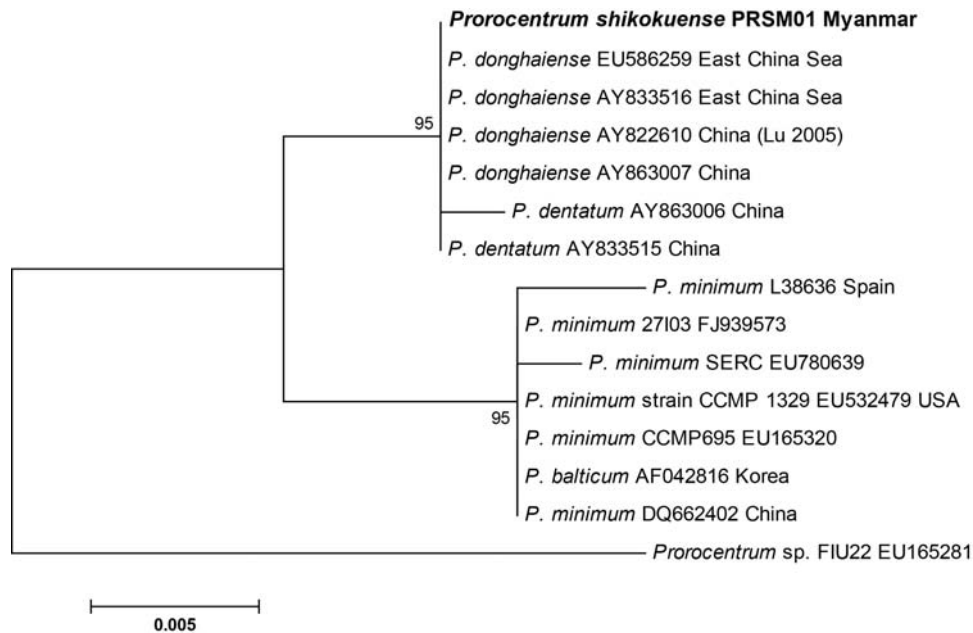


Fig.3.15. Maximum-likelihood (ML) tree for *Prorocentrum shikokuense* based on the nuclear 28S rRNA gene. An evolution model of Jukes-Cantor was used to construct a tree. Numbers at nodes are boot-strap values calculated with 1,000 replicates. Strain sequenced in this work is in bold.

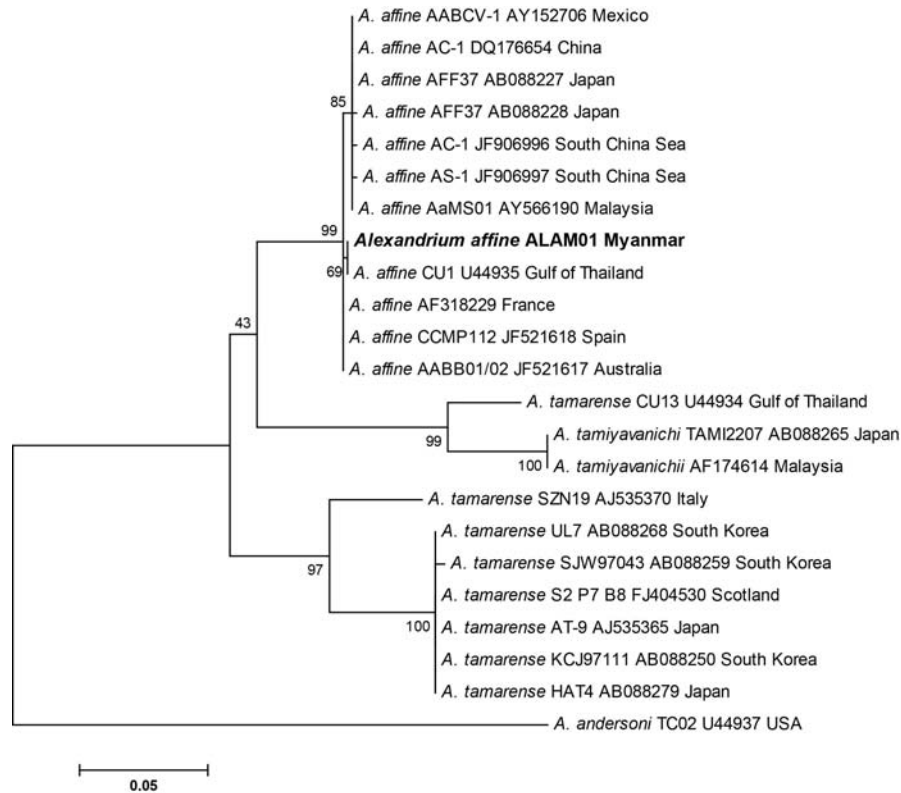


Fig.3.16. Maximum-likelihood (ML) tree for *Alexandrium affine* based on the nuclear 28S rRNA gene. An evolution model of Tamura-Nei (with G distributions) was used to construct a tree. Numbers at nodes are boot-strap values calculated with 1,000 replicates. Strain sequenced in this work is in bold.

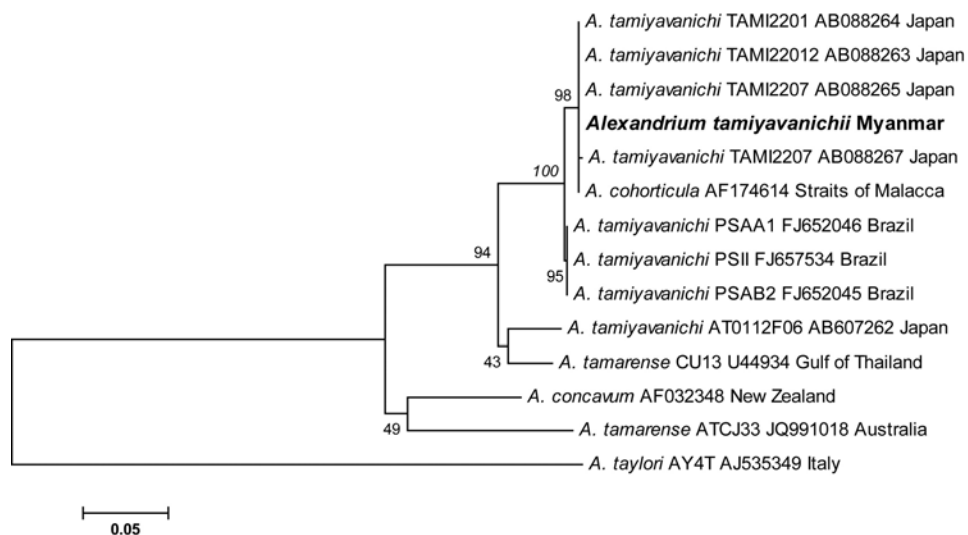


Fig.3.17. Maximum-likelihood (ML) tree for *Alexandrium tamiyavanichii* based on the nuclear 28S rRNA gene. An evolution model of Tamura-Nei (with G distributions) was used to construct a tree. Numbers at nodes are boot-strap values calculated with 1,000 replicates. *A. tamiyavanichii* sequenced in this work is in bold.

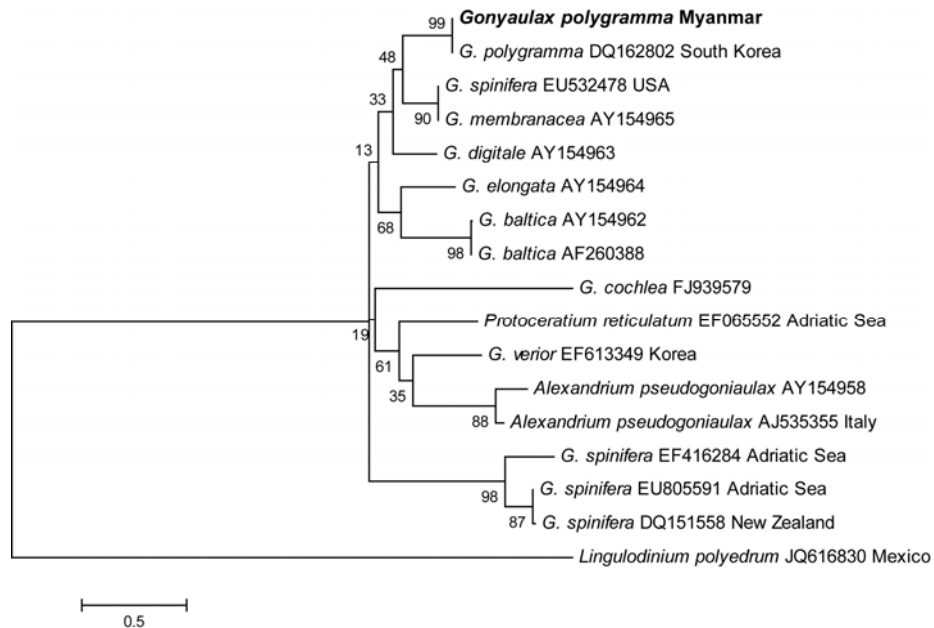


Fig.3.18. Maximum-likelihood (ML) tree for *Gonyaulax polygramma* based on the nuclear 28S rRNA gene. An evolution model of Tamura-Nei (with G distributions) was used to construct a tree. Numbers at nodes are boot-strap values calculated with 1,000 replicates. *G. polygramma* sequenced in this work is in bold.

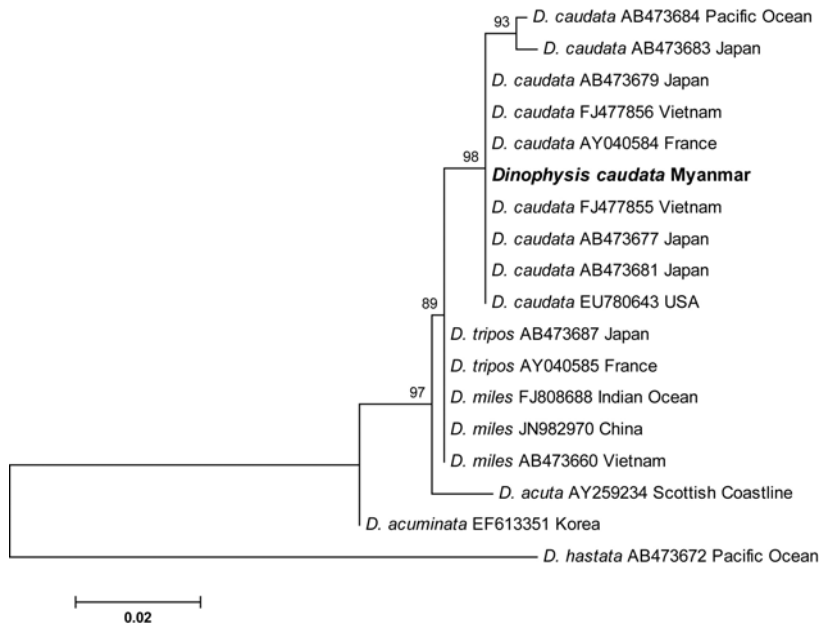


Fig.3.19. Maximum-likelihood (ML) tree for *Dinophysis caudata* based on the nuclear 28S rRNA gene. An evolution model of Hasegawa-Kishino-Yano (with G distributions) was used to construct a tree. Numbers at nodes are boot-strap values calculated with 1,000 replicates. *D. caudata* sequenced in this work is in bold.

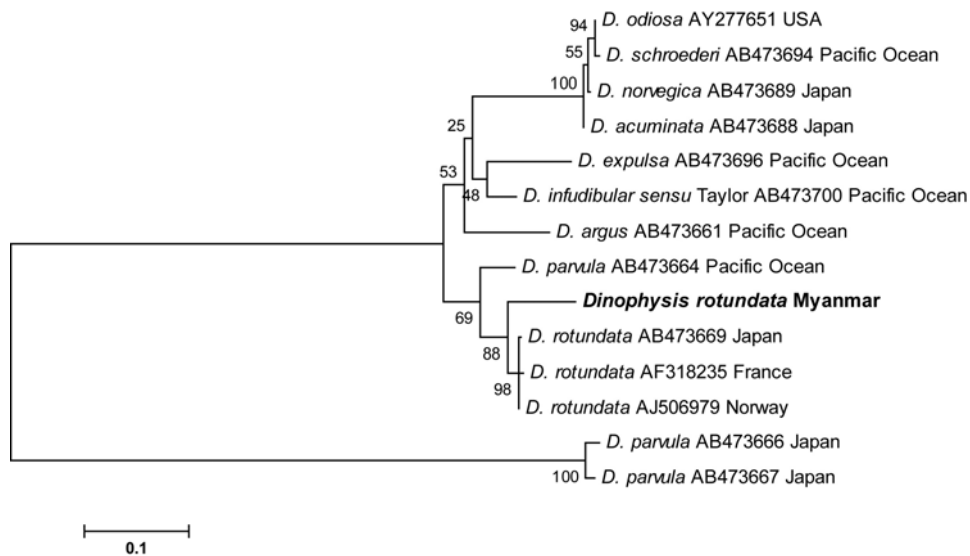


Fig.3.20. Maximum-likelihood (ML) tree for *Dinophysis rotundata* based on the nuclear 28S rRNA gene. An evolution model of Tamura-Nei (with G distributions) was used to construct a tree. Numbers at nodes are boot-strap values calculated with 1,000 replicates. *D. rotundata* sequenced in this work is in bold.

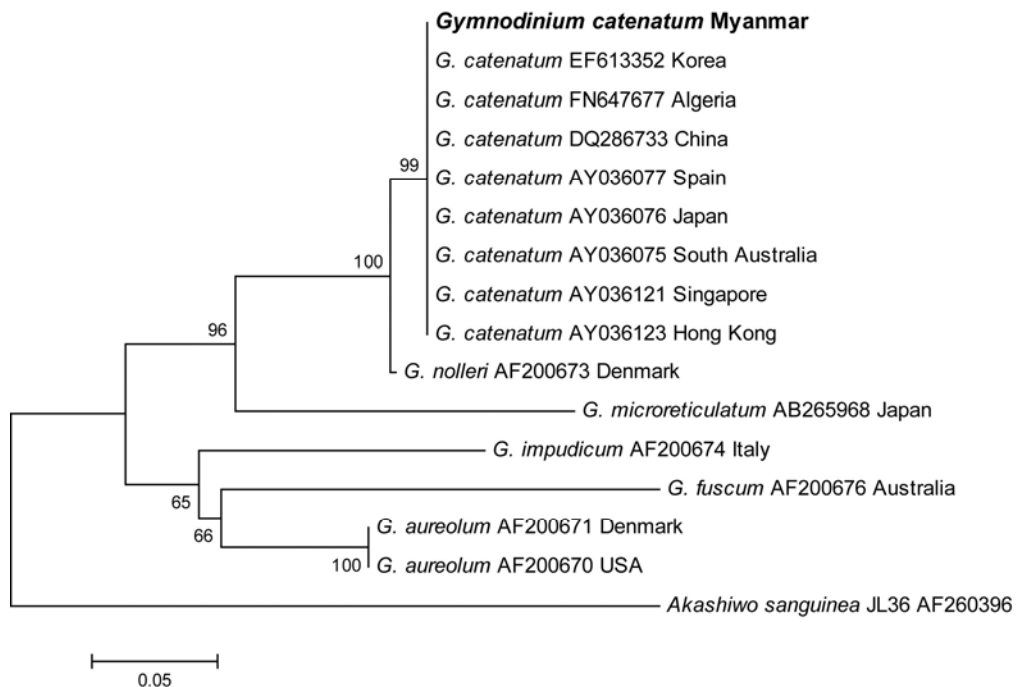


Fig.3.21. Maximum-likelihood (ML) tree for *Gymnodinium catenatum* based on the nuclear 28S rRNA gene. An evolution model of Tamura-Nei (with G distributions) was used to construct a tree. Numbers at nodes are boot-strap values calculated with 1,000 replicates. *G. catenatum* sequenced in this work is in bold.

CHAPTER 4: GROWTH CHARACTERS OF THREE RED-TIDE FORMING SPECIES (*Prorocentrum rhathymum*, *P. shikokuense*, *Alexandrium affine*) AT DIFFERENT TEMPERATURES

4.1. INTRODUCTION

In Chapter 2, the phytoplankton surveys around the Mali and Kadan Islands off the Tanintharyi coastal area were conducted thrice (May 2010, December 2010 and March 2012). One of these occasions, red-tide mainly composed by *Prorocentrum rhathymum* Loeblich was detected for the first time near the St. 6 in the March survey (Fig. 4.1). Interestingly, lesser numbers of *P. shikokuense* and *Alexandrium affine* were coexisted with *P. rhathymum* red-tide. These species were also confirmed in Chapter 3.

P. rhathymum is a benthic species and widely distributes in tropical and temperate waters. The red-tide of *P. rhathymum* was firstly reported (as *P. mexicanum*) from the Gulf of California (Ismael and Aida, 1997), and later reported by Cortés-Altamirano and Sierra-Beltrán (2003) from the same water. Al-Yamani et al. (2004) reported a bloom of *P. rhathymum* (as *P. mexicanum*) contributed to a massive fish kill of wild and culture fish of Doha, in the western side of Kuwait Bay. Pearce et al. (2005) reported association of oyster spat mortalities and high *P. rhathymum* density in Tasmania. The detection of DSP toxins associated by OA production by *P. rhathymum* was also reported from the Florida Bay (An et al., 2010) and Sabah, Malaysia (Caillaud et al., 2010).

Together with *P. rhathymum*, another red-tide forming species of *Alexandrium affine* (Inoue & Fukuyo) Balech was also found with lesser number. *A. affine* has been known to inhabit a wide range of geographical areas and has been found in temperate

and tropic waters, mainly in Japan, the Gulf of Thailand and the Philippine (Balech, 1995). In 1974, 1975 and 1977, a bloom of *A. affine* was reported (as *Protogonyaulax affinis*) in several parts of Japan (Fukuyo et al., 1985; 1990). In 1997, a bloom of *A. affine* in Ambon Bay, Indonesia was reported by Wagey et al. (2001).

The other co-occurring red-tide forming species of *Prorocentrum shikokuense* Hada ex Balech (*P. donghaiense* Lu in China) is one of the causative species of large red tides occurring in the East China Sea. In 1995, a huge red-tide of *P. shikokuense* was occurred off the Chanjiang River mouth in the East China Sea and reported as *P. donghaiense* by Lu and Goebel (2001). In advance to such reports, blooming of *P. shikokuense* was reported from Iwamatsu Bay of the Bungo Channel on the western coast of Shikoku, Ehime, and reported as new species (Hada, 1975).

Finding red-tide in this study is probably first case in Myanmar. Moreover, it is noteworthy that the red-tide was composed by three different harmful dinoflagellate species. To investigate possibility of such red-tide extension in the corresponding area, it is important to understand their growth physiology. The outbreaks of red-tides are associated with some complex ecological and oceanographic processes and can be affected by a variety of environmental factors (Sunda et al., 2006). Among them, water temperature, salinity, light and nutrient are the most basic factors for the growth of red tide organisms. Many laboratory studies have confirmed that environmental factors can significantly influence the growth rate of harmful algal species (e.g. Yamamoto et al., 2002; Xu et al., 2010). In this study, the effect of temperature on the growth of these three species were examined in the laboratory conditions.

4.2. MATERIALS AND METHODS

4.2.1. Study area

The study area (red-tide detected area) located near the mouth of a small bay near the St.6, at the northeast part of Kadan Island off the Tanintharyi coast (Fig. 4.1). This area receives terrestrial nutrients from the river runoffs, and in the same time, receives oceanic waters before the rainy season at the onset of southwest wind. The survey was carried out in March 2012, at when after passing long period from the rainy season. The surface red tide water was sampled with basket and transferred into 500 ml plastic bottle for species isolation.

4.2.2. *Prorocentrum rhathymum* cell densities in red-tide water

A 50 ml of surface red-tide water was fixed with neutralized formalin at final concentration of 10 %. *P. rhathymum* cells were counted from 10 ml of sample water using counting chamber. Lesser numbers of *P. shikokuense* and *A. affine* were also detected in this sample and enumerated in the same manner.

4.2.3. Organism and culture conditions

Clonal cultures of *Prorocentrum rhathymum*, *P. shikokuense* and *Alexandrium affine* were established by capillary pipette isolation from the red-tide water sample as described in Chapter 3.

4.2.4. Temperature experiments

Growths of *A. affine*, *P. rhathymum* and *P. shikokuense* at four different temperature conditions (15, 20, 25 and 30°C) were monitored. Each culture strain was inoculated into 4 autoclaved flasks each containing a total volume 200 ml of sterilized f/2 medium, and these cultured flasks were maintain at the stable conditions of 100 $\mu\text{mol photons m}^{-2} \text{s}^{-1}$, 33 psu salinity, 25°C, 12:12h light:dark for 3 days prior to the experiment. To avoid shock from temperature changes during transplantation, temperature was acclimated with increase or decrease 2°C each day for one flask of each species. Each acclimated species were maintained at the above temperature regimes for 3 days and checked every day to ensure the growths. From the each culture flask, a 5ml of culture which containing 17,500 cells were inoculated into triplicated autoclaved flat bottom plant culture tubes containing 30 ml f/2 medium to become a final concentration of 500 cells ml^{-1} . Daily, at 10:00 am, *in vivo* chl. *a* fluorescence was measured using a fluorometer (10-AU, Turner Designs, Sunnyvale, USA). To obtain a stable fluorescence value, fluorescence measuring was conducted in the laboratory under dim light. The culture tubes were shaken thoroughly to ensure dissociate the cells in medium because *Prorocentrum rhathymum* has benthic nature and both of these two *Prorocentrum* species produce large amount of mucilage. Measurements were conducted until the end of stationary phase. Daily division rate (μ_2 unit: division day^{-1}) was calculated for *in vivo* chl. *a* fluorescence measurement during the exponential growth phase using the following equation

$$\mu_2 = \frac{\log_2 N_1 - \log_2 N_0}{D_1 - D_0}$$

Where N_0 and N_1 are initial and final value of fluorescence in exponential phase and D_0 and D_1 are initial and final time (day).

4.3. RESULTS

4.3.1. *P. rhathymum* densities in the field sample

The average cells number (81,250 cells L⁻¹) of *P. rhathymum* were detected from the field sample of red-tide waters (Fig. 4.3). In this red-tide sample, lesser number of (2,000 cells L⁻¹) of *P. shikokuense* and (1,750 cells L⁻¹) of *A. affine* were also obtained.

4.3.2. Effects of temperature on growth

Growth of *A. affine* was not observed at temperature 15°C, but was observed at the temperature ranges from 20°C to 30°C (Fig. 4.4.a). *A. affine* exhibited the low tolerant to low temperature (15°C) hence it was more adapted to tropical environment. The growth curves suggested the optimum condition for growth to be at 20°C and 25°C with the growth rate of 0.46 division day⁻¹ (Fig. 4.4.b). At 30°C, the growth rate showed 0.39 division day⁻¹. Growth of *P. rhathymum* was observed in the temperature ranges from 15°C to 30°C (Fig. 4.4.c). *P. rhathymum* exhibited the strong tolerant to the given temperature ranges. The growth curves suggested the optimum condition for growth to be at 25°C with the growth rate of 0.62 division day⁻¹ (Fig. 4.4.d). The lowest growth rate of *P. rhathymum* (0.37 division day⁻¹) was observed at 15°C. Growth of *P. shikokuense* was observed in the temperature ranges from 15°C to 30°C. *P. shikokuense* also exhibited as *P. rhathymum* with the strong tolerant to the temperature ranges from

15°C to 30°C (Fig. 4.4.e). The optimum growth rate (0.87 division day⁻¹) was observed at temperature 15°C. *P. shikokuense*, however, grew well even at higher temperature, i.e. 0.76 division day⁻¹ at 25°C and 0.75 division day⁻¹ at 30°C (Fig. 4.4.f).

4.4. DISCUSSION

4.4.1. Effects of temperature on growth

The growth of *A. affine* was observed at the temperature range from 20°C to 30°C and the optimal growth occurred at temperatures 20°C and 25°C. The results for the temperature tolerance are in agree with the previous studies of *A. affine* from Vietnamese water (from 21°C to 27°C) (Nguyen-Ngoc, 2004). My results for the maximum division rate of 0.46 division day⁻¹ is also in close agreement with the results of Nguyen-Ngoc (2004), and also agree with previous studies of other *Alexandrium* species (0.5-0.7 division day⁻¹) by Anderson (1998). Anderson et al. (1984) reported that the growth rate of *A. tamarensense* varied significantly in temperature, with no growth below 7°C, or above 26°C. Jensen and Moestrup (1997) reported that *A. ostenfeldii* from Danish waters grew at 11.3°C to 23.7°C.

A. affine was previously reported from the Saroma Lake and Mutsu Bay (Fukuyo et al., 1985), which locate in the cool temperate zone of the northern part of Japan. By contrast, *A. affine* isolated from Myanmar water showed more tolerant to higher temperature regimes than some other *Alexandrium* species, and low tolerant to the low temperature than *A. affine* from the cool temperate region, hence *A. affine* isolated from Myanmar water was more adapted to tropical environment.

Growth of *P. rhathymum* was observed in the temperature ranges from 15°C to 30°C, and exhibited optimum growth of 0.62 division day⁻¹ at 25°C. The optimal temperature for maximum growth of *P. rhathymum* (Myanmar strain) was shown together with *P. rhathymum* from Vietnamese water (Nguyen-Ngoc, 2010). And, this result also agrees with an observed temperature 24.5°C of the *P. rhathymum* red-tide comprising 3,135,200 cells L⁻¹ reported from the Gulf of California (Ismael and Aida, 1997). It suggests the optimal temperature for the massive bloom of *P. rhathymum* may probably be around 25 °C.

P. shikokuense exhibited the strong tolerant to the temperature ranges from 15°C to 30°C with the optimal growth rate (0.87 division day⁻¹) at temperature 15°C. Well growth of *P. shikokuense* was showed even at higher temperature, i.e. 0.76 division day⁻¹ at 25°C and 0.75 division day⁻¹ at 30°C. My experimental results for *P. shikokuense* are inconsistent with the previous study of *P. donghaiense* (junior synonym of *P. shikokuense*) from East China Sea strain by Xu et al. (2010). Maximum growth of *P. donghaiense* (East China Sea strain) exhibited 0.77 division day⁻¹ at 27°C (Xu et al., 2010), while *P. shikokuense* (Myanmar strain) showed maximum growth rate of 0.87 division day⁻¹ at 15°C. In comparison with the higher growth of *P. shikokuense* (Myanmar strain) at 15°C, East China Sea strain of *P. donghaiense* showed lower growth rate (0.2 division day⁻¹) at temperature 10-15°C (Xu et al., 2010). Regardless to the phylogenetic results in Chapter 3 showing the close genetic relationship between *P. shikokuense* from Myanmar and *P. donghaiense* from Chinese waters, growth physiology was significantly different possibly due to the geographical adaptation. Massive and recurrent blooms of *P. donghaiense* were detected at the Changjiang River estuary and along the coastal water of Zhejiang proviance at China (Lu et al., 2005).

Massive blooms of *P. donghaiense* were recorded at the water temperature 17-20°C and salinity between 20-30 PSU (Lu et al., 2005).

This experimental result revealed these Myanmar strains exhibited rather high cell division under a wide temperature range, and agreement or disagreement in the temperature tolerance of other localities in the red-tide affected areas, indicating similar awareness will be needed based on local strain character.

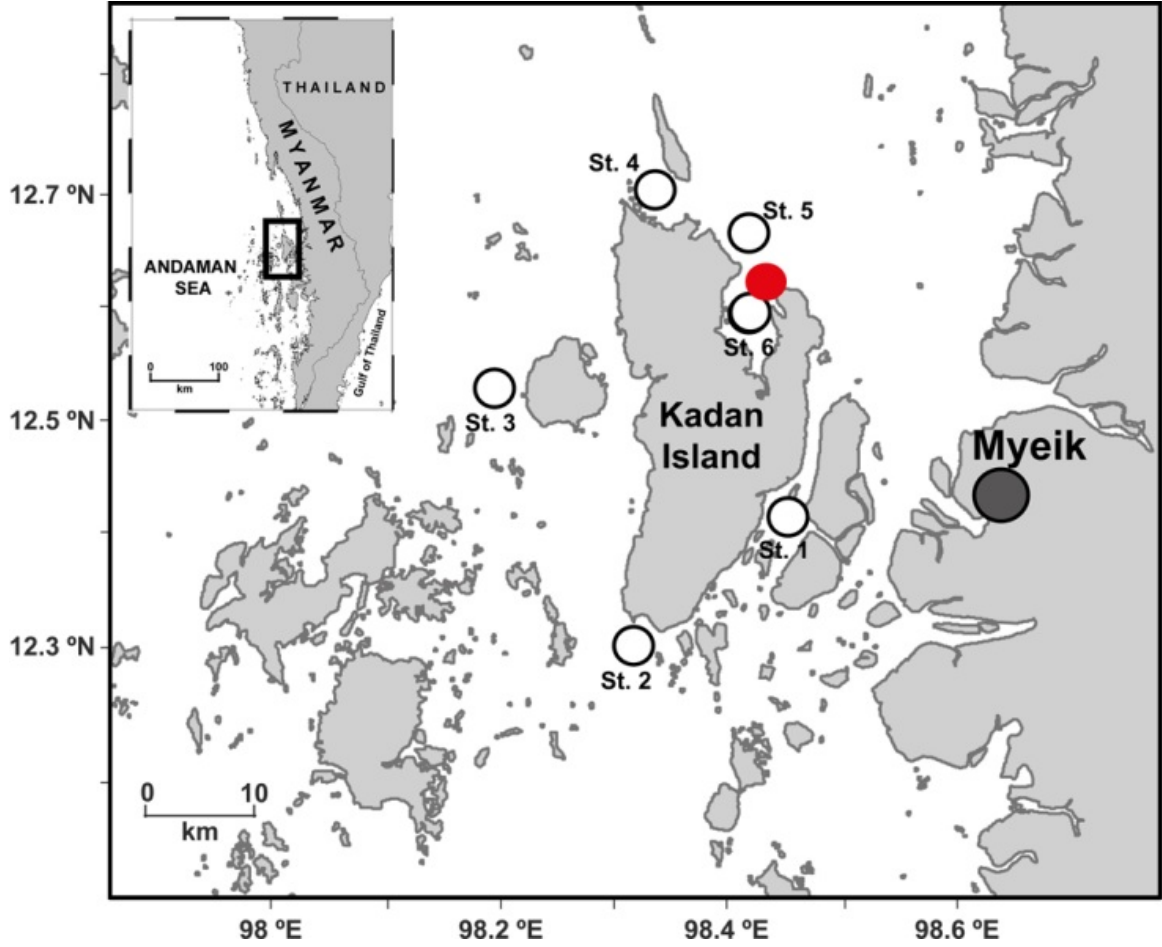


Fig.4.1. Map showing sampling location of red-tide occurring area at the northeast part of Kadan Island, Tanintharyi coast, Myanmar in March, 2012 (red circle).

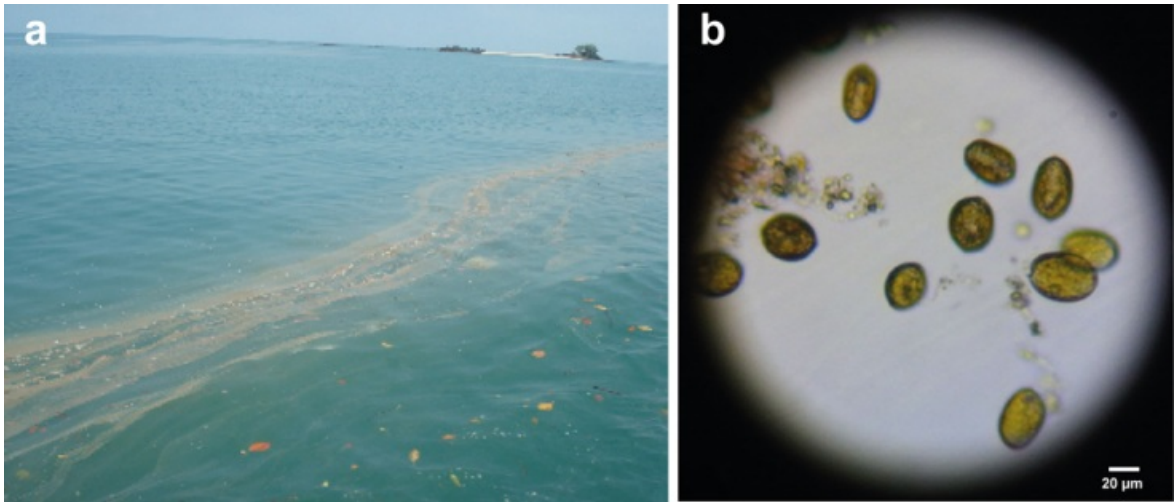


Fig.4.2. a. Red-tide of *Prorocentrum rhathymum* at the northeast part of Kadan Island in the March survey (14th March 2012), **b.** *P. rhathymum* cells in the red-tide water (observed on boat).

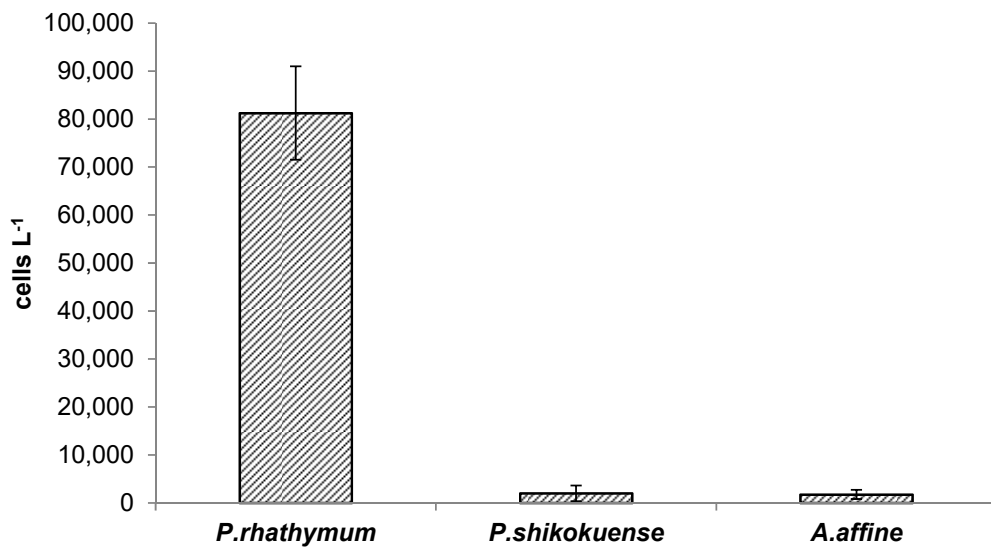


Fig.4.3. Graph showing the densities of *P. rhathymum*, *P. shikokuense* and *A. affine* detecting in the red-tide field sample. Error bars indicate the standard deviations based on triplicate counting.

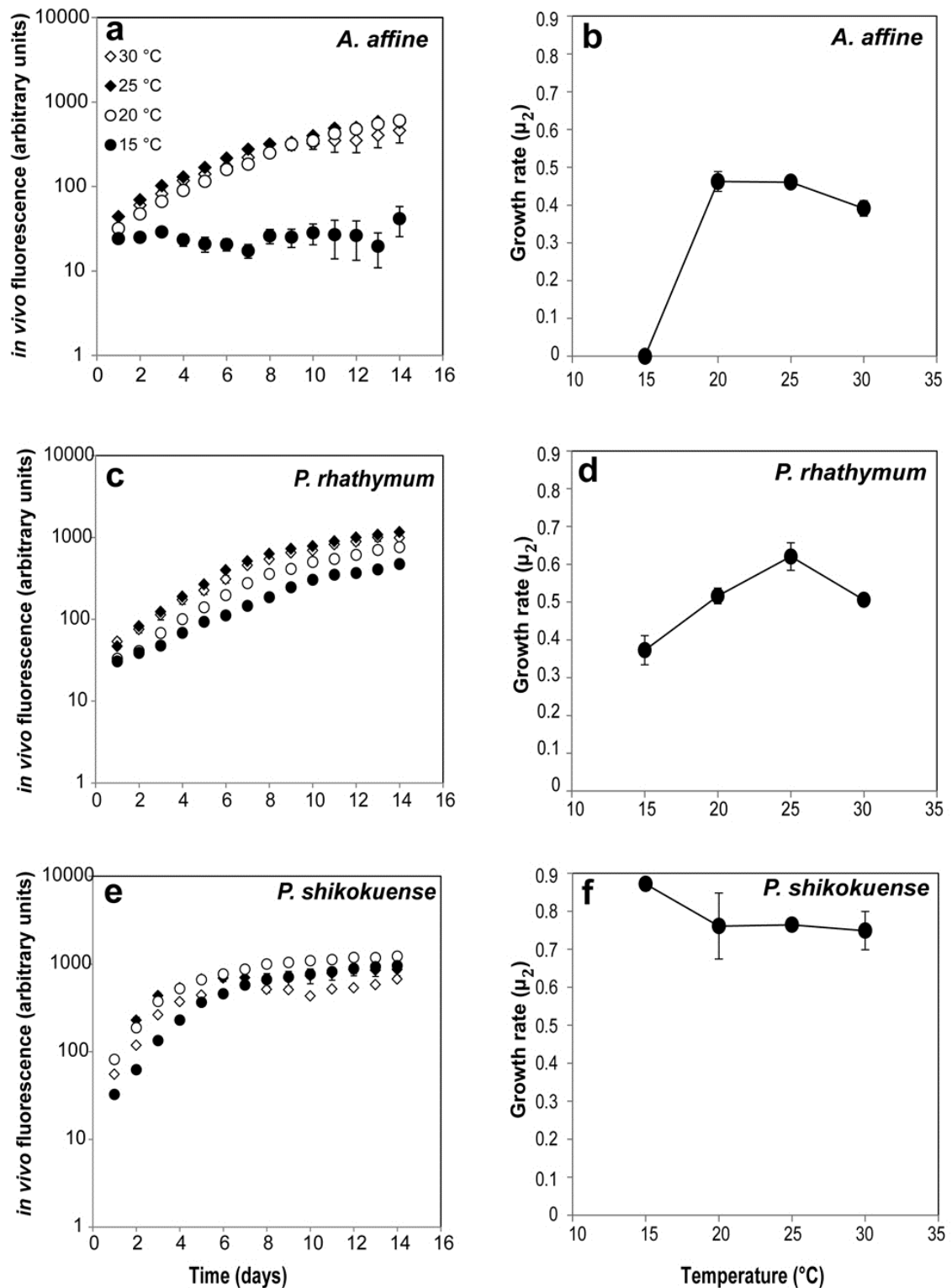


Fig.4.4. Growth curves of *A. affine* (a), *P. rathymum* (c), *P. shikokuense* (e) and growth rate (μ_2) of *A. affine* (b), *P. rathymum* (d) and *P. shikokuense* (f) at four different temperatures conditions (\bullet 15°C, \circ 20°C, \blacklozenge 25°C, \blacklozenge 30°C). Error bars indicate the standard deviations based on of triplicate cultures.

**CHAPTER 5: OCCURRENCE OF DINOFLAGELLATE CYSTS IN THE
SURFACE SEDIMENT, AND FINDING OF TOXIC *Gymnodinium catenatum*
AND *Alexandrium tamiyavanichii* FROM COASTAL WATERS OF SELANGOR,
MALAY PENINSULA**

5.1. INTRODUCTION

A bivalve, blood cockle *Anadara granosa* (Linnaeus 1758), is one of the most important culture products in Malaysia. The culture fields are intensively gathered in the coastal waters of Selangor district, Malaysia. The cultured cockles are supplied to entire domestic markets and exported to neighboring countries such as Thailand, Indonesia and Vietnam. However, it should be noted that bivalve cultures and markets may always be along with risks of contamination of shellfish toxins. Therefore, sustaining or even promoting the bivalve fisheries largely rely on the risk management for shellfish toxins and on a strict consensus for regulating contaminated shellfishes. In this context, the regular monitoring for toxic plankton is also required as well as analyzing the toxicity of harvested products. As mentioned above, paralytic shellfish poisoning (PSP) is potent poisoning and may cause serious problem on bivalve culture industry if it happens. However, regardless to the reports for occurrence of PSP causative dinoflagellates in Malay Peninsula, phytoplankton monitoring in the culture grounds of Selangor district has not been conducted yet.

For establishing plankton monitoring systems on Selangor district in future, the investigation of dinoflagellate cysts from Selangor area, west coast of Malay Peninsula was conducted. The aim of this investigation was to realize the presence or absence of PSP causative species in the sediment of blood cockle cultures ground. This study could

support understanding on the occurrence of PSP species in Selangor area to establish the PSP risks management for blood cockle culture farms. Furthermore, since Selangor coastal area faces to the Strait of Malacca, and leads to the southern Andaman Sea, connecting to Myanmar coast, it can be also regarded in a view of HAB expansion from or to the Myanmar coast. This study was conducted under a joint survey between Fisheries Research Institute, Penang, Malaysia, and Japan International Research Center for Agricultural Sciences (JIRCAS).

5.2. MATERIALS AND METHODS

5.2.1. Study area and cyst survey

Sediment samples were collected from five sampling lines named as A) Bagan Nakhoda Omar, B) Sungai Basar, C) Sekinchan, D) Kuala Selangor, E) Sungai Buloh ($3^{\circ} 45' - 3^{\circ} 13' N$ latitude, $100^{\circ} 51' - 101^{\circ} 14' E$ longitude) locating along the Selangor coastal area, west coast of Malay Peninsula (Fig. 5.1). The Selangor coast is facing with the Strait of Malacca, where influenced by monsoon. In the west coast of Malay Peninsula, rainy season is associated with the northeast monsoon (November to March) and dry season is associated with the southwest monsoon (June to September). There has a two shorter inter-monsoon period (October, April and May). Sampling was carried out in the rainy season (December 2011) and dry season (September 2011). Five sampling points were set at each sampling lines (Fig. 5.1; Table 5.1). The environmental parameters (depths, temperatures and salinities) were collected by CTD (AAQ sensor, JFE AIEC, Japan). Twenty-five sediment samples were collected for each survey using a handy core sampler (TFO corer) equipped with an inner tube of 2.6 cm diameter. The upper 2 cm

of core samples was cut and preserved with neutralized formalin at a final concentration of 2%. All preserved samples were transported to Hiroshima University, Japan to extract and observe dinoflagellate cysts.

5.2.2. Sample preparation and microscopy

Sample preparation was carried out based on Matsuoka and Fukuyo (2000); 6-29 g of sediment from each sample was chemically treated with 50 ml of 10% hydrochloric acid and 30% hydrofluoric acid (each for 24 hours) to remove carbonate and silicate particles. After each chemical treatment, samples were neutralized with distilled water for one night. The neutralized samples were sieved with 100 μm and 20 μm opening size meshes. The concentrated residue on the 20 μm mesh was suspended in 5 ml distilled water and kept in a vial. Cysts were observed under the inverted light microscope (Olympus IX71) with (DIC illumination) and identified according to some literatures (Bolch et al., 1999; Matsuoka and Fukuyo, 2000; Matsuoka et al., 2006). Dinoflagellate cysts were counted with inverted light microscope at 200 \times to 600 \times magnifications. Cysts abundance was represented as number of cyst g^{-1} sediment dry weight.

5.2.3. Plankton sampling and microscopy

Plankton sampling was carried out five times in the stations A1, B1, C1, D1 and E1 from September 2011 to February 2012. Samples were collected by vertical hauling of a plankton net (20- μm -mesh size, 20 cm in diameter, 80 cm in side length) from bottom to surface and the samples were fixed with neutralized formalin solution at final

concentration of 2%. The fixed samples were observed under light and/or fluorescence microscopes after staining with calcofluor white M2R (Fritz and Triemer, 1985) to visualize thecal plate tabulation. In the samples collected in January and February, *Gymnodinium catenatum* cells were found, but their morphological preservation was not satisfactory to examine exact species. Therefore, fresh plankton samples were observed immediately after the samplings on March and May surveys. Only in the March and May surveys, plankton samplings at the offshore stations (e.g. A3, A5, B3, B5---) were carried out in addition to the regular coastal stations (e.g. A1, B1, C1--) to seek *G. catenatum*.

5.3. RESULTS

5.3.1. Cysts

At least 43 cyst types were recorded (Table. 5.2) based on current paleontological taxonomy (Matsuoka, 1987; Rochon et al., 1999), which comprise 10 autotrophic (Fig. 5.2.A) and 33 heterotrophic types (Fig. 5.2.B). Among these 43 cyst types, 21 species could be identified to species level. The densities of autotrophic species in September were higher than those in December through the stations except line E, however the density of heterotrophic species showed higher proportion in the both surveys in the whole stations (Fig. 5.3.A,B). The highest average density of autotrophic species (13.18 cysts g⁻¹ dry sediment) was detected at the line A (Bagan Nakhoda Omar) in the September survey. At this line, round *Alexandrium* spp. cysts (Fig. 5.2.A. 10-12) were dominantly included (an average of 9.98 cysts g⁻¹ dry sediment). Among the autotrophic cysts, yessotoxin producing species, *Protoceratium reticulatum* (*Operculodinium*

centrocarpum) (Fig. 5.2.A. 5) and *Lingulodinium polyedrum* (*Lingulodinium machaerophorum*) (Fig. 5.2.A. 8) were detected. Low density of *P. reticulatum* cysts were detected especially in the September survey, and highest density (3.1 cysts g⁻¹ dry sediment) was detected at station A5, which is the only one station where *P. reticulatum* cysts detected in the December survey (Table 5.3). *L. polyedrum* cysts were detected only in the September survey with low density. Highest density (1.2 cysts g⁻¹ dry sediment) was detected at station A2 (Table 5.3). Among the autotrophic species, paralytic shellfish poisoning (PSP) causative species *Gymnodinium catenatum* Graham was detected in both survey. This is separately described in the later sections.

The highest average density of heterotrophic species (26.22 cysts g⁻¹ dry sediment) was also detected at the line A (Bagan Nakhoda Omar) in the December survey. In this heterotrophic density, *Protoperidinium denticulatum* (*Birgantedinium irregulare*) (Fig. 5.2.B. 2) (an average 8.46 cysts g⁻¹ dry sediment) and spiny round brown type cysts (Fig. 5.2.B. 15,16) (an average 4.62 cysts g⁻¹ dry sediment among the stations in the line A) dominantly occurred. The average cyst densities showed the trend in lowering to the southern lines in both September and December surveys (Fig. 5.3. a,b).

5.3.2. Cysts of *Gymnodinium catenatum* Graham

Cysts identified as *G. catenatum* are based on the following features; cyst characterized by reticulate ornaments (Fig. 5.4.a,b), two rows of finer meshes developed along the paracingulum, chasmic archeopyle along the paracingulum (Fig. 5.4.a), and larger cyst diameter (50-60 µm; Fig. 5.4.a,b). The cysts of *G. catenatum* were detected with low

numbers from 11 stations collected in September (Fig. 5.5.a) and 8 stations in December survey (Fig. 5.5.b). The maximum number of *G. catenatum* cysts (1.28 cysts g⁻¹ dry weight sediment in September) and (0.78 cysts g⁻¹ dry weight sediment in December) were found at the station A3 and A5 respectively. The average density of *G. catenatum* cyst was high (<0.6 cyst g⁻¹ dry weight sediment weight in the line A, Bagan Nakhoda Omar, Northern part of Selangor area to compare with other lines (Fig. 5.5.a,b). Although the occurrence of *G. catenatum* was not obviously different between September and December, the density of cysts decreased to southern part (Fig. 5.6).

5.3.3. Plankton of *Gymnodinium catenatum*

At the moment, plankton-monitoring focusing on harmful phytoplankton species has not been regularly conducted, however possible plankton cells identical to *G. catenatum* were found from the samples collected on December, 2011. Unfortunately, since the sample was fixed with formalin, the cells became rounded and did not maintain the original morphology (Fig. 5.4.c,d,e). However, the spherical nucleus positioned at the center of the cell and chains composed of over 4 cells suggested that this plankton was possibly identical to *G. catenatum* (Fig. 5.4.c,d,e).

5.3.4. Plankton of *Alexandrium tamiyavanichii*

Plankton samples collected on February, 2012 contained *Alexandrium* species. Based on the following features, this plankton was identified as *A. tamiyavanichii* (Fig. 5.7); triangular apical pore complex with small connecting pore (Fig. 5.7.e), the first apical

plate directly contacting with the apical pore complex, development of curtain (Fig. 5.7.b,c), additional suture running at anterior part of anterior sulcal plate (Fig. 5.7.a,d), well-developed sulcal sutures, and chains of more than 8 cells (Fig. 5.7.f,g,h). *A. tamiyavnichii* shares these features with *A. cohorticula*, but is different by lower epitheca, diagonal direction of additional suture in the anterior sulcal plate and a small connecting pore in Po plate (Balech, 1995). Based on this feature, we identified thecate dinoflagelates in the plankton samples as *A. tamiyavanichii*.

5.4. DISCUSSION

Total of 43 cyst types comprising 10 autotrophic types and 33 heterotrophic types were found in Selangor coastal area. Higher density of autotrophic cysts was found in the September survey than that in the December survey. Among these total cysts assemblage, *G. catenatum* cyst was a minor component and its density was very low. This might be due to low plankton cell densities in the Selangor coast at the moment. *G. catenatum* has been reported from Manila Bay (Fukuyo et al., 1993), Singapore (Holmes et al., 2002), Kota Kinabalu of Sabah, Malaysia (Mohamed-Noor et al., 2002), Gulf of Thailand (Lirdwitayaprasit et al., 2008), and Andaman Sea coast of Myanmar (Boonyapiwat, 2007; Chapter 2 in this study).

The occurrence of *A. tamiyavanichii* was reported from various regions of Southeast Asian waters; Manila Bay, (Furio and Gonzales, 2002), Gulf of Thailand as *Pseudogonyaulax cohorticula* (Fukuyo et al., 1989), Sebatu in the Strait of Malacca, Malaysia (Lim et al., 2004) and the Merugi Archipelago, Myanmar (Chapter 2 in this study). *A. tamiyavanichii* is also known to produce a resting cyst (Nagai et al., 2003).

However, it is very difficult to correctly identify the cysts, because simple spherical cysts characterized with transparent cyst wall without any surface ornament have also been known in *A. affine*, *A. fraterculus*, *A. pseudogonyaulax*, and *A. hiranoi*. We also observed such simple spherical cysts in surface sediments collected from Selangor coasts, but could not identify *A. tamiyavanichii* yet. These spherical *Alexandrium* cysts were found as dominant species in the autotrophic cysts assemblages from all lines in both surveys.

The distribution of *P. reticulatum* cysts was reported from the various regions of Southeast Asian coastal waters such as Indonesia, South China Sea and several basins in the Philippine (Furio et al., 2012). The occurrence of *L. polyedrum* cyst was also reported from the various regions Southeast Asian waters such as Manila Bay, Malampaya Sound, Sorsogon Bay, Juag Lagoon from Philippine and Kota Kinabalu Bay, Sipitang Bay from Malaysia (Furio et al., 2012). In this study, low density of *P. reticulatum* and *L. polyedrum* cysts were detected especially in the September survey, however *P. reticulatum* and *L. polyedrum* are not observed as plankton at the moment. Under this circumstance, cyst survey is important and significant to know the occurrences of such toxic dinoflagellates.

Selangor district is one of important areas for the cockle culture industry in the whole of Southeast Asia not only in Malaysia. From the Selangor district, high amount of blood cockles' natural spats are produced in several times for a year. Those spats are selected as seeds for the culture and exported to neighboring countries as well as domestic, because these seeds faster grow and contain higher nutritious substance compared to others (personal communication with local fishermen). However, occurrence of toxic dinoflagellates, *G. catenatum* and *A. tamiyavanichii* detected from

the cockle culture grounds suggests the PSP risk presents in Selangor district. In addition, the wide distribution of *G. catenatum* cysts also may suggest diffusion risks of *G. catenatum* cysts by the fisheries activity. Thus, we need managements on cyst contamination in the transporting cockle spats and it is important to establish toxic phytoplankton monitoring systems for cultured blood cockles in Selangor district. This study can provide the important information not only for the Selangor area, and also for Myanmar coast to establish toxic phytoplankton monitoring, and to aware the future bivalve culture in the Myanmar coast.

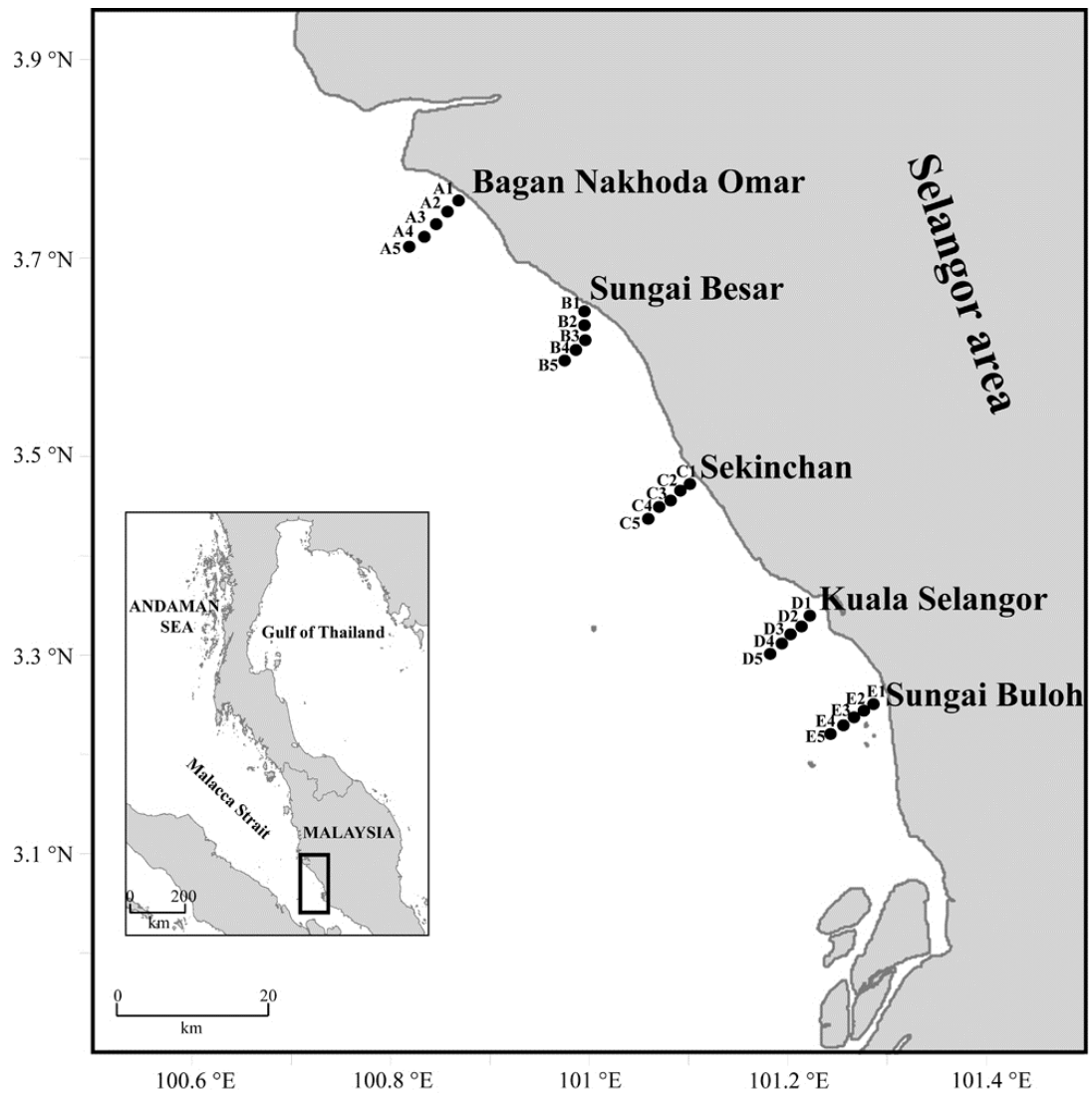


Fig.5.1. Map of the Selangor area off the west coast of the Malay Peninsula, Malacca Strait showing the sampling stations.

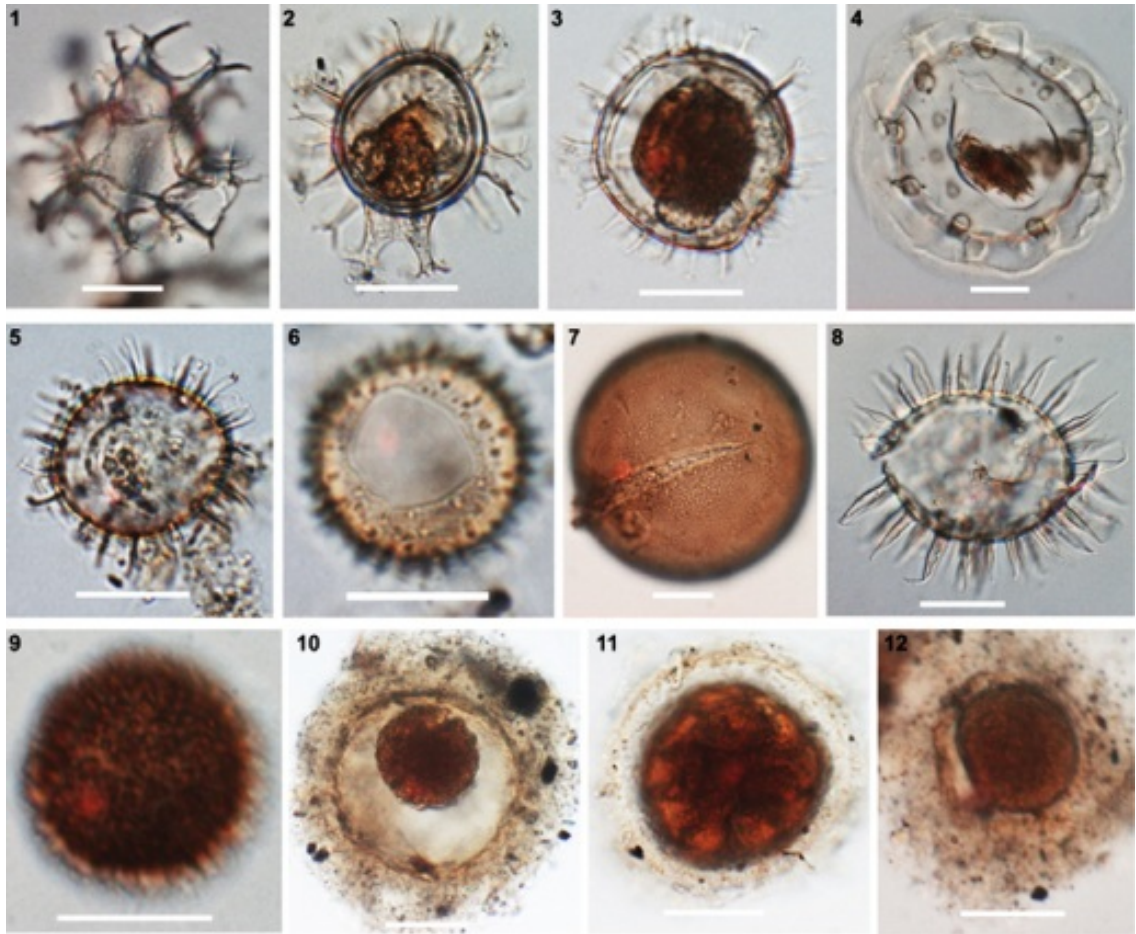


Fig.5.2.A. Light micrographs of dinoflagellate cysts. **1** *Gonyaulax* cf. *spinifera* (*Spiniferites ramosus*), **2** *Gonyaulax* sp. (*Spiniferites* cf. *delicatus*), **3** *Gonyaulax* sp. (*Spiniferites* sp.), **4** *Pyrophacus steinii* (*Tuberculodinium vancampoae*), **5** *Protoceratium reticulatum* (*Operculodinium centrocarpum*), **6** *Protoceratium* sp. (*Operculodinium islaerianum*), **7** *Gymnodinium catenatum*, **8** *Lingulodinium polyedrum* (*Lingulodinium machaerophorum*), **9** *Scrippsiella* sp., **10-12** *Alexandrium* spp.. Scale bars = 20 μ m.

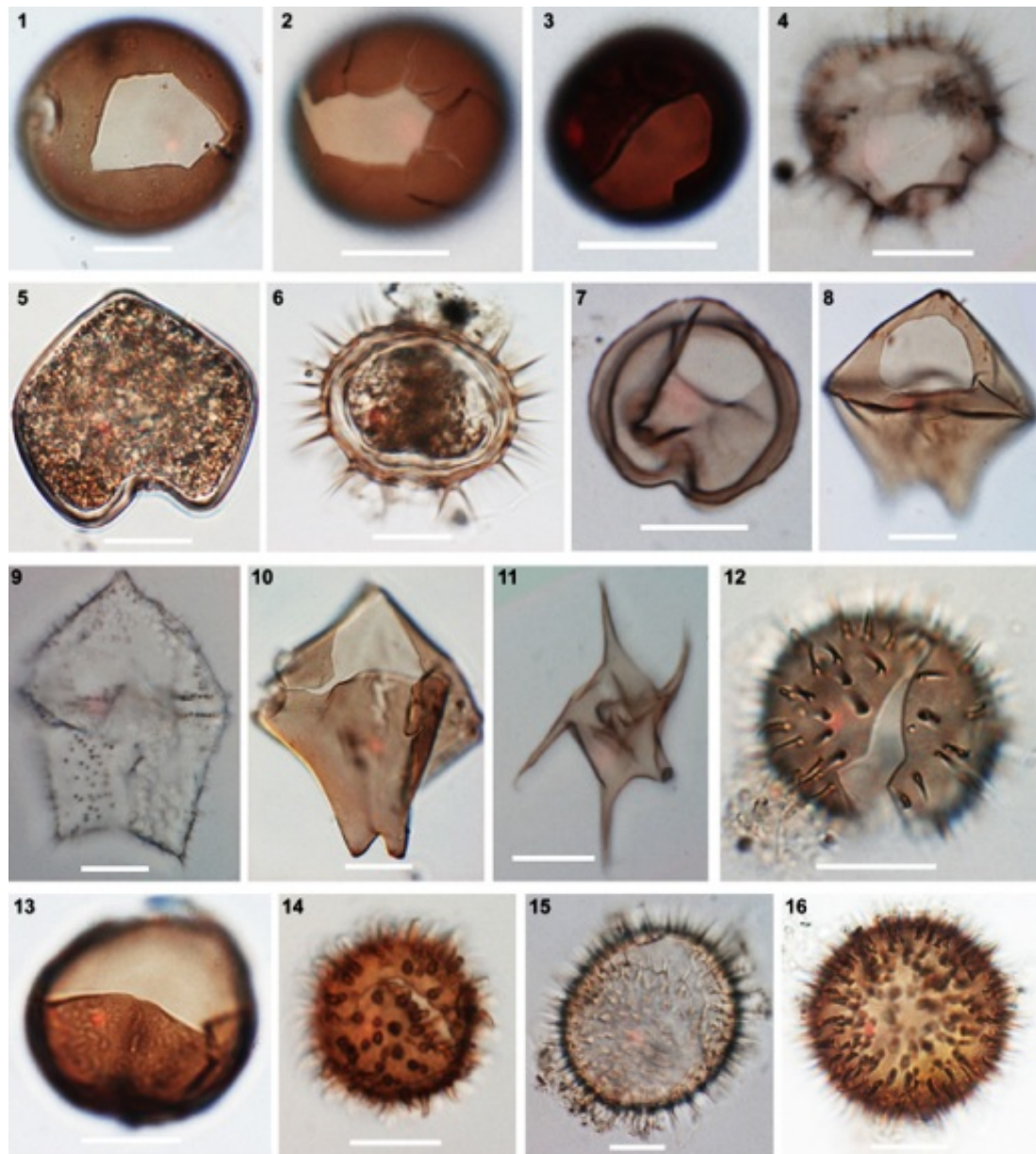


Fig.5.2.B. Light micrographs of dinoflagellate cysts. **1** *Protoperidinium* sp. 2 (*Brigantedinium majusculum*), **2** *Protoperidinium denticulatum* (*Brigantedinium irregulare*), **3** *Protoperidinium* sp. 3 (*Brigantedinium* sp.), **4** *Protoperidinium divaricatum* (*Xandarodinium variabile*), **5** *Protoperidinium oblongum* (*Votadinium calvum*), **6** *Protoperidinium conicum* (*Selenopemphix quanta*), **7** *Protoperidinium subinerme* (*Selenopemphix alticinctum*), **8** *Protoperidinium* sp. 4 (*Lejeunecysta sabrina*), **9** *Protoperidinium* sp. 14 (*Trinovantedinium capitatum*), **10** *Protoperidinium latissimum*, **11** *Protoperidinium* cf. *compressum* (*Stelladinium robustum*), **12** *Oblea acanthocysta*, **13** *Diplopsalopsis* sp., **14** *Diplopsalis* cf. *labourae*, **15,16** *Protoperidinium* spp. (Spiny round brown types). Scale bars = 20 μ m.

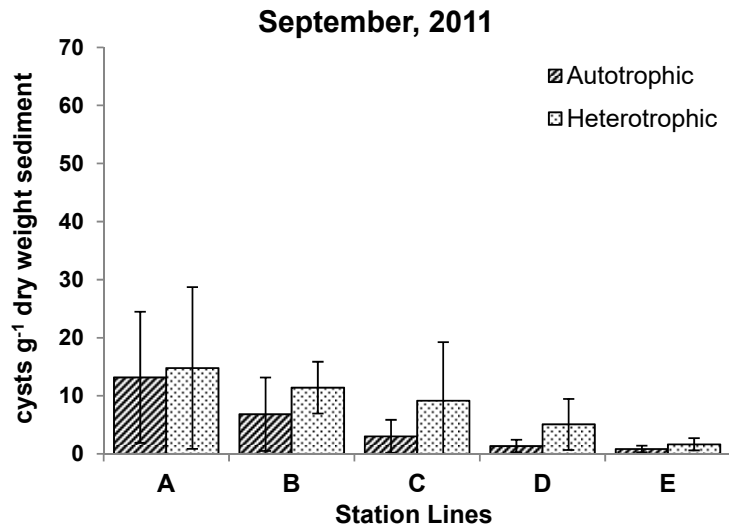


Fig.5.3.a. Graph showing the average density of autotrophic and heterotrophic cyst in each station in September, 2011. Error bars indicate the standard deviations among the composed stations in a line.

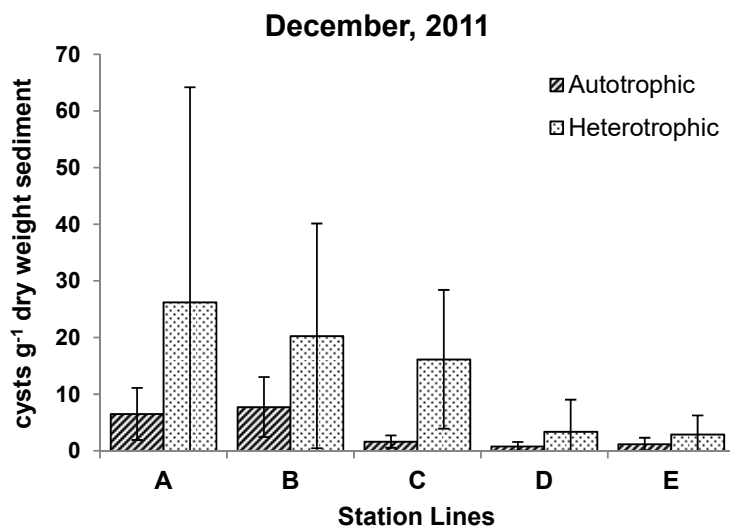


Fig.5.3.b. Graph showing the average density of autotrophic and heterotrophic cyst in each station in December, 2011. Error bars indicate the standard deviations among the composed stations in a line.

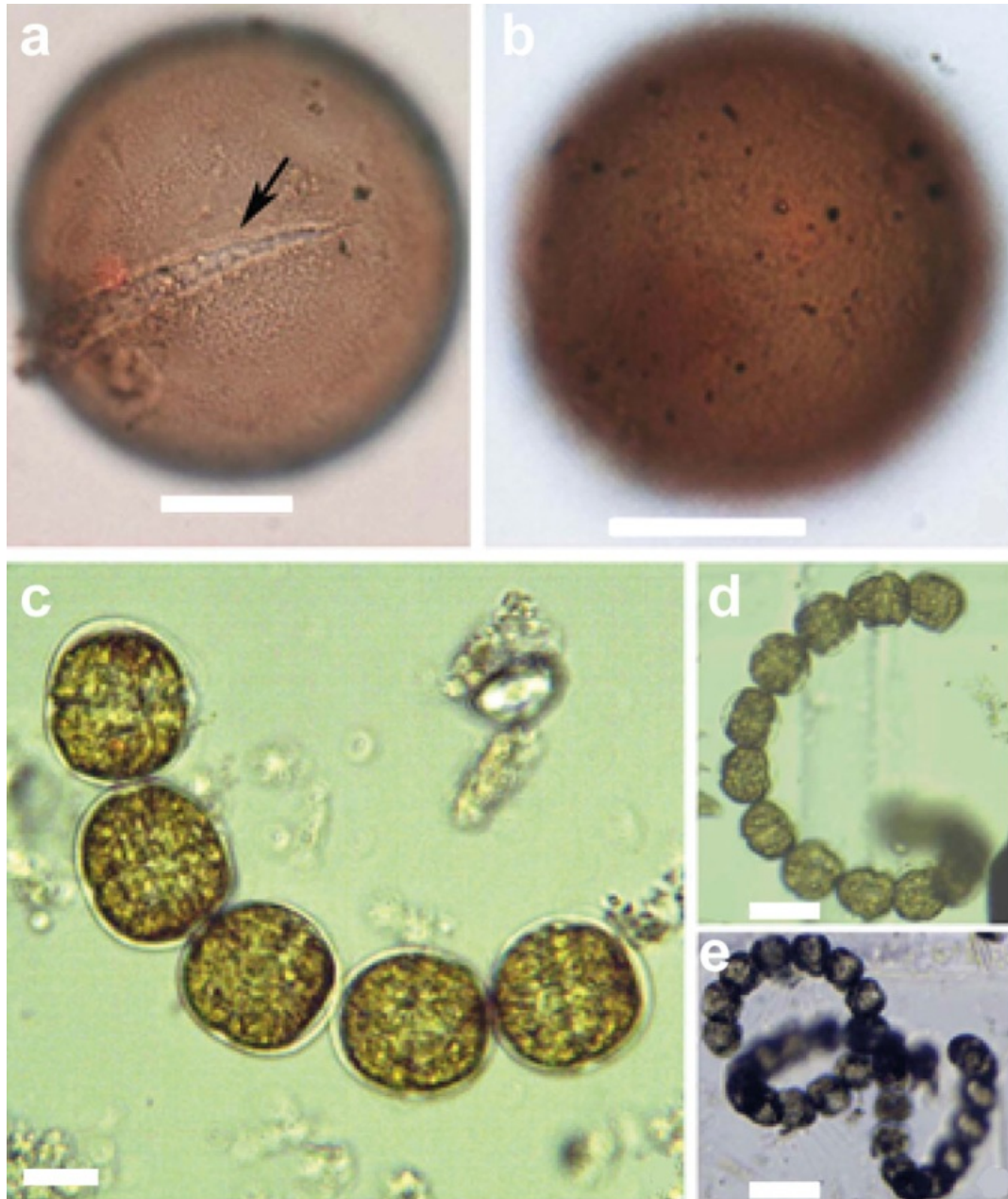


Fig.5.4. Light micrographs of cysts and plankton of *Gymnodinium catenatum* found in Selangor area. **a**; cyst showing a large chasmic archeopyle, **b**; cyst showing surface reticulate ornaments, **c**; plankton forming a chain composed of four cells, **d**; chain containing of ca. 16 cells, **e**; chain consisting ca. 32 cells. All plankton cells deformed due to formalin fixation. Scale bars: **a-c** = 20 μm , **d,e** = 50 μm .

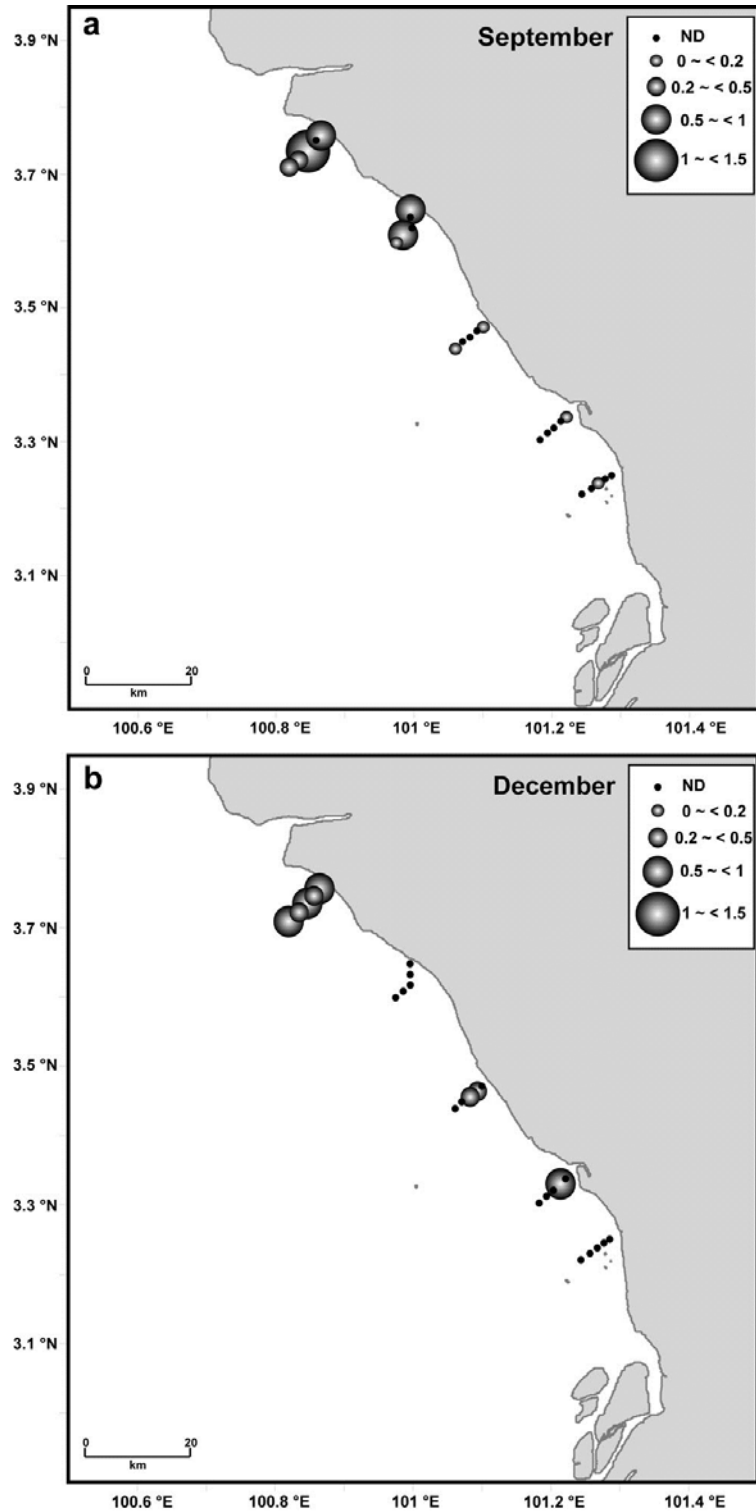


Fig.5.5. **a.** Map of Selangor area showing the occurrence of the cyst of *Gymnodinium catenatum* in the September survey. **b.** Map of Selangor area showing the occurrence of the cysts of *Gymnodinium catenatum* in the December survey. (ND: Not detected) (Cysts g⁻¹ dry weight sediment)

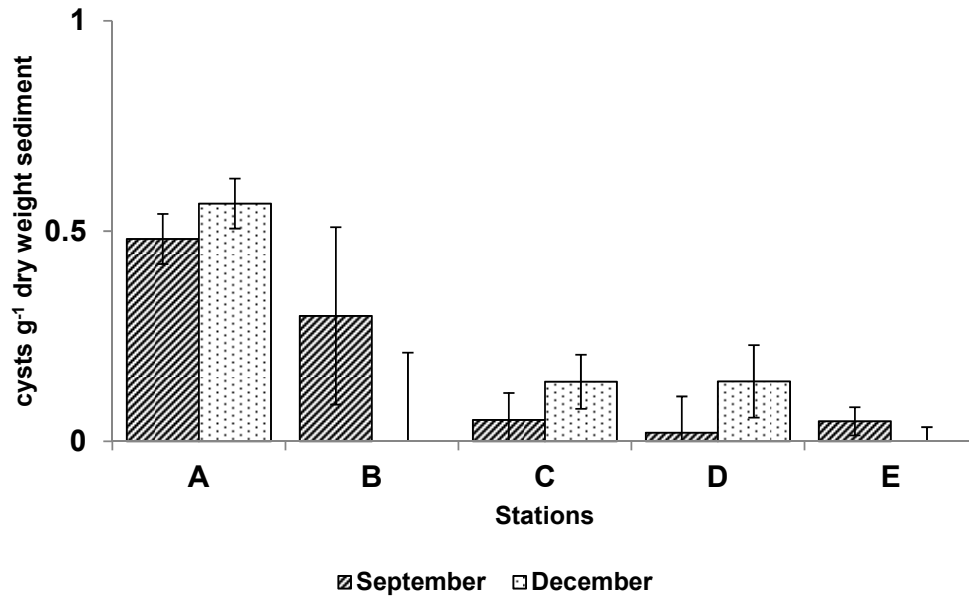


Fig.5.6. Graph showing the average density of *Gymnodinium catenatum* cysts in five sampling lines of Selangor area. Error bars indicate the standard deviations among the composed stations in a line.

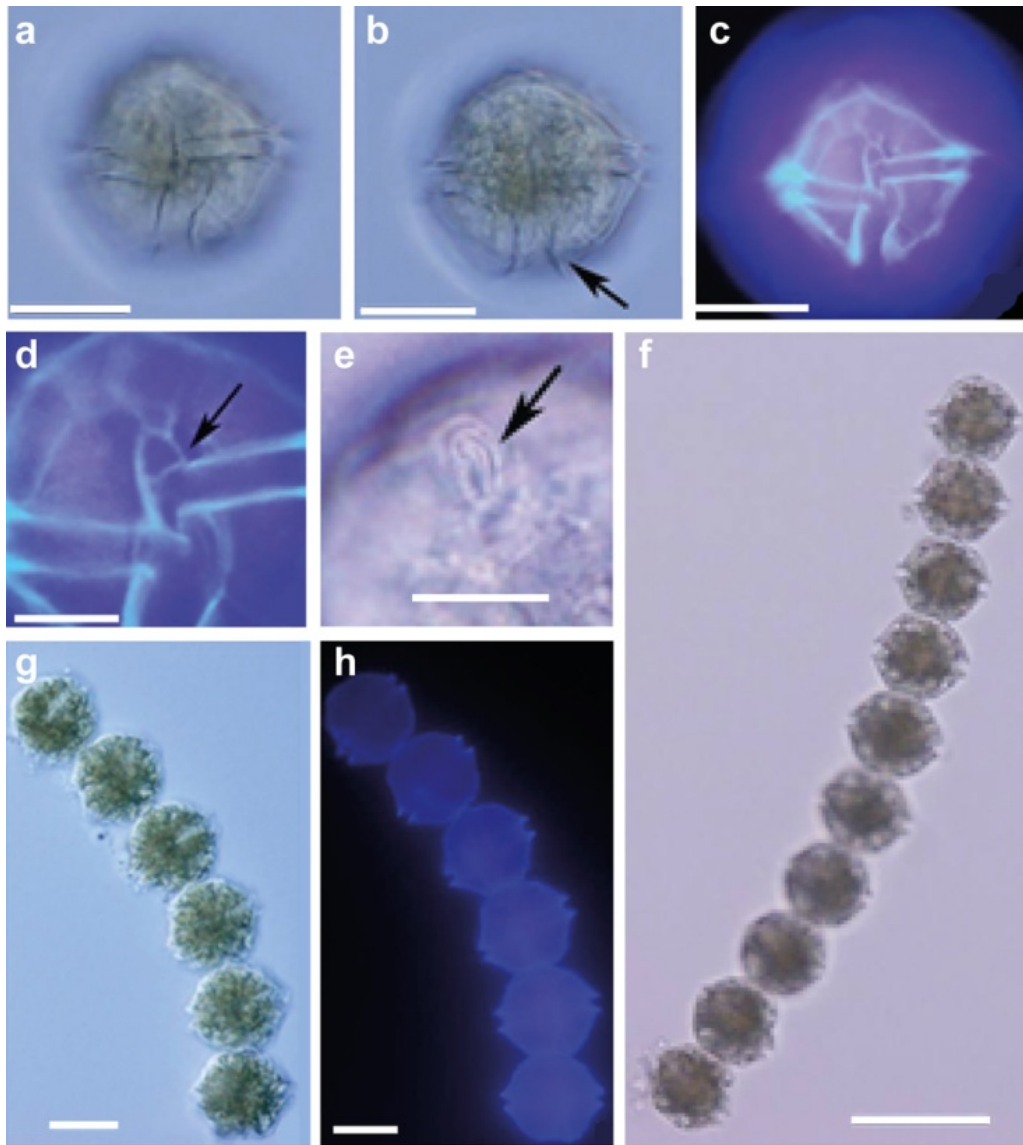


Fig.5.7. Light and fluorescence micrographs of planktonic cells of *Alexandrium tamiyavanichii* collected from Selangor area. **a,b** Outline of a single cell and well developed extension of sulcal lists (arrow), **c** Fluorescence micrograph of a single cell, **d** Fluorescence micrograph showing anterior sulcal plate (arrow), **e** Light micrograph showing apical pore plate (arrow), **f** Chain consisting of ten cells, **g** Normal light micrograph showing 6 cells, **h** Fluorescence micrograph showing 6 cells. (All fluorescence micrographs are taken using Calcofluor, which can stain the cellulose thecal plate). Scale bars: **a-c,f,g** = 20 μm , **d,e** = 10 μm .

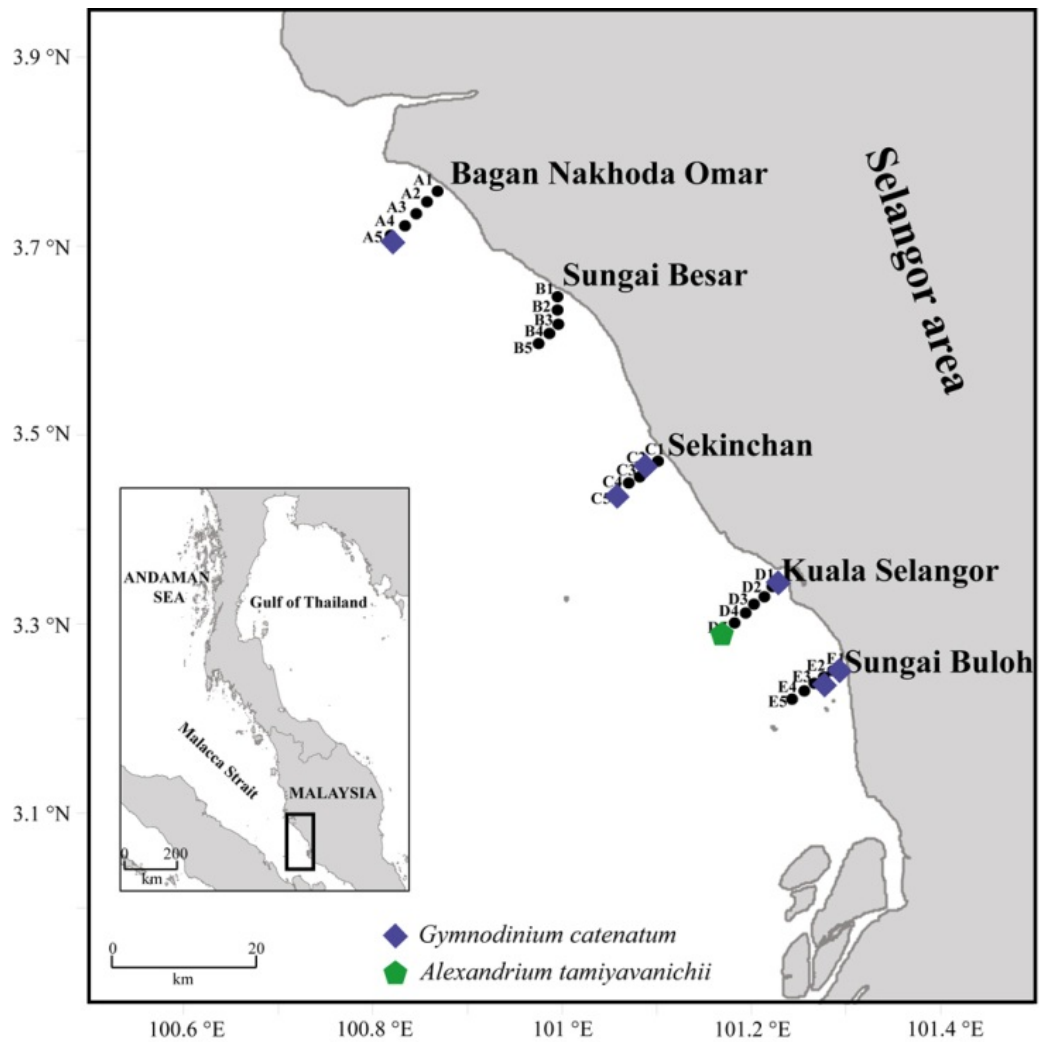


Fig.5.8. Map showing presences of planktonic cells of *Gymnodinium catenatum* and *Alexandrium tamiyavanichii*.

Table 5.1. Sampling locations at the west coast of Malay Peninsula, depths and environmental parameters (September and December, 2011).

Stations	Latitude (°N)	Longitude (°E)	Depths	Temperature (°C)		Salinity (psu)	
				September	December	September	December
A1	3.75713	100.86508	1.2	28.665	28.919	30.029	29.549
A2	3.74686	100.85722	2.2	29.007	29.401	29.622	28.293
A3	3.73425	100.84577	4.2	29.387	29.701	29.924	29.903
A4	3.72222	100.83380	4.8	29.463	29.613	30.205	30.178
A5	3.71150	100.81961	16.1	29.627	29.550	30.365	30.184
B1	3.64702	100.99563	1	28.366	29.083	29.153	28.161
B2	3.63330	100.99555	2.9	29.009	29.828	29.757	29.545
B3	3.61819	100.99605	6.3	29.528	29.827	29.882	29.685
B4	3.60833	100.98644	8.3	29.578	29.777	29.910	29.943
B5	3.59755	100.97569	10.3	29.573	29.721	30.149	30.097
C1	3.47152	101.10069	3.3	30.328	30.276	29.313	28.608
C2	3.46494	101.09258	5.7	30.211	29.982	29.786	29.042
C3	3.45672	101.08183	8.4	30.132	29.912	29.935	29.643
C4	3.44936	101.07122	11.5	30.101	29.828	30.082	29.492
C5	3.43891	101.06027	9.9	29.741	29.802	29.766	29.756
D1	3.33677	101.22113	0.6	29.990	30.077	28.665	26.628
D2	3.32955	101.21302	1.8	29.861	30.167	29.374	25.196
D3	3.32102	101.20355	2.8	29.615	29.908	29.509	28.620
D4	3.31252	101.19436	4	30.108	29.785	28.846	29.747
D5	3.30188	101.18280	17.4	29.864	29.582	30.499	30.215
E1	3.24981	101.28583	1.9	29.720	29.865	28.833	28.670
E2	3.24494	101.27686	8.1	29.971	29.704	29.365	29.659
E3	3.23802	101.26719	7.2	29.910	29.545	29.382	29.878
E4	3.22980	101.25661	5.6	29.730	29.553	29.763	30.094
E5	3.22155	101.24425	9.4	29.788	29.610	29.973	27.435

Table 5.2. List of dinoflagellate cysts recorded from the Selangor area, west coast of Malay Peninsula.

No.	Biological name	Paleontological name	Stations									
			(September, 2011)					(December, 2011)				
			A	B	C	D	E	A	B	C	D	E
Autotrophic species												
Gonyaulacales												
1	<i>Alexandrium</i> spp.		+	+	+	+	+	+	+	+	+	+
2	<i>Gonyaulax</i> cf. <i>spinifera</i>	<i>Spiniferites ramosus</i>	+		+	+		+	+			
3	<i>Gonyaulax</i> sp.	<i>Spiniferites</i> cf. <i>delicatus</i>	+	+		+	+		+	+		
4	<i>Gonyaulax</i> sp.	<i>Spiniferites</i> sp.	+	+	+		+					
5	<i>Lingulodinium polyedrum</i>	<i>Lingulodinium machaerophorum</i>	+	+	+	+						
6	<i>Protoceratium reticulatum</i>	<i>Operculodinium centrocarpum</i>	+	+	+		+					
7	<i>Protoceratium</i> sp.	<i>Operculodinium islaertianum</i>						+	+			+
8	<i>Pyrophacus steinii</i>	<i>Tuberculodinium vancampoae</i>	+	+	+	+	+	+	+	+	+	+
Gymnodiniales												
9	<i>Gymnodinium catenatum</i>		+	+	+	+	+	+	+	+	+	+
Peridinales												
10	<i>Scrippsiella</i> sp.		+									
Heterotrophic species												
Peridinales												
11	<i>Protoperidinium</i> sp.1	<i>Brigantedinium</i> cf. <i>cariacoense</i>	+	+	+	+	+	+	+	+	+	+
12	<i>Protoperidinium denticulatum</i>	<i>Brigantedinium irregulare</i>	+	+	+	+	+	+	+	+	+	+
13	<i>Protoperidinium</i> sp.2	<i>Brigantedinium majusculum</i>		+	+	+	+	+	+	+	+	+

Table 5.2 continued

No.	Biological name	Paleontological name	Stations											
			(September, 2011)					(December, 2011)						
			A	B	C	D	E	A	B	C	D	E		
14	<i>Protoperidinium</i> sp.3	<i>Brigantedinium</i> sp.	+	+	+	+	+	+	+	+	+	+	+	+
15	<i>Protoperidinium leonis</i>	<i>Lejeunecysta concreta</i>	+	+	+	+	+	+	+	+	+	+	+	+
16	<i>Protoperidinium</i> sp.4	<i>Lejeunecysta sabrina</i>	+	+	+	+	+	+	+	+	+	+	+	+
17	<i>Protoperidinium</i> sp.5	<i>Lejeunecysta</i> sp. 1	+	+	+	+	+	+	+	+	+	+	+	+
18	<i>Protoperidinium</i> sp.6	<i>Lejeunecysta</i> sp. 2	+	+	+	+	+	+	+	+	+	+	+	+
19	<i>Protoperidinium</i> sp.7	<i>Lejeunecysta</i> sp. 3	+	+	+	+	+	+	+	+	+	+	+	+
20	<i>Protoperidinium</i> sp.8	<i>Lejeunecysta</i> sp. 4	+	+	+	+	+	+	+	+	+	+	+	+
21	<i>Protoperidinium oblongum</i>	<i>Votadinium calvum</i>	+	+	+	+	+	+	+	+	+	+	+	+
22	<i>Protoperidinium</i> sp.9	<i>Votadinium</i> sp.1	+	+	+	+	+	+	+	+	+	+	+	+
23	<i>Protoperidinium</i> sp.10	<i>Votadinium</i> sp.2	+	+	+	+	+	+	+	+	+	+	+	+
24	<i>Protoperidinium conicum</i>	<i>Selenopenphix quanta</i>	+	+	+	+	+	+	+	+	+	+	+	+
25	<i>Protoperidinium subinerme</i>	<i>Selenopenphix alicinctum</i>	+	+	+	+	+	+	+	+	+	+	+	+
26	<i>Protoperidinium divaricatum</i>	<i>Xandarodinium variabile</i>	+	+	+	+	+	+	+	+	+	+	+	+
27	<i>Protoperidinium abei</i>	<i>Stelladinium abei</i>	+	+	+	+	+	+	+	+	+	+	+	+
28	<i>Protoperidinium</i> cf. <i>compressum</i>	<i>Stelladinium robustum</i>	+	+	+	+	+	+	+	+	+	+	+	+
29	<i>Protoperidinium</i> sp.11	<i>Stelladinium</i> sp.1	+	+	+	+	+	+	+	+	+	+	+	+
30	<i>Protoperidinium</i> sp.12	<i>Stelladinium</i> sp.2	+	+	+	+	+	+	+	+	+	+	+	+
31	<i>Protoperidinium</i> sp.13	<i>Stelladinium</i> sp.3	+	+	+	+	+	+	+	+	+	+	+	+
32	<i>Protoperidinium</i> sp.14	<i>Trinovantedinium capitatum</i>	+	+	+	+	+	+	+	+	+	+	+	+

Table 5.2 continued

No.	Biological name	Paleontological name	Stations (September, 2011)					Stations (December, 2011)					
			A	B	C	D	E	A	B	C	D	E	
33	<i>Protoperidinium latissimum</i>		+	+	+	+	+	+	+	+	+	+	+
34	<i>Protoperidinium</i> spp.	Spiny round brown types	+	+	+	+	+	+	+	+	+	+	+
35	<i>Protoperidinium</i> sp.15		+	+	+	+	+	+	+	+	+	+	+
36	<i>Protoperidinium</i> sp.16		+	+	+	+	+	+	+	+	+	+	+
37	<i>Protoperidinium</i> sp.17	New form 1	+	+	+	+	+	+	+	+	+	+	+
38	<i>Protoperidinium</i> sp.18	New form 2		+	+				+				+
39	<i>Protoperidinium</i> sp.19	New form 3	+										
40	<i>Protoperidinium</i> sp.20	New form 4	+			+			+		+		
41	<i>Oblea acanthocysta</i>		+	+	+	+	+	+	+	+	+	+	+
42	<i>Diplopsalopsis</i> sp.			+					+		+		+
43	<i>Diplopsalis</i> cf. <i>labourae</i>		+	+	+	+	+	+	+	+	+	+	+

Table 5.3. Density of autotrophic cysts from Station A (Bagan Nakhoda Omar), Selangor area.

No.	Biological name	Paleontological name	Stations A (Cysts g ⁻¹ dry sediment weight)									
			Stations (September, 2011)					Stations (December, 2011)				
			1	2	3	4	5	1	2	3	4	5
Autotrophic species												
1	<i>Alexandrium</i> spp.		8.8	7.4	27	0.7	6.0	0.7	2.7	7.4	2.3	3.9
2	<i>Gonyaulax</i> cf. <i>spinifera</i>	<i>Spiniferites ramosus</i>	0.8	0.3	0	0	1.1	0	0	0	0	3.9
3	<i>Gonyaulax</i> sp.	<i>Spiniferites</i> cf. <i>delicatus</i>	0.3	0	0	0.1	0	0	0	0	0	0
4	<i>Gonyaulax</i> sp.	<i>Spiniferites</i> sp.	0	0.6	0.6	0	0	0	0	0	0	0
5	<i>Lingulodinium polyedrum</i>	<i>Lingulodinium machaerophorum</i>	0	1.2	0	0	0	0	0	0	0	0
6	<i>Protoceratium reticulatum</i>	<i>Operculodinium centrocarpum</i>	0.2	0.6	1.3	0	0.7	0	0	0	0	3.1
7	<i>Protoceratium</i> sp.	<i>Operculodinium islaerianum</i>	0	0	0	0	0	0	0	0	0	0.8
8	<i>Pyrophacus steinii</i>	<i>Tuberculodinium vancampoae</i>	2.4	1.8	1.3	0	0	1.5	0.9	1.2	0.5	0.8
9	<i>Gymnodinium catenatum</i>		0.5	0	1.3	0.2	0.4	0.7	0.5	0.6	0.2	0.8
10	<i>Scrippsiella</i> sp.		0.3	0	0	0	0	0	0	0	0	0
			13.3	11.9	31.5	1.0	8.2	2.9	4.1	9.2	3.0	13.3

Table 5.4. Density of heterotrophic cysts from Station A (Bagan Nakhoda Omar), Selangor area.

No.	Biological name	Paleontological name	Stations A (Cysts g ⁻¹ dry sediment weight)									
			Stations (September, 2011)					Stations (December, 2011)				
			1	2	3	4	5	1	2	3	4	5
Heterotrophic species												
1	<i>Protooperidinium</i> sp.1	<i>Brigantedinium</i> cf. <i>cariacoense</i>	0	0	0	0	10	0	0.4	0.6	0.7	9.4
2	<i>Protooperidinium</i> <i>denticulatum</i>	<i>Brigantedinium</i> <i>irregularare</i>	2.7	0.6	7.6	0.8	12	2.6	3.6	7.3	1.8	27
3	<i>Protooperidinium</i> sp.2	<i>Brigantedinium</i> <i>majusculum</i>	0	0	0	0	0	0	0	0	1.4	0
4	<i>Protooperidinium</i> sp.3	<i>Brigantedinium</i> sp.	0	0	0	0	0	0	0	0	0	4.7
5	<i>Protooperidinium</i> <i>leonis</i>	<i>Lejeunecysta</i> <i>concreta</i>	0	0	0	0	0	0.4	0	0	0	0.8
6	<i>Protooperidinium</i> sp.4	<i>Lejeunecysta</i> <i>sabrina</i>	0	0	0	0	0	0	0	0	0	0
7	<i>Protooperidinium</i> sp.5	<i>Lejeunecysta</i> sp. 1	0	0	0.6	0	0	0	0	0	0	0
8	<i>Protooperidinium</i> sp.6	<i>Lejeunecysta</i> sp. 2	0	0	0	0	0	0.4	0	0.2	0	0
9	<i>Protooperidinium</i> sp.7	<i>Lejeunecysta</i> sp. 3	0	0.6	0	0	0	0	0	0	0	0
10	<i>Protooperidinium</i> sp.8	<i>Lejeunecysta</i> sp. 4	0	0	0	0	0	0	0	0	0	0
11	<i>Protooperidinium</i> <i>oblongum</i>	<i>Votadinium</i> <i>calvum</i>	1.1	0.3	0.6	0	0.3	0	0.9	0.6	0.2	1.6
12	<i>Protooperidinium</i> sp.9	<i>Votadinium</i> sp.1	0.5	0.3	1.2	0	1.8	0	0	0	0	0
13	<i>Protooperidinium</i> sp.10	<i>Votadinium</i> sp.2	0	0	0	0	0	0	0	0	0	0
14	<i>Protooperidinium</i> <i>conicum</i>	<i>Selenopemphix</i> <i>quanta</i>	0	0	0	0	0	0	0	0.6	0	3.1
15	<i>Protooperidinium</i> <i>subinermis</i>	<i>Selenopemphix</i> <i>alticinctum</i>	0.5	0.3	0.6	0	2.5	0	0.4	1.2	0.2	0
16	<i>Protooperidinium</i> <i>divaricatum</i>	<i>Xandarodinium</i> <i>variabile</i>	0.8	0.3	0	0	0	0	0	0	0	0
17	<i>Protooperidinium</i> <i>abei</i>	<i>Stelladinium</i> <i>abei</i>	0.3	0.6	0	0	0	0	1.2	0.2	0.8	0.8

Table 5.4 continued

No.	Biological name	Paleontological name	Stations A (Cysts g ⁻¹ dry sediment weight)									
			Stations (September, 2011)					Stations (December, 2011)				
			1	2	3	4	5	1	2	3	4	5
18	<i>Protoperidinium cf. compressum</i>	<i>Stelladinium robustum</i>	0.3	0.3	0	0	0.3	0	0	0.6	0.2	1.6
19	<i>Protoperidinium</i> sp.11	<i>Stelladinium</i> sp.1	0	0	0	0	0	0	0	0	0	0
20	<i>Protoperidinium</i> sp.12	<i>Stelladinium</i> sp.2	0.8	0.6	0	0	0	0.4	0	0	0	0
21	<i>Protoperidinium</i> sp.13	<i>Stelladinium</i> sp.3	0	0.3	0	0	1.4	0	0.4	1.2	0	1.6
22	<i>Protoperidinium</i> sp.14	<i>Trinovantedinium capitatum</i>	0.8	0.9	0	0	2.5	0	0	0.6	0.2	7.0
23	<i>Protoperidinium latissimum</i>		0	0	0	0	0.3	0	0	0	0.2	0
24	<i>Protoperidinium</i> spp.	Spiny round brown types	1.9	0.3	1.9	0.1	3.5	0	0.4	1.2	0.5	21
25	<i>Protoperidinium</i> sp.15		0	0	0	0	0.3	0.4	0.4	0	0.7	0.8
26	<i>Protoperidinium</i> sp.16		0	0	0.6	0	0	0	0.4	0	0.5	1.6
27	<i>Protoperidinium</i> sp.17	New form 1	0.8	3.1	0	0	1.4	0.4	0.9	1.8	0.7	3.9
28	<i>Protoperidinium</i> sp.18	New form 2	0	0	0	0	0	0	0	0	0	0
29	<i>Protoperidinium</i> sp.19	New form 3	0.3	0	0	0	0	0	0	0	0	0
30	<i>Protoperidinium</i> sp.20	New form 4	0	0	0	0	0.3	0	0	0	0	0
31	<i>Oblea acanthocysta</i>		0.5	0	1.3	0	1.4	0	0	0	0	8.6
32	<i>Diplopsalopsis</i> sp.		0	0	0	0	0	0	0	0	0	0
33	<i>Diplopsalis cf. labourae</i>		0.5	0.3	0	0	0	0	0	0.6	0	0
			11.8	8.8	14.4	0.9	38	3.8	8.6	17.5	7.7	93.5

Table 5.5. Density of autotrophic cysts from Station B (Sungai Besar), Selangor area.

No.	Biological name	Paleontological name	Stations B (Cysts g ⁻¹ dry sediment weight)									
			Stations (September, 2011)					Stations (December, 2011)				
			1	2	3	4	5	1	2	3	4	5
Autotrophic species												
1	<i>Alexandrium</i> spp.		15	2.8	1.9	3.1	2.7	8.7	11	9.1	1.8	1.9
2	<i>Gonyaulax</i> cf. <i>spinifera</i>	<i>Spiniferites ramosus</i>	0	0	0	0	0	0	0	0	0	0.6
3	<i>Gonyaulax</i> sp.	<i>Spiniferites</i> cf. <i>delicatus</i>	0	0	0.4	0.8	0	0	0.5	0	0	0
4	<i>Gonyaulax</i> sp.	<i>Spiniferites</i> sp.	1.5	0.8	0.2	0.8	0	0	0	0	0	0
5	<i>Lingulodinium polyedrum</i>	<i>Lingulodinium machaerophorum</i>	0	0	0.2	0	0	0	0	0	0	0
6	<i>Protoceratium reticulatum</i>	<i>Operculodinium centrocarpum</i>	0.5	0	0	0	0	0	0	0	0	0
7	<i>Protoceratium</i> sp.	<i>Operculodinium islaerianum</i>	0	0	0	0	0	1.2	0	0	0	0
8	<i>Pyrophacus steinii</i>	<i>Tuberculodinium vancampoe</i>	0	0.8	0.4	0	0.2	2.9	0.9	0	0	0
9	<i>Gymnodinium catenatum</i>		0.5	0	0	0.8	0.2	0	0	0	0	0
10	<i>Scrippsiella</i> sp.		0.5	0	0	0	0	0	0	0	0	0
			18	4.4	3.1	5.5	3.1	12.8	12.4	9.1	1.8	2.5

Table 5.6. Density of heterotrophic cysts from Station B (Sungai Besar), Selangor area.

No.	Biological name	Paleontological name	Stations B (Cysts g ⁻¹ dry sediment weight)									
			Stations (September, 2011)					Stations (December, 2011)				
			1	2	3	4	5	1	2	3	4	5
Heterotrophic species												
1	<i>Protoperidinium</i> sp.1	<i>Brigantedinium cf. cariacense</i>	0.5	0.4	1.2	0	0.2	2.9	0.5	2.1	0.2	1.0
2	<i>Protoperidinium denticulatum</i>	<i>Brigantedinium irregulare</i>	3.5	1.6	2.7	2.4	0.8	10	1.9	3.2	0.9	3.5
3	<i>Protoperidinium</i> sp.2	<i>Brigantedinium majusculum</i>	3.0	0.4	0.8	0.8	1	1.2	4.2	1.1	0.9	0.3
4	<i>Protoperidinium</i> sp.3	<i>Brigantedinium</i> sp.	1.5	0	0.4	0	0.2	2.3	0.5	0.5	0.2	0.3
5	<i>Protoperidinium leonis</i>	<i>Lejeunecysta concreta</i>	0.5	0	0.2	0	0	0	0	0	0	0
6	<i>Protoperidinium</i> sp.4	<i>Lejeunecysta sabrina</i>	0.5	0	0	1.6	1.0	1.2	1.4	0	0.2	0.3
7	<i>Protoperidinium</i> sp.5	<i>Lejeunecysta</i> sp. 1	0.5	0	0	0.8	0	0	0	0	0.2	0
8	<i>Protoperidinium</i> sp.6	<i>Lejeunecysta</i> sp. 2	0.5	0	0	0	0	1.2	0	0	0	0
9	<i>Protoperidinium</i> sp.7	<i>Lejeunecysta</i> sp. 3	0	0	0.2	0	0.2	1.2	0	0	0	0
10	<i>Protoperidinium</i> sp.8	<i>Lejeunecysta</i> sp. 4	1.0	0	0	0	0	0.6	0	0.5	0	0
11	<i>Protoperidinium oblongum</i>	<i>Votadinium calvum</i>	0.5	0	0.6	0	0.6	4.1	2.3	1.1	0.2	0
12	<i>Protoperidinium</i> sp.9	<i>Votadinium</i> sp.1	0	0	0	0	0	0.6	0	0.5	0	0
13	<i>Protoperidinium</i> sp.10	<i>Votadinium</i> sp.2	0	0	0	0	0	0	0	0	0	0
14	<i>Protoperidinium conicum</i>	<i>Selenopemphix quanta</i>	0	0	0	0	0	0	0	0	0.2	0.6
15	<i>Protoperidinium subinerme</i>	<i>Selenopemphix alticinctum</i>	0.5	0	0.4	0.8	0.2	0	0.5	0	0.7	0
16	<i>Protoperidinium divaricatum</i>	<i>Xandarodinium variabile</i>	0	0	0	0	0	0	0	0	0	0
17	<i>Protoperidinium abei</i>	<i>Stelladinium abei</i>	0	0	0	0	0.4	0	0	0	0	0

Table 5.6 continued

No.	Biological name	Paleontological name	Stations B (Cysts g ⁻¹ dry sediment weight)														
			Stations (September, 2011)					Stations (December, 2011)									
			1	2	3	4	5	1	2	3	4	5	1	2	3	4	5
18	<i>Protooperidinium</i> cf. <i>compressum</i>	<i>Stelladinium robustum</i>	0	0	0	0	0.2	0	0.9	0	0.2	0	0.2	0	0	0	
19	<i>Protooperidinium</i> sp.11	<i>Stelladinium</i> sp.1	0	0	0	0	0	0.6	0.9	0	0.4	0	0	0	0	0	
20	<i>Protooperidinium</i> sp.12	<i>Stelladinium</i> sp.2	0	0	0	0	0	0.6	0	0	0	0	0	0	0	0	
21	<i>Protooperidinium</i> sp.13	<i>Stelladinium</i> sp.3	0.5	1.2	0.6	0	0.2	1.2	0	0	0	0	0	0	0	0	
22	<i>Protooperidinium</i> sp.14	<i>Trinovantedinium capitatum</i>	2.5	0	0.6	1.6	0	4.6	0	0.5	0	0	0	0	0	0	
23	<i>Protooperidinium latissimum</i>		0	0	0	0	0.2	0.6	0	0	0	0	0	0	0	0	
24	<i>Protooperidinium</i> spp.	Spiny round brown types	1.5	1.2	1.9	0.8	0.4	12	4.7	2.7	0.9	0.6	0.6	0.6	0.6	0.6	
25	<i>Protooperidinium</i> sp.15		0.5	0.4	0.6	0.8	0.8	0.6	0	0.5	0	0	0	0	0	0	
26	<i>Protooperidinium</i> sp.16		0.5	0	0.4	0	0	0	0	0	0	0	0	0	0	0	
27	<i>Protooperidinium</i> sp.17	New form 1	0.5	2.4	0.6	0	0.4	6.4	0.9	0.5	0.4	0	0	0	0	0	
28	<i>Protooperidinium</i> sp.18	New form 2	0	0	0	0	0.4	0	0	0	0	0	0	0	0	0	
29	<i>Protooperidinium</i> sp.19	New form 3	0	0	0	0	0	0	0	0	0	0	0	0	0	0	
30	<i>Protooperidinium</i> sp.20	New form 4	0	0	0	0	0	0	0.5	0	0	0	0	0	0	0	
31	<i>Oblea acanthocysta</i>		0	0.4	0	0.8	0.8	0	0	0	0	0	0	0	0	0	
32	<i>Diplopsalopsis</i> sp.		0.5	0	0	0	0	1.2	0.9	0	0.2	0.3	0.3	0.3	0.3	0.3	
33	<i>Diplopsalis</i> cf. <i>labourae</i>		0	0.4	0	0	0	1.2	0	0.5	0	0	0	0	0	0	
			19	8.4	11.2	10.4	8.0	54.3	20.1	13.7	5.8	7.5	7.5	7.5	7.5	7.5	

Table 5.7. Density of autotrophic cysts from Station C (Sekinchan), Selangor area.

No.	Biological name	Paleontological name	Stations C (Cysts g ⁻¹ dry sediment weight)									
			Stations (September, 2011)					Stations (December, 2011)				
			1	2	3	4	5	1	2	3	4	5
Autotrophic species												
1	<i>Alexandrium</i> spp.		0.8	1.3	3.7	6.2	0.3	2.7	1.2	0.9	1.3	0
2	<i>Gonyaulax</i> cf. <i>spinifera</i>	<i>Spiniferites ramosus</i>	0	0	0.2	0.8	0	0	0	0	0	0
3	<i>Gonyaulax</i> sp.	<i>Spiniferites</i> cf. <i>delicatus</i>	0	0	0	0	0	0	0	0.4	0	0
4	<i>Gonyaulax</i> sp.	<i>Spiniferites</i> sp.	0	0	0.4	0	0	0	0	0	0	0
5	<i>Lingulodinium polyedrum</i>	<i>Lingulodinium machaerophorum</i>	0	0.2	0.2	0	0	0	0	0	0	0
6	<i>Protoceratium reticulatum</i>	<i>Operculodinium centrocarpum</i>	0	0.2	0	0	0	0	0	0	0	0
7	<i>Protoceratium</i> sp.	<i>Operculodinium islaerianum</i>	0	0	0	0	0	0	0	0	0	0
8	<i>Pyrophacus steinii</i>	<i>Tuberculodinium vancampoeae</i>	0	0.2	0.4	0	0	0.3	0	0	0.6	0
9	<i>Gymnodinium catenatum</i>		0.1	0	0	0	0.1	0	0.2	0.5	0	0
10	<i>Scrippsiella</i> sp.		0	0	0	0	0	0	0	0	0	0
			0.9	1.9	4.9	7.0	0.4	3.0	1.4	1.8	1.9	0

Table 5.8. Density of heterotrophic cysts from Station C (Sekinchan), Selangor area.

No.	Biological name	Paleontological name	Stations C (Cysts g ⁻¹ dry sediment weight)									
			Stations (September, 2011)					Stations (December, 2011)				
			1	2	3	4	5	1	2	3	4	5
Heterotrophic species												
1	<i>Protopteridinium</i> sp.1	<i>Brigantedinium</i> cf. <i>carriacoense</i>	0.1	0	0.4	2.9	0.7	0	0	1.8	3.2	1.5
2	<i>Protopteridinium denticulatum</i>	<i>Brigantedinium irregulare</i>	0.2	0	1.1	5.8	1.4	0.5	3.2	8.3	9.5	3.5
3	<i>Protopteridinium</i> sp.2	<i>Brigantedinium majusculum</i>	0.4	0.8	0.8	5	1	0	1.2	0.9	3.2	1.5
4	<i>Protopteridinium</i> sp.3	<i>Brigantedinium</i> sp.	0	0	0.4	0	0.1	0	0	0.4	0	0
5	<i>Protopteridinium leonis</i>	<i>Lejeunecysta concreta</i>	0.1	0	0	0	0	0	0	0	0.6	0
6	<i>Protopteridinium</i> sp.4	<i>Lejeunecysta sabrina</i>	0	0.2	0	0.4	0.1	0	0.2	0.9	0	0.5
7	<i>Protopteridinium</i> sp.5	<i>Lejeunecysta</i> sp. 1	0	0	0	0.8	0	0	0	0	0.6	0
8	<i>Protopteridinium</i> sp.6	<i>Lejeunecysta</i> sp. 2	0	0	0.2	0	0	0.3	0	0.4	0.6	0
9	<i>Protopteridinium</i> sp.7	<i>Lejeunecysta</i> sp. 3	0	0.2	0	0	0	0	0	0	0	0.5
10	<i>Protopteridinium</i> sp.8	<i>Lejeunecysta</i> sp. 4	0	0	0	0	0	0	0	0	0	0
11	<i>Protopteridinium oblongum</i>	<i>Votadinium calvum</i>	0.4	0.8	0.2	0.4	0.3	0.3	2.0	0.9	2.5	1.0
12	<i>Protopteridinium</i> sp.9	<i>Votadinium</i> sp.1	0	0.8	0	0	0	0	0.5	0	0.6	0.5
13	<i>Protopteridinium</i> sp.10	<i>Votadinium</i> sp.2	0	0	0	0	0	0	0	0	0	0
14	<i>Protopteridinium conicum</i>	<i>Selenopemphix quanta</i>	0	0	0.4	0.8	0	0	0	0	0	0
15	<i>Protopteridinium subinerme</i>	<i>Selenopemphix alticinctum</i>	0	0	0.2	0.4	0.1	0.3	0.2	0.4	1.3	1.5
16	<i>Protopteridinium divaricatum</i>	<i>Xandarodinium variabile</i>	0	0	0	0	0	0	0	0	0	0
17	<i>Protopteridinium abei</i>	<i>Stelladinium abei</i>	0	0.2	0	0.8	0	0	0	0	0	0.5

Table 5.8 continued

No.	Biological name	Paleontological name	Stations C (Cysts g ⁻¹ dry sediment weight)															
			Stations (September, 2011)					Stations (December, 2011)										
			1	2	3	4	5	1	2	3	4	5	1	2	3	4	5	
18	<i>Protoperidinium cf. compressum</i>	<i>Stelladinium robustum</i>	0	0	0	0	0	0	0	0	0	0	0	0	0	0.4	0	0
19	<i>Protoperidinium</i> sp.11	<i>Stelladinium</i> sp.1	0	0.2	0	0	0	0	0	0	0	0	0	0	0.4	1.3	0	0
20	<i>Protoperidinium</i> sp.12	<i>Stelladinium</i> sp.2	0	0	0	0	0	0	0	0	0	0	0	0	0	0	0	0
21	<i>Protoperidinium</i> sp.13	<i>Stelladinium</i> sp.3	0	0	0.2	0.8	0.1	0	0	0	0	0	0	0	0	1.3	0	0
22	<i>Protoperidinium</i> sp.14	<i>Trinovantedinium capitatum</i>	0	0	0.2	0.4	0.1	0	0	0	0	0.4	0	0	0	0	0	0
23	<i>Protoperidinium latissimum</i>		0	0	0	0	0	0.1	0	0.2	0	0	0.6	0	0	0	0	0
24	<i>Protoperidinium</i> spp.	Spiny round brown types	0	1.0	1.1	3.3	0	0.5	1	2.3	3.8	2.5						
25	<i>Protoperidinium</i> sp.15		0.1	0.5	0.4	0.8	0	0	0	0	0	0	0	0	0	0	0	0
26	<i>Protoperidinium</i> sp.16		0	0	0	0	0	0	0	0	0.4	0	0	0	0	0	0	0
27	<i>Protoperidinium</i> sp.17	New form 1	0	0.2	1.1	0.8	0.5	0	0.5	0.9	1.9	0.5						
28	<i>Protoperidinium</i> sp.18	New form 2	0	0	0	0.4	0	0	0.5	0.4	0	0	0	0	0	0	0	0
29	<i>Protoperidinium</i> sp.19	New form 3	0	0	0	0	0	0	0	0	0	0	0	0	0	0	0	0
30	<i>Protoperidinium</i> sp.20	New form 4	0	0	0	0	0	0	0	0	0	0	0	0	0	0	0	0
31	<i>Oblea acanthocysta</i>		0	0	1.3	2.9	0.3	0	0.2	0	1.9	0.5						
32	<i>Diplopsalopsis</i> sp.		0	0	0	0	0	0	0	0	0	0	0	0	0	0	0	0
33	<i>Diplopsalis cf. labourae</i>		0	0	0	0	0	0	0.2	0	0	0	0	0	0	0	0	0
			1.3	4.9	8	26.7	4.8	1.9	9.9	19.2	34.8	15						

Table 5.9. Density of autotrophic cysts from Station D (Kuala Selangor), Selangor area.

No.	Biological name	Paleontological name	Stations D (Cysts g ⁻¹ dry sediment weight)									
			Stations (September, 2011)					Stations (December, 2011)				
			1	2	3	4	5	1	2	3	4	5
Autotrophic species												
1	<i>Alexandrium</i> spp.		1.0	0.6	0	0.3	2.8	0.9	0	0	0	0.6
2	<i>Gonyaulax</i> cf. <i>spinifera</i>	<i>Spiniferites ramosus</i>	0	0	0.6	0	0	0	0	0	0	0
3	<i>Gonyaulax</i> sp.	<i>Spiniferites</i> cf. <i>delicatus</i>	0	0	0.3	0	0	0	0	0	0	0
4	<i>Gonyaulax</i> sp.	<i>Spiniferites</i> sp.	0	0	0	0.1	0	0	0	0	0	0
5	<i>Lingulodinium polyedrum</i>	<i>Lingulodinium machaerophorum</i>	0	0	0.3	0	0	0	0	0	0	0
6	<i>Protoceratium reticulatum</i>	<i>Operculodinium centrocarpum</i>	0	0	0	0	0	0	0	0	0	0
7	<i>Protoceratium</i> sp.	<i>Operculodinium islaerianum</i>	0	0	0	0	0	0	0	0	0	0.6
8	<i>Pyrophacus steinii</i>	<i>Tuberculodinium vancampoeae</i>	0.1	0	0	0.1	0.4	0.4	0	0	0.2	0.6
9	<i>Gymnodinium catenatum</i>		0.1	0	0	0	0	0	0.7	0	0	0
10	<i>Scrippsiella</i> sp.		0	0	0	0	0	0	0	0	0	0
			1.2	0.6	1.2	0.5	3.2	1.3	0.7	0	0.2	1.8

Table 5.10. Density of heterotrophic cysts from Station D (Kuala Selangor), Selangor area.

No.	Biological name	Paleontological name	Stations D (Cysts g ⁻¹ dry sediment weight)											
			Stations (September, 2011)					Stations (December, 2011)						
			1	2	3	4	5	1	2	3	4	5		
Heterotrophic species														
1	<i>Protoperidinium</i> sp.1	<i>Brigantedinium</i> cf. <i>carriacoense</i>	0	0.2	1.4	0.1	0	0	0	0	0	0	0	0
2	<i>Protoperidinium</i> <i>denticulatum</i>	<i>Brigantedinium</i> <i>irregularare</i>	0.7	0.8	4.6	0.3	2.4	0	0	0	0	0	0	3.8
3	<i>Protoperidinium</i> sp.2	<i>Brigantedinium</i> <i>majusculum</i>	0.1	0.2	0.8	0	0	0	0.6	0	0.2	1.3		
4	<i>Protoperidinium</i> sp.3	<i>Brigantedinium</i> sp.	0	0.2	0	0	0	0	0	0	0	0	0	0
5	<i>Protoperidinium</i> <i>leonis</i>	<i>Lejeunecysta</i> <i>concreta</i>	0	0	0.3	0	0	0	0	0	0	0	0	0
6	<i>Protoperidinium</i> sp.4	<i>Lejeunecysta</i> <i>sabrina</i>	0.1	0.4	0.6	0	0	0	0	0	0	0	0	0
7	<i>Protoperidinium</i> sp.5	<i>Lejeunecysta</i> sp. 1	0	0	0	0.1	1.6	0	0	0	0	1.3		
8	<i>Protoperidinium</i> sp.6	<i>Lejeunecysta</i> sp. 2	0	0	0	0	0	0	0	0	0	0	0	0
9	<i>Protoperidinium</i> sp.7	<i>Lejeunecysta</i> sp. 3	0.1	0	0	0	0	0	0	0	0	0	0	0
10	<i>Protoperidinium</i> sp.8	<i>Lejeunecysta</i> sp. 4	0	0	0	0	0	0	0	0	0	0	0	0
11	<i>Protoperidinium</i> <i>oblongum</i>	<i>Votadinium</i> <i>calvum</i>	0.2	0	0.3	0.4	1.2	0	0.7	0	0.5	2.5		
12	<i>Protoperidinium</i> sp.9	<i>Votadinium</i> sp.1	0	0.2	0	0	0	0	0	0	0	0	0	0
13	<i>Protoperidinium</i> sp.10	<i>Votadinium</i> sp.2	0	0	0	0.1	0.4	0	0	0	1.3			
14	<i>Protoperidinium</i> <i>conicum</i>	<i>Selenopemphix</i> <i>quanta</i>	0	0	0	0	0	0.4	0	0	0.2	0		
15	<i>Protoperidinium</i> <i>subinermis</i>	<i>Selenopemphix</i> <i>alticinctum</i>	0.1	0	0.8	0.1	0	0	0	0	0	0	0	0
16	<i>Protoperidinium</i> <i>divaricatum</i>	<i>Xandarodinium</i> <i>variabile</i>	0	0	0	0	0	0	0	0	0	0	0	0
17	<i>Protoperidinium</i> <i>abei</i>	<i>Stelladinium</i> <i>abei</i>	0	0	0.3	0	0	0	0	0	0	0	0	0.6

Table 5.10 continued

No.	Biological name	Paleontological name	Stations D (Cysts g ⁻¹ dry sediment weight)																	
			Stations (September, 2011)					Stations (December, 2011)												
			1	2	3	4	5	1	2	3	4	5	1	2	3	4	5			
18	<i>Protopteridinium cf. compressum</i>	<i>Stelladinium robustum</i>	0	0	0	0	0	0	0	0	0	0	0	0	0	0	0	0	0	0
19	<i>Protopteridinium</i> sp.11	<i>Stelladinium</i> sp.1	0	0	0	0	0	0	0	0	0	0	0	0	0	0	0	0.2	0	0
20	<i>Protopteridinium</i> sp.12	<i>Stelladinium</i> sp.2	0	0	0	0	0	0	0	0	0	0	0	0	0	0	0	0	0	0
21	<i>Protopteridinium</i> sp.13	<i>Stelladinium</i> sp.3	0	0	0	0.1	0	0	0	0	0	0	0	0	0	0	0	0	0	0
22	<i>Protopteridinium</i> sp.14	<i>Trinovantedinium capitatum</i>	0.1	0	0	0	0	0	0	0	0	0	0	0	0	0	0	0	0	0
23	<i>Protopteridinium latissimum</i>		0	0	0	0	0	0.8	0	0	0	0	0	0	0	0	0	0	0	0
24	<i>Protopteridinium</i> spp.	Spiny round brown types	0.2	0	0	0.2	0.4	0	0.7	0	0	0	0	0	0	0	0	0	0	1.3
25	<i>Protopteridinium</i> sp.15		0.1	0.2	0.3	0	0	0	0	0	0	0	0	0	0	0	0	0	0	0
26	<i>Protopteridinium</i> sp.16		0	0	0	0	0.4	0	0	0	0	0	0	0	0	0	0	0	0	0
27	<i>Protopteridinium</i> sp.17	New form 1	0.1	0.2	1.4	0.1	0.4	0	0	0	0	0	0	0	0	0	0	0	0	1.3
28	<i>Protopteridinium</i> sp.18	New form 2	0	0	0	0	0	0	0	0	0	0	0	0	0	0	0	0	0	0
29	<i>Protopteridinium</i> sp.19	New form 3	0	0	0	0	0	0	0	0	0	0	0	0	0	0	0	0	0	0
30	<i>Protopteridinium</i> sp.20	New form 4	0	0	0.3	0	0	0	0	0	0	0	0	0	0	0	0	0	0	0
31	<i>Oblea acanthocysta</i>		0.1	0	0	0	0	0	0	0	0	0	0	0	0	0	0	0	0	0
32	<i>Diplopsalopsis</i> sp.		0	0	0.3	0.2	0	0	0	0	0	0	0	0	0	0	0	0	0	0
33	<i>Diplopsalis cf. laboureae</i>		0	0	0	0	0.4	0	0	0	0	0	0	0	0	0	0	0	0	0
			1.9	2.4	11.4	1.7	8	0.4	2	0	1.1	13.4								

Table 5.11. Density of autotrophic cysts from Station E (Sungai Buloh), Selangor area.

No.	Biological name	Paleontological name	Stations E (Cysts g ⁻¹ dry sediment weight)									
			Stations (September, 2011)					Stations (December, 2011)				
			1	2	3	4	5	1	2	3	4	5
Autotrophic species												
1	<i>Alexandrium</i> spp.		1.3	0	0.5	0.1	1.0	0.7	0.8	3.2	0.8	0.4
2	<i>Gonyaulax</i> cf. <i>spinifera</i>	<i>Spiniferites ramosus</i>	0	0	0	0	0	0	0	0	0	0
3	<i>Gonyaulax</i> sp.	<i>Spiniferites</i> cf. <i>delicatus</i>	0	0.3	0	0	0	0	0	0	0	0
4	<i>Gonyaulax</i> sp.	<i>Spiniferites</i> sp.	0	0	0	0	0	0	0	0	0	0
5	<i>Lingulodinium polyedrum</i>	<i>Lingulodinium machaerophorum</i>	0	0	0	0	0	0	0	0	0	0
6	<i>Protoceratium reticulatum</i>	<i>Operculodinium centrocarpum</i>	0.2	0	0	0.1	0	0	0	0	0	0
7	<i>Protoceratium</i> sp.	<i>Operculodinium islaerianum</i>	0	0	0	0	0	0	0	0	0	0
8	<i>Pyrophacus steinii</i>	<i>Tuberculodinium vancampoae</i>	0.2	0.3	0	0	0	0	0	0	0	0
9	<i>Gymnodinium catenatum</i>		0	0	0.2	0	0	0	0	0	0	0
10	<i>Scrippsiella</i> sp.		0	0	0	0	0	0	0	0	0	0
			1.7	0.6	0.7	0.2	1.0	0.7	0.8	3.2	0.8	0.4

Table 5.12. Density of heterotrophic cysts from Station E (Sungai Buloh), Selangor area.

No.	Biological name	Paleontological name	Stations E (Cysts g ⁻¹ dry sediment weight)												
			Stations (September, 2011)					Stations (December, 2011)							
			1	2	3	4	5	1	2	3	4	5			
Heterotrophic species															
1	<i>Protopteridinium</i> sp.1	<i>Brigantedinium</i> cf. <i>cariacoense</i>	0	0.3	0	0	0	0	0	0	0	0.8	0.4	0	0
2	<i>Protopteridinium denticulatum</i>	<i>Brigantedinium irregularare</i>	0.8	1.7	0.2	0.3	0.2	0.2	0.2	0.2	0.2	3.9	0.4	0.4	2.0
3	<i>Protopteridinium</i> sp.2	<i>Brigantedinium majusculum</i>	0	0	0	0.1	0	0	0	0	0	0	0	0	0
4	<i>Protopteridinium</i> sp.3	<i>Brigantedinium</i> sp.	0	0.3	0	0	0	0	0.2	0	0	0	0	0	0
5	<i>Protopteridinium leonis</i>	<i>Lejeunecysta concreta</i>	0	0	0	0	0	0	0	0	0	0	0	0	0
6	<i>Protopteridinium</i> sp.4	<i>Lejeunecysta sabrina</i>	0	0	0	0.2	0	0	0	0	0.8	0	0.4	0	0
7	<i>Protopteridinium</i> sp.5	<i>Lejeunecysta</i> sp. 1	0	0	0.2	0	0	0	0	0	0.8	0.4	0	0	0
8	<i>Protopteridinium</i> sp.6	<i>Lejeunecysta</i> sp. 2	0	0.3	0.2	0.1	0	0	0	0	0	0	0	0	0
9	<i>Protopteridinium</i> sp.7	<i>Lejeunecysta</i> sp. 3	0	0	0	0	0	0	0	0	0	0	0	0	0
10	<i>Protopteridinium</i> sp.8	<i>Lejeunecysta</i> sp. 4	0	0	0	0	0	0	0	0	0	0	0	0	0
11	<i>Protopteridinium oblongum</i>	<i>Votadinium cavum</i>	0.3	0.3	0	0.1	0.4	0	0.4	0	1.6	0.4	0	0	0
12	<i>Protopteridinium</i> sp.9	<i>Votadinium</i> sp.1	0	0	0	0	0	0	0	0	0	0	0	0	0
13	<i>Protopteridinium</i> sp.10	<i>Votadinium</i> sp.2	0	0	0	0	0	0	0	0	0	0	0	0	0
14	<i>Protopteridinium conicum</i>	<i>Selenopemphix quanta</i>	0	0	0	0	0	0	0	0	0	0	0	0	0
15	<i>Protopteridinium subimerme</i>	<i>Selenopemphix alticinctum</i>	0	0	0	0	0	0	0	0	0	0	0	0	0
16	<i>Protopteridinium divaricatum</i>	<i>Xandarodinium variabile</i>	0	0	0	0	0	0	0	0	0	0	0	0	0
17	<i>Protopteridinium abei</i>	<i>Stelladinium abei</i>	0	0	0	0	0	0	0	0	0	0	0	0	0

Table 5.12 continued

No.	Biological name	Paleontological name	Stations E (Cysts g ⁻¹ dry sediment weight)											
			Stations (September, 2011)					Stations (December, 2011)						
			1	2	3	4	5	1	2	3	4	5		
18	<i>Protoperidinium cf. compressum</i>	<i>Stelladinium robustum</i>	0	0	0	0	0	0	0	0	0	0	0	0
19	<i>Protoperidinium</i> sp.11	<i>Stelladinium</i> sp.1	0	0	0	0	0	0	0	0	0	0	0	0
20	<i>Protoperidinium</i> sp.12	<i>Stelladinium</i> sp.2	0	0	0	0	0	0	0	0	0	0	0	0
21	<i>Protoperidinium</i> sp.13	<i>Stelladinium</i> sp.3	0	0	0	0	0	0	0	0	0	0	0	0
22	<i>Protoperidinium</i> sp.14	<i>Trinovantedinium capitatum</i>	0	0	0	0	0	0.2	0	0	0	0	0	0
23	<i>Protoperidinium latissimum</i>		0	0	0	0	0	0	0	0	0	0	0	0
24	<i>Protoperidinium</i> spp.	Spiny round brown types	0	0.3	0.7	0	0.6	0	0.8	0	0	0	0	0.4
25	<i>Protoperidinium</i> sp.15		0	0	0	0	0	0	0	0	0	0	0	0
26	<i>Protoperidinium</i> sp.16		0	0	0	0.1	0	0	0	0	0	0	0	0
27	<i>Protoperidinium</i> sp.17	New form 1	0	0	0	0	0	0	0	0	0.4	0	0	0
28	<i>Protoperidinium</i> sp.18	New form 2	0	0.3	0	0	0	0	0	0	0	0	0	0
29	<i>Protoperidinium</i> sp.19	New form 3	0	0	0	0	0	0	0	0	0	0	0	0
30	<i>Protoperidinium</i> sp.20	New form 4	0	0	0	0	0	0	0	0	0	0	0	0
31	<i>Oblea acanthocysta</i>		0	0	0	0	0	0	0	0	0	0	0	0
32	<i>Diplopsalopsis</i> sp.		0	0	0	0	0	0	0	0	0	0	0	0
33	<i>Diplopsalis cf. labourae</i>		0.2	0	0	0	0	0	0	0	0	0	0	0
			1.3	3.5	1.3	0.9	1.2	0.6	8.7	2	0.8	2.4		

CHAPTER 6: GENERAL DISCUSSION

6.1. General overview of studies

In this study, results of four main parts were described. The results of first three parts are regarding to the phytoplankton surveys from the Tanintharyi coastal area, southern Myanmar coast, and the results of fourth part is regarding to the dinoflagellate cysts survey from the Selangor area, west coast of Malay Peninsula. This coastal area faces to the Strait of Malacca, and leads to the southern Andaman Sea, connecting to Myanmar coast. Chapter 2 was concerning to the occurrences of phytoplankton communities and dinoflagellate cysts around the Mali and Kadan Islands, Tanintharyi coast. Chapter 3 was concerning the harmful dinoflagellates species and confirmation of their identification based on their morphologies and molecular phylogenetic data sets. Chapter 4 was concerning to the growth physiology of three red-tide forming species (*Alexandrium affine*, *Prorocentrum rhathymum* and *P. shikokuense*), which isolated from Myanmar water. Chapter 5 was concerning the occurrence of dinoflagellate cysts, and the occurrence of PSP causative species (i.e. *Alexandrium tamiyavanichii* and *Gymnodinium catenatum*) in the planktonic and cysts assemblages from the Selangor district.

6.2. Phytoplankton occurrences in the southern Myanmar coast

From the results of Chapter 2, the occurrences of phytoplankton community with a list of dinoflagellates and diatoms species were shown. Diverse dinoflagellates species were

listed in the pre-rainy season surveys (57 species in May, 2010 and 67 species in March, 2012) than the post-rainy season survey (26 species in December, 2010), and it is assumed that the dinoflagellate species diversity in two different seasons were significantly derived from the differences of climate and/or oceanographic systems before and after the rainy season. That is, the occurrence of the higher diversity of dinoflagellates species in the May and March surveys indicated that an oligotrophic environment in the late dry season was favorable for dinoflagellates. On the other hand, the occurrences of diverse diatoms species and massive diatoms blooms in the post-rainy season survey (December, 2010) explained the flooding of nutrient-rich terrestrial water into the coastal areas in prolonged rainy weather during the southwest monsoon. The simultaneous occurrence of oceanic species such as *Ornithocercus* spp. and *Podolampas bipes* with neritic species (e.g. *Prorocentrum* spp., *Gonyaulax* spp. and *Alexandrium tamiyavanichii*) in the May and March surveys insisted oceanic waters were mixing with the coastal waters in this season.

Such understandings for the oceanographic characters, namely, typical neritic environment in the post-rainy season followed by rather oligotrophic environment in the late dry season (pre-rainy season) and mixture with oceanic waters, were firstly revealed by the phytoplankton observations under this study. In addition, among the occurrence of dinoflagellate cysts in the surface sediment, high diversities of heterotrophic cysts were characteristic of the Myanmar coast, and high abundance of heterotrophic cysts in the December survey indicated richness of prey plankters after the rainy season.

6.3. Occurrences of potentially harmful dinoflagellates

From the results of Chapter 3, total 21 species of potentially harmful dinoflagellates were found in the Tanintharyi coastal area. From this study, toxin-producing species, which can cause shellfish poisoning including paralytic shellfish poisoning (PSP) such as *Alexandrium tamiyavanichii*, *Gymnodinium catenatum*, diarrhetic shellfish poisoning (DSP)-causative species such as *Dinophysis caudata*, *D. miles*, *D. rotundata*, *D. infundibulus* and potentially okadaic acid (OA) producing species *Prorocentrum rhathymum*, and yessotoxin (YTX)-producing species *Gonyaulax spinifera*, *Lingulodinium polyedrum*, and several red-tide forming species such as *Alexandrium affine*, *Gonyaulax polygramma*, *Prorocentrum micans*, *P. sigmoides*, *P. shikokuense*, *Ceratium furca*, *C. fusus*, *Scrippsiella trochoidea* and *Noctiluca scintillans* were identified. Among them, 10 species were reexamined with detail morphological observation and DNA (28S rRNA gene) analyses. These potentially harmful species mainly occurred in the pre-rainy season (May, 2010 and March, 2012). These occurrences suggest that the corresponding area may have risks of HABs, and late dry seasons should be regarded as to be potentially suffered from harmful events.

6.4. Growth characters of three red-tide forming species (*Prorocentrum rhathymum*, *P. shikokuense* and *A. affine*) at different temperatures

The results of Chapter 4 are based on the finding of red-tide near St. 6, at the northeast part of Kadan Island in the March, 2012 survey. This red-tide is noteworthy by comprising three different harmful dinoflagellate species such as, *P. rhathymum*, *P. shikokuense* and *A. affine*. The clonal cultures of these harmful species were

successfully established from this red-tide water. To understand the growth physiology of these species, temperature experiments were conducted at four different temperature regimes (15, 20, 25, 30°C) using these culture strains of Myanmar water. Among these three species, *P. rhathymum* and *P. shikokuense* showed the high tolerance to the given temperature ranges, while *A. affine* had less tolerance to low temperature (15°C). Temperature tolerance and optimal temperature for the maximum growths of *A. affine* and *P. rhathymum* showed similar with those of previous studies (Nguyen-Ngoc, 2004; Ismael et al., 1997). The optimal temperature for maximum growth of *P. shikokuense* showed significant difference from that of *P. donghaiense* (junior synonym of *P. shikokuense*) in the East China Sea by Xu et al. (2010), regardless to the genetic identity among these local strains. The temperature experiments using these culture strains provide the well understandings on the relationship of temperatures and growth rates of the local strains in comparison with other studies from different geographical areas. This understanding is beneficial for prediction the occurrence of red-tide events in the coastal area based on one of the environmental factors of water temperature.

6.5. Occurrence of dinoflagellate cysts in the surface sediment, and finding of toxic *Gymnodinium catenatum* and *Alexandrium tamiyavanichii* from coastal water of Selangor, Malay Peninsula

The result of Chapter 5 is based on the occurrence of toxic dinoflagellates in the Selangor district, west coast of Malay Peninsula. Selangor coastal area is an important for blood cockle culture industry. This coastal area faces to the Strait of Malacca, and leads to the southern Andaman Sea, connecting to Myanmar coast. To understand the

HAB expansion from or to the Myanmar coast, and regard to a future model of HAB risk management in shellfish culture fields, both planktonic and cyst forms of harmful dinoflagellate species were investigated as a multi-nation cooperative research. From this result, 43 cyst types comprising 10 autotrophic types and 33 heterotrophic types were found. In the plankton and cyst samples, PSP causative dinoflagellates, *G. catenatum* was detected with low density. The occurrence of another PSP causative species, *A. tamiyavanichii* was not confirmed in the cysts survey, however, their planktonic form was confirmed. The occurrence of toxic dinoflagellates, *G. catenatum* and *A. tamiyavanichii* from the cockle culture grounds suggests the PSP risk may present in this area, and also diffusion risks of *G. catenatum* cysts by the fisheries activity. This finding of these toxic species in Selangor district and Myanmar coast notified that HAB expansion from or to the Myanmar coast, and alarmed to establish toxic phytoplankton monitoring system and managements on cyst contamination in the transporting cockle spats.

6.6. Significance of this study

1. This is the first detail study of phytoplankton and dinoflagellate cysts from Myanmar's foremost marine fisheries area, Tanintharyi coast. It provides species lists and micrographs of phytoplankton and dinoflagellate cysts from Myeik coast. It should be beneficial for the future phytoplankton studies, especially for phytoplankton monitoring.
2. The influences of drastic seasonal change on the diversities of diatoms and dinoflagellates off Myeik coast were recognized. Diverse occurrence of diatom in the

post-rainy season indicated the high productivity of this coastal region. The high abundance of heterotrophic cysts in the December survey also indicated the richness of prey plankters after the rainy season. Diverse dinoflagellates comprising the oceanic and the neritic species indicated the mixing of oceanic water in the coastal area in the pre-rainy season. These factors are represented as the characteristic of Tanintharyi coastal region. High diversity of diatoms and dinoflagellates off the Myeik coast is proving the high Myanmar marine capture fisheries.

3. On the other hand, many potentially harmful dinoflagellates, including red-tide and shellfish poisoning causative species were detected especially in the pre-rainy season surveys. This information should be useful for future HAB risk managements, and warned to establish the regular monitoring of harmful dinoflagellates for better prediction of HAB.

4. Furthermore, the culture strains of three red-tide forming species from red-tide water of Myanmar were successfully established, and relationship of temperatures and growth rates of local strains was understood by laboratory experiments. The understanding of local strains characters should be beneficial for prediction of the occurrence of red-tide events based on water temperature.

5. The potent paralytic shellfish poisoning (PSP) causative species (i.e. *G. catenatum* and *A. tamiyavanichii*) were found in the blood cockle culture area, Selangor district. These species were also detected off the Myeik coast. These finding are the important information to establish the toxic phytoplankton monitoring system and management on cyst contamination in the bivalve transportation.

6.7. Future studies

The occurrence of high diversities of diatoms and dinoflagellates species in the Tanintharyi coastal seems to be supported by various characteristic environments of Myeik coast such as large mangrove forests, numerous rivers, and drastic climate change (tropical monsoon regimes). Meanwhile, in Myanmar, rapid economic changes are leading to degradation of these characteristic environments by human activities such as over-fishing, harvesting mangrove forest and urbanizing in coastal area. Moreover, there is no appropriate measure (e.g. primary productivity) to control sustainable fisheries. Therefore, future phytoplankton study must be investigated to understand the basic information of primary productivity in this coastal area, and suitable control should be created on fish catch.

Recently, harmful event reports have been increasing from the Southeast Asian coast including red-tide and shellfish poisoning. The finding of many harmful dinoflagellate species in the pre-rainy season surveys and red-tide incident on the March, 2012 survey alarmed to establish the phytoplankton monitoring system in Myanmar coastal area. Based on the understanding from this study, the phytoplankton studies must be continued in regard not only for primary productivity and also for future HAB risk events.

Investigations of bio-toxin analysis for marine fishery products such as bivalve have been conducted in 2009 under the collaborated project with DOF, Myanmar and MFRD, Singapore. However, in Myanmar, the bio-toxin analysis is still difficult to perform regularly due to poor technology and high causes. In this circumstance, toxic dinoflagellate monitoring is one of useful technique for the safety of shellfish toxin by

early warning. The finding of toxic dinoflagellate species in the May and March surveys alarmed that frequent and well monitoring system for harmful dinoflagellate species should be conducted in the Tanintharyi coast especially during the dry season. Therefore, phytoplankton study is essential in regards to Myanmar sustainable fisheries, and food safety not only for export purpose and also for local consumers. Moreover, in harmful dinoflagellate monitoring, both fresh and fixed samples should be examined not to lose unarmored species, since most of these are harmful.

REFERENCES

- Abé, T. H. (1981). *Studies on the family Peridiniidae. An unfinished monograph of the armoured dinoflagellata*. Tokyo: Publ. Seto Mar. Biol. Lab., Special Publication Series, No. 6. 412 pages.
- Aligizaki, K., Nikolaidis, G., Katikou, P., Baxevanis, A. D. and Abatzopoulos, T. J. (2009). Potentially toxic epiphytic *Prorocentrum* (Dinophyceae) species in Greek coastal waters. *Harmful Algae*, 8, 299-311.
- Al-Yamani, F. Y., Bishop, J., Ramadhan, E., Al-Husaini, M. and Al-Ghadban, A. N. (2004). *Oceanographic atlas of Kuwait's waters*. Safat: Kuwait Institute for Scientific Research. 203 pages.
- Al-Yamani, F. Y. and Saburova, M. A. (2010). *Illustrated guide on the flagellates of Kuwait's intertidal soft sediments*. Safat: Kuwait Institute for Scientific Research. 197 pages.
- An, T., Winshell, J., Scorzetti, G., Fell, J. W. and Rein, K. S. (2010). Identification of okadaic acid production in the marine dinoflagellate *Prorocentrum rhathymum* from Florida Bay. *Toxicon*, 55, 653-657.
- Anderson, D. M., Kulis, D. M. and Binder, B. J. (1984). Sexuality and cyst formation in the dinoflagellate *Gonyaulax tamarensis*: cyst yield in bath cultures. *J. Phycol.*, 20, 418-425.
- Anderson, D. M. (1998). Physiology and bloom dynamics of toxic *Alexandrium* species, with emphasis on life cycle transitions. In: D. M. Anderson, A. D. Cembella, and G. M. Hallegraeff (Eds.), *Physiological Ecology of Harmful Algal Blooms*. Berlin: Springer-Verlag Berlin Heidelberg. pp. 29-48
- Anderson, D. M., Alpermann, T. J., Cembella, A. D., Collos, Y., Masseret, E. and Montresor, M. (2012). The globally distributed genus *Alexandrium*: Multifaceted roles in marine ecosystems and impacts on human health. *Harmful algae*, 14, 10-35.
- Anton, A., Teoh, P. L., Mohd-Shaleh, S. R. and Mohammad-Noor, N. (2008). First occurrence of *Cochlodinium* blooms in Sabah, Malaysia. *Harmful Algae*, 7, 331-336.

- Armstrong, M. and Kudela, R. (2006). Evaluation of California isolates of *Lingulodinium polyedrum* for the production of yessotoxin. *Afr. J. Marine Sci.*, 28, 399-401.
- Azanza, R. V. and Taylor, F. J. R. (2001). Are *Pyrodinium* blooms in the Southeast Asian region recurring and spreading? A view at the end of the millennium. *Ambio*, 30, 356-364.
- Azanza, R. V., Siringan, F. P., Diego-Mcglone, M. L. S., Yñiguez, A. T., Macalalad, N. H., Zamora, P. B., Agustin, M. B. and Matsuoka, K. (2004). Horizontal dinoflagellate cyst distribution, sediment characteristics and benthic flux in Manila Bay, Philippines. *Phycol. Res.*, 52, 376-386.
- Azanza, R. V., David, L. T., Borja, R. T., Baula, I. U. and Fukuyo, Y. (2008). An extensive *Cochlodinium* bloom along the western coast of Palawan, Philippines. *Harmful Algae*, 7, 324-330.
- Balech, E. (1988). *Los dinoflagelados del Atlantico sudoccidental*. Madrid: Publ. Espec. Inst. Esp. Oceanogr. No.1. 310 pages.
- Balech, E. (1994). Three new species of the genus *Alexandrium* (Dinoflagellata). *Trans. Am. Microsc. Soc.*, 113, 216-220.
- Balech, E. (1995). *The genus Alexandrium Halim (Dinoflagellata)*. Sherkin Island: Sherkin Island Marine Station. 151 pages.
- Bolch, C. J. S., Negri, A. P. and Hallegraeff, G. M. (1999). *Gymnodinium microreticulatum* sp. nov. (Dinophyceae): a naked, microreticulate cyst-producing dinoflagellate, distinct from *Gymnodinium catenatum* and *Gymnodinium nolleri*. *Phycologia*, 38, 301-313.
- Boonyapiwat, S., Tienpisut, K. and Ngowsakul, W. (2007). Abundance and distribution of phytoplankton in Myanmar waters. In: *Preliminary report on fishery resources survey in the waters of Myanmar MV. SEAFDEC 2 Cruise no. 23-1/2007. TD/RES/128*. Bangkok: Southeast Asian Fisheries Development Center. pp. 1-9.
- Boonyapiwat, S., Sada, M. N., Mandal, J. K. and Sinha M. K. (2008). Species composition, abundance and distribution of phytoplankton in the Bay of Bengal. In: *The Ecosystem-Based Fishery Management in the Bay of Bengal*. Bangkok: Department of Fisheries, Ministry of Agriculture and Cooperatives. pp. 53-64.
- Bralewska, J. M and Witek, Z. (1995). Heterotrophic dinoflagellates in the ecosystem of the Gulf of Gdansk. *Mar. Ecol. Prog. Ser.*, 117, 241-248.

- Caillaud, A., Iglesia, P. D. L., Campàs, M., Elandalousi, L., Fernández, M., Mohammad-Noor, N., Andree, K. and Diogène, J. (2010). Evidence of okadaic acid production in a cultured strain of the marine dinoflagellate *Prorocentrum rhathymum* from Malaysia. *Toxicon*, 55, 633-637.
- Cembella, A. D. (1989). Occurrence of okadaic acid, a major diarrhetic shellfish toxin, in natural populations of *Dinophysis* spp. from the eastern coast of North America. *J. Appl. Phycol.*, 1, 307-310.
- Ciminiello, P., Fattorusso, E., Forino, M., Magno, S., Poletti, R., Satake, M., Viviani, R. and Yasumoto, T. (1997). Yessotoxin in mussels of the northern Adriatic Sea. *Toxicon*, 35, 177-183.
- Clarke, K. R. and Warwick, R. M. (2001). *Change in marine communities: An approach to statistical analysis and interpretation* (2nd ed.), PRIMER-E. Plymouth: Plymouth Marine Laboratory. 172 pages.
- Collins, C., Graham, J., Brown, L., Bresnan, E., Lacaze, J. P. and Turrell, E. A. (2009). Identification and toxicity of *Alexandrium tamarense* (Dinophyceae) in Scottish waters. *J. Phycol.*, 45, 692-703.
- Cortés-Altamirano, R. and Sierra-Beltrán, A. P. (2003). Morphology and taxonomy of *Prorocentrum mexicanum* and reinstatement of *Prorocentrum rhathymum* (Dinophyceae). *J. Phycol.*, 39, 221-225.
- Currie, R. I., Fisher, A. E. and Hargreaves, P. M. (1973). The Arabian Sea upwelling. In: B. Zeitschel and S. A. Gerlach (Eds.), *The biology of the Indian Ocean 3*. New York: Springer-Verlag. pp. 37-52.
- D'Costa, P. M., Anil, A. C., Patil, J. S., Hegde, S., D'Silva, M. S. and Chourasia, M. (2008). Dinoflagellates in a mesotrophic, tropical environment influenced by monsoon. *Estuar. Coast. Shelf Sci.*, 77, 77-90.
- Department of Fisheries (2010). *Fishery Statistic (2009-2010)*. Yangon: Department of Fisheries, Ministry of Livestock and Fisheries. 122 pages.
- Dodge, J. D. (1988). An SEM study of thecal division in *Gonyaulax* (Dinophyceae). *Phycologia*, 27, 241-247.
- Dodge, J. D. (1989). Some revisions of the Family Gonyaulacaceae (Dinophyceae) based on scanning electron microscope study. *Bot. Mar.*, 32, 275-298.

- Dugan, K. A., Lawrence, H. S., Hares, D. R., Fisher, C. L. and Budowle, B. (2002). An improved method for post-PCR purification for mtDNA sequence analysis. *J. Forensic Sci.*, *47*, 811-818.
- FAO and NACA (2003). *Myanmar aquaculture and inland fisheries*. Bangkok: Regional office for Asia and the Pacific. 60 pages.
- FAO (2010). *The state of world fisheries and aquaculture 2010*. Rome: Food and Agriculture Organization of the United Nations. 197 pages.
- Fraga, S., Anderson, D. M., Bravo, I., Reguera, B., Steidinger, K. A. and Yentsch, C. M. (1988). Influence of upwelling relaxation on dinoflagellates and shellfish toxicity in Ria de Vigo, Spain. *Estuar. Coast. Shelf Sci.*, *27*, 349-361.
- Fritz, L. and Triemer, R. E. (1985). A rapid simple technique utilizing calcofluor white M2R for the visualization of dinoflagellate thecal plates. *J. Phycol.*, *21*, 662-4.
- Fukuyo, Y. (1981). Taxonomical study on benthic dinoflagellates collected in coral reefs. *B. Jpn. Soc. Sci. Fish.*, *47*, 967-978.
- Fukuyo, Y., Yoshida, K. and Inoue, H. (1985). *Protogonyaulax* in Japanese coastal waters. In: D. M. Anderson, A. W. White and D. G. Baden (Eds.), *Toxic Dinoflagellates*. New York: Elsevier Science. pp. 27-32.
- Fukuyo, Y., Yoshida, K., Ogata, T., Ishimaru, T., Kodama, M., Pholpunthin, P., Wisessang, S., Phanichyaakarn, V., and Piyakarnchana, T. (1989). Suspected causative dinoflagellates of paralytic shellfish poisoning in the Gulf of Thailand. In: T. Okaichi, D. M. Anderson, and T. Nemoto (Eds.), *Red Tides: Biology, Environmental Science, and Toxicology*. New York: Elsevier. pp. 403-406.
- Fukuyo, Y., Takano, H., Chihara, M. and Matsuoka, K. (1990). *Red tide organisms in Japan: An illustrated taxonomic guide*. Tokyo: Uchida Rukakuho. 407 pages.
- Fukuyo, Y., Kodama, M., Ogata, T., Ishimaru, T., Matsuoka, K., Okaichi, T., Maala, A. M. and Ordonez, J. A. (1993). Occurrence of *Gymnodinium catenatum* in Manila Bay, the Philippines. In: T. J. Smayda and Y. Shimizu (Eds.), *Toxic Phytoplankton Blooms in the Sea*. New York: Elsevier. pp. 875-880.
- Fukuyo, Y., Kodama, M., Omura, T., Furuya, K., Furio, E. F., Cayme, M., Lim, P. T., Ha, D. V., Kotaki, Y., Matsuoka, K., Iwataki, M., Sriwoon, R., and Lirdwitayaprasit, T. (2011). Ecology and oceanography of harmful marine microalgae (Project-2). In: S. Nishida, M. D. Fortes, and N. Miyazaki (Eds.), *Coastal Marine Science in Southeast Asia – Synthesis Report of the Core*

University Program of the Japan Society for the Promotion of Science: Coastal Marine Science (2001-2010). Tokyo: Terra Scientific Publishing Company. pp. 23-48.

- Furio, E. F., Fukuyo, Y., Matsuoka, K. and Gonzales, C. L. (1996). The vertical distribution of resting cysts of PSP-producing dinoflagellate *Pyrodinium bahamense* var. *compressum* in Manila Bay, Philippines. In: T. Yasumoto, Y. Oshima and Y. Fukuyo, (Eds.), *Harmful and Toxic Algal Blooms*. Paris: IOC-UNESCO. pp. 185-188.
- Furio, E. F. and Gonzales, C. (2002). Toxic red tide and paralytic shellfish poisoning profiles in the Philippines. In: C. L. Gonzales, S. Sakamoto, F. E. Furio, T. Ogata, M. Kodama and Y. Fukuyo (Eds.), *Practical Guide in Paralytic Shellfish Poisoning Monitoring in the Philippines*. Manila: BFAR and JICA. pp. 3-27.
- Furio, E. F., Azanza, R. V., Fukuyo, Y. and Matsuoka, K. (2012). Review of geographical distribution of dinoflagellate cysts in Southeast Asian coasts. *Coast. Mar. Sci.*, 35, 20-33.
- Giesen, W., Wulffraat, S., Zieren, M. and Scholten, L. (2006). *Mangrove guidebook for Southeast Asia*. Bangkok: FAO Regional Office for Asia and the Pacific. 769 pages.
- Godhe, A., Karunasagar, I. and Karlson, B. (2000). Dinoflagellate cysts in recent marine sediments from SW India. *Bot. Mar.*, 43, 39-48.
- Grindley, J. R. and Taylor, F. J. R. (1962). Red water and mass-mortality of fish near Cape Town. *Nature*, 195, 1324.
- Guillard, R. R. L. (1975). Culture of phytoplankton for feeding marine invertebrates. In: W. L. Smith and M. H. Chanley (Eds.), *Culture of Marine Invertebrate Animals*. New York: Plenum Press. pp. 26-60.
- Guindon, S. and Gascuel, O. (2003). A simple, fast, and accurate algorithm to estimate large phylogenies by maximum likelihood. *Syst. Biol.*, 52, 696-704.
- Hada, Y. (1975). On two new species of the genus *Prorocentrum* Ehrenberg belonging to Dinoflagellida. *Hiroshima Shudo Daigaku Ronshu*, 16, 31-38.
- Hallegraeff, G. M. (1993). A review of harmful algal blooms and their apparent global increase. *Phycologia*, 32, 79-99.

- Hallegraeff, G. M. and Jeffrey, S. W. (1993). Annually recurrent diatom blooms in spring along the New South Wales coast of Australia. *Aust. J. Mar. Freshwater Res.*, *44*, 325-334.
- Hallegraeff, G. M. (2004). Harmful algal blooms: a global overview. In: G. M. Hallegraeff, D. M. Anderson and A. D. Cembella (Eds.), *Manual on Harmful Marine Microalgae, Monographs on Oceanographic Methodology*, *11*. Paris: UNESCO. pp. 383-388.
- Hallegraeff, G. M., Blackburn, S. I., Doblin, M. A. and Bolch, C. J. S. (2012). Global toxicology, ecophysiology and population relationships of the chainforming PST dinoflagellate *Gymnodinium catenatum*. *Harmful Algae*, *14*, 130-143.
- Hansen, G., Daugbjerg, N. and Henriksen, P. (2000). Comparative study of *Gymnodinium mikimotoi* and *Gymnodinium aureolum*, comb. nov. (= *Gyrodinium aureolum*) based on morphology, pigment composition, and molecular data. *J. Phycol.*, *36*, 394-410.
- Harland, R. (1982). A review of recent and quaternary organic-walled dinoflagellate cysts of the Genus *Protoperidinium*. *Palaeontology*, *25*, 369-397.
- Harland, R., Nordberg, K. and Filipsson, H. L. (2006). Dinoflagellate cysts and hydrographical change in Gullmar Fjord, west coast of Sweden. *Sci. Total Environ.*, *355*, 204-231.
- Hasle, G. R. and Syvertsen, E. E. (1997). Marine diatoms. In: C. R. Tomas (Ed.), *Identifying marine phytoplankton*. San Diego, California: Academic Press. pp. 5-386.
- Hernández-Becerril, D. U., Cortés Altamirano, R. and Alonso, R. (2000) The dinoflagellate genus *Prorocentrum* along the coasts of the Mexican Pacific. *Hydrobiologia*, *418*, 111-121.
- Holmes, M. J., Teo, S. L. M., Lee, F. C. and Khoo, H. W. (1999). Persistent low concentrations of diarrhetic shellfish toxins in green mussels *Perna viridis* from the Johor Strait, Singapore: first record of diarrhetic shellfish toxins from South-East Asia. *Mar. Ecol. Prog. Ser.*, *181*, 257-268.
- Holmes, M. J., and Teo, S. L. M. (2002). Toxic marine dinoflagellates in Singapore waters that cause seafood poisonings. *Clin. Exp. Pharmacol. P.*, *29*, 829-836.
- Hong, D. D., Hien, H. T. M., Thu, N. H., Anh, H. L. and Luyen, Q. H. (2008). Phylogenetic analyses of *Prorocentrum* spp. and *Alexandrium* spp. isolated from

- northern coast of Vietnam based on 18S rDNA sequence. *J. Env. Bio.*, 29, 535-542.
- Hoppenrath, M., Elbrächter, M. and Drebes, G. (2009). *Marine phytoplankton. Selected microphytoplankton species from the North Sea around Helgoland and Sylt*. Stuttgart: Schweizerbart Science. 264 pages
- Ismael, G. I. and Aida, M. L. (1997). First record of a *Prorocentrum rhathymum* (Prorocentraceae) red tide in the Gulf of California. *Rev. Biol. Trop.*, 45, 1263-1271.
- Jensen, M. Ø. and Moestrup, Ø. (1997). Autecology of the toxic dinoflagellates *Alexandrium ostenfeldii*: life history and growth at different temperature and salinities. *Eur. J. Phycol.*, 32, 9-18.
- Kamba, M. and Yuki, K. (1980). Plankton of Burmese coasts. *Inst. Oceanic Res. and Develop. Tokai Univ. Notes*, 2, 89-146.
- Karunasagar, I., Karunasagar, I., Oshima, Y. and Yasumoto, T. (1990). A toxin profile for shellfish involved in and outbreak of paralytic shellfish poisoning in India. *Toxicon*, 28, 868-870.
- Kim, C. J., Yoshimatsu, S. A., Sako, Y. and Kim, C. H. (2004). Molecular identification of the toxic *Alexandrium tamiyavanichii* (Dinophyceae) by the whole-cell FISH method. *J. Fish. Sci. Tech.*, 7, 175-183.
- Kim, K. Y. and Kim, C. H. (2007). Phylogenetic relationships among diverse dinoflagellate species occurring in coastal waters off Korea inferred from large subunit ribosomal DNA sequence data. *Algae*, 22, 57-67.
- Koizumi, Y., Kohno, J., Matsuyama, N., Uchida, T. and Honjo, T. (1996). Environmental features and the mass mortality of fish and shellfish during the *Gonyaulax polygramma* red tide occurred in the round Uwajima Bay, Japan, in 1994. *Nippon Suisan Gakkaishi*, 62, 217-224.
- Lam, C. W. Y. and Yip, S. S. Y. (1990). A three-month red tide event in Hong Kong. In: E. Graneli, B. Sundstrom and D. M. Anderson (Eds.), *Toxic Marine Phytoplankton*. New York: Elsevier. pp. 481-486.
- Larsen, J. and Moestrup, Ø. (1992). Potentially toxic phytoplankton, Genus *Dinophysis* (Dinophyceae) Leaflet No. 180. In: J. A. Lindley (Ed.), *ICES Identification Leaflets for Plankton*. Copenhagen: International Council For The Exploration Of The Sea. pp. 1-12.

- Lee, J. S., Igarashi, T., Fraga, S., Dahl, E., Hovgaard, P. and Yasumoto, T. (1989). Determination of diarrhetic shellfish toxins in various dinoflagellate species. *J. Appl. Phycol.*, *1*, 147-152.
- Lee, J. H. W., Hodgkiss, I. J., Wong, K. T. M. and Lam, I. H. Y. (2005). Real time observations of coastal algal blooms by an early warning system. *Estuar. Coast. Shelf Sci.*, *65*, 172-190.
- Lilly, E. L., Halanych, K. M. and Anderson, D. M. (2007). Species boundaries and global biogeography of the *Alexandrium tamarense* complex (Dinophyceae). *J. Phycol.*, *43*, 1329-1338.
- Lim, P. T., Leaw, C. P. and Uspu, G. (2004). First incidence of paralytic shellfish poisoning of the east coast of Peninsula Malaysia. In: S. M. Phang, V. C. Chong, S. S. Ho, N. Mokhtar and J. L. S. Ooi (Eds.), *Marine Science into the New Millennium: New Perspectives and Challenges*. Kuala Lumpur: University of Malaysia Maritime Research Center. pp. 661-667.
- Lirdwitayaprasit, P., Nuangsang, C., Puewkhao, P., Rahman, M. J., Oo, A. H. and Sein, A. W. (2008). Composition, abundance and distribution of fish larvae in the Bay of Bengal. In: *The Ecosystem-Based Fishery Management in the Bay of Bengal*. Bangkok: Department of Fisheries, Ministry of Agriculture and Cooperatives. pp. 93-124.
- Lirdwitayaprasit, T., Panuksubkasul, D., Takata, Y., Sato, S., Kodama, M. and Fukuyo, Y. (2008). Occurrence of *Gymnodinium catenatum* in the Gulf of Thailand. *Mar. Res. Indonesia*, *33*, 87-89.
- Loeblich, A. R. III, Sherley, J. L. and Schmidt, R. J. (1979). The correct position of flagellar insertion in *Prorocentrum* and description of *Prorocentrum rhathymum* sp. nov. (Pyrrhophyta). *J. Plank. Res.*, *1*, 113-120.
- Lu, D. D. and Goebel, J. (2001). Five red tide species in genus *Prorocentrum* including the description of *Prorocentrum donghaiense* Lu sp. nov. from the East China Sea. *Chin. J. Oceanol. Limnol.*, *19*, 337-344.
- Lu, D., Goebel, J., Qi, Y., Zou, J., Han, X., Gao, Y. and Li, Y. (2005). Morphological and genetic study of *Prorocentrum donghaiense* Lu from the East China Sea, and comparison with some related *Prorocentrum* species. *Harmful Algae*, *4*, 493-505.
- Marasigan, A. N., Sato, S., Fukuyo, Y. and Kodama, M. (2001). Accumulation of a high level of diarrhetic shellfish toxins in the green mussel *Perna viridis* during a

- bloom of *Dinophysis caudata* and *Dinophysis miles* in Sapien Bay, Panay Island, the Philippines. *Fish. Sci.*, 67, 994-996.
- Margalef, R. (1956). Estructura y dinámica de la 'purga de mer' en la Ria de Vigo. *Investigacion Pesquera*, V, 113-134.
- Matsuoka, K. (1984). Cyst and theca of *Protoperidinium avellana* (Meunier) Balech, (Dinophyceae). *Bull. Faculty of Liberal Arts, Nagasaki Univ., (Natural Science)*, 25, 37-47.
- Matsuoka, K. (1985). Organic-walled dinoflagellate cysts from surface sediments of Nagasaki Bay and Senzaki Bay, West Japan. *Bull. Faculty of Liberal Arts, Nagasaki Univ., (Natural Science)*, 25, 21-115.
- Matsuoka, K. (1987). Organic-walled dinoflagellate cysts from surface sediments of Akkeshi Bay and Lake Saroma, North Japan. *Bull. Faculty of Liberal Arts, Nagasaki Univ., (Natural Science)*, 28, 35-123.
- Matsuoka, K. (1988). Cyst-theca relationships in the Diplopsalid group (Peridinales, Dinophyceae). *Rev. Palaeobot. Palyno.*, 56, 95-122.
- Matsuoka, K. (1999). Eutrophication process recorded in dinoflagellate cyst assemblages—a case of Yokohama Port, Tokyo Bay, Japan. *Sci. Total Environ.*, 231, 17-35.
- Matsuoka, K. and Fukuyo, Y. (2000). *Technical guide for modern dinoflagellate cyst study*. WESTAPAC-HAB/WESTPAC/IOC. 29 pages.
- Matsuoka, K., Fujii, R., Hayashi, M., and Wang, Z. (2006). Recent occurrence of toxic *Gymnodinium catenatum* Graham (Gymnodiniales, Dinophyceae) in coastal sediments of West Japan. *Palaeontological Research*, 10, 117-125.
- McMinn, A. (1991). Recent dinoflagellate cysts from Estuaries on the Central Coast of new South Wales, Australia. *Micropaleontology*. 37, 269-287.
- Moestrup, Ø., Akselman, R., Cronberg, G., Elbraechter, M., Fraga, S., Halim, Y., Hansen, G., Hoppenrath, M., Larsen, J., Lundholm, N., Nguyen, L. N. and Zingone, A. (Eds.) (2009 onwards). IOC-UNESCO Taxonomic Reference List of Harmful Micro Algae. Available online at <http://www.marinespecies.org/HAB>. Accessed on 24 December 2012.
- Mohamed-Abubaker-Sithik, A., Thirumaran, G., Arumugam, R., Ragupathi-Rajakannan, R. and Anantharaman, P. (2009). Studies of phytoplankton diversity

from Agnitheertham and Kothandaramar Koil coastal waters; Southeast coast of India. *Global J. Env. Res.*, 3, 118-125.

Mohammad-Noor, N., Anton, A. and Alexander, J. (2002). HAB species in Sabah, Malaysia: New records of *Alexandrium tamiyavanichii* and *Gymnodinium* sp. The 10th International Conference on Harmful Algae, 21-25 October 2002, Florida, USA. (Abstract).

Mohammad-Noor, N., Daugbjerg, N., Moestrup, Ø and Anton, A. (2005). Marine epibenthic dinoflagellates from Malaysia – a study of live cultures and preserved samples based on light and scanning electron microscopy. *Nord. J. Bot.*, 24, 629-690.

Nagai, S., Itakura, S., Matsuyama, Y., and Kotani, Y. (2003). Encystment under laboratory conditions of the toxic dinoflagellate *Alexandrium tamiyavanichii* (Dinophyceae) isolated from the Seto Inland Sea, Japan. *Phycologia*, 42, 646-653.

Nakajima, I., Oshima, Y. and Yasumoto, T. (1981). Toxicity of benthic dinoflagellates in Okinawa. *B. Jpn. Soc. Sci. Fish.*, 47, 1029-1033.

Naqvi, S. W. A., George, M. D., Narvekar, P. V., Jayakumar, D. A., Shailaja, M. S., Sardessai, S., Sarma, V. V. S. S., Shenoy, D. M., Naik, H., Maheswaran, P. A., KrishnaKumari, L., Rajesh, G., Sudhir, A. K. and Binu, M. S. (1998). Severe fish mortality associated with 'red tide' observed in the sea of Cochin. *Current Science*, 75, 543-544.

Naustvoll, L. J. (2000). Prey size spectra and food preferences in thecate heterotrophic dinoflagellates. *Phycologia*, 39, 187-198.

Nguyen-Ngoc, L. (2004). An autecological study of the potentially toxic dinoflagellate *Alexandrium affine* isolated from Vietnamese waters. *Harmful Algae*, 3, 117-129.

Nguyen-Ngoc, L. (2010). Ecophysiology of *Ostreopsis* and *Prorocentrum* species (i.e., adaptive strategies, physiological characteristics, life cycle traits, temperature preferences and tolerances, growth rates). In: *Open Science Meeting on Harmful Algal Blooms in Benthic Systems. Honolulu, 21-23 June 2010*. (Abstract, p. 21)

Nguyen, N. V. (2009). *Taxonomic study on dinoflagellates belonging to the order Dinophysiales (Dinophyceae)*. The University of Tokyo: The Graduate School of Agricultural and Life Sciences. (Doctoral Thesis), 224 pages.

- Nie, D. and Wang, C. C. (1941). Dinoflagellata of the Hainan region. III. On *Metadinophysis sinensis*, a new genus and species of Dinophysidae. *Sinensia*, 12, 217-226.
- Nishitani, G., Nagai, S., Sakiyama, S. and Kamiyama, T. (2008). Successful cultivation of the toxic dinoflagellate *Dinophysis caudata* (Dinophyceae). *Plank. Benth. Res.*, 3, 78-85.
- Okaichi, T. and Nishio, S. (1976). Identification of ammonia as the toxic principle of red tide of *Noctiluca miliaris*. *Bull. Plankton Soc. Jpn.*, 23, 75-80.
- Okaichi, T. (1997). Red tides. In: T. Okaichi (Ed.), *Red tides* (2nd ed.). Tokyo: Kouseisha-Kouseikaku (in Japanese). pp. 15-23.
- Padmakumar, K. B., SreeRanjima, G., Fanimol, C. L., Menon, N. R. and Sanjeevan, V. N. (2010). Preponderance of heterotrophic *Noctiluca scintillans* during a multi-species diatom bloom along the southwest coast of India. *Int. J. Oceans Oceanogr.*, 4, 55-63.
- Pastoureaud, A., Dupuy, C. and Chrétiennot-Dinet, M. J. (2003). Red coloration of oysters along the French Atlantic coast during the 1998 winter season: implication of nanoplanktonic cryptophytes. *Aquaculture*, 228, 225-235.
- Pauly, D. and Christensen, V. (1995). Primary production required to sustain global fisheries. *Nature*, 374, 255-257.
- Paz, B., Riobó, P., Fernández, M. L., Fraga, S. and Franco, J. M. (2004). Production and release of yessotoxins by the dinoflagellates *Protoceratium reticulatum* and *Lingulodinium polyedrum* in culture. *Toxicon*, 44, 251-258.
- Pearce, I., Handlinger, J. H. and Hallegraeff, G. M. (2005). Histopathology in Pacific oyster (*Crassostrea gigas*) spat caused by the dinoflagellate *Prorocentrum rhathymum*. *Harmful Algae*, 4, 61-74.
- Porumb, F. (1992). On the development of *Noctiluca scintillans* under eutrophication of Romanian Black Sea waters. In: R. A. Vollenweider, R. Marchetti and R. Viviani (Eds.), *Marine Coastal Eutrophication*. Amsterdam: Elsevier. pp. 907-918.
- Radi, T. and Vernal, A. D. (2004). Dinocyst distribution in surface sediments from the northeastern Pacific margin (40-60°N) in relation to hydrographic conditions, productivity and upwelling. *Rev. Palaeobot. Palyno.*, 128, 169-193.

- Reid, P. C. (1977). Peridiniacean and Glenodiniacean dinoflagellate cysts from the British Isles. *Nova Hedwigia*, 18, 429-462.
- Relox, Jr. J. R. and Bajarias, F. (2003). Harmful algal blooms (HABs) in the Philippines. In: Workshop on Red Tide Monitoring in Asian Coastal Waters. University of Tokyo, Japan. (Abstract)
- Rhodes, L., McNabb, P., Salas, M. D., Briggs, L., Beuzenberg, V. and Gladstone, M. (2006). Yessotoxin production by *Gonyaulax spinifera*. *Harmful Algae*, 5, 148-155.
- Riccardi, M., Guerrini, F., Roncarati, F., Milandri, A., Cangini, M., Pigozzi, S., Riccardi, E., Ceredi, A., Ciminiello, P., Dell'Aversano, C., Fattorusso, E., Forino, M., Tartaglione, L. and Pistocchi, R. (2009). *Gonyaulax spinifera* from the Adriatic Sea: Toxin production and phylogenetic analysis. *Harmful Algae*, 8, 279-290.
- Rochon, A., Vernal, A. D., Turon, J. L., Matthiessen, J. and Head, M. J. (1999). *Distribution of recent dinoflagellate cysts in surface sediments from the North Atlantic Ocean and adjacent seas in relation to sea-surface parameters*, AASP contributions series number 35. Dallas: American Association of Stratigraphic Palynologists Foundation. 147 pages.
- Scholin, C. A., Herzog, M., Sogin, M. and Anderson, D. M. (1994). Identification of group- and strain-species genetic markers for globally distributed *Alexandrium* (Dinophyceae). II. Sequence analysis of a fragment of the LSU rRNA gene. *J. Phycol.*, 30, 999-1011.
- SEAFDEC Mission Report (2006). Survey and information collection on surimi industry and catch data in Myanmar from 26 February to 5 March 2006. Bangkok: Southeast Asian Fisheries Development Center. 19 pages.
- Sherr, E. B. and Sherr, B. F. (2002). Significance of predation by protists in aquatic microbial food webs. *Antonie van Leeuwenhoek*, 81, 293-308.
- Sidharta, B. R. and Ahyadi, H. (2007). Possible occurrence of toxic and harmful phytoplankton in Lembar Bay, Lombok, Indonesia. *Mar. Res. Indonesia.*, 32, 197-202.
- Smayda, T. J. (1997). Harmful algal blooms: Their ecophysiology and general relevance to phytoplankton blooms in the sea. *Limnol. Oceanogr.*, 42, 1137-1153.

- Steidinger, K. A. and Tangen, K. (1997). Dinoflagellates. In: C. R. Tomas (Ed.), *Identifying marine phytoplankton*. San Diego, California: Academic Press. pp. 387-584.
- Su-Myat, Maung-Saw-Htoo-Thaw, Matsuoka, K., Khin-Ko-Lay and Koike, K. (2012). Phytoplankton surveys off the southern Myanmar coast of the Andaman Sea: an emphasis on dinoflagellates including potentially harmful species. *Fish Sci.*, *78*, 1091-1106.
- Sunda, W. G., Graneli, E. and Gobler, C. J. (2006). Positive feedback and the development and persistence of ecosystem disruptive algal blooms. *J. Phycol.*, *42*, 963-974.
- Sweeney, B. M. (1975). Red tides I have known. In: V. R. LoCicero (Ed.), *Toxic dinoflagellate blooms*. Wakefield, Massachusetts: Massachusetts Science and Technology Foundation. pp. 225-234.
- Takahashi, Y., Takishita, K., Koike, K., Maruyama, T., Nakayama, T., Kobiyama, A. and Ogata, T. (2005). Development of molecular probes for *Dinophysis* (Dinophyceae) plastid: a tool to predict blooming and explore plastid origin. *Mar. Biotechnol.*, *7*, 95-103.
- Takano, Y. and Matsuoka, K. (2011). A comparative study between *Prorocentrum shikokuense* and *P. donghaiense* (Prorocentrales, Dinophyceae) based on morphology and DNA sequences. *Plank. Benth. Res.*, *6*, 179-186.
- Tamura, K., Peterson, D., Peterson, N., Stecher, G., Nei, M. and Kumar, S. (2011). MEGA5: Molecular Evolutionary Genetics Analysis using maximum likelihood, evolutionary distance, and maximum parsimony methods. *Mol. Biol. Evol.*, *28*, 2731-2739.
- Taylor, F. J. R. (1975). *The phytoplankton of water adjacent to a tropical Asian mangrove area*. A report to UNESCO. 32 pages.
- Taylor, F. J. R. (1976). *Dinoflagellates from the International Indian Ocean Expedition*. Stuttgart: E. Schweizerbart'sche Verlagbuchhandlung. 234 pages.
- Taylor, F. J. R. (1987). Ecology of dinoflagellates. In: *The Biology of Dinoflagellates. Botanical Monographs Volume 21*. Oxford: Blackwell Scientific. pp. 398-502.
- Taylor, F. J. R., Fukuyo, Y. and Larsen, J. (1995). Taxonomy of harmful dinoflagellates. In: G. M. Hallegraeff, D. M. Anderson and D. D. Cembella (Eds.), *Manual on Harmful Marine Microalgae, IOC Manuals and Guides No. 33*. Paris: UNESCO. pp. 283-317.

- Usup, G. and Azanza, R. V. (1998). Physiology and bloom dynamics of the tropical dinoflagellate *Pyrodinium bahamense*. In: D. M. Anderson, A. D. Cembella and G. M. Hallegraeff (Eds.), *Physiological Ecology of Harmful Algal Blooms*, NATO ASI Series Vol. G 41. Berlin: Springer. pp. 81-94.
- Usup, G., Pin, L. C., Ahmad, A. and Teen, L. P. (2002). *Alexandrium* (Dinophyceae) species in Malaysian waters. *Harmful Algae*, 1, 265-275.
- Usup, G., Leaw, C. P. and Asmat, A. (2002). Increasing importance of harmful algal blooms in Malaysia. In: Omar et al. (Eds.) *Proceedings of the Regional Symposium on Environment and Natural Resources 10-11 April 2002*. pp.144-153.
- Wagey, G. A., Taylor, F. J. R. and Harrison, P. J. (2001). Bloom of the dinoflagellate *Alexandrium affine* (Inoue and Fukuyo) Balech, in tropical Ambon Bay, Indonesia. In: G. M. Hallegraeff, S. I. Blackburn, C. J. Bolch and R. J. Lewis (Eds.), *Harmful Algal Blooms 2000*. Paris: IOC-UNESCO. pp. 120-123.
- Xu, N., Duan, S., Li, A., Zhang, C., Cai, Z. and Hu, Z. (2010). Effects of temperature, salinity and irradiance on the growth of the harmful dinoflagellate *Prorocentrum donghaiense* Lu. *Harmful Algae*, 9, 13-17.
- Yamamoto, T., Oh, S. J. and Kataoka, Y. (2002). Effects of temperature, salinity and irradiance on the growth of the toxic dinoflagellate *Gymnodinium catenatum* (Dinophyceae) isolated from Hiroshima Bay, Japan. *Fish. Sci.*, 68, 356-363.